RIA 43

XLIII Reunião Ibérica de Adsorção

Book of Abstracts

Porto, Portugal

1-4 September, 2024

SPONSORS

Institutional Support

Gold

SILVER

Bronze

Coffee Break Sponsor

*This event was financially supported by national funds through FCT/MCTES (PIDDAC) reference ALiCE, LA/P/0045/2020 (DOI: 10.54499/LA/P/0045/2020)

Table of Contents

Opening & Closing Lectures

PL1: 25 Abril 1974 - 50 years: The democratization of higher education and scientific research in Portugal
My adsorption journey

A. E. Rodrigues[1,2]

(1) LSRE-LCM—Laboratory of Separation and Reaction Engineering-Laboratory of Catalysis and Materials, Faculty of Engineering, University of Porto, Rua Dr. Roberto Frias, 4200-465 Porto, Portugal

(2)ALiCE—Associate Laboratory in Chemical Engineering, Faculty of Engineering, University of Porto, Rua Dr. Roberto Frias, 4200-465 Porto, Portugal

Closing Session: RIA@Porto: 20 years later

J. L. Figueiredo[1,2]

(1) LSRE-LCM—Laboratory of Separation and Reaction Engineering-Laboratory of Catalysis and Materials, Faculty of Engineering, University of Porto, Rua Dr. Roberto Frias, 4200-465 Porto, Portugal

(2)ALiCE—Associate Laboratory in Chemical Engineering, Faculty of Engineering, University of Porto, Rua Dr. Roberto Frias, 4200-465 Porto, Portugal

Plenary Lectures

RIA 43
XLIII Reunião Ibérica de Adsorção
Porto, Portugal
1-4 September 2024

PL2: Chromatographic Downstream Processing of Biopharmaceuticals

J. P. B. Mota

LAQV-REQUIMTE, Department of Chemistry, NOVA School of Science and Technology, NOVA University of Lisbon, 2829-516 Caparica, Portugal

Continuous manufacturing has seen widespread adoption across various industries, yet its integration into biotechnology has been met with hesitation, as traditional batchwise processing remains the norm. However, transitioning to continuous operations holds immense potential to enhance productivity and significantly reduce the operational footprint. Furthermore, continuous processes enable robust purification of delicate biomolecules, facilitated by a comprehensive suite of unit operations tailored for continuous downstream processing in biopharmaceuticals.

Of these operations, chromatography stands out as particularly advanced in continuous mode, having resolved the inherent challenges associated with batch definitions. This advancement not only streamlines regulatory compliance but also paves the way for broader implementation of continuous downstream processing. The impetus for embracing continuous manufacturing strategies in the future will be driven by economic pressures, operational flexibility, and considerations for parametric release.

A straightforward approach to continuous chromatography involves running multiple columns in parallel, allowing for seamless cycling of loading, washing, elution, regeneration, and re-equilibration processes. While each step may have differing durations, optimizations can be made to consolidate steps within a single cycle, thereby enhancing efficiency. Nonetheless, loading often emerges as the most time-intensive step, potentially leading to idle columns and reduced productivity. Strategies such as distributing loading across multiple columns can mitigate this issue, albeit at the expense of increased equipment costs.

Remarkable progress has been made in industrial-scale continuous purification processes, notably through rapid cycling of membrane chromatography units, enabling the processing of significant volumes of cell culture supernatant. Moreover, advancements in high-throughput development and modeling have facilitated the rapid optimization of adsorption and elution conditions, seamlessly translatable from batchwise to continuous operations.

In the realm of chromatography applied to biomolecules, scalability poses no inherent challenge, with various operation principles extensively explored. Notable among these are rotating chromatography devices and periodic countercurrent chromatography techniques, which operate in a pseudocontinuous manner, achieving cyclic steady state operation.

This review aims to elucidate the downstream processing of biopharmaceuticals, with a focus on the impementation of continuous chromatography. The pivotal drivers for transitioning from batchwise to continuous operation encompass gains in productivity, operational flexibility, and the potential for implementing process-control strategies essential for parametric or real-time release. While continuous chromatography introduces complexity, its benefits in productivity and flexibility far outweigh the challenges, making it an increasingly attractive prospect for biotechnological applications.

PL3: Paving the way for sustainable industrial futures

Mercedes Maroto-Valer

Research Centre for Carbon Solutions (RCCS), School of Engineering and Physical Sciences, Heriot-Watt University, Edinburgh, Scotland

1. Clustering for success: A place-based approach to industrial decarbonisation

On the path to net zero, all sector emissions need to be targeted, with the fastest rate of decarbonisation occurring by early 2030s. A key component of global reduction efforts focus on energy intensive industries, which according to the International Energy Agency [1], contribute over a quarter of the total global carbon dioxide (CO_2) emissions. Mitigation of emissions from industry, however, is challenging, as it requires a two-fold transition away from fossil fuels involving the use of low-carbon energy sources (e.g. renewables, hydrogen or bioenergy), as well as moving away from fossil fuel based carbon feedstocks.

In a growing number of economies, industrial decarbonisation strategies focus on large clusters of energy intensive industries. This 'cluster' or 'place-based' approach capitalises on the fact that industries co-locate large-scale infrastructure, such as electricity and heat generation, with access to manufacturing and chemical supply chains and distribution facilities. Effective industrial decarbonisation seeks to harness the scale of industrial clusters to co-create local and regional opportunities for cost-effective solutions to decarbonise, while remaining competitive on a global scale. These clusters include large energy-intensive industries, such as iron and steel, cement, refineries and chemical manufacturing. As well as being emissions intensive, these industrial clusters are major economic contributors to both their local economy and their communities, meaning techno and socio-economic factors are also at play.

Around half of UK industrial emissions are generated from clusters[2], and therefore, decarbonisation of industrial clusters is of critical importance to the UK's ambition of cutting greenhouse gas emissions to net zero by 2050. Action on decarbonising clusters is being achieved through supporting both strategic and deployment plans formulated by industry within clusters and also by engagement with research and innovation through IDRIC - the Industrial Decarbonisation Research and Innovation Centre (www.idric.org). IDRIC had established a multi-disciplinary research and innovation programme addressing key cross-cutting challenges through a whole systems approach to accelerate the development and deployment of low carbon solutions, including carbon capture, utilisation and storage (CCUS), hydrogen, fuel switching, and negative emissions technologies.

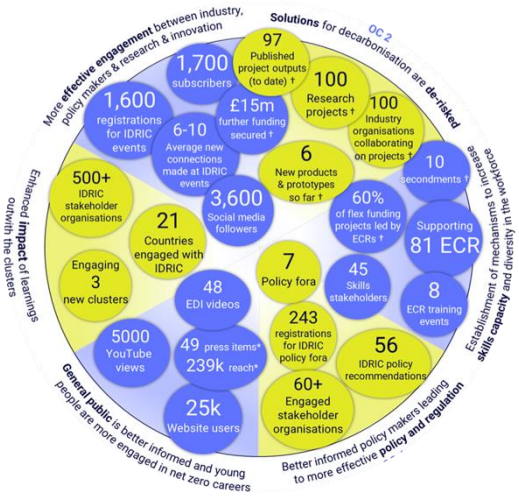

Figure 1. Key outputs and outcomes from IDRIC's work in the last 18 months.

IDRIC has become an essential catalyst, bringing together critical stakeholders across academia, industry and policy to collaborate on research and innovation to reduce barriers to development, and to accelerate deployment. This is essential to reach and maintain the pace and scale necessary for industrial decarbonisation, and to achieve economic and employment benefit from the transition to net zero. Figure 1 shows key outputs and outcomes from IDRIC's work in the last 18 months across the research and innovation portfolio. A strong community has been built across the research and industrial landscape and clear advantages can be seen to using clusters as sites to accelerate the industrial transition.

Cluster initiatives worldwide are still at an early stage, and it is important for this approach to be adopted internationally taking advantage of wider knowledge exchange which has the potential to prevent duplication of effort, speed up work and bring in new innovations.

2. The role of adsorption technologies for industrial decarbonisation

Carbon capture, utilisation and storage (CCUS) technologies are critical to reducing industrial emissions at lowest cost globally. Currently, CCUS facilities under development can capture about 361 million tonnes of CO_2 per year, whilst International Energy Agency (IEA) estimates that around 1 Giga tonne of CO_2 per year needs to be captured and stored. Through a series of research and innovation projects, IDRIC is addressing technical and socio-economic key barriers to accelerate deployment of CCUS, e.g. novel materials with high loading and cyclic capacity, dynamic storage capacity, access to UK CO_2 storage capacity appraisal, fast-tracking routes to market and skills shortages.

A range of adsorption technologies are emerging for capturing CO_2 emissions from industrial sources, including advanced adsorbent materials, as well as innovations in the capture process and regeneration methods [4]. A wide range of porous adsorbents have been developed, including carbons, zeolites, silicas, activated alumina and molecular organic frameworks (MOFs), with a large number of them containing amine–functionalised groups.

There are critical challenges to accelerate the commercialisation of adsorption technologies for CO_2 capture from industrial sources, ranging from fundamental understanding of adsorption materials, development of adsorbents with improved properties and process optimisation. This presentation will highlight some of IDRIC's work to address these barriers, including: integration of developments in material science with system analysis and process engineering; synergistic process for carbon capture, waste heat recovery and hydrogen production; and CO_2 capture with improved hydrogen recovery processes. Finally, the integration of adsorption technologies for direct air capture and hybrid systems combining CO_2 capture with conversion will also be discussed.

3. References

[1] International Energy Agency, Energy system - industry, www.iea.org/energy-system/industry, Accessed 27th August 2024.
[2] HM Government Industrial Decarbonisation Strategy, March 2021, https://www.gov.uk/government/publications/industrial-decarbonisation-strategy, Accessed 27th August 2024.
[3] UK Government's Carbon Budget Delivery Plan, March 2023, https://www.gov.uk/government/publications/carbon-budget-delivery-plan, Accessed 27th August 2024.
[4] Dziejarski, B., Serafin, J., Andersson, K. & Krzyżyńska, R. *Materials Today Sustainability* **24**, 100483 (2023).

4. Acknowledgements

IDRIC has received support from the UKRI ISCF Industrial Challenge award number EP/V027050/1, under the UKRI Industrial Decarbonisation Challenge (IDC), and EPSRC funding EP/Z53125X/1.

.

RIA43
XLIII Reunião Ibérica de Adsorção
Porto, Portugal
1-4 September 2024

PL4: Revealing the Potential of Zeolites: Enhancing Solutions for Separation Processes

Susana Valencia

Instituto de Tecnología Química, Universitat Politècnica de València − Consejo Superior de Investigaciones Científicas, 46022, Valencia, Spain

Gas and vapour separations can be complex and energy-intensive, driving the search for more sustainable options. The use of porous materials as selective adsorbents has been proposed as a very efficient solution. Zeolites, in particular, can be tailored to meet the specific needs of these separations, maximizing unit production and diminishing energy demand. This presentation aims to show how zeolites can be applied in different separations, such as those involving CO2 adsorption and other processes where all silica zeolites can perform successfully. Examples include separations of olefins from paraffins, separations of linear and monobranched from multibranched alkanes, and the recovery of bioalcohols from fermentation media by vapour phase adsorption processes. These examples illustrate how the properties of zeolites influence adsorption processes and how these properties can be modified to be adapted to the required separation with the objective of enhancing productivity and selectivity using these materials as selective adsorbents.

Keynotes

KN1: Thermochemical Energy Storage of Traditional and Blended Refrigerants in Porous Materials

Azahara Luna Triguero

Eindhoven University of (TUe), The Netherlands

Traditional refrigerants, known for their high Global Warming Potential (GWP), are being phased out from most applications. This research explores their potential use in adsorption-based energy storage systems. By combining micro- and mesoporous materials with refrigerants and evaluating their performance in energy storage, we aim to gain a better understanding of the underlying mechanisms and identify more sustainable alternatives. One of the alternatives being considered is the use of blended refrigerants. This work focuses on the challenges of assessing and predicting the behavior of classical refrigerants, such as the crucial role of defined interactions and molecular models in the simulation. Additionally, it assesses the impact of postprocessing models and data analysis on performance indicators, providing insights into the efficiency and behavior of refrigerants-materials pairs. This research aims to evaluate the energy storage potential of blended refrigerants in porous materials with the ultimate goal of minimizing the environmental impact of refrigeration systems and establishing key performance indicators that contribute to the development of more sustainable solutions

KN2: Quest of porous materials via the valorization of organic and inorganic Wastes

S. Youssef Belmabkhout

ACER CoE, Mohammed VI Polytechnic University, Ben Guerir, Morocco

The large-scale production of a variety of end products, such as energy, electronics, fertilizers, etc. has led to a dramatic increase in the number and size of several industries, which then generate hazardous pollutants that are all too often released into the surrounding environment. Increasing levels of pollution is driving the research community to discover new ways to capture toxic pollutants from industrial waste streams and also to valorize industrial waste through the subsequent production of valuable commodities. One way to valorize waste products is to convert them into functional materials. Among the various useful products that can be synthesized from waste, the preparation of porous physical adsorbents has attracted recent attention. Metal-organic frameworks (MOFs), mesoporous silicas, and zeolites are among the various functional solid-state sorbents that have shown huge promise for many industrially relevant applications. However, overcoming obstacles ahead, such as the difficulty of producing those porous sorbents at a scale due to the high cost of the precursors used to assemble them is critical. Preparing porous materials from waste sources could help to overcome the sustainable production challenge while simultaneously valorizing the waste and addressing environmental concerns. In this work, the transformation of phosphogypsum, solid waste products generated in huge amounts from the different value chains of the phosphate industry, into advanced Ca-MOFs and zeolites, as well as the simultaneous valorization of tannery effluents and waste plastic bottles into water adsorbing Cr-terephthalate MOFs. The combination of tannery effluent and organic linker extracted from waste plastic bottles led to a successful assembly of Cr-terephthalate (Cr-BDC) MOFs with potential application for water related applications. The structural attributes of the prepared porous sorbents and their performance in different applications were confirmed by various techniques including XRD, SEM-EDX, FTIR, TGA-DSC-MS, TEM, NMR, ICP-OES, N2 sorption at cryogenic conditions, CO2 sorption at different temperatures, and room temperature water, methanol, and ethanol sorption analyses. The advances made in this study represent significant progress in (i) applying sustainability principles and pave the way for circular economy targets and (ii) in pavin the way to scale of adsorbents from different families of solid state materials.

KN3: Hybrid Membrane-PSA Systems for Hydrogen Recovery from Ammonia Cracking and CO_2 Capture from Flue Gas

José Antonio Delgado Dobladez

Facultad de Ciencias Químicas, Universidad Complutense de Madrid, 28040 Madrid/SPAIN.

e-mail: jadeldob@ucm.es

1. Introduction – Hybrid membrane-PSA systems can be advantageous over systems based on only one of these technologies for performing bulk gas separations. An example of separation where a hybrid membrane system can be used is the recovery of hydrogen from ammonia cracking. In recent years, hydrogen has been proposed as an energy carrier to decarbonize industry and transportation. Hydrogen has a low energy density and a high cost of transport. Due to the problem of low energy density of hydrogen, other ways of transporting hydrogen in liquid form have been proposed, including different hydrocarbons, methanol and ammonia. The use of liquid ammonia as a hydrogen carrier has several advantages: (i) high hydrogen content (18% by weight), (ii) ease of liquefaction, (iii) physical properties similar to LPG so that existing storage and transport technology can be used. To recover hydrogen from ammonia, a reforming unit is required. Most commercial units produce and forming gas mixture (N_2 and H_2) for various industrial applications and rarely include any additional steps to produce hydrogen at high purities [1]. Considering that currently most of the high purity hydrogen is obtained by PSA processes, it is logical to think that a PSA process can also be used in this separation. The purification of hydrogen from an ammonia reforming (or cracking) process by PSA has been studied first to obtain hydrogen suitable for use in fuel cells (ammonia content less than 0.1 ppm, nitrogen content less than 300 ppm). Secondly, the improvements that can be obtained using a hybrid membrane-PSA system have been evaluated. Both studies have been carried by simulation with PSASIM® software.

Carbon capture utilization and storage (CCUS) is a key technology to combat climate change by reducing CO_2 emissions. The conventional technology for CO_2 capture is nowadays absorption using liquid solvents, mainly amines. An important drawback of this technology is the degradation of amines and their corrosive character. CO_2 capture with solid adsorbents by PSA does not have this problem. US Department of Energy has proposed purity and recovery targets of captured CO_2 for a CO_2 capture technology [2], a minimum purity of 95% (to facilitate liquefaction) and a minimum recovery of 90%. The CO_2 capture from flue gas by PSA has been studied and compared with the CO_2 capture with a hybrid membrane-PSA process.

2. Results and Discussion - The adsorbents used in the PSA process for hydrogen recovery from ammonia cracking have been chosen considering the molecular properties of the impurities to be removed (ammonia and nitrogen). Thus, a layered bed containing silica gel and 5A zeolite has been proposed for this process. The adsorption isotherms of ammonia, nitrogen and hydrogen in these adsorbents have been taken from the literature [3,4]. The composition and conditions of the feed mixture to be treated have been taken from a feasibility study carried out by a consortium of companies formed by Siemens, Engie, Science & Technology Facilities Council and Ecuity [1]. With a single PSA process, it is possible to achieve the required hydrogen purity specifications, but the loss of hydrogen in the tail gas is quite important. With a hybrid membrane-PSA process, it is possible to obtain hydrogen with the required purity with high recovery (above 98%).

For CO_2 capture from flue gas, a CO_2/N_2 feed mixture with 15% CO_2 at 25ºC and 1 bar has been considered [2]. BPL activated carbon has been used as adsorbent [5]. With a single PSA process,

it is possible to achieve the required CO_2 recovery, but the purity target is quite far away. With a hybrid membrane-PSA process, it is possible to achieve both purity and recovery targets.

3. Conclusions - Hydrogen recovery from ammonia cracking and CO_2 capture from flue gas using PSA and hybrid membrane-PSA processes have been studied. The synergy that exists in a hybrid membrane-PSA process allows to achieve simultaneously high purity and high recovery in the two separations considered.

4. References

[1] https://assets.publishing.service.gov.uk/media/5ea1705fd3bf7f7b4cadb7c5/HS420_-_Ecuity_-_Ammonia_to_Green_Hydrogen.pdf
[2] T.T. Nguyen, G.K.H. Shimizu, A. Rajendran, *Chem. Eng. J.*, **452**, (2023) p. 139550.
[3] J. Helminen, J. Helenius, E. Paatero, I. Turunen, *J. Chem. Eng. Data*, **46(**2), (2001) p. 391.
[4] M.R. Rahimpour, M. Ghaemi, S.M. Jokar, O. Dehghani, M. Jafari, S. Amiri, S. Raeissi, *Chem. Eng. J.*, **226**, (2013) p. 444.
[5] P. Brea, J.A. Delgado, V.I. Agueda, M.A. Uguina, *Sep. Purif. Tech.*, **179**, (2017) p. 61

KN4: New possibilities with liquid stationary phases

Mirjana Minceva

Technical University of Munich, Germany

In liquid-liquid chromatography, centrifugal partition chromatography (CPC), and countercurrent chromatography (CCC), the mobile phase and the stationary phase are the two phases of a liquid biphasic system composed of two or more solvents. The stationary phase is held in place during operation by the application of centrifugal force in a specially designed column. Separation of a sample mixture is achieved due to the different distribution of the solutes between the two liquid phases. Either phase of the biphasic solvent system, the upper or the lower phase, may be used as the stationary phase. The roles of the phases and flow direction may be switched during a separation run, giving rise to various operating modes not otherwise realizable with solid stationary phases (adsorbents). These features, combined with the nearly limitless choice of solvents, make the technology extremely versatile and allow for the creation of tailor-made biphasic liquid systems, i.e., tailor-made mobile and stationary phases. This high operational flexibility renders centrifugal partition chromatography highly adaptable to different separation tasks. This talk will cover recent developments in liquid-liquid chromatography, focusing on process design and optimization using a model-based approach with the perspective “from molecule to process”.

KN5: The role of adsorption in the production of bio-methane

S. Ganesan [(1)], A. Abubakar [(1)], R. Canevesi [(1)], C. A. Grande [(1,2)]

[(1)] Laboratory of Intensification of Materials and Processes (IMAP). King Abdullah University of Science and Technology (KAUST), Thuwal, 23955-6900, Saudi Arabia. E-mail: carlos.grande@kaust.edu.sa

[(2] Chemical Engineering Program, Physical Science and Engineering (PSE) Division, King Abdullah University of Science and Technology (KAUST), Thuwal, 23955-6900, Saudi Arabia

1. Introduction – Biogas is a sustainable source of energy that can be used to produce electricity but that can also be used for decarbonizing transportation. The emissions related to the transportation sector is 24% of total CO_2 emissions and is a difficult sector to decarbonize as there are multiple source points. Bio-methane has the potential to have a significant share of this market.

Adsorption in general is a very suitable technique to assist in the production of bio-methane. Adsorption processes are available to remove contaminants from biogas like siloxanes, H_2S and other minor molecules (biogas conditioning). Moreover, pressure swing adsorption (PSA) is a state-of-the-art technology for biogas upgrading (bulk removal of CO_2). In recent years, adsorbent materials have also been used for enhanced storage of bio-methane. Indeed, using a suitable material in a storage tank, the pressure of bio-methane can be significantly reduced with tremendous impact in weight reduction of the storage tank.

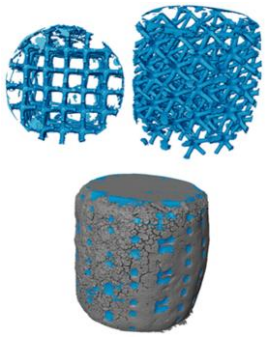

Figure 1. Low porosity carbon monolith for bio-methane storage

In this work, we present some developments in PSA technology for biogas upgrading, specifically in the deployment of new PSA cycles that aim to be customized for different users depending on production volumes. We also introduce a new approach to make carbon-based monoliths for storage of bio-methane with tailored porosity aiming to dramatically enhance the carbon packing in the storage tank but with minimal impact in gas diffusion. An example of the produced monolith is shown in Figure 1. Our ultimate objective is to demonstrate that adsorption technologies can have a significant role in transitioning to sustainable mobility in different regions of the planet.

2. Experimental – Carbon monoliths were prepared by using a customized 3D printed sacrificial template and phenolic resins. The template was designed using different lattice structures to demonstrate the flexibility of the method. Using a sequential pyrolysis, it is possible to first remove the sacrificial template and then carbonize the phenolic resin. Further activation with CO_2 contributes in increasing the surface area of the carbon monoliths.

PSA simulations of a biogas upgrading process were done in gPROMS (Siemens, UK). The adsorbent material used is carbon molecular sieve that has a kinetic selectivity towards CO_2. Different cycles were simulated, including a dual PSA unit for simultaneous production of bio-methane and high-purity CO_2.

3. Results and Discussion –

3.1- PSA for biogas upgrading

One of the important variables to consider in bio-methane production is the location of the PSA unit. In many countries with low income and cities with million inhabitants, temperature is in the range of 20 – 35 ^{o}C all year round. In other colder countries, population is smaller and temperatures are also lower, in few cases below zero. A cost-efficient PSA unit for processing 10000 m^3/h of biogas is not a mere scale-up of a unit that process 200 m^3/h. Furthermore, some countries like Denmark have very tight rules on methane emissions in the CO_2 stream.

Our initial simulations indicate that there are two ways to obtain simultaneously high-purity in the bio-methane stream as well as in the CO_2-rich stream. Either we use a multi-column PSA unit with two depressurization steps and a rinse with purified CO_2, or we use a dual-PSA technology. In the dual PSA technology, the role of the first PSA unit is to produce high purity CO_2 and the second PSA unit enhances the purity of the bio-methane. Our results indicate that with both configurations it is possible to produce bio-methane with purity over 97% and CO_2 purity over 99.5%.

3.2- Production of activated carbon for bio-methane storage

We have successfully demonstrated that it is possible to produce activated carbon monoliths with a porosity of 9%, 15 and 21% with different types of 3D printed sacrificial lattices. Using a targeted pyrolysis process, the polymer of the sacrificial lattice (rich in oxygen) is combusted leaving transport pores that also facilitate the carbonization of the phenolic resin used. Further activation with CO_2 contribute to enhance the surface area to over 1000 m^2/g. The pore network was maintained as confirmed by computer tomography (CT).

Breakthrough curves of diluted N_2 and CO_2 were measured to characterize the dispersion of gas in the monolith and diffusional resistances. The results obtained confirmed the CT observations: the transport pores created by the sacrificial lattice are open and continuous over the entire structure of the monolith. These results are now under scale-up procedure and optimization of the activation process to enhance the adsorption of methane.

4. Conclusions – This work aims to demonstrate that adsorption technologies have an enormous potential to valorize biogas as a sustainable fuel to decarbonize the transportation sector. We have proven that PSA units can render bio-methane quality with low CH4-emissions to the atmosphere using different cycle configurations which allow customization of these processes to attend different markets. Moreover, we have shown that 3D printing can assist in generating tailored monoliths where diffusion issues can be minimized in dealing with low porosity storage of bio-methane.

5. References

[1] A. Abubakar, R.L.S. Canevesi, D.A.L. Sanchez and C.A. Grande, *Chem. Eng. J*, ***489***, (2024)151450.

Oral Communications

O1: Post-combustion CO_2 Capture using Ion-exchanged binder-free NaY beads

E. Aly [(1), (2), (3)], L. F. A. S. Zafanelli [(1),(2)], A. Henrique [(1),(2)], K. Gleichmann [(4)], A. E. Rodrigues [(5)], F. A. D. S. Freitas [(3)], J. A. C. Silva [(1),(2)]

[(1)] *Centro de Investigação de Montanha (CIMO), Instituto Politécnico de Bragança, Campus Santa Apolónia, 5300-253 Bragança, Portugal.*
ezzeldin@ipb.pt
[(2)] *Laboratório Associado para a Sustentabilidade e Tecnologia em Regiões de Montanha (SusTEC), Instituto Politécnico de Bragança, Campus de Santa Apolónia, 5300-253 Bragança, Portugal*
[(3)] *Aveiro Institute of Materials, CICECO, Chemistry Department, University of Aveiro, Campus Universitario de Santiago, 3810-193, Aveiro, Portugal*
[(4)] *Chemiewerk Bad Köstritz GmbH, Heinrichshall 2, 07586 Bad Köstritz, Deutschland / Germany*
[(5)] *Laboratory of Separation and Reaction Engineering (LSRE), Associate Laboratory LSRE/LCM, Department of Chemical Engineering, Faculty of Engineering, University of Porto, 4099-002, Porto, Portugal*
zafanelli@ipb.pt; adriano_henrique@ipb.pt; k.gleichmann@cwk-bk.de; arodrig@fe.up.pt; fsilva@ua.pt; jsilva@ipb.pt

1. Introduction - Ion-exchange processes on zeolites hold promise for improving adsorption mechanisms critical for post-combustion CO_2 capture (PCC). Zeolites offer advantages such as favourable CO_2 adsorption isotherms, rapid kinetics, non-toxicity, and cost-effectiveness, making them attractive candidates for carbon capture applications. In this study, we focus on exploring the impact of ion-exchange (K^+ and Ca^{2+}) on bare NaY zeolite for PCC. Fixed-bed breakthrough experiments were conducted on various ion-exchanged zeolites, including K(23)Y, K(58)Y, K(95)Y, Ca(56)Y, and Ca(71)Y, within a temperature range of 306 K to 344 K and pressures reaching up to 350 kPa. The objective of these experiments is to investigate the equilibrium, kinetics, and dynamic characteristics of the sorption process, covering both single and binary mixtures of CO_2 and N_2. Performance parameters such as selectivity and working capacity were evaluated based on the experimental outcomes. Following data collection, a mathematical model was calibrated utilizing Aspen Adsorption v10 software to simulate fixed-bed performance under standard PCC conditions.

2. Experimental - The FAU type-Y zeolites investigated in this study were synthesized in a binder-free form, denoted as Köstrolith NaYBFK, with a Si/Al ratio of 2.5. The synthesis was conducted at the laboratory facilities of *Chemiewerk Bad Köstritz GmbH (Germany)*. A single and multicomponent breakthrough apparatus was employed to investigate the dynamics of fixed-bed adsorption involving CO_2 and N_2, alongside obtaining adsorption equilibrium data. The apparatus configuration is depicted in Image 1. The isotherms for both single and multicomponent adsorption were modelled using the Dual-site Langmuir (DSL) isotherm. Aspen Adsorption v10 package was used for the numerical simulation of fixed bed adsorption in both single and binary-component breakthrough experiments.

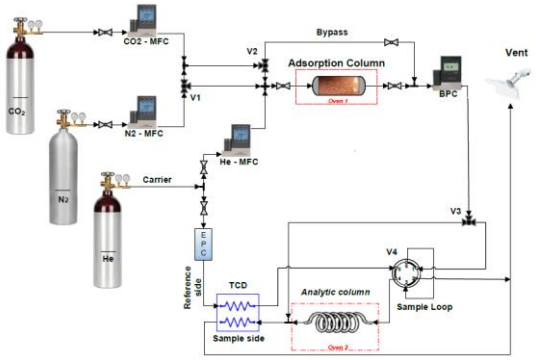

Image 1. Schematic drawing of the experimental set-up used to perform single- and multi-component breakthrough experiments

3. Results and Discussion - In Image 2, the CO_2 and N_2 adsorption behaviors, along with the CO_2/N_2 selectivity at 306 K, are shown. These include isotherms for bare binder-free NaY and ion-exchanged zeolites: K(23)Y, K(58)Y, K(95)Y, Ca(56)Y, and Ca(71)Y. Notably, the sorption hierarchy at low pressures (up to 50 kPa) follows the order: Ca(71)Y < Ca(56)Y < NaY < K(23)Y < K(58)Y < K(95)Y. For instance, at 25 kPa and 306 K, CO_2 loading for bare NaY is 4.05 mol·kg^{-1}, rising to 4.29 for K(23)Y, 4.59 for K(58)Y, and peaking at 4.72 for K(95)Y, indicating a 16% improvement over NaY. Conversely, Ca(56)Y exhibits a loading of 2.63 mol·kg^{-1}, and Ca(71)Y records a lower loading of 2.01 mol·kg^{-1}, indicating less than half the adsorption compared to commercial NaY. At pressures exceeding 200 kPa, K(23)Y and NaY exhibit

the highest CO_2 loadings, followed by K(58)Y and K(95)Y. The N_2 isotherms show a more linear trend compared to CO_2, with a similar sorption hierarchy, but with considerably lower loadings. The observed N_2 loadings suggest zeolites containing smaller monovalent cations, like binder-free K(23)Y and NaY, exhibit slightly lower N_2 uptake compared to other K^+ exchanged adsorbents, potentially contributing to higher CO_2/N_2 selectivities and enhancing CO_2 separation efficiency in industrial applications. Analysis of the CO_2/N_2 selectivity profile in Image 2c reveals consistent superior performance by binder-free zeolite K(23)Y across various conditions. For instance, at 306 K and 50 kPa, the CO_2/N_2 selectivity for K(23)Y is 41, surpassing those of NaY (38), K(58)Y (35), K(95)Y (28), Ca(56)Y (26), and Ca(71)Y (24). This sustained elevation highlights K(23)Y's notable proficiency in preferentially adsorbing CO_2 over N_2, suggesting potential applicability in PCC processes. Under standard PCC conditions, binary breakthrough experiments were performed on all binder-free FAU zeolites using a gas mixture containing 15% CO_2 and 85% N_2 (mol. %) at 101.3 kPa and 306 K. To evaluate CO_2 separation efficiency, various adsorbent metrics, including CO_2 loadings, selectivities, and working capacities, were analyzed. The findings suggest that binder-free K(23)Y exhibits considerable promise for PCC applications, demonstrating the highest binary selectivity at 101, a binary loading of 3.53 $mol \cdot kg^{-1}$, and the highest working capacities of 2.37 $mol \cdot kg^{-1}$, 0.71 $mol \cdot kg^{-1}$, 0.15 $mol \cdot kg^{-1}$ across a range of Vacuum Swing Adsorption (VSA) PCC processes, considering regeneration pressures of 3, 10, and 15 kPa, respectively, relative to a feed pressure of 101.3 kPa. Image 3 shows the simulated and experimental breakthrough curves, along with temperature fronts for binary CO_2/N_2 adsorption in binder-free K(23)Y at 306 K. The simulated data generated with Aspen Adsorption accurately mirrors the dynamic data, capturing both concentration and temperature profiles. This alignment positions Aspen Adsorption as a valuable tool for designing cyclic adsorption processes employing FAU-Y zeolites in PCC applications.

4. Conclusions - The results of this study highlight the considerable potential of binder-free K(23)Y as a promising adsorbent for the separation of CO_2 from post-combustion streams. The data derived from this research are actively informing the development of a cyclic process, intended to optimize the practical application and effectiveness of this adsorption system for CO_2 recovery utilizing FAU Y-type zeolites.

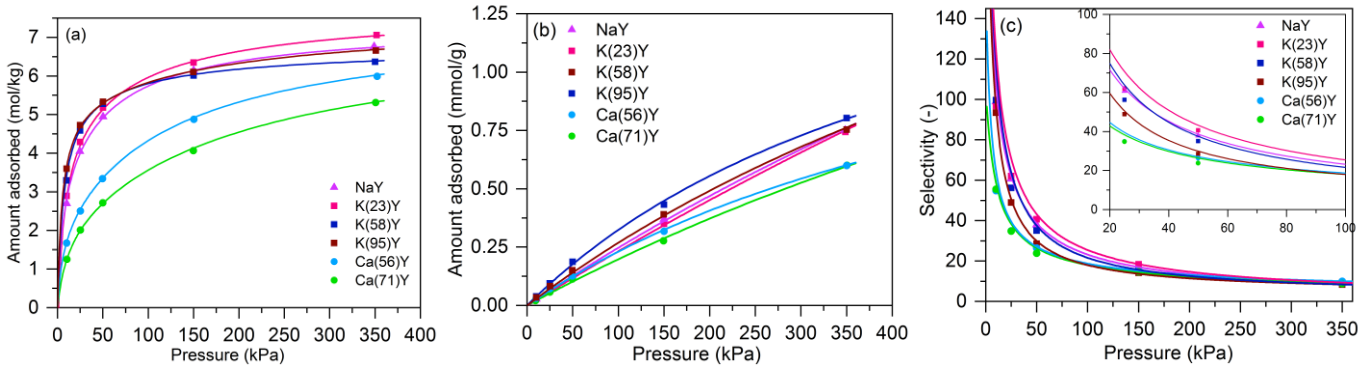

Image 2. Comparison of (a) CO_2 and (b) N_2 adsorption isotherms and (c) CO_2/N_2 at 306 K among binder-free NaY, K(23)Y, K(58)Y, K(95)Y, Ca(56)Y, and Ca(71)Y zeolite. Experimental = symbols; DSL isotherm = lines.

5. Acknowledgments - This work was supported by national funds through FCT/MCTES (PIDDAC): (1) project PTDC/EQU-EPQ/0467/2020 (DOI:10.54499/PTDC/EQU-EPQ/0467/2020); (2) CIMO, UIDB/00690/2020 (DOI: 10.54499/UIDB/00690/2020) and SusTEC, LA/P/0007/2020 (DOI: 10.54499/LA/P/0007/2020); (3) CICECO –Aveiro Institute of Materials, UIDB/50011/2020 & UIDP/50011/2020 & LA/P/0006/2020.

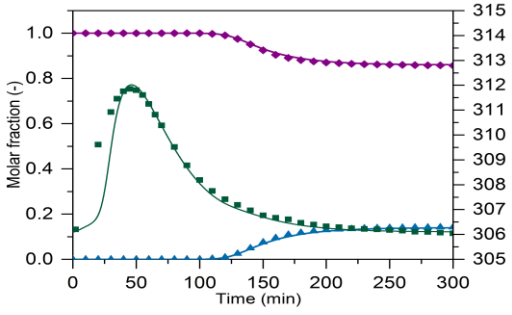

Image 3. Breakthrough curves for binder-free K(23)Y zeolite in binary CO_2 (15%) (▲) and N_2 (85%)(♦) fixed bed experiments and temperature fronts (■) at 306 K. Experimental = symbols; Aspen numerical predictions = lines.

O2: Rational Doping Strategy of Porous Materials for Hydrogen Storage: CNTs study case

S. Rezaie [(1)], A. Luna-Triguero [(2)]

(1) Energy Technology, Department of Mechanical Engineering, Eindhoven University of Technology, 5600 MB Eindhoven, The Netherlands
(2) Eindhoven Institute for Renewable Energy Systems (EIRES), Eindhoven University of Technology, PO Box 513, Eindhoven 5600 MB, The Netherlands
Principal Author's e-mail: s.rezaie@tue.nl

1. Introduction – The increase in global energy demand along with the pollution caused by the use of fossil fuels has sent a clear message to use a clean and renewable energy source. The use of hydrogen gas along with other renewable energy sources such as solar and wind energy is the most promising way to provide sufficient energy [1]-[3]. Hydrogen is the most abundant element on earth, which can achieve a maximum efficiency of about 65% in fuel cells. This amount is higher than gasoline (22%), diesel (45%) and other fossil fuels. In addition, hydrogen is a non-toxic energy source that does not emit any CO_2 upon combustion. Water vapor and heat are the only byproducts of burning hydrogen [4].
Despite its potential, the practical utilization of hydrogen as a fuel source hinges on effective hydrogen storage. Storage enables energy to be available when needed, ensuring a consistent supply that complements other renewable sources to mitigate fluctuations in energy production due to varying weather conditions and seasons [5], [6]. As an example, excess energy generated during summer days can be used to produce and store hydrogen, which can be tapped during winter when solar energy production is limited [6]. In this scenario, hydrogen storage is paramount for using hydrogen as fuel.
The critical challenge in using solid hydrogen storage lies in identifying a suitable material capable of reversibly storing hydrogen. According to the Department of Energy of the US (DOE) standards, efficient materials for hydrogen storage applications should exhibit gravimetric capacity with a lower limit of about 5.5 wt% by 2025 and an ultimate goal 6.5 wt% [7], [8]. In addition, the binding energy should be in the range of 0.15 to 0.6 eV for reversible hydrogen storage [9].

2. Experimental – Present study provides simulations conducted using density functional theory (DFT). However, the simulation outcomes, including binding energy, charge transfer, adsorption behaviour, and bond length, have been systematically compared with multiple experimental findings. The results exhibit both quantitative and qualitative agreement with the experimental data.

3. Results and Discussion - This study introduces a systematic approach for selecting optimal doping on porous materials, emphasizing the intricate interplay between doping with the material's structure and the interaction between doping and hydrogen. Our proposed approach serves as a framework for evaluating and predicting the performance of doped materials. To validate the efficacy of our strategy, we conduct a comprehensive investigation in carbon nanotubes (CNTs). Applying our criteria, we systematically screen several dopants in CNTs (Figure 1). The results highlight Cu-doped CNTs as promising candidates for hydrogen storage applications. Focusing on Cu-doped CNTs, we analysed binding energy, charge transfer, partial density of states (PDOS), and desorption temperature to assess the performance of modified CNTs. Additionally, we explore the feasibility of doped CNTs featuring various sizes of copper clusters and the effect on the release temperature, i.e., complete regeneration [10].

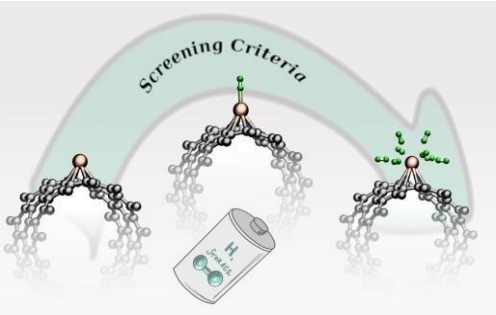

Figure 1. Screening criteria.

4. Conclusions - The findings indicate that incorporating 5 to 6% copper impurity onto CNT surfaces renders these nanostructures highly applicable for reversible hydrogen storage near ambient conditions [10]. The evaluation of our proposed strategy demonstrates that this approach serves as a robust framework for assessing and predicting the performance of doped materials, offering valuable insights for both computational and experimental design.

5. References

[1] S. Sharma, S. Basu, N. P. Shetti, and T. M. Aminabhavi, "Waste-to-energy nexus for circular economy and environmental protection: Recent trends in hydrogen energy," Science of the Total Environment, vol. 713, Apr. 2020, doi: 10.1016/j.scitotenv.2020.136633.

[2] J. O. Abe, A. P. I. Popoola, E. Ajenifuja, and O. M. Popoola, "Hydrogen energy, economy and storage: Review and recommendation," International Journal of Hydrogen Energy, vol. 44, no. 29. Elsevier Ltd, pp. 15072–15086, Jun. 07, 2019. doi: 10.1016/j.ijhydene.2019.04.068.

[3] D. J. Durbin and C. Malardier-Jugroot, "Review of hydrogen storage techniques for on board vehicle applications," International Journal of Hydrogen Energy, vol. 38, no. 34. pp. 14595–14617, Nov. 13, 2013. doi: 10.1016/j.ijhydene.2013.07.058.

[4] S. Niaz, T. Manzoor, and A. H. Pandith, "Hydrogen storage: Materials, methods and perspectives," Renewable and Sustainable Energy Reviews, vol. 50. Elsevier Ltd, pp. 457–469, May 30, 2015. doi: 10.1016/j.rser.2015.05.011.

[5] G. Reiter and J. Lindorfer, "Global warming potential of hydrogen and methane production from renewable electricity via power-to-gas technology," International Journal of Life Cycle Assessment, vol. 20, no. 4, pp. 477–489, Apr. 2015, doi: 10.1007/s11367-015-0848-0.

[6] K. Kajiwara, H. Sugime, S. Noda, and N. Hanada, "Fast and stable hydrogen storage in the porous composite of MgH2 with Nb2O5 catalyst and carbon nanotube," J Alloys Compd, vol. 893, Feb. 2022, doi: 10.1016/j.jallcom.2021.162206.

[7] T. Rimza et al., "Carbon-Based Sorbents for Hydrogen Storage: Challenges and Sustainability at Operating Conditions for Renewable Energy," ChemSusChem, vol. 15, no. 11. John Wiley and Sons Inc, Jun. 08, 2022. doi: 10.1002/cssc.202200281.

[8] H. W. Langmi, N. Engelbrecht, P. M. Modisha, and D. Bessarabov, "Hydrogen storage," in Electrochemical Power Sources: Fundamentals, Systems, and Applications Hydrogen Production by Water Electrolysis, Elsevier, 2021, pp. 455–486. doi: 10.1016/B978-0-12-819424-9.00006-9.

[9] S. M. Aceves, G. D. Berry, J. Martinez-Frias, and F. Espinosa-Loza, "Vehicular storage of hydrogen in insulated pressure vessels," Int J Hydrogen Energy, vol. 31, no. 15, pp. 2274–2283, Dec. 2006, doi: 10.1016/j.ijhydene.2006.02.019.

[10] S. Rezaie, and A. Luna-Triguero, "A comprehensive approach for doping selection and assessment in porous materials for hydrogen storage: CNTs study case," Chemical Engineering Journal, vol. 489, p.151270, Jun. 2024, doi: https://doi.org/10.1016/j.cej.2024.151270.

O3: Simulated Moving Bed Reactor to Valorise Glycerol into Solketal: Coupling Green Chemicals and Process Intensification

I. Corrêa [1,2], R. P. V. Faria [1,2], A E. Rodrigues [1,2]

[1] *LSRE-LCM – Laboratory of Separation and Reaction Engineering - Laboratory of Catalysis and Materials, Faculty of Engineering, University of Porto, Rua Dr. Roberto Frias, 4200-465 Porto, Portugal*
[2] *ALiCE – Associate Laboratory in Chemical Engineering, Faculty of Engineering, University of Porto, Rua Dr. Roberto Frias, 4200-465 Porto, Portugalup201902799@up.pt*
ruipvfaria@gmail.com
arodrig@fe.up.pt

1. Introduction – Solketal is one of the most promising solutions for glycerol valorisation due to its properties as diesel additive, with the capability of enhancing fuel octane number and oxidation stability, diminishing particle emissions and gum formation, and enhancing properties at low temperatures. Furthermore, solketal has the potential to be used as jet fuel additive due to its anti-freezing property. Reinserting solketal in the biodiesel production chain complies with the Circular Economy model, which is of great economic and environmental interest [1].
The reaction for solketal synthesis is reversible, thus the conversion is thermodynamically limited. The SMBR stands out as a sorption-enhanced Process Intensification strategy able to improve the efficiency of reactive systems by combining separation by adsorption and chemical reaction using a hybrid stationary phase with catalytic activity and adsorption selectivity between the products. This way, by adsorbing one of the products, the reaction equilibrium shifts towards product formation.
In the Conventional SMBR, a feed stream composed of a reactive mixture is fed to a four-section unit, with synchronous time switch (t*) and constant flow rates. Unlike most SMBR processes, for solketal synthesis, none of the reactants can be used as desorbent, due to miscibility issues. For this reason, two non-conventional strategies were developed, the Multifeed, where the reactants are fed in different positions, and the ModiCon SMBR, where the reactants are fed at different moments of t*. Both strategies take advantage of the different affinities of the reactants with the stationary phase to promote their countercurrent contact, maximize their interaction, and, consequently, solketal's output.
In practice, to implement all these operations, it is necessary to build a highly versatile unit. The valve system strategy is a key factor in ensuring the flexibility of the unit. The distributed valve design was selected for the novel pilot scale unit built at LSRE-LCM, the Supercritical Fluid Simulated Moving Bed Reactor (SF-SMB(R)), where the experimental validation of solketal synthesis was performed.

2. Experimental - The optimizations of the Conventional and Five-section SMBR were performed following the two-step procedure proposed by Faria et al. The TMBR steady-state model is used to find the feed and extract flowrates, and solid velocity (decision variables) that result in the maximum productivity (objective function), under the purity constraints of 97% (desorbent free) for solketal in the raffinate and water in the extract stream. In the first step, the optimal unit configuration (number of columns in each section) was defined. Then, for the best column configuration, a sensitivity analysis was carried out to the safety factor (SF) applied to sections 1 and 4 (solid and liquid regeneration sections) [2].
The ModiCon SMBR is a dynamic operation, therefore it requires the equations to be solved dynamically until reaching the cyclic steady state. This makes it unviable to reproduce the method that relies on the steady-state model. The rigorous SMBR must be used instead. Thus, the column configuration and SFs that achieved the highest productivity in the Conventional SMBR and the t* that achieved the highest in the Five-section SMBR were used as inputs for the ModiCon. The model equations were solved using gPROMS ®, v. 7.0.7.
The SMBR simulation studies and the experimental validation were performed in the SF-SMB(R). This unit comprises eight fixed-bed columns with 15 cm in length and 2.12 cm in diameter.

3. Results and Discussion - The best column configuration for the Conventional SMBR is the 1-2-4-1. Since acetone is carried in the direction of the fluid flow, most of the reaction takes place in Section III, and this reactant is present in significant amounts only in the column immediately before the feed port, therefore there is no need for more than two columns in Section II. The reaction thermodynamic limitation is what hinders the performance of the Conventional SMBR since it is necessary more columns in the sections where the reaction occurs. As for the regeneration sections, only one column in each section is necessary. The combination of SF that achieves the highest productivity and that provides a sufficient T/SMBR equivalence is 40% in Section I and 15% in Section IV. At this point, t* is 25.7 min, the productivity is 1.086 $kg_{Solk} \cdot L_{Ads}^{-1} \cdot day^{-1}$ and the DC is 26.24 $L_{Desorbent} \cdot kg_{Prod}^{-1}$.

The study on the column configuration of the Five-section SMBR reveals that the reaction and the separation of acetone and solketal take place almost exclusively in Section IIIB, and the performance is strongly driven by the available reactive region. The configuration that maximizes the number of columns in Section IIIB is 1-1-1-4-1. The combination of SF that achieves the highest productivity and that provides a good T/SMBR equivalence is 40% in Section I and 25% in Section IV. At this point, t* is 23.14 min, the productivity is 7.03 $kg_{Solk} \cdot L_{Ads}^{-1} \cdot day^{-1}$, with DC is 5.02 $L_{Desorbent} \cdot kg_{Prod}^{-1}$. Also, the reactants feed ratio is 1.03, which results in an excess of acetone of nearly 5%.
For the ModiCon operation, such acetone excess is granted when glycerol is fed during 49% of the t* and acetone in the remaining time. The performance of the ModiCon SMBR is slightly superior to the Five-section SMBR. Using the t* of 23.14 min and a combination of SF of 40% and 25%, the productivity reaches 8.13 $kg_{Solk} \cdot L_{Ads}^{-1} \cdot day^{-1}$, with DC of 4.30 $L_{Desorbent} \cdot kg_{Prod}^{-1}$.
The SF-SMB(R) was built in a way that to implement the non-conventional strategies, it is only required to select it in the software, with almost no intervention in the physical equipment. The advantage of the ModiCon SMBR over the Multifeed is that its operation is slightly more robust.

4. Conclusions - The productivity results of both non-conventional operations are within the range reported for similar processes and prove that solketal may be produced by a continuous chromatographic reactor. The major advantage of using such strategies is the possibility of operating with higher flow rates and, consequently, obtaining better performance parameters. It is noteworthy that between the proposed non-conventional operation, the ModiCon strategy can achieve a productivity 14% higher due to being able to process an even higher feed flow rate while achieving a DC 14% lower.
Despite the Conventional SMBR performing poorly, experimentally validating it is a groundbreaking step in solketal production and indeed the first step to implementing this process on a large scale.

5. References

[1] J. A. Melero, G. Vicente, G. Morales, M. Paniagua, J. Bustamante, Fuel. 89 (2010) 2011–2018.
[2] R.P.V. Faria, J. C. Gonçalves, I. Corrêa, A. M. Ribeiro, A. E. Rodrigues, Industrial & Engineering Chemistry Research, 61(39) (2022) p. 14531-14545.

O4: Efficient Hybrid Modeling and Sorption Model Discovery for Non Linear Advection-Diffusion-Sorption Systems: A Systematic Scientific Machine Learning Approach

V. Santana[(1)], C. Rackauckas[(2)], A.M. Ribeiro[(3)], I. Nogueira[(4)]

[(1)] *Norwegian University of Science and Technology*
[(2)] *Massachusetts Institute of Technology*
[(3)] *University of Porto*

Mathematical modeling is a crucial aspect of science and engineering, with two main approaches in chemical engineering: mechanistic/classical and empirical [1]. The former relies on conservation equations, transport, and thermodynamic expressions, while the latter is based on observations without assumptions about the underlying physics. Hybrid models, which merge empirical equations and physics knowledge, have gained increasing attention in engineering [1],[5]

Hybrid serial models in chemical engineering may combine first-principles derived equations with a universal approximator, like Artificial Neural Networks (ANNs), to replace one or more terms of the equation resulting in an object named Universal Differential Equation [6]. Applications of hybrid models have mainly focused on bioreaction engineering, with ANNs replacing kinetic reaction laws [7], [8]. However, the computational challenge of fitting ANNs' parameters in a differential equation has limited their application in more complex systems such as the ones described by partial differential equations (PDEs) [7], [9], [10]. Some works have pioneered the application of UDEs in advection-diffusion-sorption PDEs [9],[11].

Gradient-based or Hessian-based optimizers are preferred for training neural networks [12], but calculating accurate and efficient gradients remains an open issue in UDEs for advection-diffusion-sorption PDEs. Automatic Differentiation (AD) can provide high-accuracy gradients but can be computationally demanding and numerically unstable for non-linear advection-diffusion-sorption PDE problems [13]. This work demonstrates a feasible and efficient way for training hybrid non-linear advection-diffusion-sorption PDE problems using gradient-based optimizers. The present work also addresses the interpretability of ANNs' predictions by using symbolic or sparse regression on ANNs' output [6]. This approach reduces computational burden and allows for finding a combination of simple functions that share similar properties with the trained ANN. The in-silico dataset used in this work simulates breakthrough curves of a hypothetical single-component non-linear advection-diffusion-sorption system with various isotherms and kinetic models [14].

Overall, this work aims to help engineers efficiently introduce hybrid modeling in packed-bed separation for improving predictive power or discovering mass-transfer kinetics directly from breakthrough curves data. The methodology includes the in-silico dataset building process, hybrid model proposition, numerical aspects of the hybrid model solution and gradient calculation, and sparse regression details.

The ANN architecture is typically chosen before training, with hyperparameter optimization used in traditional deep learning to select the best architecture for a problem [6], [15]. In this work, one-layer or two-layer ANNs with hyperbolic tangent activation were used, and a varying number of neurons between 15 and 25 were chosen using grid search. Learning rates were set to 0.05 with ADAM optimizer [12] and exponential learning rate decay every 20 iterations and a 0.985 drop factor over 180 iterations. After the second fit with ADAM, the BFGS method [16] was employed until convergence.

Numerical solution of the hybrid PDE model and gradient calculation are crucial as stability and speed of gradient calculation are influenced by discretization and numerical integration method. In fixed-bed chromatography literature, Orthogonal Collocation on Finite Elements (OCFEM) is preferred [17] due to its high accuracy with steep gradients in concentration profiles. OCFEM is used with cubic Hermite polynomials [18] and zeros of shifted orthogonal Legendre polynomials as collocation points. A total of 42 evenly spaced finite elements were used, and the resulting ODE was solved using a fixed-leading coefficient adaptive-order adaptive-time BDF method (FBDF) implemented in DifferentialEquations.jl [19].

Gradient calculation for the hybrid model is formulated using an L2-norm-based discrete cost function. Continuous or discrete adjoint sensitivity analysis is preferred for calculating gradients when the sum of parameters and equations is large. The quadrature adjoint with JIT-compiled reverse-mode AD vector-jacobian product with FBDF solver is used for solving the adjoint problem in this work, as it was the most performant and stable method [13]

In summary, the presented method employs a one-layer or two-layer ANNs with hyperbolic tangent activation, grid search to select the number of neurons, ADAM optimizer, and BFGS method for training. OCFEM is used for discretization, and the adjoint sensitivity analysis is chosen for gradient calculation

using the quadrature adjoint with JIT-compiled reverse-mode AD vector-jacobian product and FBDF solver. This approach provides a stable and efficient way to train hybrid models in non-linear advection-diffusion-sorption PDE systems.

The results show that the UDE approach fits breakthrough training data well, with errors compatible with simulated noise and no apparent auto-correlation in time. It performs well in the test set for desorption and adsorption from another steady state, and the uptake rate is close to the training noiseless ground-truth data. Similar conclusions can be drawn for other models. The hybrid approach also fits breakthrough training data well, with good performance in the test set and uptake rate close to noiseless ground-truth data. However, in some cases, the uptake rate is underestimated despite the good fitting of breakthrough data.

Sparse and symbolic regression techniques were used to obtain polynomials for Langmuir, Sips, and Vermeulen's isotherms with LDF and improved LDF kinetics. The obtained polynomials resemble the true kinetic models that produced the data, and the train and test set predictions were very close to the noisy observations. Symbolic regression did not require tuning the sparsity parameter and produced simpler expressions with fewer terms. A Taylor expansion analysis demonstrated why polynomials with positive integer exponents found in sparse and symbolic regression explain the observations well.

[1] J. Sansana et al., Recent trends on hybrid modeling for Industry 4.0, Computers and Chemical Engineering, vol. 151. Elsevier Ltd, Aug. 01, 2021. doi: 10.1016/j.compchemeng.2021.107365.
[2] L. von Rueden, S. Mayer, R. Sifa, C. Bauckhage, and J. Garcke, Combining Machine Learning and Simulation to a Hybrid Modelling Approach: Current and Future Directions, Lecture Notes in Computer Science (including subseries Lecture Notes in Artificial Intelligence and Lecture Notes in Bioinformatics), vol. 12080 LNCS, pp. 548-560, 2020, doi: 10.1007/978-3-030-44584-3_43.
[3] I. Pan, L. R. Mason, and O. K. Matar, Data-centric Engineering: integrating simulation, machine learning and statistics. Challenges and opportunities, Chem Eng Sci, vol. 249, p. 117271, 2022, doi: 10.1016/j.ces.2021.117271.
[4] M. von Stosch, R. Oliveira, J. Peres, and S. Feyo de Azevedo, Hybrid semi-parametric modeling in process systems engineering: Past, present and future, Comput Chem Eng, vol. 60, pp. 86-101, 2014, doi: 10.1016/j.compchemeng.2013.08.008.
[5] M. Raissi, P. Perdikaris, and G. E. Karniadakis, Physics-informed neural networks: A deep learning framework for solving forward and inverse problems involving nonlinear partial differential equations, J Comput Phys, vol. 378, pp. 686-707, 2019, doi: 10.1016/j.jcp.2018.10.045.
[6] C. Rackauckas et al., Universal Differential Equations for Scientific Machine Learning, pp. 1-55, Jan. 2020, [Online]. Available: http://arxiv.org/abs/2001.04385
[7] S. Feyo De Azevedo, B. Dahm, and F. R. Oliveira, Hybrid modelling of biochemical processes: A comparison with the conventional approach, Comput Chem Eng, vol. 21, no. SUPPL.1, 1997, doi: 10.1016/s0098-1354(97)87593-x.
[8] H. J. Zander, R. Dittmeyer, and J. Wagenliuber, Dynamic modeling of chemical reaction systems with neural networks and hybrid models, Chem Eng Technol, vol. 22, no. 7, 1999, doi: 10.1002/(SICI)1521-4125(199907)22:7<571::AID-CEAT571>3.0.CO;2-5.
[9] H. Narayanan, M. Luna, M. Sokolov, P. Arosio, A. Butte, and M. Morbidelli, Hybrid Models Based on Machine Learning and an Increasing Degree of Process Knowledge: Application to Capture Chromatographic Step, Ind Eng Chem Res, p. acs.iecr.1c01317, Jul. 2021, doi: 10.1021/acs.iecr.1c01317.
[10] H. Narayanan, T. Seidler, M. F. Luna, M. Sokolov, M. Morbidelli, and A. Butte, Hybrid Models for the simulation and prediction of chromatographic processes for protein capture, J Chromatogr A, vol. 1650, p. 462248, 2021, doi: 10.1016/j.chroma.2021.462248.
[11] T. Praditia, M. Karlbauer, S. Otte, S. Oladyshkin, M. V. Butz, and W. Nowak, Finite Volume Neural Network: Modeling Subsurface Contaminant Transport, Apr. 2021, [Online]. Available: http://arxiv.org/abs/2104.06010
[12] D. P. Kingma and J. L. Ba, Adam: A method for stochastic optimization, in 3rd International Conference on Learning Representations, ICLR 2015 - Conference Track Proceedings, 2015.
[13] Y. Ma, V. Dixit, M. J. Innes, X. Guo, and C. Rackauckas, A Comparison of Automatic Differentiation and Continuous Sensitivity Analysis for Derivatives of Differential Equation Solutions, 2021 IEEE High Performance Extreme Computing Conference, HPEC 2021, no. 2, 2021, doi: 10.1109/HPEC49654.2021.9622796.
[14] Z. Li et al., A numerical modelling study of SO2 adsorption on activated carbons with new rate equations, Chemical Engineering Journal, vol. 353, no. July, pp. 858-866, 2018, doi: 10.1016/j.cej.2018.07.119.
[15] S. Kim, W. Ji, S. Deng, Y. Ma, and C. Rackauckas, Stiff neural ordinary differential equations, Chaos, vol. 31, no. 9, 2021, doi: 10.1063/5.0060697.
[16] J. Nocedal and S. J. Wright, Numerical Optimization Second Edition. 2006.

[17] B. A. Finlayson, ORTHOGONAL COLLOCATION ON FINITE ELEMENTS, Chem Eng Sci, vol. 30, no. 1, pp. 587-596, 1974, doi: 10.1016/0378-4754(80)90097-X.
[18] I. A. Ganaie, S. Arora, and V. K. Kukreja, Cubic Hermite Collocation Method for Solving Boundary Value Problems with Dirichlet, Neumann, and Robin Conditions, International Journal of Engineering Mathematics, vol. 2014, pp. 1-8, Feb. 2014, doi: 10.1155/2014/365209.
[19] C. Rackauckas, M. Innes, Y. Ma, J. Bettencourt, L. White, and V. Dixit, DiffEqFlux.jl - A Julia Library for Neural Differential Equations, no. February, 2019, [Online]. Available: http://arxiv.org/abs/1902.02376

O5: Improving conventional drinking water treatment: can biomass-derived PACs get the job done?

M.A. Andrade [(1)], E. Mesquita [(2)], R.M.C. Viegas [(2)], A.P. Carvalho [(1)], M.J. Rosa [(2)], A.S. Mestre [(2)]

[(1)] *Centro de Química Estrutural, Institute of Molecular Sciences, Faculdade de Ciências, Universidade de Lisboa, Campo Grande, 1749-016 Lisboa, Portugal*
mvandrade@ciencias.ulisboa.pt
[(2)] *Urban Water Unit, Hydraulics and Environment Department, LNEC - National Laboratory for Civil Engineering, Av. Brasil 101, 1700-066 Lisboa, Portugal*
emesquita@lnec.pt; rviegas@lnec.pt; mjrosa@lnec.pt; ana.carvalho@ciencias.ulisboa.pt; asmestre@ciencias.ulisboa.pt

1. Introduction – The presence of micropollutants in natural waters, as pharmaceutical compounds (PhCs), natural organic matter (NOM) and cyanotoxins (naturally produced by cyanobacteria in drinking water source reservoirs under some conditions), that resist to conventional treatments, calls for the development of advanced drinking water treatment (DWT) processes [1]. Activated carbon adsorption is considered one of the best available, consolidated, and cost-effective technologies to tackle these current water quality challenges in conventional water treatment plants. The development of advanced DWT processes calls for high-performing powdered activated carbons (PACs), as those prepared within the EMPOWER+ project, by physical (steam or CO_2) activation of carbonized pine nut shells (PNS, a by-product of the food industry). In the present work, the aim is to assess the combined PAC/coagulant performance towards PhCs and NOM removal using the fraction with particle sizes from 20 to 75 µm of a PNS-derived PAC and a commercial carbon in a conventional treatment, coagulation/flocculation/sedimentation (CFS), aiming to improve this process in a DWT plant.

2. Experimental – Pine nut shells (PNS), a by-product of the food industry (PT), were hand-crushed and carbonized under N_2 flow. The chars obtained were milled to obtain powdered material (<150 µm), which were then sieved, according to the desired particle size, and afterwards steam activated following an established protocol (LIFE Impetus project) [2]. Samples of activated carbons obtained were merged into distinct batches, according to resembling experimental conditions and textural parameters. The particle size distribution of these batches, and of the as-received commercial carbons was characterized by sieving and the PAC fractions were characterized regarding textural properties, density, moisture content and pH_{PZC}. Particle size was assessed by Laser Diffraction Spectrometry. The performance of the fraction 20_75 µm of a PNS-PAC, S2, and a commercial carbon, NSAUF was tested in real surface water (Guimarães, PT) spiked with PhCs, regarding their adsorption capacity and/or adsorption kinetics towards PhCs, namely carbamazepine (CBZ, 250 µg/L), diclofenac (DCF, 250 µg/L), and sulfamethoxazole (SMX, 100 µg/L) and NOM (natural occurring concentration, TOC= 2 mg/L). For the PAC/CFS studies, conditions of enhanced coagulation were used, and the assays with PACs S2 and NSAUF 20_75 µm addressed the simultaneous PAC and coagulant addition to real surface water with spiked PhCs, evaluating PhCs and TOC removal, according to the conditions described in Figure 1.

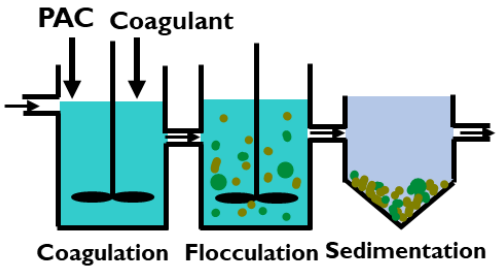

Figure 1- Experimental set up for PAC/CFS assays.

3. Results and Discussion – Overall, very similar results for PACs_20_75, S2 and NSAUF for the removal of the PhCs and NOM in real surface water were obtained in the adsorption assays. The adsorption of CBZ, DCF, and SMX to activated carbons followed the same trend observed in previous studies, with higher removals of CBZ (hydrophobic and neutral) and DCF (moderately hydrophobic compound and negatively charged) than those of SMX (hydrophilic and anionic). Adsorption isotherm data was modelled with the Freundlich model, and the Homogeneous Surface Diffusion model (HSDM) was used for fitting adsorption kinetics data; the Kf and Ds constants were also determined. The integrated modelling resulting from the combination of the 2 models allowed to forecast the PhCs removal as a function of PAC doses and contact time (Figure 2).

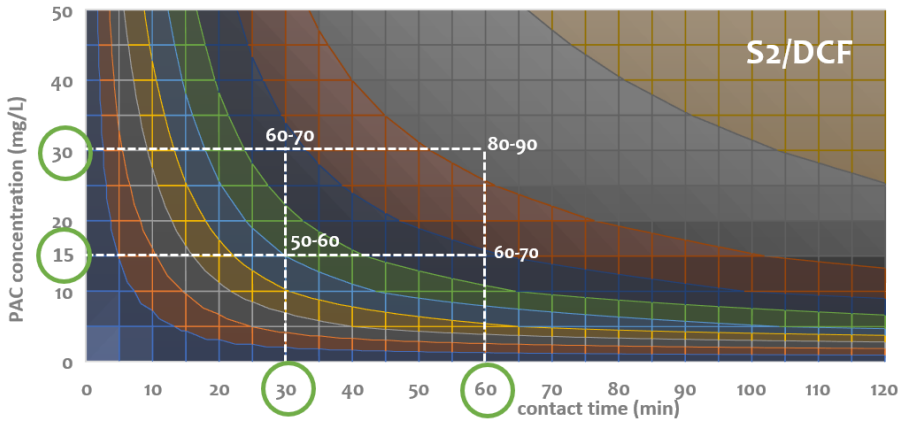

Figure 2 - DCF removal predictions from a real surface water with PAC S2 20-75 µm, for a DCF spiked concentration of 250 µg/L.

From the results obtained for PAC/CFS assays using fraction 20-75 of the commercial carbon NSAUF, the highest removal was observed for CBZ, reaching 90% for the PAC/CFS *vs* 69 % for CFS. Regarding SMX and CBZ, higher removals were also obtained for PAC/CFS, reaching 30% of removal, while CFS alone only allowed to remove 6-9% of these compounds. Regarding organic matter, the PAC/CFS achieved 21% of NOM removal, while for CFS alone, it was only 13%. Assays with the PNS/PAC in real PT surface water are currently ongoing.

4. Conclusions – High-performing PNS-derived PACs towards the removal of PhCs and NOM in real PT surface waters spiked with PhCs were obtained from a Portuguese industrial by-product by steam activation. Modelling of the adsorption data allowed the prediction of the PhCs removal as a function of PAC dose and contact time. A PNS/PAC and a commercial carbon were applied simultaneous with a coagulant, and the first results for PAC/CFS assays point out the incremental benefit of PAC addition in this technology, towards PhCs and NOM removal in the DWT process.

Acknowledgements – Centro de Química Estrutural is a Research Unit funded by Fundação para a Ciência e Tecnologia (FCT) through projects UIDB/00100/2020 and UIDP/00100/2020 (DOI 10.54499/UIDB/00100/2020 and 10.54499/UIDP/00100/2020). Institute of Molecular Sciences is an Associate Laboratory funded by FCT through project LA/P/0056/2020 (DOI 10.54499/LA/P/0056/2020). Authors thank FCT financial support to EMPOWER+ Project (PTDC/EQU-EQU/6024/2020, DOI 10.54499/PTDC/EQU-EQU/6024/2020). ASM and MAA thank FCT for, respectively, the Assistant Researcher CEECIND/01371/2017 (DOI 10.54499/CEECIND/01371/2017/CP1387/CT0013) and the Junior Research contracts in the EMPOWER+ project. The authors acknowledge Salmon & Cia for providing the commercial material Norit SA UF.

5. References

[1] M. Campinas, C. Silva, R.M.C. Viegas, R. Coelho, H. Lucas, M.J. Rosa, *J. Water Process Eng*. **40** (2021) p. 101833.
[2] A. S. Mestre, R. M. C. Viegas, E. Mesquita, M. J. Rosa, A.P. Carvalho, *J. Hazard. Mat*. **437** (2022) p. 129319.

O6: Carbon capture from wet flue gas in a dual-site dynamic Metal Organic Framework

E. Borrego-Marin[(1)], V. Colombo[(2)], C. Montoro[(3)], E. Barea[(1)], L. M. Rodríguez-Albelo[(4)], J. A. Rodriguez Navarro[(1)]

[(1)] Departamento de Química Inorgánica, Universidad de Granada, Av. Fuentenueva S/N, 18071, Granada, Spain.
emiliobm@ugr.es
[(2)] Department of Chemistry, Università degli Studi di Milano, Milano, Italy.
[(3)] Departamento de Química Inorgánica, Universidad Autónoma de Madrid, Cantoblanco, Madrid, España
[(4)] Departamento de Ingeniería y Ciencia de los Materiales y del Transporte, Universidad de Sevilla, Sevilla, España.
jarn@ugr.es, valentina.colombo@unimi.it, carmen.montoro@uam.es, lralbelo@us.es, ebarea@ugr.es

1. Introduction

Separation processes account for 10-15 % of global energy consumption. Among gas separation processes, carbon dioxide capture from wet flue gases represents one of the greater challenges in view of the Global Warming problem. However, the high moisture content in flue gas represents a problem as a consequence of the competitive nature of water adsorption. In this regard, much effort has been devoted to develop porous materials that possess high affinity CO2 adsorption sites and low interaction with water molecules [1]. For instance, classical crystalline porous materials such as zeolites and rigid metal-organic frameworks (MOFs) exhibit regular and rigid porous structures that determine the selective access of a guest molecule with a certain size, shape and physicochemical properties [2].
By contrast, soft porous coordination polymers (Soft-PCPs) are a unique class of porous crystalline materials that combine pore regularity of crystalline porous materials with transformability of enzymes. Indeed, soft-PCPs exhibit reversible transformability between states (bistable or multistable) with long-range structural ordering, and permanent porosity. The observed phase transition is highly dependent on the adsorbate-adsorbent interaction energy. This behaviour leads to gate-opening and breathing effects inducing stepwise changes in the amount of adsorbed gas at a specific pressure termed as "gate pressure" (Image 1) [3]. This phenomenon is regarded as highly promising for gas storage and separation processes, rendering larger working capacities and selectivities in comparison to conventional rigid adsorbents. Considering all the above, there is much interest in finding materials showing gas adsorption induced bistable phase (gated adsorption) but exhibiting low or negligible crystal cell volume change to avoid any problems with adsorption bed scale up and/or pressure drops in the gas separation system. The negligible volume change will also a allow to achieve intrinsic thermal management.

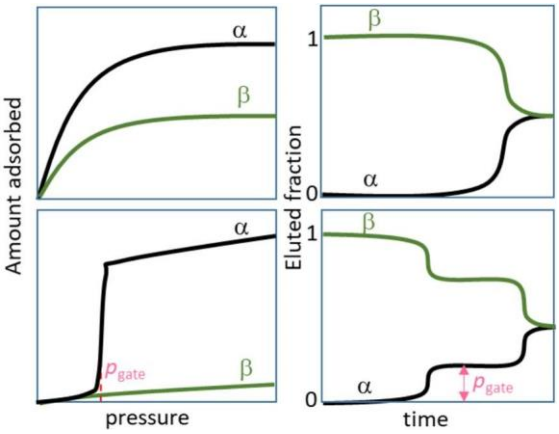

Figure 1. Comparative adsorption behaviour in rigid vs flexible porous materials. Single component adsorption isotherms for α and β gases (top left) and breakthrough curve (top right) for a rigid microporous material; Single component adsorption isotherms for α and β gases (down left) and breakthrough curve (down right) in a flexible microporous material.

2. Experimental

In this work, we synthesized the MOF system [Cu(FMA)(4,4'-Bpe)$_{0.5}$] (FMA= fumarate; 4,4'-Bpe= trans-bis(4-pyridyl)ethylene), named as **1**, as a suitable material for selective CO2 capture from wet flue gas. This material was characterized using different techniques: powder X-ray diffraction; CO_2, N_2 and H_2O adsorption isotherms; thermogravimetric analysis; etc. In situ single crystal X-ray diffraction experiments were carried out to locate CO_2 and H_2O guest binding sites and determine the mechanism of interaction.
We have also carried out multicomponent N_2, CO_2, H_2O breakthrough curve experiments in dry and wet at variable temperature (273 K, 288 K and 298 K) and gas composition.

3. Results and Discussion

In situ single crystal X-ray diffraction results show that the crystal structure of as synthetized (**1**·H2O) exhibits a 3D double interpenetrated framework consisting of square grid layers of paddlewheel dinuclear $Cu_2(COO)_4$ secondary building units (SBUs) connected by fumarate (FMA) ligands. The 2D square grids are pillared by 4,4'-Bpe linkers through the axial sites of the $Cu_2(COO)_4$ SBUs to form a 3D framework The guest water molecules are accommodated in a C2 axis and strongly interacting by H-bonding with two O-atoms fumarate moieties (O-H···O(FMA) = 2.175 Å). When the system is activated, there is a 2.6 % cell volume expansion along with a pyridine rotary disorder on the Bpe connectors. Ulterior, single crystal X-ray diffraction measurements on an environmental cell loaded with CO_2 are indicative that CO_2 guest incorporation takes place on the same binding pockets previously occupied by the water guest molecules with short contacts with FMA. CO_2 accommodation is responsible for the pyridine ring moieties reordering along with negligible crystal cell volume modification.

In order to clarify the adsorption behavior of the system under complex gas mixtures we performed multicomponent N_2, CO_2, H_2O breakthrough curve experiments. We observed that CO_2 partial pressure plays a significant role in the efficiency of the gas separation process (Image II). When the CO_2 partial pressure is below the gate pressure (P_{CO2}=0.2 bar) we observe the characteristic shape of a breakthrough curve for full CO_2/N_2 separation. By contrast, when the CO_2 relative pressure is above the gate pressure value, we observe a stepwise behaviour in the breakthrough curves. Noteworthy, while the first step in the breakthrough curve is invariant the shape of the second step is highly dependent on the excess pressure above the gate pressure value. Increasing CO_2 concentration in the incoming stream give rise to well defined second step with decreasing breakthrough times. Noteworthy, a higher CO_2 partial pressure value (P_{CO2}= 0.8 bar) give rise to a single step with a breakthrough time of aprox. 160 s accounting for 2.08 mmolg-1 of CO_2 adsorbed.

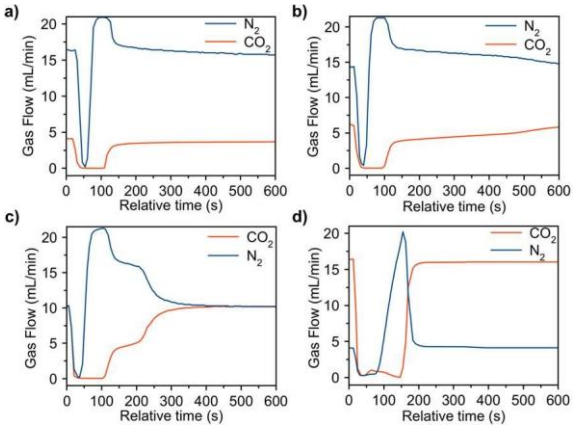

Figure 2. Study of impact of inlet gas composition on the efficiency of the N2, CO2 separation process by breakthrough curve measurements on a chromatographic bed of 1. (a) PN2= 0.8 bar; PCO2 = 0.2 bar; (b) PN2= 0.3 bar; PCO2 = 0.7 bar; (c) PN2= 0.5 bar; PCO2 = 0.5 bar; (d) PN2= 0.2 bar; PCO2 = 0.8 bar. Conditions of breakthrough curve measurements Ptotal= 1 bar, flow= 20 mL min-1 and T= 273 K.

4. Conclusions

We have demonstrated that the MOF system [Cu(FMA)(4,4'-Bpe)$_{0.5}$] (FMA= fumarate; 4,4'-Bpe= trans-bis(4-pyridyl)ethylene) behaves as a flexible porous framework that exhibits a complex adsorption process related to pyridine (Bpe) residues rotation and dual guest accommodation sites. Multicomponent N_2, CO_2, H_2O breakthrough curve measurements are indicative of full CO_2 separation at low and high pressures and partial separation at medium pressure values (above the gate pressure). Moreover, the CO_2 adsorption process is unaffected by moisture which can be related to distinct CO_2 and H_2O binding sites as ascertained by operando single crystal X-ray diffraction measurements.

5. References

[1] P.G. Boyd, A. Chidambaram, E. García-Díez et al. *Nature*, **576**, (2019) p. 253–256.
[2] P. A. Wright. "Microporous Framework Solids", *RSC Publishing*, Cambridge, 2008.
[3] S. Horike, S. Shimomura, S. Kitagawa. *Nat. Chem*, **1**, (2009) p. 695.

O7: Development of materials for potential use in water harvesting

A. Pereira [(1,2)], M. Barata , A. F. P. Ferreira[(1,2)], A. E. Rodrigues[(1,2)], A. M. Ribeiro[(1,2)], M. J. Regufe[(1,2)*]

[(1)] *LSRE-LCM - Laboratory of Separation and Reaction Engineering – Laboratory of Catalysis and Materials, Faculty of Engineering, University of Porto, Rua Dr. Roberto Frias, 4200-465 Porto, Portugal*
[(2)] *ALiCE - Associate Laboratory in Chemical Engineering, Faculty of Engineering, University of Porto, Rua Dr. Roberto Frias, 4200-465 Porto, Portugal*
A. Pereira: ajmp@fe.up.pt
A. F. P. Ferreira: aferreir@fe.up.pt; A. E. Rodrigues: arodrig@fe.up.pt; A. M. Ribeiro: apeixoto@fe.up.pt; M. J. Regufe: mjregufe@fe.up.pt

1. Introduction

Climate change, per Intergovernmental Panel on Climate Change reports, has led to shifts in Europe's climate, with rising temperatures and altered precipitation patterns. Portugal has witnessed increasing mean and extreme temperatures, along with decreasing annual precipitation. Climate models project continued temperature rise and precipitation decrease, with southern Portugal potentially facing a 30% drop and the northern region a 15% reduction by 2100 under a scenario of 3°C global warming. [1].

Direct water capture via adsorption offers a promising solution to water scarcity, showing advantages including low energy consumption, simple system designs, and cost-effectiveness [2].

Adsorption-based methods, especially Electric Swing Adsorption (ESA), hold great promise for water harvesting. In ESA, adsorbents regenerate via Joule heating, leading to faster heating, increased process efficiency, and smaller equipment size. [3].

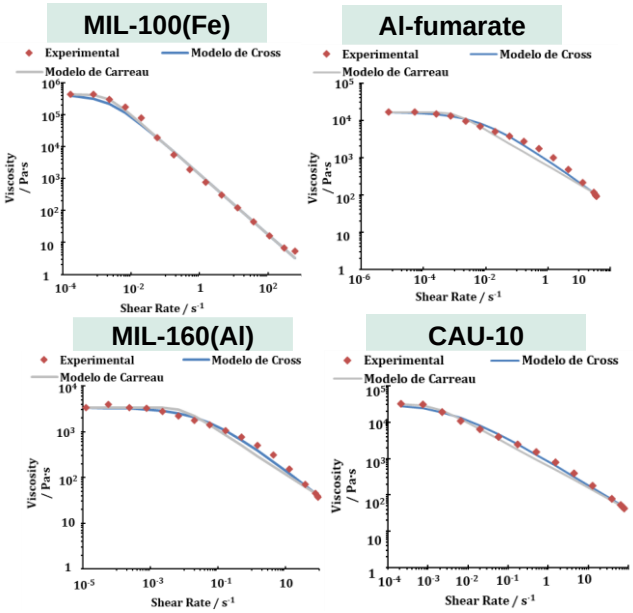

Image 1. Shear rate-dependent viscosity.

2. Material and Methods

Al-Fumarate, CAU-10, MIL-160(Al), and MIL-100(Fe) adsorbents, provided by KRICT, were combined with graphite for electrical conductivity for potential use in ESA. Carboxymethylcellulose (CMC) was added as a binder for mechanical stability and ink pseudoplasticity. Each ink formulation comprised 45%wt. MOF, 45%wt. graphite, and 10%wt. CMC, and were prepared using the Caleva Multi Lab Extruder. Dry components were initially mixed, followed by gradual addition of distilled water to achieve a uniform paste. The ink behaviour was evaluated using an Anton Paar GmbH MCR 92 rheometer at 298 K with a 0.5 mm gap between parallel plates.

The structured adsorbent was created using an extruder module (Structur3D Printing, Canada) and the Ultimaker 2+ 3D printer. After ink homogeneity was attained, it was loaded into a syringe and placed in the extruder module. Initially, the prepared inks were tested in a syringe, with manual pressure applied to print small lines, which were then dried for 24 hours at room temperature.

The four ink formulations were evaluated, and the best one was selected for printing using the 3D printer and Discovery module.

The ink-dried formulations and MOF powders were characterized via N_2 adsorption at 77 K and CO_2 adsorption isotherm at 273 K using a Micromeritics ASAP 2420 Accelerated Surface Area and Porosimetry System (USA). Prior to analysis, samples were degassed and activated at 423 K under vacuum to determine specific surface area and pore volume.

Water vapor adsorption equilibrium at 303 K was measured with a magnetic suspension balance (MSB, Rubotherm®, Bochum, Germany).

3. Results and Discussion

Rotational tests evaluated viscosity variation with shear rate, indicating pseudoplastic behaviour (Image 1). Amplitude sweep analysis plotted storage (G') and loss (G'') moduli against ink deformation, with G' initially surpassing G'', but for higher deformation values this trend reversed.

Four ink formulations were prepared, each exhibiting distinct characteristics upon drying. Al-Fumarate ink lines maintained structural integrity and mechanical resilience with no deformation, and the same was verified for the CAU-10 ink. MIL-160(Al) ink lines experienced length reduction and slight flattening, likely due to higher water content. In addition, the dried lines of this ink showed small mechanical resistance. MIL-100(Fe) ink lines also reduced in length but retained structural integrity and resistance to pressure.

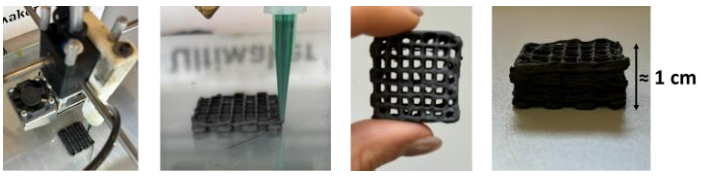

Image 2. 3D-printed Al-Fumarete + graphite monolith.

After drying, the ink samples were tested for electrical resistance to assess their suitability for direct heating by Joule effect. The Al-Fumarate ink exhibited the lowest electrical resistance ((0.18 – 0.24) x 10^3 Ω), followed by CAU-10 ink ((0.5 – 0.72) x 10^3 Ω), MIL-100(Fe) ink ((30 – 50) x 10^4 Ω), and MIL-160(Al) ((80 – 120) x 10^4 Ω).

The analysis of N2 adsorption at 77 K and CO2 isotherms at 273 K provided insights into specific surface area and pore volumes of the dried ink samples. Results showed a reduction in both parameters compared to the original MOFs, attributed to the shaping process and inclusion of graphite which has a very low surface area. After considering the results of hand-printed lines, textural characterization, and electrical resistance measurements, the ink composed of Al-Fumarate, graphite, and CMC was chosen for printing. During printing, some flattening occurred, but this was mitigated by adding kaolin and adjusting the water content in ink production. Additionally, a different printing nozzle was selected, and an external convection heat source was used. Monoliths with dimensions of 3 cm x 3 cm (Image 2) were successfully printed without structural deformations during drying.

Water vapor adsorption equilibrium was evaluated at 303 K, revealing adsorption capacities of approximately 8.06 and 10.43 mol·kg^{-1} at relative humidity levels of about 38% and 61%, respectively.

4. Conclusions

The ink formulation comprising Al-Fumarate + graphite exhibited favourable attributes for testing, considering its pseudoplastic behaviour, low electrical resistance, and measured surface area and pore volume when compared to the other formulations. The resulting 3D-printed material demonstrated robustness suitable for conducting water capture adsorption tests.

Acknowledgments

This work is financially supported by national funds through the FCT/MCTES (PIDDAC), under the project 2022.01973.PTDC - H2O-3DCapture - Water harvesting - sustainable solution based on a gas-adsorption process using innovative 3D-printed hybrid materials, with DOI 10.54499/2022.01973.PTDC (https://doi.org/10.54499/2022.01973.PTDC). This work was supported by national funds through FCT/MCTES (PIDDAC): LSRE-LCM, UIDB/50020/2020 (DOI: 10.54499/UIDB/50020/2020) and UIDP/50020/2020 (DOI: 10.54499/UIDP/50020/2020); and ALiCE, LA/P/0045/2020 (DOI: 10.54499/LA/P/0045/2020). Ana Pereira acknowledges her Ph.D. scholarship 2022.10612.BD funded by FEDER funds through NORTE 2020 and by national funds through FCT/MCTES.

5. References

[1] C. Schleussner, I. Menke, E. Theokritoff, N. van Maanen, A. Lanson, Climate impacts in portugal, Clim Analytics, (2020).

[2] M. Ejeian, R. Wang, Adsorption-based atmospheric water harvesting, Joule, 5 (2021) 1678-1703.

[3] P.D. Sullivan, M.J. Rood, G. Grevillot, J.D. Wander, K.J. Hay, Activated Carbon Fiber Cloth Electrothermal Swing Adsorption System, Environmental Science & Technology, 38 (2004) 4865-4877.

O8: Structural Changes In ZIFs Upon Liquid-Phase Adsorption

J. Farrando-Pérez[(1)], A. Missyul[(2)], J. Silvestre-Albero[(1)]

[(1)] Department of Inorganic Chemistry/University Institute of Materials, University of Alicante, Spain.
Judit.farrando@ua.es
[(2)] ALBA synchrotron light source, Cerdanyola del Valles, Spain

1. Introduction –Chemical contamination in water and air streams requires the development of novel adsorbents able to retain/concentrate these pollutants selectively and with a high adsorption capacity. Activated carbons, zeolites, silicas, and metal-organic materials are among the most frequently used adsorbents to this end. Utilizing MOFs for this purpose offers a significant advantage in terms of customization, as the pore structure of these materials can be tailored to match specific applications, rendering them a highly versatile tool for adsorption processes. Among them, ZIFs, a sub-class of MOFs, are characterized by a high specific surface area, a flexible and ultra-hydrophobic pore structure and high chemical and thermal stability[1]. These properties and the simple synthesis make them ideal adsorbents for gas and liquid-phase adsorption processes. Compared to conventional adsorbents, ZIFs can suffer structural changes upon adsorption. Gate-opening, phase transition, breathing, etc., have been widely reported in the literature for ZIFs upon an external stimulus[2,3]. However, these changes are less described for liquid-phase adsorption processes, despite their relevance for the adsorption performance and the selectivity of the process. Based on these premises, the aim of this study is to transfer knowledge from previous gas-phase studies and perform a comparative analysis of the most relevant structural changes that occurs in ZIFs during liquid-phase adsorption processes, specifically in the adsorption of aromatic contaminants. This comparison will be achieved through the integration of adsorption studies, chemical and structural characterization techniques, as well as synchrotron-based measurements conducted prior to and post-adsorption.

2.Experimental

Synthesis of ZIF-71. A solution of zinc acetate (0.73 g) in 150 mL of methanol and a solution of 4,5-dichloroimidazole (2.2 g) in 150 mL of methanol were combined and stirred for 30 minutes and left to stand at room temperature for 24 h. The methanol was then removed by decantation, and the remaining crystals were soaked in chloroform for two days. To recover the crystals, the solution was centrifuged, and the crystals were vacuum-dried at 100°C for 24 h.

Adsorption experiments. Phenol and chlorobenzene quantification was performed using UV-Vis spectroscopy analysis. Kinetic studies were conducted under an initial concentration of 50 ppm (phenol) and 75 ppm (chlorobenzene), with various time intervals between 0 and 24 h. Adsorption isotherms were conducted at different initial concentrations ranging from 25 to 100 ppm at room temperature. For chlorobenzene experiments, 15 mg of MOF were used, while for phenol experiments, 50 mg of ZIF-71 were used.

3. Results and Discussion - The initial results derived from the evaluation of the kinetics (Image 1. Left) and isotherms of the phenol and chlorobenzene adsorption process were remarkably surprising. Although both molecules were similar in size, there was a significant difference in the amount of contaminant adsorbed by the MOF. In order to understand the variation in adsorbate behaviour, synchrotron-based measurements were performed both before and after the adsorption processes. X-ray diffraction analyses revealed a highly selective phase transition from ZIF-71 to ZIF-72 when used as adsorbent in liquid phase adsorption processes. (Image 1. Right)

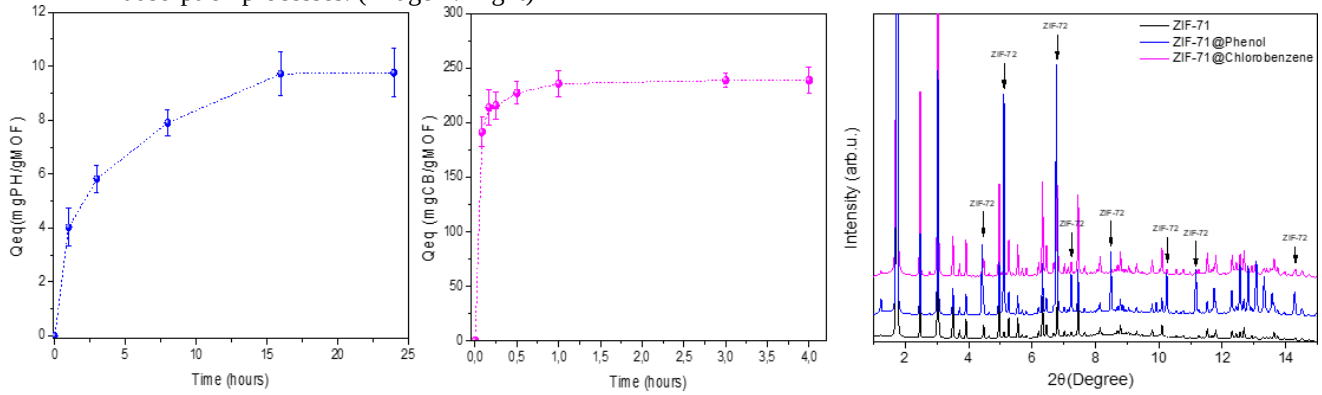

Image 1. Adsorption process kinetics for Phenol and Chlorobenzene solutions using ZIF-71 as an adsorbent (left). Synchrotron X-ray diffraction pattern of ZIF-71 at 300 K before and after adsorption process of both pollutants.

In order to study this phenomenon in greater depth, the same measurements were carried out but heating the material to 180 ºC, the evaporation temperature of the phenol. As illustrated in Image 2, there is a notable augmentation in the ZIF-72 phase post-heating, indicating an irreversible transition under these conditions.

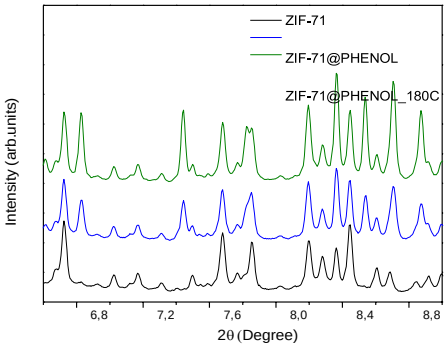

Image 2. Synchrotron X-ray diffraction pattern of ZIF-71@PHENOL at 300 K before and after heating treatment.

4. Conclusions - Structural changes or phase transitions in materials known as Zeolitic Imidazolate Frameworks (ZIFs) have been demonstrated in gas-phase adsorption processes over recent years. However, the present study has provided a new perspective by revealing that these materials exhibit similar behavior in liquid-phase adsorption processes. In particular, it has been observed that the ZIF-71 material undergoes a highly selective phase transition to ZIF-72 when employed as an adsorbent for various aromatic contaminants in the liquid phase.

5. References

[1] R.P. Lively, M.E. Dose, J.A. Thompson, B.A. McCool, R.R. Chance, W.J. Koros. Chem. Commun., 2011, 47, 8667–8669.
[2] M.E. Casco, Y.Q. Cheng, L.L. Daemen, D. Fairen-Jimenez, E.V. Ramos-Fernández, A.J. Ramirez-Cuesta, J. Silvestre-Albero. Chem. Commun., 2016, 52, 3639.
[3] J. Gandara-Loe, A. Missyul, F. Fauthe, L.L. Daemen, Y.Q. Cheng, A. Ramirez-Cuesta, P.I. Ravikovitch, J. Silvestre-Albero. J. Mater. Chem. A, 2019, 7, 14552-14558.

O9: New activated carbons produced from pine nut shells – their potential for drinking water treatment

E. Mesquita [(1)], M. Andrade [(2)], H. Costa [(2)], R. M. C. Viegas [(1)], A. P. Carvalho [(2)], A. S. Mestre [(2)], M. J. Rosa [(1)]

[(1)] Urban Water Unit, Hydraulics and Environment Department, LNEC - National Laboratory for Civil Engineering, Av. Brasil 101, 1700-066 Lisboa, Portugal
emesquita@lnec.pt
[(2)] Centro de Química Estrutural, Institute of Molecular Sciences, Faculdade de Ciências, Universidade de Lisboa, Campo Grande, 1749-016 Lisboa, Portugal mvandrade@ciencias.ulisboa.pt; fc49741@alunos.ciencias.ulisboa.pt; rviegas@lnec.pt; ana.carvalho@ciencias.ulisboa.pt; asmestre@ciencias.ulisboa.pt; mjrosa@lnec.pt

1. **Introduction** – Activated carbon (AC) adsorption is considered one of the best available technologies for removing organic micropollutants resistant to conventional drinking water treatment (DWT) processes, such as pharmaceutical compounds (PhCs), pesticides, perfluoroalkyl substances (PFAS), natural organic matter (NOM) oxidation byproducts produced during DWT and naturally occurring cyanotoxins or organic compounds that confer taste and odour to water. The efficacy of this technology largely depends on the adequate AC selection, ensuring that it has suitable physical, textural, and characteristics for adsorbing target contaminants and matching the physicochemical characteristics of the water to be treated [1].

This communication presents EMPOWER+ project results, in particular the application of the new pine nut shell (PNS) activated carbons in two different water treatment technologies: i) fine PAC, with particle size under 20 µm, for a DWT advanced technology combining adsorption and filtration through low-pressure membrane systems (microfiltration or ultrafiltration) and ii) granular activated carbon (GAC), as an adsorbent medium for point-of-use (PoU) potable water purification' devices.

The performance of the new ACs was compared with that of commercial AC, regarding their efficacy on the removal of i) a mixture of PhCs from different therapeutic classes with distinct physicochemical properties that condition their adsorption, namely, carbamazepine (CBZ), diclofenac (DCF) and sulfamethoxazole (SMX); ii) microcystin-LR (MC-LR), a cyanotoxin frequently detected in surface water bodies and whose control is mandatory under the EU drinking water directive [2]; iii) NOM, present in all surface water bodies, is the main precursor of undesirable disinfection byproducts produced in DWT plants and/or in the water distribution systems, moreover, NOM interferes with micropollutants' adsorption onto AC, mainly by pore blocking and/or competition for adsorption sites; iv) hypochlorite (commonly referred as free chlorine) is often used in DWT for water disinfection and to maintain the microbiological stability of water in distribution networks and, depending on its concentration, may confer taste to tap water.

2. Experimental – Adsorption tests were conducted with PNS-PAC and commercial PAC, in jar test equipment, using synthetic water (non-chlorinated tap water supplemented with tannic and salicylic acids, as NOM surrogates) or water samples from a DWT plant. These waters were spiked with known concentrations of CBZ, DCF and SMX or non-purified MC-LR (*Microcystis sp.* cell extract); the microcontaminants were quantified, after solid-phase extraction, by liquid chromatography (SPE/HPLC-DAD) and NOM was quantified as dissolved or total organic carbon (DOC or TOC), using a TOC analyzer (with persulphate- UV oxidation method) and by measuring water absorbance at 254 nm (A254).

NOM, MC-LR and chlorine removals from tap water by PNS-GAC and commercial GAC were evaluated and compared. Adsorption tests were carried out in batch conditions, for assessing NOM adsorption capacity at equilibrium, and through rapid small-scale column tests (RSSCT) to assess NOM and residual chlorine breakthrough curves. MC-LR removal by GAC filters was also evaluated after NOM breakthrough curve plateau has been reached. NOM and MC-LR were quantified as described above, and the standard N, N-diethyl-p-phenylenediamine (DPD) colorimetric method was used to quantify residual chlorine.

3. Results and Discussion - PhCs´ adsorption onto PNS-PAC followed the same trend observed in previous studies [1], with higher removals of CBZ (hydrophobic compound with neutral charge) and DCF (moderately hydrophobiccompound with negative overall charge) than SMX (hydrophilic and anionic compound). Their removal rates by PNS-PAC and by the benchmarked AC were similar, for 1 hour contact

time; and for 24 hours contact time, the new PACs surpassed the commercial PAC in SMX removal – rates of 70 - 78% where achieved (20 to 40 percentage points higher than the commercial carbon). This result is remarkable since SMX, due to its hydrophilicity, is typically less adsorbable than the other tested PhCs. The removal of NOM by the PNS-PAC was higher than that recorded with commercial PAC, for 24-hour contact time, particularly for aromatic organic matter, as suggested by A254 results. Regarding MC-LR, the tests with 30 mg/L PAC showed MC-LR removals of 40% and 90% for contact times of 0.5 h and 1 h, respectively (comparable to those obtained with the commercial PAC).

The results of the EMPOWER+ project are being modelled using mechanistic adsorption models, namely by the Homogeneous Surface Diffusion model (HSDM) and the Equivalent Background Compound model (EBCM), which will enable to estimate contaminant removal rates as a function of any PAC dose and contact time applied. On the other hand, these and other adsorption test results will be used to feed a predictive tool, already applied in previous studies, which will identify descriptors related to contaminant properties, activated carbon, and water matrix that best describe the adsorption mechanisms.

The PNS-GACs showed higher NOM removals than those obtained with the commercial GAC, in the batch adsorption tests. This was corroborated in RSSCT in which, despite presenting similar TOC and A254 breakthrough curves, the amount of TOC adsorbed per GAC unit mass was higher in PNS-GAC columns. Moreover, in NOM saturated columns PNS-GAC showed higher MC-LR removal capacity. Both PNS-GAC and commercial-GAC columns removed 100% of the residual chlorine from the inlet tap water over 100 bed volumes (BV), decreasing to 90% over another 200 BV. The RSSCT´s results will allow the up-scaling and the performance prediction of the PoU drinking water purification systems.

4. Conclusions - Pine nut shells (available in Portugal) allow the production of PAC or GAC with high performance in removing emerging contaminants and NOM from water. The results, obtained in tests conducted under conditions that allow modelling of real-scale applications, confirm the high potential of this biomass to produce high-performance activated carbons, applicable in different water treatment technologies (e.g., PAC/coagulation/flocculation/sedimentation and PAC/low-pressure membrane filtration) and in PoU systems for drinking water purification.

5. References

[1] Viegas, R.M.C., Mestre, A.S.; Mesquita, E.; Machuqueiro, M.; Andrade, M., Carvalho, A.P.; Rosa, M.J. (2022) “Key Factors for Activated Carbon Adsorption of Pharmaceutical Compounds from Wastewaters: A Multivariate Modelling Approach”. Water, 14(2), 166. https://doi.org/10.3390/w14020166.
[2] Directive (EU) 2020/2184 of the European Parliament and of the Council of 16 December 2020 on the quality of water intended for human consumption (recast) – The Drinking Water Directive (DWD).

Acknowledgments: Centro de Química Estrutural is a Research Unit funded by Fundação para a Ciência e a Tecnologia (FCT), through projects UIDB/00100/2020 (https://doi.org/10.54499/UIDB/00100/2020) and UIDP/00100/2020 (https://doi.org/10.54499/UIDP/00100/2020). Institute of Molecular Sciences is an Associate Laboratory funded by FCT through project LA/P/0056/2020 (https://doi.org/10.54499/LA/P/0056/2020). Authors thank FCT financial support to EMPOWER+ Project(PTDC/EQU-EQU/6024/2020, DOI 10.54499/PTDC/EQU-EQU/6024/2020). Ana S. Mestre and Marta A. Andrade thank FCT for, respectively, the Assistant Researcher contract CEECIND/01371/2017 (DOI 10.54499/CEECIND/01371/2017/CP1387/CT0013) and the Junior Research contract in the EMPOWER+project. The authors acknowledge Salmon & Cia and Chemviron for donating commercial activated carbonsamples, respectively, Norit SA UF and F400. Grupo Cecilio is acknowledge for providing the biomass (pine nut shell) for new activated carbons preparation.

O10: Analysing the role of nanopore confinement on the regeneration of exhausted carbons

Florian Olivier[(1,2)], Sebastien Schaefer[(2)], Isabelle Laidin[(3)], Benoit Cagnon[(2)], Conchi Ania[(1)]*

[(1)] *CEMHTI (UPR 3079) CNRS, Université d'Orléans, 45071 Orléans, France.*
[(2)] *ICMN (UMR 7374) CNRS, Université d'Orléans, 45071 Orléans, France.*
[(3)] *Jacobi Carbons, Vierzon, France.*

* *conchi.ania@cnrs-orleans.fr*

1. Introduction – Despite adsorption on activated carbons (ACs) is a mature technology for the removal of emerging pollutants, the cost associated to the carbon regeneration still represents a major limitation and the regeneration cycle is essential from the points of view of environmental and economic sustainability [1]. Hence, the reactivation of saturated activated carbons is a crucial aspect in the upgrading and restructuring of existing water and wastewater treatment plants. In this context, the objective of this study is to investigate the regeneration of exhausted commercial ACs currently used in different industrial facilities, emphasizing on the impact of the regeneration conditions after several adsorption/regeneration cycles in the porosity and uptake capacity of the regenerated carbons. Conventional thermal regeneration and novel methodologies based on advanced oxidation processes using radical species have been applied for the regeneration of the spent carbons [2-4]. Two case studies of spent activated carbons from a wastewater treatment plant in Spain, and the regeneration factory of Jacobi Carbons in France will be discussed in terms of the quality of the regenerated carbons.

2. Results and Discussion – A detailed study of the textural properties and surface chemistry of saturated ACs has been carried out after different cycles of regeneration in order to understand the mechanisms associated with this process. The results obtained allow identifying the main parameters of the carbon adsorbents controlling the efficiency of the regeneration. For the thermal-induced regeneration process, the desorption mechanism seemed to be governed by the average nanopore size, with higher desorption energies in pores below 1.3 nm (Figure 1). The desorption rate decreased for pores above 1 nm, pointing out the importance of the confinement state of the adsorbed phase (i.e., more disordered state in large pores). For the radical-assisted regeneration, ozonation and photochemical irradiation have been applied to carbons with varied saturation degree. Data has shown that the efficiency of the reactivation process depends on the saturation state of the carbon and the density of radical species formed.

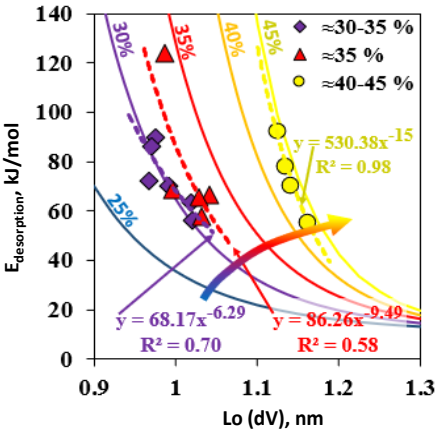

Figure 1. Correlation between the average micropore size of the carbons and the activation energy for desorption.

3. Conclusions - A detailed analysis of the textural properties and surface chemistry of saturated carbons has showed that medium-sized micropores govern the adsorption and thermal-assisted regeneration mechanism. A partial regeneration -maintained over several cycles- is obtained upon thermal treatment of non-functionalized carbons at moderate temperature. For radical-assisted regeneration, efficiencies between 50-80% were obtained at varied operating conditions. The presence of water coadsorbed in the porosity of the carbons is important to guarantee the activation and diffusion of the radical species.

Funding Acknowledgements: H2020 (Project Ô, 776816); region Centre Val de Loire (ARD-MATEX).

4. References

[1] Roskill Report. Activated Carbon, Global Industry, Markets and Outlook, 2017.
[2] E. Caliskan, J.M. Bermudez, J.B. Parra, J.A. Menéndez, M. Mahramanlioglu, C.O. Ania, J. Environ. Manag., **102** (2012) p. 134.
[3] L.F. Velasco, R.J. Carmona, J. Matos, C.O. Ania, Carbon **73** (2014) p. 206.
[4] C. Macias, C.O. Ania. BET 23P4307 EMO/SF n° 23306872.5 (patent application 2023).

O11: Physical Characterization of Porous Carbons for Gas Storage and Separation Applications

N. Prieto [(1)], O. Maulik [(2)], K. Struckhoff [(3)]

[(1)] *Anton Paar Quantatec, Boynton Beach, FL USA, nathalia.prieto@anton-paar.com*
[(2)] *Anton Paar, Graz, Austria, ornov.maulik@anton-paar.com*
[(3)] *Anton Paar Quantatec, Boynton Beach, FL USA, katie.struckhoff@anton-paar.com*

1. Introduction – Porous carbon-based materials have become one of the most popular solutions to address hydrogen storage and carbon capture and storage due to their abundance in the universe. Carbons that have undergone thermal treatments along with solvent impregnation produce desirable nanoporous carbons with high surface area and, ultimately, these surfaces and pores allow for excellent performance of the material in these storage and separation applications. In order to structurally characterize nanoporous carbons and to further correlate those structural properties with performance, low pressure gas sorption (N_2 (77 K) and CO_2 (273 K)) can be utilized to determine material properties including surface area, pore size distribution, and pore volume. In addition to the evaluation of these properties, it is significantly important to characterize directly the performance properties of a material by performing measurements at the temperature and pressure of the application.

In this work, a diverse variety of nanoporous carbons synthesized in different ways were characterized using low pressure gas sorption, both N_2 (77 K) and CO_2 (273 K), coupled with state-of-the-art quenched solid density functional theory (QSDFT) for pore size and volume analysis. Further evaluation was done at high pressure and higher, real operation temperature conditions using gases including carbon dioxide, hydrogen, and ammonia. These data provide performance insight such as adsorption capacity, adsorption kinetics, and even provide cycle stability of the materials.

2. Experimental – Low pressure gas sorption experiments were performed using either an Anton Paar Nova 800 or an Autosorb 6100 instrument, depending on the experiment. High pressure gas sorption data was measured on the Anton Paar iSorb HP. Prior to the measurements, samples were degassed at 573 K (or lower) overnight under turbomolecular pump vacuum.

3. Results and Discussion – As an example, two base activated carbons, one by KOH and one by NaOH, were characterized with nitrogen and carbon dioxide adsorption. Coupling these gases allows one to assess narrow micropores in the material down to as small as 0.35 nm. The DFT pore size distributions from the two individual isotherms were merged to generate the complete nanopore size distribution in one curve (Image 1).

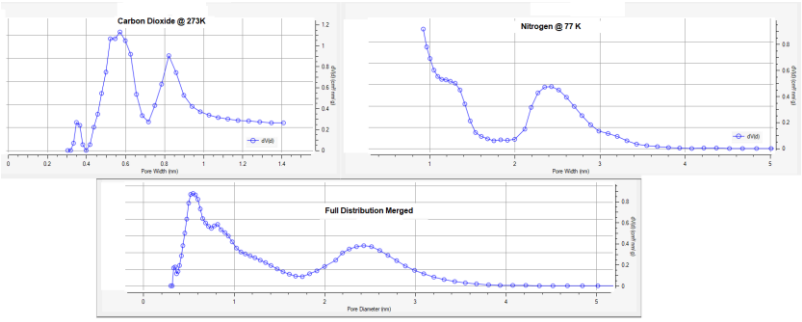

Image 1.

The high pressure H_2 adsorption isotherms of the same two base activated carbons were measured at two different temperatures, 77 K and 298 K. The surface excess hydrogen isotherms are shown in Image 2. One can clearly see the adsorption at cryogenic temperature far exceeds the room temperature adsorption. In addition, regardless of activation conditions or differences in the low pressure data, the adsorption capacity for the two samples is in agreement for both samples at both temperatures.

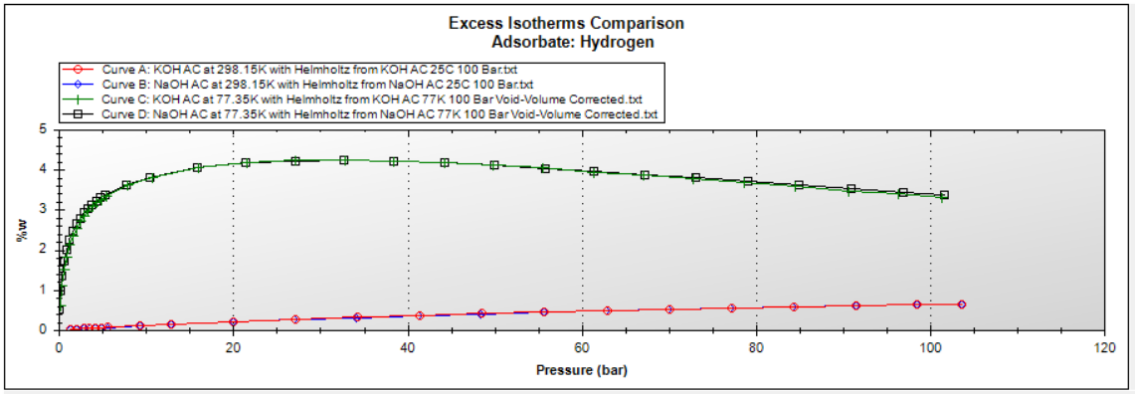

Image 2.

4. Conclusions – Gas sorption, both low and high pressure, is a crucial tool for characterizing nanoporous carbons. A full micro- and mesopore size distribution was generated by merging the DFT pore size distributions from N_2 (77 K) and CO_2 (273 K). The hydrogen storage capacity was measured to 100 bar at 77 K and 298 K and clearly shows the differences in uptake capacity depending on the temperature. This information can be used to guide applications in gas storage and separations.

O12: Revealing the potential of poly(heptazine imides)-based adsorbents for CO_2 capture

P. Ouro [1,2], I. Krivtsov [2], M. Sardo [1], L. Mafra, [1] M. Ilkaeva [2]

[1] *CICECO - Aveiro Institute of Materials, University of Aveiro, 3810-193, Aveiro, Portugal*
pedrooouro@ua.pt
[2] *UNIOVI - Department of* Chemical and Environmental Engineering, *University of Oviedo, 33006, Oviedo, Spain*
ilkaevamarina@uniovi.es

1. **Introduction -** A promising new class of polymeric carbon nitrides (PCNs), the poly(heptazine imides) (PHIs), has emerged as a potential candidate for CO_2 adsorption due to its cost-effectiveness, stability at temperatures up to 450 ºC, and moisture-resistance (*e.g.*, not observed in MOFs, leading to structural collapse). PHIs present a facile and rapid synthesis, via molten-salt approach, a microporous structure, and show a high CO_2 adsorption capacity (~ 4 mmol/g), according to preliminary results. However, the semi- crystalline nature of these materials has made it challenging to establish the mechanisms of CO_2 uptake, unclear to this date. In this work, an in-depth study of PHIs for application in CO_2 adsorption is showcased. Solid-state nuclear magnetic resonance (ssNMR) helped characterizing the structure and adsorption mechanism (unveiling interactions between the framework and ^{13}C-enriched CO_2, at an atomic-level), leading to a clear understanding of PHIs and consequentially the potential for fine tuning towards CO_2 adsorption.

2. **Experimental -** PHIs were synthesized through a rapid and tuneable molten-salt approach, using low-cost precursors and a salt, as presented in **Image 1.**

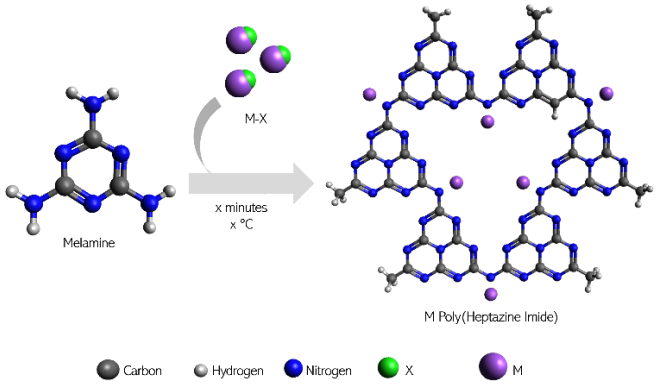

Image 1. Synthetic pathway of PHIs

By varying the precursor's concentration, and temperature setup, control over crystallinity and textural properties (surface area, porous structure, etc.) were achieved.

3. Results and Discussion - The obtained results show (i) an increase in crystallinity when comparing PHIs to traditional PCNs, (ii) an increase in CO_2 adsorption capacity with an increase in dwell time under certain temperatures during synthesis, (iii) higher CO_2 adsorption than any other PHIs reported for the purpose of CO_2 capture (as per our knowledge), (iv) high selectivity for CO_2 in binary gas mixtures (CO_2/N_2), and (v) an adsorption mechanism comprised of physisorption, with mostly solid-like physisorbed CO_2 species.

4. Conclusions - The main conclusions of the work and its most relevant contributions consist of unveiling of the most accurate CO_2 adsorption mechanism for this material up to date, the establishment of a direct link between crystallinity and CO_2 adsorption capacity, which can be easily tuned during the synthesis, and the highest CO_2 adsorption capacity registered for PHIs to date.

5. Acknowledgements - This work was developed within the scope of the project CICECO-Aveiro Institute of Materials, UIDB/50011/2020 DOI: 10.54499/UIDB/50011/2020), UIDP/50011/2020 (DOI:10.54499/UIDP/50011/2020) & LA/P/0006/2020 (DOI: 10.54499/LA/P/0006/2020), financed from national funds through the FCT/MCTES (PIDDAC). The NMR spectrometers are part of the National NMR Network (PTNMR) and are partially supported by Infrastructure Project 022161 (cofinanced by FEDER

through COMPETE 2020, POCI and PORL and FCT through PIDDAC). This work has received funding from the European Research Council (ERC) under the European Union's Horizon 2020 research and innovation program (grant agreement 865974).

O13: Adsorption of carbon dioxide, water and hydrogen in lithium alkoxide functionalized Cu-BTC metal-organic frameworks

K. Wortelboer [1,2,3], V. Menkovski [2,3], J. M. Vicent-Luna [1], S. Calero [1]

[1] *Materials Simulation and Modelling, Department of Applied Physics and Science Education, Eindhoven University of Technology, PO Box 513, 5600MB Eindhoven, The Netherlands.*
[2] *Data and AI cluster, Eindhoven University of Technology*
[3] *Eindhoven Artificial Intelligence Systems Institute, Eindhoven University of Technology*
k.a.wortelboer1@tue.nl, v.menkovski@tue.nl, j.vicent.luna@tue.nl, s.calero@tue.nl

1. Introduction - Metal-organic frameworks (MOFs) are promising materials for adsorption, catalysis and storage. Different choices of clusters and linkers make for a wide variety of MOFs with different properties. Functional groups of different nature can be included to modify the material's surface. For example, CO_2 adsorption in the Cu-BTC MOF improves when lithium is added to the material [1,2]. Here, we study how the concentration and specific distribution of lithium-alkoxide (OLi) functional groups in Cu-BTC affect adsorption of CO_2, H_2 and H_2O.

2. Experimental - The model of Cu-BTC is functionalized by replacing hydrogen atoms on the BTC linkers with OLi groups. The atomic positions can be selected with various algorithms, such as randomly or clustered together, to obtain different frameworks with wide variety in configurations (see Figure 1). The functionalized structures are relaxed with the M3GNet [3] machine learned force field. Furthermore, the structure is copied and its atoms slightly perturbed before relaxation to create multiple relaxed versions of a framework. We performed Monte Carlo simulations to obtain the adsorption properties of CO_2, H_2, and H_2O in all the relaxed versions using RASPA software [4]. The different relaxations lead to a distribution in the heat of adsorption for each framework and molecule.

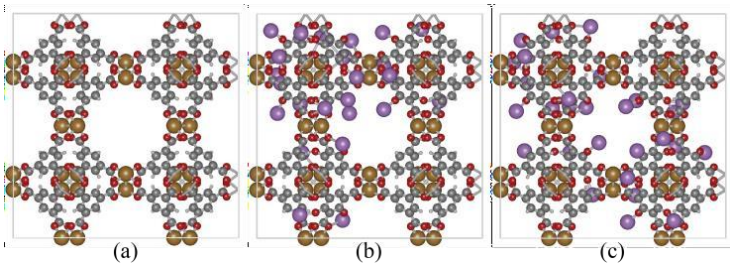

Figure 1. **a)** Single unit cell of pristine Cu-BTC **b)** Cu-BTC functionalized with OLi groups clustered together **c)** OLi at random atomic positions

3. Results and Discussion – We created 120 frameworks with different numbers of OLi groups. Each framework has 50 relaxed versions, starting from different perturbed atom positions. As expected, CO_2 and H_2O heats of adsorption increase with the number of OLi groups. However, there is a significant spread in mean heat of adsorption between frameworks with equal number of OLi groups, especially for H_2O (see Figure 2). For H_2, being generally non-reactive, the effect of the added groups is minima

4. Conclusions – We found that the heats of adsorption for CO_2 and H_2O in Cu-BTC increase when the framework is functionalized with lithium-alkoxide, while the heat of adsorption for H_2 is almost unaffected. Our results show that not only the number of OLi groups, but also their distribution within the framework affect the heat of adsorption. These findings can help designing novel adsorbents with improved features.

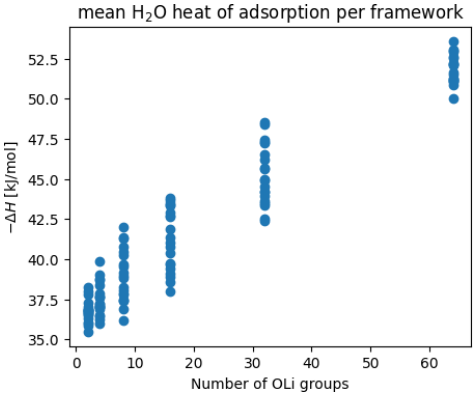

Figure 2. Heat of adsorption for H2O in Cu-BTC with lithium- alkoxide functional groups. Each data point represents the mean of 50 different relaxed versions of a framework with the OLi groups at unique atomic positions.

5. References

[1] L. Zhou, Z. Niu, X. Jin, L. Tang, L. Zhu, ChemistrySelect. 3, 12865–12870 (2018).
[2] J. Hu, J. Liu, Y. Liu, X. Yang, J. Phys. Chem. C. 120, 10311–10319 (2016).
[3] C. Chen, S. P. Ong, Nat Comput Sci. 2, 718–728 (2022).
[4] D. Dubbeldam, S. Calero, D. E. Ellis, R. Q. Snurr, Molecular Simulation. 42, 81–101 (2016).

O14: Structural modifications of pure silica MEL zeolite studied by in situ X-Ray diffraction during adsorption of propane

Alberto Barros, Silvia Martí, Miguel Palomino, Susana Valencia, Fernando Rey

Instituto de Tecnología Química, Universitat Politècnica de València – Consejo Superior de Investigaciones Científicas (UPV-CSIC), 46022 Valencia (Spain).
frey@itq.upv.es
abarpar@itq.upv.es, silvimaarti@gmail.com, miparo@itq.upv.es, svalenci@itq.upv.es

1. Introduction – Structural deformations of zeolites during adsorption processes have been reported previously for MFI [1], RHO [2] and many AlPO-zeotypes [3,4] among others. These structural modifications generally imply an increment of the adsorption capacity above certain pressure, evidenced by the presence of sharp increments in the adsorption isotherm profiles. This is accompanied by the appearance/disappearance of X-Ray diffraction (XRD) peaks indicating the occurrence of the phase transition without changes in the atomic connectivity (i.e. symmetry change). Additionally, it has been found that this phase transition does not depend solely on the gas pressure, but also on the nature of the adsorbate. For instance, CO_2 when adsorbed on a zeolite RHO of Si/Al ratio close to 5 induces a phase transition at a pressure around 2 bar, while CH_4 does not. This peculiarity provides of very high CO_2/CH_4 selectivity to zeolite RHO for this relevant gas separation [2].
The Ar adsorption isotherm of pure silica ZSM-11 (MEL structure) shows an abrupt increase at 0.002 P/P_0. Molecular simulation studies have attributed this sharp step in the isotherm to structural modifications of the tetragonal symmetry of MEL structure [5].
In this work, we have studied the structural modifications of the pure silica ZSM-11 zeolite upon adsorption of propane by in-situ X-Ray diffraction techniques compared to its adsorption isotherm.

2. Experimental – Synthesis of pure silica ZSM-11 zeolite was carried out following methods reported previously [6]. The calcined material was outgassed at 400ºC under high vacuum for 12 hours prior to any adsorption measurement. The Ar adsorption isotherms were measured at 77, 87, 92 and 97 K in an ASAP-2020 (from Micromeritics) equipped with a Cryotune attachment (from 3P analytics) that allows an accurate control of the temperature between 77 to 300 K. The propane adsorption isotherm on pure silica ZSM-11 sample was measured using a BELSORP Max-II instrument at 298 K. The pure-silica ZSM-11 sample was calcined in situ under inert atmosphere at 873 K for 8 h and subsequently cooled down at 303 K in an Anton-Paar XRK-900 reaction chamber attached to an Empyrean X-Ray diffractometer. Then, mixtures of propane/helium at different proportions were fluxed through the sample while X-Ray diffractions patterns were collected for four eight hours each. The X-Ray diffraction patterns obtained at the same partial pressure were carefully examined and those that are identical were added (assuming that equilibrium was reached), while those that showed dissimilarities were discarded.

3. Results and Discussion – The Ar adsorption isotherms collected at different temperatures are shown in Figure 1. There, it is observed that the pure-silica MEL zeolite shows a very sharp step in the isotherms, being this step shifted to higher pressures as the temperature increases. When these isotherms are plotted versus partial pressure of propane, the abrupt adsorption step appear at the same P/P_0 values in all isotherms.

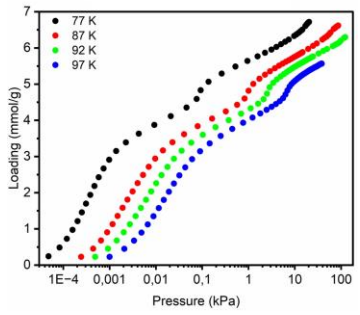

Figure 1: Ar adsorption isotherms on pure-silica ZSM-11 at different temperatures

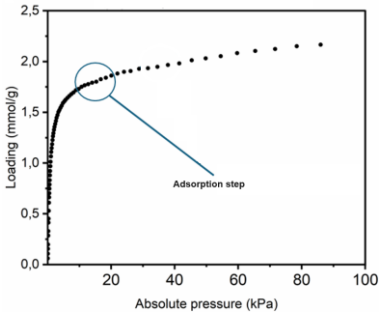

Figure 2: Propane adsorption isotherm at 298 K on pure silica ZSM-11.

Attempts to fit the Ar isotherms by applying different models were unsuccessful and thus, the heat of adsorption in the whole range of loading were not calculated.
The heat of adsorption at propane loading below the abrupt step of the isotherms (i.e. below 3 mmol/g) gives a value of approximately 12 kJ/mol, which is of the order of values reported in literature for Ar adsorbed on non-polar surfaces.
The propane adsorption isotherm on pure silica ZSM-11 at 298 K is shown in Figure 2, where a subtle step is observed at 20 kPa of pressure. The step also precludes the fitting of the experimental isotherm by

applying Langmuir based models (Toth, Dual Site, etc). The presence of this step may indicate that a phase transformation takes place at 20 kPa of pressure of propane in pure silica ZSM-11, as was suggested to occur with Ar.

Thus, we performed an in-situ structural study by submitting the sample to different partial pressures of propane in He while recording the XRD patterns. All patterns of the pure silica ZSM-11 recorded at different propane pressures can be indexed in the same tetragonal symmetry. However, the unit cell volume increases with the propane loading as it is shown in Figure 3. Thus, these results indicate that there is no phase transition as occurs in other zeolites, such as MFI or RHO. However, the unit cell expansion is not linear with the propane uptake and there is an inflection point in the expansion curve at approximately 1.8 mmol/g of adsorbed propane on ZSM-11, which approximately corresponds to the sharp step observed in the adsorption isotherm of propane.

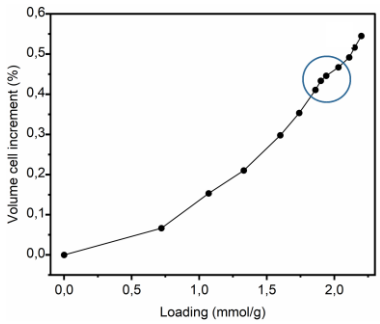

Figure 3: Variation of the tetragonal unit cell volume of MEL structure with the propane loading.

Consequently, the increase observed in the propane uptake at 20 kPa must be attributed to an abrupt expansion of the tetragonal unit cell rather than to a phase transition, since there is no symmetry change along the whole range of propane pressure studied here.

5. References

[1] E. García-Pérez, J.B. Parra, C.O. Ania, D. Dubbeldam, T.J.H. Vlugt, J.M. Castillo, P.J. Merkling, S. Calero, *J. Phys. Chem. C*, **112**, (2008) p. 9976.
[2] M. Palomino, A. Corma, J.L. Jordá, F. Rey, S. Valencia, *Chem. Commun*., **48**, (2012) p. 215.
[3] A. Krajnc, J. Varlec, M. Mazaj, A. Ristic, N. Zabukovec Logar, G. Mali, *Adv. Energy Mater*., **7**, (2017) 1601815.
[4] J. Varlec, A. Krajnc, M. Mazaj, A. Ristic, K. Vanatalu, A. Oss, A. Samoson, V. Kaucic, G. Mali, *New J. Chem*., **40**, (2016) p. 4178.
[5] V. Sánchez-Gil, E.G. Noya, J.M. Guil, E. Lomba, S. Valencia, I. da Silva, L. Pusztai, L. Temleitner, *J. Phys. Chem. C*, **120**, (2016) p. 2260.
[6] O. Terasaki, T. Ohsuna, H. Sakuma, D. Watanabe, Y. Nakagawa, R.C. Medrud, *Chem. Mater*., **8**, (1996) p. 463.

O15: Ferromagnetic metal organic framework (MOF)/alginate hybrid beads for induction heating enabled atmospheric water harvesting

R. Sharma [(1)], G. Saab, M. Schoukens, T.R.C. Van Assche, J.F.M. Denayer

[(1)] Department of Chemical Engineering, Vrije Universiteit Brussel, B-1050 Belgium.
Ravi.Sharma@vub.be

With global concern over **freshwater scarcity** escalating and traditional water supply methods like desalination, facing challenges due to high costs and energy consumption, researchers have diverted their attention to non-traditional water resources such as **atmospheric water vapor**. Earth's atmosphere holds ~ 10 % of freshwater in the form of vapor or droplets, which could address global water issues[1].

Various methods, including cooling air below dew point temperature, using desiccants, and employing porous materials like silica gel, zeolites, pristine MOFs, and MOFs impregnated with hygroscopic salts have been proposed for **atmospheric water harvesting (AWH)**[2]. Among MOFs, sorbents like MOF-801-P, MOF-841, MOF-808, MOF-303 have exhibited promising performance[3]. However significant challenges persist, particularly in achieving structural forms and efficient water recovery methods[4]. Hybrid structures, like hydrogel-MOF composites, offer a potential solution, with recent innovations including the incorporation of LiCl into polyacrylamide hydrogel and the use of sunlight as a means of efficient energy for water release technology[5,6]. However, despite the proven feasibility, low productivity remains a long-standing challenge for **solar-driven AWH devices**[7].

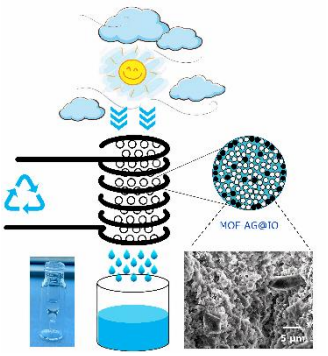

Graphical Abstract

In addressing these challenges, this work introduces a novel hybrid ferromagnetic MOF-alginate composite (**MOF-AG@IO**) beads for atmospheric water harvesting. Synthesized instantaneously at room temperature via **ionic gel polymerization technique**, the composite beads (MOF-AG@IO) were comprised of a hydrophilic hydrogel network embedded with hydrophilic substances i.e., MOF-808 and $CaCl_2$, and iron oxide (Fe_3O_4), as magnetic susceptor. SEM-EDX and XRD analysis confirmed the successful incorporation of MOF-808 crystals in the hydrogel together with $CaCl_2$ and Fe_3O_4 particles. The composite beads exhibited **high water** capturing **capacity** from the atmosphere i.e., **~1.02 $gH_2O/g_{MOF\text{-}AG@IO}$**, 75 % RH, 25 °C and, owing to Fe_3O_4 presence, **quick water releasing** capability (**~ 85 % water release within the first 30 min.**) when exposed to magnetic induction, a technology not limited by the natural day-light cycle. Furthermore, it displayed outstanding cyclic stability, enduring up to 10 consecutive cycles. These remarkable performance characteristics translated into an **excellent potential water productivity** of up to 9.11 $LH_2O/kg_{MOF\text{-}AG@IO}$/day at 75 %RH, 25 °C and 10.3 $LH_2O/ kg_{MOF\text{-}AG@IO}$/day in outside conditions (open-air environment, VUB campus, Etterbeek).

Overall, this work presents a new conceptual advance of hybrid composite materials which takes advantage of its constituent properties. The rapid and uniform heating provided by induction heating, a technology not constrained by natural sunlight, positions these findings as an important platform for **next-generation electrified water harvesting technologies**.

References

1. UN Water & UNESCO. UN Water (2022).
2. Kandeal, A. W. et al. Sustain. Energy Technol. Assessments 52, 102000 (2022).
3. Furukawa, H. et al. J. Am. Chem. Soc. 136, 4369–4381 (2014).
4. Babaei, H. et al. Nat. Commun. 2020 111 11, 1–8 (2020).
5. Kim, H. et al. Science (80-.). 356, 430–434 (2017).
6. Fathieh, F. et al. Sci. Adv. 4, (2018).
7. Li, T. et al. Nat. Commun. 2022 131 13, 1–11 (2022).

RIA 43
XLIII Reunião Ibérica de Adsorção
Porto, Portugal
1-4 September 2024

O16: Scaling-up PILC production for CO_2 capture applications

T. Frade[(1)], M.M.G. Jesus, A. Al Mohtar[(1)], M.L. Pinto [(1,*)]

[(1)] *CERENA, Departamento de Engenharia Química, Instituto Superior Técnico, Universidade de Lisboa, Campus Alameda, 1049-001, Lisboa, Portugal.*
moises.pinto@tecnico.ulisboa.pt

1. Introduction – In the efforts for a future complete decarbonization of the industry, the removal of carbon dioxide from flue gases originated from stationary sources plays an important role. Some possible technologies for such removal are processes based on adsorption with the use solid absorbent materials, which need to have the appropriate properties for such application. Recently, we demonstrated that pillared clays (PILCs) are interesting materials for CO_2 removal from flue gases produced by cement plants with estimated low separation costs [1]. However, for a future industrial implementation of such process, a large amount of PILCs needs to be produced. In the present contribution, we will summarize our recent work on the optimization and scale-up of the PILCs production. Two main aspects were considered for the optimization: minimization of water used and the decrease in the preparation time during the washing step.

2. Experimental – The stating point for the synthesis optimization was inspired on previously established synthesis procedures [2,3]. Briefly, the stating clay is a natural clay supplied by Sibelco (Portaclay A90). A solution of $ZrOCl_2$ 0.1M was used has source of the oligomeric species to intercalate. This solution was added slowly to a stirred suspension of clay (10 to 40 g/L) with a ratio of 25 mL Zr solution per gram of clay. After ageing, the solid content was increased in some cases by centrifugation and washed in dialysis tubes until the target conductivity was achieved. After that, a further increase in the solid content was required in some cases to obtain a tick paste that could be extruded and calcined at 350ºC. The final obtained calcined extrudates were after characterized and the adsorption properties for pure gases and mixtures studied.

3. Results and Discussion -

Table 1 summarizes the conditions for the different optimization trials done for the production optimization. The batch 1 and 5 were produced in pilot scale reactors of 30 and 50 L respectively.

Table 1. Conditions used in the preparation of the different batches of PILCs.

	Batch Number					
Synthesis Conditions	1	2	3.1	3.2	4	5
Intercalation –water/clay ratio (L water/kg clay)	100	100	100		50	25
Centrifugation before dialysis	Yes	Yes	Yes		No	No
Dialysis – clay/water ratio inside the tubes (g clay/L water)	≈10 g clay/L water	Dry clay paste	≈30 g clay/L water		≈20 g clay/L water	≈40 g clay/L water
Dialysis – Final conductivity (µS/cm)	1000	1000	1000	10	1000	1000
Drying after dialysis	No	No	Yes	Yes	Yes	No

In all cases, except in batch 2, we were able to produce PILCs with surface areas and porous volumes close to those obtained and reported previously [2,3]. The most important parameters for the assessment of these materials are the adsorption properties. As can be observed in the Figure 1, the results demonstrate that a high selectivity for CO_2 over N_2 and O_2 is obtained. In the case of batch produced with more concentrated suspension (batch 5), the conditions are already very interesting for production at large scale since a four times water reduction was achieved and a tick paste can be obtained immediately after the dialysis to be directly extruded in pellets.

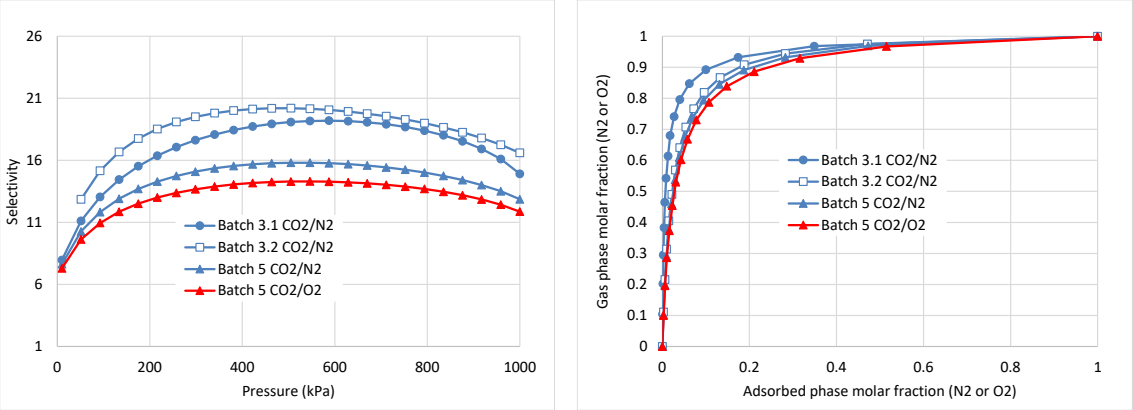

Figure 1. Selectivity for the separation of CO_2 from N_2 or O_2 (left) and *xy* phase diagrams of the adsorption of CO_2/N_2 or CO_2/O_2 mixtures at 500 kPa.

The breakthrough curves obtained with CO_2/N_2 mixtures confirmed the selectivity of the mixture for the separation of CO_2. The presence of moisture in the mixture was also studied and results indicate that although a small reduction on the capacity is noticed, the selectivity is maintained.

4. Conclusions – The results demonstrate that PILCs can be produced in batch pilot reactors with the appropriate adsorption properties for future applications in CO_2 capture from flue gases. Moreover, since the PILCs are produced from natural clays trough water-based processes at ambient pressure and relatively low temperatures, they present a cost effective and environmentally friendly alternative to be used the large scale adsorption processes.

5. References

[1] J. Tingelinhas, C. Saragoça, A. Al Mohtar, M. Mateus and M. L. Pinto, Pillared Clays as Cost-Effective Adsorbents for Carbon Capture by Pressure Swing Adsorption Processes in the Cement Industry. *Ind. Eng. Chem. Res.* **62** (2023), p 5613–5623.
[2] P. R. Pereira, J. Pires, M. Brotas De Carvalho, Zirconium pillared clays for carbon dioxide/methane separation. 1. Preparation of adsorbent materials and pure gas adsorption. Langmuir **14** (1998), 4584–4588.
[3] D. Jerónimo, J.M. Guil, B.M. Corbella, H. Vasques, A. Miranda, J.M. Silva, A. Lobato, J. Pires, A.P. Carvalho Acidity characterization of pillared clays through microcalorimetric measurements and catalytic ethylbenzene test reaction. Appl. Catal. A Gen. **330** (2007), 89–95.

RIA 43
XLIII Reunião Ibérica de Adsorção
Porto, Portugal
1-4 September 2024

O17: Exploring metal biosorption onto non-living algae: truth and myths

H. Passos [(1)(2)], A.R.F. Carreira[(3)], J.A.P. Coutinho[(3)]

[(1)]LSRE-LCM – Laboratory of Separation and Reaction Engineering – Laboratory of Catalysis and Materials, Faculty of Engineering, University of Porto, Porto, Portugal
[(2)]ALiCE – Associate Laboratory in Chemical Engineering, Faculty of Engineering, University of Porto, Porto, Portugal.
hpassos@fe.up.pt
[(3)]CICECO - Aveiro Institute of Materials, Department of Chemistry, University of Aveiro, 3810-193 Aveiro, Portugal
ritafutre@ua.pt; jcoutinho@ua.pt

1. Introduction

Metal overexploitation is likely to cause metal depletion, resulting in industrial supply and demand limitations and subsequent price inflation. Exploring secondary metal sources such as wastewaters, electrical and electronic waste and acid mine drainage waters as alternative metal-rich sources may help to overcome this issue. Aqueous secondary metal sources may contain low metal concentrations, requiring a pre-concentration step. Bioremediation is a naturally occurring process that can be used to pre-concentrate metals present in effluents. Among the available sorbents, algae are deemed as an effective, cheap and biocompatible metal sorbent. Despite their popularity, there is a shortage of studies directly comparing the efficiency of macroalgae, microalgae and blue-green algae (cyanobacteria), especially in multi-metallic systems.

2. Results and Discussion

Herein, the sorption capacity of eleven varieties of cyanobacteria, macroalgae and microalgae was evaluated in multi-elemental solutions of Co^{2+}, Cu^{2+}, Ni^{2+} and Zn^{2+} to find the most promising bio-concentrators. The elemental composition of the evaluated biomass was correlated with sorption capacity. Biomass samples containing higher carbon, nitrogen and hydrogen percents display less sorption capacity.[1] Higher oxygen percents did not translate into better sorption capacity values, regardless of the importance of oxygenated groups for metal sorption. The role of Ca^{2+} and K^{+} ion-exchange in metal sorption was also determined. The most promising biomasses release higher amounts of Ca^{2+} and K^{+} to the aqueous media than less effective sorbents. From the initial screening, the best cyanobacteria, macro- and microalgae were selected to conduct process optimization. Parameters such as pH, initial metal concentration, the metal counterion and the sorption kinetics were evaluated.[2] All biomass showed better metal sorption capacity values at pH 5. The optimal metal concentration depends on the binding sites availability of each biomass. Regardless of the optimal metal concentration, metal sorption in mono-elemental assays is better than in multi-elemental assays. Sargassum sp. showed the best sorption capacity throughout the study. As a result, this brown macroalga was selected for kinetic studies. Metal sorption reached equilibrium after 360 min. Langmuir and Freundlich's models were applied to the kinetic data to understand the underlying sorption mechanisms better. Langmuir presented a better fit to the experimental data, indicating that sorption occurred through chemisorption. Once again, ion-exchange played an important role in metal sorption. Algae incineration allowed to pre-concentrate metals by 4639-fold when compared to the initial aqueous solution concentration. As a proof of concept, Sargassum sp. was applied to acid mine drainage (AMD) at its original pH (2), pH 4 and pH 5.[3] The biomass-to-algae was tailored based on the optimization studies in synthetic multi-metallic solutions. Despite being a promising metal pre-concentrator in synthetic solutions, Sargassum sp. sorption capacity in AMD was underwhelming. The existing gaps in this field are discussed, including algae cultivation, water decontamination emphasis in detriment to metal recovery and cost performance of algae as opposed to commercial and waste-based metal sorbents.

4. Conclusions - This study highlights the potential of algae as effective biosorbents for metal pre-concentration from wastewaters. However, despite promising results, the application in real-world scenarios revealed limitations, underscoring the need for further research. Addressing these gaps, including optimization of algal cultivation and cost-performance analysis, is crucial for advancing algae-based bioremediation technologies for sustainable metal recovery.

This work was supported by national funds through FCT/MCTES (PIDDAC): LSRE-LCM, UIDB/50020/2020 (DOI: 10.54499/UIDB/50020/2020) and UIDP/50020/2020 (DOI: 10.54499/UIDP/50020/2020); ALiCE, LA/P/0045/2020 (DOI: 10.54499/LA/P/0045/2020); CICECO, UIDB/50011/2020, UIDP/50011/2020 & LA/P/0006/2020.

5. References

[1] A.R.F. Carreira, T. Veloso, I.P.E. Macário, J.L. Pereira, S.P.M. Ventura, H. Passos, J.A.P. Coutinho, *Chemosphere* **314** (2023) 137675.
[2] A.R.F. Carreira, N. Schaeffer, H. Passos, J.A.P. Coutinho, *Chem. Eng. Res. Des.* **192** (2023) 546–555.
[3] A.R.F. Carreira, H. Passos, J.A.P. Coutinho, *Green Chem.* **25** (2023) 5775-5788.

O18: Electrified Temperature Vacuum Swing Adsorption post combustion carbon capture, a cyclic simulation study

M. Gholami, M. Schoukens, T. Van Assche, J. F.M. Denayer

(1) *Department of Chemical Engineering, Vrije Universiteit Brussel, 1050 Brussels, Belgium.*
Mohsen.Gholami@VUB.be
Matthias.Schoukens@vub.be, Tom.Van.Assche@vub.be, Joeri.Denayer@vub.be

1. Introduction – Electrification of adsorbent thermal regeneration for the purpose of carbon capture has been explored by investigating different electric heating technologies including Joule, microwave, and induction heating [1–4]. For enhancing the performance of these processes, the electric heating has been combined with the evacuation effect, in a so called temperature vacuum swing adsorption (TVSA) process [5]. Research on electrified TVSA suggests that for optimal results, heating should precede evacuation, and cooling should be done with a stream of gas [6]. However, it is still difficult to make a clear statement about the required temperature before evacuation, and about the required degree of evacuation. Since the heating rate has a direct impact on the desorption rate and energy consumption, in this work the regeneration step of an electrically heated TVSA process (hereafter E-TVSA) was comprehensively investigated and different effects were evaluated in more detail.

2. Model development – a comprehensive simulator that has been developed in MATLAB (verified in our previous work) was used to study the E-TVSA carbon capture cycle [7]. For the study of the E-TVSA process, the adsorption time, heating power, and evacuation pressure were considered as independent variables. Since this work aims to analyse the regeneration step under the combined effect of evacuation and electrified heating, a comprehensive parametric analysis was performed over the whole range of adsorption time, heating power and evacuation pressure (Table 1). In total, 2717 case studies were simulated (to cyclic steady state) for E-TVSA.

Table 1: Range of the parameters used in the study of the E-TVSA process.

	Adsorption time (s)	Heating power MW/m^3 adsorbent	Evacuation pressure (kPa)
Parameter range	300-600	0.60-1.81	1-10
Number of points	11	13	19

3. Results and Discussion - While the primary aim of this paper is to evaluate the impact of evacuation and electrical heating on the overall energy consumption of TVSA carbon capture, the examination of the thermodynamic cycle and bed profiles can provide additional insights (Image 1).

The full assessment of the mentioned parameters in table 1 was done by plotting the contours of KPIs of purity, recovery, productivity, and specific energy consumption in 44 contours which will be presented in the conference. Besides this full analysis, some specific conditions were explored in more detail including effect of adsorption time at a constant heating power and evacuation pressure (Image 2).

The evacuation pressure and heating power, on one hand affect the KPIs, on the other hand discern the distribution of energy usage between evacuation and heating, as both functions rely on electricity as a source of power. As illustrated in Image 3, the contour plot of evacuation energy breakdown at an adsorption time of 450 s implies that in the full range of applied heating power and evacuation pressure, the evacuation energy lies between 10 to 60 % of the total consumed energy (Image 3).

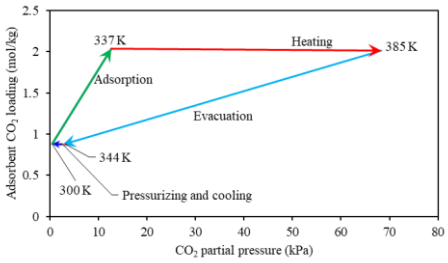

Image 1: E-TVSA process cycle, adsorption step (green), heating step (red), evacuation step (light blue), pressurizing (orange), cooling (dark blue)

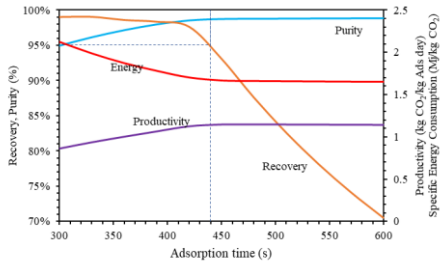

Image 2: Plot of KPIs versus adsorption. The dotted line represents the adsorption time beyond which the recovery drops below 95 %.

4. Conclusions - In this study, a comprehensive mathematical model was developed to simulate the performance of a fully electrified TVSA (E-TVSA) carbon capture process. Overall, this model provides a valuable tool for understanding and exploring the performance of the E- TVSA carbon capture process.
When comparing E-TVSA and VSA, it is noteworthy that the production rate and specific energy consumption of E-TVSA are in the same order as that of VSA. However, E-TVSA surpasses VSA in terms of purity and recovery rates, which indicates its superiority over VSA.

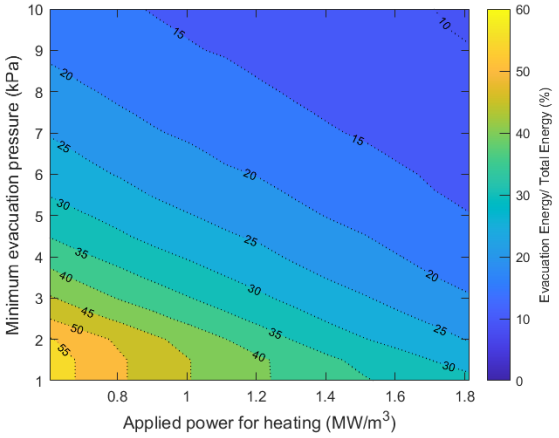

Image 3: Contours of evacuation energy breakdown

5. Acknowledgements
The authors would like to acknowledge
VLAIO for the financial support (HBC.2021.0255).

6. References

[1] H. Li, M. M. Sadiq, K. Suzuki, R. Ricco, C. Doblin, A. J. Hill, S. Lim, P. Falcaro, and M. R. Hill, *Adv. Mater.* **28**, (2016) p. 1839.
[2] Y. Gomez-Rueda, B. Verougstraete, C. Ranga, E. Perez-Botella, F. Reniers, and J. F. M. Denayer, *Chem. Eng. J.* **446**, (2022) p. 137345.
[3] B. Verougstraete, M. Schoukens, B. Sutens, N. Vanden, Y. De Vos, M. Rombouts, and J. F. M. Denayer, *Sep. Purif. Technol.* **299**, (2022) p. 121660.
[4] K. Newport, K. Baamran, A. A. Rownaghi, and F. Rezaei, *Ind. Eng. Chem. Res.* **61**, (2022) p. 18843.
[5] M. Schoukens, M. Gholami, G. V Baron, T. Van Assche, and J. F. M. Denayer, *Chem. Eng. J.* **459**, (2023) p. 141587.
[6] Q. Zhao, F. Wu, Y. Men, X. Fang, J. Zhao, P. Xiao, P. A. Webley, and C. A. Grande, *Chem. Eng. J.* **358**, (2019) p. 707.
[7] M. Gholami, M. Schoukens, T. R. C. Van Assche, and J. F. M. Denayer, *Sep. Purif. Technol.* **343**, (2024) p. 127140.

O19: CO_2 Capture from Flue Gas – Modelling of the Cyclic Sorption/Desorption on a K-promoted Hydrotalcite

J. Martins[(1),(2)], R. Seabra[(2),(3)], A. Ferreira[(2),(3)], M. Ribeiro[(2),(3)], A. Rodrigues[(2),(3)], L.M. Madeira[(1),(2)*]

[1] LEPABE, Faculty of Engineering of the University of Porto; [2] ALiCE, Faculty of Engineering of the University of Porto; [3] LSRE - LCM, Faculty of Engineering of the University of Porto.

** mmadeira@fe.up.pt*

1. Introduction – To avoid harsher consequences of global warming, efforts must be made to significantly reduce greenhouse gas emissions, for instance, through the development of carbon capture, utilization, and sequestration (CCUS) technologies [1]. Flue gas is a post-combustion stream generated at power plants, composed of CO_2 (a greenhouse gas) and N_2 (apart from other minor impurities), and so it is a viable option to be considered for CCUS processes [1]. The aim of this work is to study (through simulation and experimental activity) a process for the capture of CO_2 (through sorption) in a commercial solid material, a K-promoted hydrotalcite (MG30K). Hydrotalcites are layered double hydroxides ($MgO\text{-}Al_2O_3$), which, among the alternative sorbents, are relevant due to their operating conditions (suitable for temperature and pressure swing processes in the range of 200 to 400 °C), as well as their low costs, chemical and mechanical stability, sufficiently fast sorption kinetics and reasonable cyclic working capacity [2,3].

2. Experimental – A column was filled with MG30K in pellet form (*ca.* 30 g), and inserted into an experimental installation where breakthrough tests were carried out at atmospheric pressure and 350 °C. The experiments were performed by feeding to the packed-bed, alternately, a simulated flue gas stream (15 % of CO_2 balanced in N_2), during the sorption stages, and an inert stream (N_2), during the regeneration stages, thus creating sorption/desorption cycles. The inlet flow rate was kept constant at 100 $mL_N \cdot min^{-1}$. During these experiments, the composition and flow rate of the outlet stream of the column were registered, as well as the temperature inside the column.
For the modelling and simulation study, a one-dimensional (1D) heterogeneous dynamic fixed-bed model, designed for continuous cyclic operation, was developed and implemented in gPROMS® software. The model integrates comprehensive mass and energy balances and employs the Ergun equation to account for pressure drop. For the equilibrium sorption data, a bi-Langmuir model was chosen to describe the overall CO_2 sorption, while an Elovich-type equation was utilized to effectively describe the sorption kinetics.

3. Results and Discussion – Figure 1 shows the CO_2 outlet fraction (a)) and temperature history (b)) obtained during one breakthrough test in which two sorption/desorption cycles were carried out. In Figure 1 a), it is possible to observe that the sorption/desorption steps were carried out for long periods (>7 000 s) to ensure maximum CO_2 capture. The equilibrium behavior was characterized using a bi-Langmuir model, which considered two distinct sorption sites. The kinetics of CO_2 interactions with the heterogeneous surface sites of the hydrotalcite were modelled using an Elovich-type equation, which accounted for variations in activation energy for sorption and desorption based on surface coverage of the two sites [2,3]. The thermal positive peaks in Figure 1 b), observed during CO_2 sorption, are attributed to the heat of sorption, while the sharp breakthrough curves, Figure 1 a) are due to its favorable equilibrium isotherm.

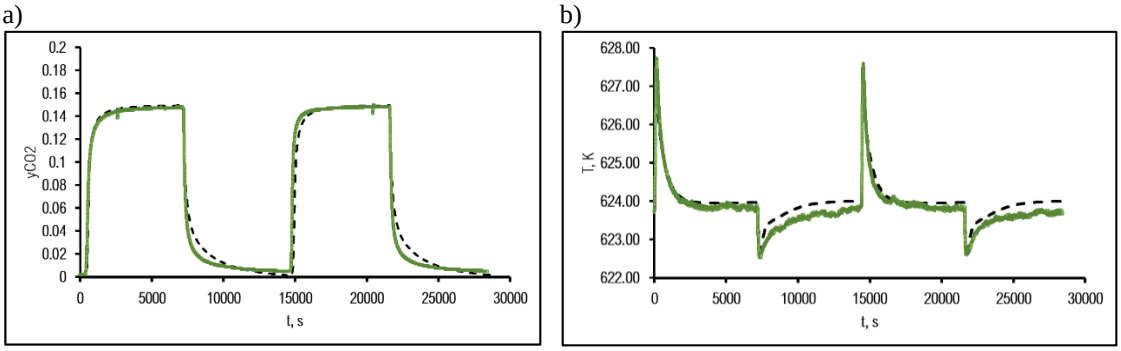

Figure 1. History of the outlet fraction of CO_2, a), and temperature inside the column, b). The experiment was carried out at atmospheric pressure and 350 °C. The green line corresponds to the experimental data, while the black dashed line represents the simulated data.

From the analysis of Figure 1, it is possible to conclude that the model is capable of accurately predicting the adsorption and desorption behavior of CO_2 on the K-promoted hydrotalcite at the stated conditions. However, more experimental and simulation efforts will be made to enhance the model predictions and extend it to other conditions, including different temperatures, feed compositions (different CO_2 and steam contents) and pressures.

4. Conclusions - In this study, long sorption cycles of CO_2 on a K-promoted hydrotalcite were performed. A model was successfully developed to describe the cyclic CO_2 sorption and desorption in the packed-bed system. This model incorporated mass, momentum, and energy balances, along with assumptions tailored to the specific properties of the hydrotalcite-based sorbent. The model accurately predicted the mass and temperature dynamics observed during the experimental CO_2 sorption and desorption cycles.

5. Acknowledgments - This work was supported by national funds through FCT/MCTES (PIDDAC): LEPABE, UIDB/00511/2020 (DOI: 10.54499/UIDB/00511/2020) and UIDP/00511/2020 (DOI: 10.54499/UIDP/00511/2020); LSRE-LCM, UIDB/50020/2020 (DOI: 10.54499/UIDB/50020/2020) and UIDP/50020/2020 (DOI: 10.54499/UIDP/50020/2020) and ALiCE, LA/P/0045/2020 (DOI: 10.54499/LA/P/0045/2020), and by CYCON project (funded by Air Liquide). J. M. is grateful to the FCT for her Ph.D. grant (DFA/BD/4663/2020), financed by national funds of the Ministry of Science, Technology and Higher Education and the ESF through the POCH.

6. References

[1] X. Wang, C. Song, Renew. Front. Energy Res. 8 (2020) 560849.
[2] K. Coenen, F. Gallucci, E. Hensen, M. van Sint Annaland, Chem. Eng. J. 355 (2019) 520–531.
[3] V. Martins, C. Miguel, J. Gonçalves, A. Rodrigues, L. Madeira, Chem. Eng. J. 434 (2022) 134704.

O20: Synthetic and sustainable carbon materials as competitive electrocatalysts for oxygen reduction reactions

E. Martínez-Díaz[1], A. Arenillas[1], A.B. García[1], S. García-Granda[2], N. Rey-Raap[1]

(1) Instituto de Ciencia y Tecnología del Carbono (INCAR-CSIC). Departamento de Procesos Químicos Sostenibles. Grupo de Investigación de Materiales para Energía, Medio Ambiente y Catálisis (MATENERCAT), 33011, Oviedo.
elisa.martinez@incar.csic.es
(2) Departamento de Química Analítica, Universidad de Oviedo-CINN-CSIC, 33006 Oviedo.

1. Introduction

Hydrogen is postulated as the energy vector of the future for the generation of clean energy. This transformation takes place in a fuel cell, in which two electrochemical reactions are involved: the hydrogen oxidation reaction (HOR) and the oxygen reduction reaction (ORR). Among these reactions, the ORR exhibits the sluggishest kinetics, being essential the development of highly efficient electrocatalysts. Currently, commercial electrocatalysts are based on platinum, a scarce and costly element that greatly limits its widespread applicability. Therefore, the development of low-cost, abundant and sustainable electrocatalysts with high electroactivity is of paramount importance. Carbon materials derived from biomass residues are currently being evaluated, as they are abundant and widely available. However, the presence of impurities and, above all, the variability in the composition of these raw materials make them unreliable. In this context, synthetic carbon materials are the best strategy for new and efficient electrocatalyst as they can be obtained with very well controlled porous and chemical properties, from many different precursors and wihtout impurities. Hence, the objective of this work focuses on the development of new, sustainable, low-cost, highly available, and electrochemical active synthetic carbon materials to beused as electrocatalysts in the ORR.

2. Experimental

The synthetic carbons were synthesized using fluoroglucinol, glyoxylic acid, and tritilendiamine (TEDA) as main reactants. The synthesis process was optimized by promoting the polymerization reaction by microwave heating, reducing considerable the time of the process to 2.5 hours. The precursor mixture, in an open container, was heated at 50°C at atmospheric pressure in a multimode microwave equipment withtemperature and power control. The product was oven-dried at 60°C to obtain synthetic polymer spheres (S)containing C, O, H and N in its composition. These spheres were further functionalized to increase its nitrogen content. To this end, functionalization with melamine through thermal treatment using two different strategies was applied:

1. The synthetic polymer spheres (S) were mixed with melamine and treated at 850°C (N-CS-850) and 1000°C (N-CS-1000) in a nitrogen atmosphere for 1 hour.
2. The synthetic polymer spheres (S) were carbonized at 850°C (CS-850) and 1000°C (CS-1000) ina nitrogen atmosphere for 1 hour; and subsequent, mixed with melamine and treated at 1000°C (CS-850-N-1000 and CS-1000-N-1000) in a nitrogen atmosphere for 1 hour.

All the synthetic materials were characterized based on their morphology (SEM), porosity (N_2 adsorption-desorption isotherms at 77K), chemical composition (elemental analysis and XPS) and tested as electrocatalysts in the ORR by performing cyclic and linear voltammetry in a rotating disk electrode.

3. Results and Discussion

The morphology of the carbonized samples is shown in Figure 1a and 1b. It can be observed that, regardless of the temperature employed, both materials obtained through microwave-assisted polymerization are micrometer-sized spheres, with approximately 2 microns in diameter. The surface area of these spheres increases notably after carbonization (Figure 1c), with a slight increase with the increase of carbonization temperature, i.e. from 564 to 610 $m^2\ g^{-1}$ by increasing from 850 to 1000ºC (Table 1). Moreover, the surfacearea is even further increased after the functionalization with melamine, reaching a specific surface area ofup to 1069 $m^2\ g^{-1}$ for the sample CS-1000-N-1000. All the samples are microporous materials as can be observed from textural parameters shown in Table 1. However, it is worth to mention that the external surface area is notably increased in the samples tretated at 1000ºC, specially the N-funcionalised samples at 1000ºC.

The porosity of the electrocatalysts plays a fundamental role in the oxygen reduction reaction, since it determines the diffusion of reactants and products in the medium and the electrochemical active surface area of the catalyst. The aim is to obtain materials that exhibit in the linear voltammetry test an onset potential as low as possible (ca. 1 V) and a current density as high as possible, since both parameters are indicative of high electrochemical activity of the electrocatalyst. In addition, it is necessary that the ORR mechanism works in a direct way (i.e. 4 e^- mechanism) thus avoiding the generation of undesirable by-products that may deteriorate the electrocatalyst and the electrode.

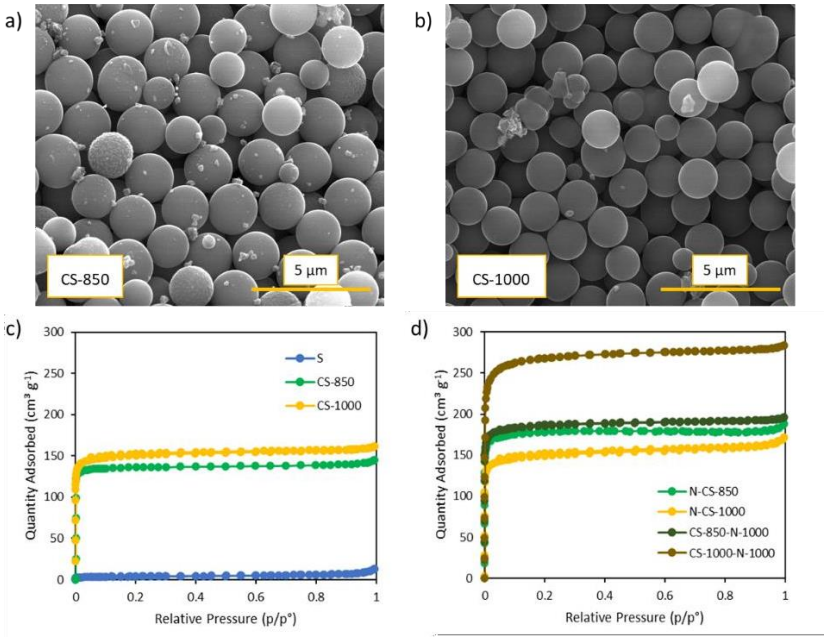

Figure 1. SEM micrograph of carbon spheres CS-850 (a) and CS-1000 (b), and N_2 adsorption-desorption isotherms at 77K for non-carbonized and carbon spheres (c) and the N-doped spheres studied (d).

Table 1. Textural characterization obtained from N_2 adsorption-desorption isotherms at 77K.

	S_{BET} (m^2/g)	S_{ext} (m^2/g)	V_{DR} (cm^3/g)	V_{meso} (cm^3/g)	V_p (cm^3/g)
S	14	7	0.01	0.02	0.02
CS-850	564	8	0.21	0.01	0.22
CS-1000	610	15	0.23	0.02	0.25
N-CS-850	683	17	0.26	0.03	0.29
N-CS-1000	599	27	0.23	0.04	0.26
CS-850-N-1000	756	14	0.28	0.01	0.3
CS-1000-N-1000	1069	23	0.42	0.02	0.44

The electrochemical test performed revealed that the synthetic polymer carbons with higher specific and external external surface area show better electrochemical performance, with excellent onset potential andcurrent densities, and a direct mechanism through 4 e^-.

4. Conclusions

Synthetic carbon materials obtained from sustainable precursors using microwave-assisted polymerization and functionalization with melamine exhibit excellent electrochemical performance towards the ORR, thussuggesting that they can be further optimized to become competitive against the commercial reference material Pt/C as electrocatalyst in fuel cells for clean energy generation.

Acknowledgements

This work was funded by Domingo Martínez Foundation (MACSO project) and MCIN/AEI/10.13039/501100011033/FEDER-UE through PID2022-139493OA-100 and PID2020-113001RB-100 projects.

O21: Enhancing the sustainability of activated carbon materials application in water treatment

Ana S. Mestre[1*], Daniela Perpétua[1], Filipe M. Leandro[1], Isabell Ober[1], Marta A. Andrade[1], Elsa Mesquita[2], Rui M.C. Viegas[2], Maria João Rosa[2], Ana P. Carvalho[1]

[(1)] *Centro de Química Estrutural, Institute of Molecular Sciences, Faculdade de Ciências, Universidade de Lisboa, Campo Grande, 1749-016 Lisboa, Portugal.*

asmestre@fc.ul.pt

[(2)] *Urban Water Unit, Hydraulics and Environment Department, LNEC—National Laboratory for Civil Engineering, Av. Brasil 101, 1700-066 Lisboa, Portugal.*

fc53056@alunos.ciências.ulisboa.pt; filipe.m.leandro@gmail.com; isiober99@gmail.com; mvandrade@fc.ul.pt; emesquita@lnec.pt; rviegas@lnec.pt; mjrosa@lnec.pt; apcarvalho@fc.ul.pt

1. Introduction – Technologies based on activated carbon's adsorption play a key role in water treatment given their versatility and non-specificity that allows to tackle more stringent water quality standards [1]. These technologies are being implemented in full-scale water treatment to cope with need to remove contaminants of emerging concern (CECs), including pharmaceutical compounds (PhCs), and consequently the amount of activated carbon materials exhausted with CEC is expected to increase, calling for a deeper knowledge on their regeneration and reuse. While granular activated carbons (GACs) applied in column filters are commonly thermally regenerated in dedicated industrial facilities, powdered activated carbons (PACs) applied in slurries are not. In fact, spent PACs are collected mixed with the water treatment sludge, which limits their recirculation and possible further regeneration. Thus, in the present work we aim to present contributions to enhance sustainability of activated carbons' application in water treatment by: (i) developing novel sustainable activated carbons from Portuguese biomass with high adsorption performance, (ii) addressing thermal regeneration of GACs exhausted with PhCs and (iii) presenting preliminary data on magnetic PACs (MPACs) and their performance for removing PhCs and natural organic matter in experimental conditions that mimic their application in drinking water treatment.

2. Experimental – Both for the assays with GACs and PACs a commercial and a lab-made material were tested. The lab-made materials were prepared by pyrolysis of pine nut shell (PNS) followed by griding and sieving to the desired particle size and further steam activation [2]. The commercial materials were Norit GAC830 (cGAC) for the assays with GAC and Norit SA UF (NSAUF) for the assays with PAC. GAC assays were performed with fractions presenting particle sizes of 850-600 µm, while the tested PACs were composed of particles < 150 µm. GACs' liquid phase kinetic and equilibrium adsorption studies were conducted with caffeine and paracetamol in single-solute conditions. The GAC thermal regeneration was tested in inert atmosphere or steam flow, both at 600 ºC during 1 h. Along with the regeneration efficiency, the changes on textural properties and surface chemistry of the regenerated materials were evaluated. Selected PACs were further magnetized by co-precipitation of iron salts to form magnetic iron oxides nanoparticles (NPs). Both PACs and MPACs were tested in multi-solute solutions containing sulfamethoxazole, diclofenac and carbamazepine in a water matrix whose organic and mineral content mimic a surface water source for drinking water production. The PACs and MPACs were characterized by N_2 adsorption, pH at the point of zero charge (pH_{PZC}) and nanoparticle content (%NP).

3. Results and Discussion – The equilibrium adsorption isotherm data of both GACs for caffeine and paracetamol fitted the Langmuir model (Image 1). The results reveal superior adsorption capacity for the lab-made GAC/PNS in comparison to cGAC (caffeine: 400 *vs* 250 mg/g; paracetamol: 394 *vs* 200 mg/g) in line with the higher volume of micro and mesopores of the lab-made material (GAC/PNS: A_{BET} = 1228 m^2/g, V_{micro} = 0.42 cm^3/g and V_{meso} = 0.20 cm^3/g; cGAC: A_{BET} = 831 m^2/g, V_{micro} = 0.29 cm^3/g and V_{meso} = 0.16 cm^3/g). The kinetic assays revealed that caffeine adsorption was always faster than that of paracetamol. The saturation/regeneration/reuse assays revealed the influence of several factors in the regeneration efficiency (RE). Over several thermal regeneration cycles of cGAC, RE in N_2 atmosphere was higher than in steam regeneration (4 cycles for caffeine: 98,5-81,9 % *vs* 154,0-53,6 %; 3 cycles for paracetamol: 78,8-33,5 % *vs* 60,0-25,6 %), in line with the mass loss (13-26 % for steam *vs* 18-46 % for N_2). The higher initial maximum adsorption capacity of GAC/PNS reflected in better overall adsorption capacity than the cGAC over several regeneration cycles, with both GACs generally presenting similar RE at the same regeneration cycle.

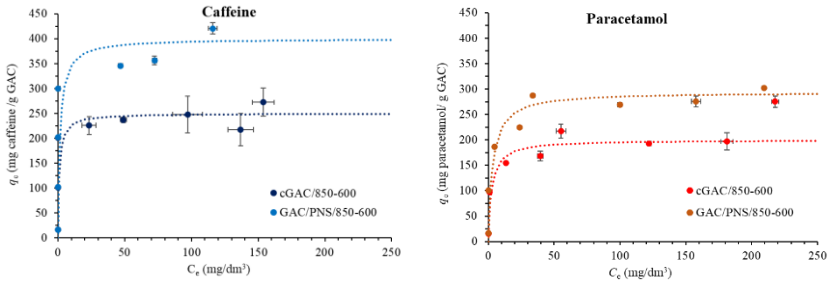

Image 1 – Adsorption isotherms of caffeine and paracetamol on the mentioned GAC materials at 30 ºC. Points correspond to experimental data and lines to Langmuir isotherm model fitting (6 mg GAC/20 cm^3 PhC solutions 5-300 mg/dm^3 and 24 h of contact time. Error bars included.

At full scale water treatment, GAC is usually used as column filter medium at final treatment stages. GAC filters act as a permanent barrier for contaminants and GAC is replaced when their breakthrough is observed. PAC can be applied in different stages of water treatment, taking advantage of their small particle size, which favors target contaminants' adsorption kinetic. In a real scenario, the competitive adsorption of natural organic matter entails several problems as, for example, slower kinetics and lower removal efficiencies of CECs. Typically, PAC is applied as a slurry and mixed with other reactants in non-dedicated treatment tanks or is dosed in a devoted contact tank, and the contact times usually do not allow the usage of PAC's total adsorption capacity. Separation of exhausted PACs from water treatment sludges is not possible but PAC magnetization is an interesting approach to overcome this issue, as it will allow easier separation of the MPACs and subsequent regeneration.

Preliminary data on the magnetization of a commercial PAC (NSAUF) and a lab-made PAC (PAC/PNS) reveal that, as expected, the incorporation of magnetic iron nanoparticles (NP) reflects in lower adsorption capacity, directly correlated with the %NP. The performance of the PACs and MPACs was assessed with 10 mg/dm^3 to 25 mg/dm^3 (M)PAC doses in short-term isotherm conditions that mimic (M)PAC application in conventional coagulation, flocculation and sedimentation (CFS) separation processes or PAC/membrane filtration (PAC/MF). The corrected masses of MPAC (considering only the PAC content) attain removal efficiencies for the three target PhCs similar to those of the correspondent PAC and following the trend carbamazepine > diclofenac > sulfamethoxazole.

4. Conclusions – The novel GACs prepared from pine nut shell have higher adsorption capacity for PhCs than the commercial counterpart. The experimental data reveal the thermal regeneration efficiency is mainly dependent on the PhCs adsorbed, being higher for caffeine. Thus, the use of GAC with higher adsorption capacity will reflect in higher removal efficiencies along several regeneration/reuse cycles. Preliminary data on MPACs point that their performance for the removal in PhCs and NOM in multi-solute conditions follow the trend of the PAC texture and correlates with their NP content.

5. References

[1] A.S. Mestre, M. Campinas, R.M.C. Viegas, E. Mesquita, A.P. Carvalho, M.J. Rosa (2022). Chapter 17 - Activated carbons in full-scale advanced wastewater treatment. In D. Giannakoudakis, L. Meili, & I. Anastopoulos (Eds.), Advanced Materials for Sustainable Environmental Remediation, Elsevier, 2022. https://doi.org/10.1016/B978-0-323-90485-8.00001-1

[2] A.S. Mestre, R.M.C. Viegas, E. Mesquita, M.J. Rosa, A.P. Carvalho, *J. Hazard. Mater.*, **437**, (2022) p. 129319.

Acknowledgements – Centro de Química Estrutural is a Research Unit funded by Fundação para a Ciência e Tecnologia (FCT) through projects UIDB/00100/2020 and UIDP/00100/2020 (DOI 10.54499/UIDB/00100/2020 and 10.54499/UIDP/00100/2020). Institute of Molecular Sciences is an Associate Laboratory funded by FCT through project LA/P/0056/2020 (DOI 10.54499/LA/P/0056/2020). Authors thank FCT financial support to EMPOWER+ Project (PTDC/EQU-EQU/6024/2020, DOI 10.54499/PTDC/EQU-EQU/6024/2020). ASM and MAA thank FCT for, respectively, the Assistant Researcher CEECIND/01371/2017 (DOI 10.54499/CEECIND/01371/2017/CP1387/CT0013) and the Junior Research contracts in the EMPOWER+ project. The authors acknowledge Salmon & Cia for providing the commercial materials Norit GAC830 and Norit SA UF.

O22: Influence of humidity on CO2 solid sorbent performance: insight and challenges

Connor Hewson[(a)], Sean McIntyre[(a)], Lisa Mingzhe Sun[(a)] Dan Burnett[(a)], Daryl Williams[(a,b)] Paul Iacomi[(a)]

[(a)] *Surface Measurement Systems Ltd., Alperton, London, HA0 4PE*
piacomi@surfacemeasurementsystems.com
[(b)] *Department of Chemical Engineering, Imperial College London, SW7 2AZ*

Solid sorbents such as zeolites, MOFs, and finely divided metal oxides are one of the most promising candidates for the implementation of carbon capture (CC), both for direct air capture (DAC) solutions and point sources. Bringing a promising material from the lab to industry requires a realistic screening of its performance in process relevant conditions. The main goal from a materials standpoint is identifying and screening sorbents with the necessary affinity at the relevant CO_2 concentration (from 400 ppm up to 100%), long term usability, and thermal properties [1].

One of the most pertinent challenges relies in the presence of humidity in the process stream, leading to several possible effects on a material's CO_2 capture potential. Water molecules compete with CO_2 for sorption sites in many materials (zeolites and most MOFs). In others the presence of a certain amount of humidity can increase total amount adsorbed, or speed up the sorption kinetics, as in the case of amine-based materials [2] and alkali or alkaline earth metal carbonation processes [3]. Even in non-interacting scenarios, the coadsorption of water at high humidity levels leads to higher energy requirements during the regeneration since besides CO_2 also water must be desorbed.

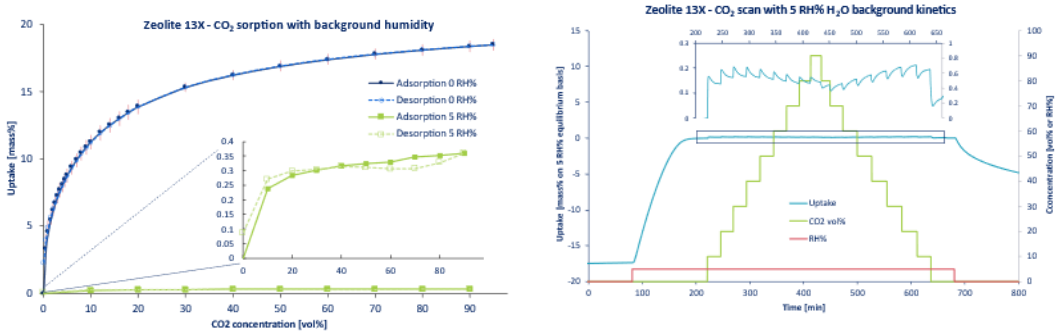

Image 1. (left) Apparent decrease of CO2 uptake in 13X on the presence of 5% relative humidity and (right) details of the kinetics of sorption, evidencing a subtle displacement of water by CO2.

Therefore, assessing the influence of moisture on the CO_2, and the amount taken up of each from a multicomponent mixture, is of crucial importance. In this work we explore several methods of accomplishing this difficult task – gravimetry and breakthrough analysis – and then walk through several examples on prototypical materials – Zeolite 13X, CALF-20, Lewatit VP OC 1065.

References

[1] M.-Y. (Ashlyn) Low, L. V. Barton, R. Pini, C. Petit, *Chem. Eng. Res. Des.* **2023**, *189*, 745–767.

[2] T. Wang, K. S. Lackner, A. Wright, *Environ. Sci. Technol.* **2011**, *45*, 6670–6675.

[3] P. López-Arce, L. S. Gómez-Villalba, S. Martínez-Ramírez, M. Álvarez De Buergo, R. Fort, *Powder Technol.* **2011**, *205*, 263–269.

O23: Adsorption process of a multi-metal leaching liquor from the waste of integrated circuits for gold purification using ion-exchange technology

Silva, Márcia A-D.[1]; Martelo, Liliana M.[2]; Bastos, Margarida M.S.M.[3] and Soares, Helena M.V.M.[4*]

(1) REQUIMTE/LAQV, (2) ALiCE/ LEPABE Departamento de Engenharia Química, Faculdade de Engenharia, Universidade do Porto, rua Dr. Roberto Frias, 4200-465 Porto, Portugal.
up201502999@fe.up.pt
(2) lmartelo@fe.up.pt, (3) mbastos@fe.up.pt, (4) hsoares@fe.up.pt

1. **Introduction –** In recent decades, the amount of gold available in mineral ores has decreased; so, it is necessary to find alternative Au resources since its demands are still growing. One of the promising possibilities to balance this deficit is recycling Au from the vast waste of electrical and electronic equipmentgenerated every year, for which the waste of integrated circuits (ICs), mainly found in surface-mounted inprinted circuit boards, can be an important contribution. ICs are mainly constituted of silica (SiO_2, 62 % wt.) reinforced with brominated epoxy resin (14 % wt,) and a large resource of metals, such as Cu (22 % wt.), Fe (1 % wt.), and precious metals, such as Au (0.3% wt.) and Ag (0.7 % wt.) [1-2].
   In this work, after applying a two-step physical pre-treatment to the waste of ICs, Au was concentrated in the non-magnetic fraction. Subsequently, an optimized hydrometallurgical process to extract Au from thisfraction was developed and resulted in a multi-metal leachate solution containing Ag, Al, Au, Cr, Cu, Fe, Ni, Pb, Sn, and Zn.
   Purification of Au from this multi-metal leachate may be achieved using several methods, such as, solventextraction, electrowinning and selective precipitation. The multiplicity of metals and its low concentration($\leq$ 1 g/L) makes difficult to recover individual metals efficiently through these traditional approaches, resulting in a low Au purity grade product [3-4]. So, in this work, an adsorption process through ion- exchange technology using a strong anionic exchange resin was implemented. This process revealed to be more efficient in separating and concentrating Au from the other metals and, thus, increasing its purity yieldat the end of the developed process. Additionally, the simplicity and the possibility to regenerate the resin and reuse it multiple times, makes this process a cost-effective and environmentally friendly option.

2. **Experimental -** A two-step physical treatment was developed to expose the metallic fraction enriched in Au: fragmentation of the ICs samples using a hydraulic press followed by a magnetic separation. The non-magnetic fraction (containing the Au) was subjected to a hydrometallurgical process for 3 hours at 40
   °C with a liquid/solid ratio (mL/g) of 40, in a solution of 2.5 M hydrochloric acid (HCl) and 0.34 M sodiumhypochlorite (NaClO). At the end, 88.6% wt. of the total Au was extracted from the non-magnetic ICs samples. Besides Au, the leachate solution contains other metals, mainly Cu and Ni. So, the next step was to separate and concentrate Au from the leachate solution. A chromatographic glass column (di = 6.6 mm,h = 100 mm) was used in continuous mode with a strong anionic exchange resin, a polystyrene structure crosslinked with divinylbenzene, with functionalized groups of mixed tertiary amine and quaternary ammonium commercialized by the name Purogold™ A194 Resin. Elution was performed using 0.5 M of sulfuric acid (H_2SO_4) and 0.25M thiourea (CSN_2H_4) for 120 minutes. For both adsorption and elution steps,a flow rate of 0.252 mL/min was used. Between adsorption and elution, the resin was washed with 30 ml of distilled water, and after elution, the resin was washed with 60 ml of deionized water and reused seven times for analysis again.

3. **Results and Discussion** - Ion exchange technology was selected and investigated to optimize Au purification from the real leachate achieved according to the experimental conditions described above. Purogold™ A194 Resin was selected since it demonstrated a high total exchange capacity, and a higher amount of Au is adsorbed in a shorter period of time when compared to other resins described in the literature [5].

   The aim was to separate and concentrate selectively Au from other metals by optimizing the process flow and the resin loading. After optimization studies, it was concluded that the ideal time of elution was obtainedafter 26 hours at a flow rate of 0.252 mL/min. The adsorption behaviour of all the metals under optimized experimental conditions are shown in **Figure 1**, unless for Al, Cu and Ni, which were not adsorbed to the resin since the beginning of the experiment.

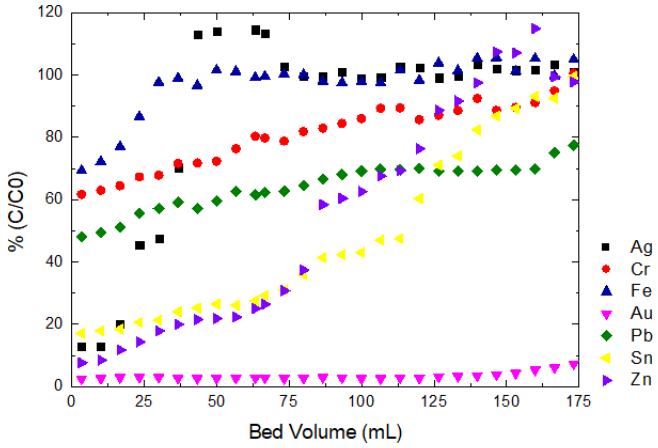

Figure 1 Ratio between the metal concentrations in the outlet, C, and in the inlet solution, C_0, *versus* Bed volume.

From the analysis of **Figure 1,** it can be observed that, besides Au, which is totally adsorbed to the resin, as $AuCl_4^-$ species, until 150 Bed Volume, Sn, Zn and Pb were partially adsorbed in the beginning of the experiment being progressively displaced from the resin. This adsorption behaviour is explained by the formation of anionic chloride complexes ($SnCl^-/SnCl^{2-}$, $PbCl^-/PbCl^2$ (95,3%), and $ZnCl^-/ZnCl^{-2}$ (96,6%), respectively). The other profile corresponds to the other metals, initially, adsorbed, but, at end of the adsorption process reached almost 100% C/C_0 (others than Pb). This phenomenon can be explained by the substitution of the reactive site in the resin already occupied by those metals by $AuCl_4^-$ species, which presents higher affinity. These results show that Purogold™ A194 resin proved to have high affinity for Auwith the following selectivity order relatively to the other metals present in the leachate: Au > Zn > Sn > Pb > Cr >>Fe > Cu ≈≡ Ni ≈ Al.
After elution, 91% of the Au was eluted from the resin with a purity grade of 85%, being Sn (7.5% wt) andPb (4.3% wt) the major contaminants.

4. **Conclusions –** This study shows that Purogold™ A194 resin is a good choice for purifying Au from a multi-metal solution resultant from leaching the non-magnetic Au enriched fraction of ICs. This process inits entirety proves to be simple and with a final product of high purity**.** Its high purity percentage makes it useful in a vast variety of industries, including jewellery.

5. References

[1] B. Niu, E. Shanshan, Z. Xu, and J. Guo, Journal of Cleaner Production, 415 (2023) p. 137815. [2] Y. Liu, K. Li, J. Guo, and Z. Xu, J Clean Prod, 197 (2018), p. 1488–1497.
[3] D. Bożejewicz, K. Witt, M. A. Kaczorowska, W. Urbaniak, and B. Ośmiałowski, Int J Mol Sci, 22 (17) (2021) p. 9123
[4] K. Y. Tomizaki, T. Okamoto, T. Tonoda, T. Imai, and M. Asano, Int J Mol Sci, 21 (14), (2020) p. 1- 12.
[5] I. F. F. Neto and H. M. V. M. Soares, Waste Management, 135 (2021), p 90–97.

Acknowledgments
This work is financially supported by national funds through the FCT/MCTES (PIDDAC), under the project PTDC/CTA-AMB/3489/2021 - RECY-SMARTE - Sustainable approaches for recycling discarded mobile phones, with DOI **10.54499/PTDC/CTA-AMB/3489/2021** (https://doi.org/10.54499/PTDC/CTA- AMB/3489/2021).

O24: H_2 purification by PSA using Norit R2030 as the adsorbent and IAST model to predict the multicomponent adsorption equilibrium

M. Bessa [1] [2], A. Ferreira [1] [2], A. Rodrigues [1] [2], A. M. Ribeiro [1] [2]

[1] *LSRE-LCM – Laboratory of Separation and Reaction Engineering - Laboratory of Catalysis and Materials, Faculty of Engineering, University of Porto, Rua Dr. Roberto Frias, 4200-465 Porto, Portugal*
[2] *ALiCE – Associate Laboratory in Chemical Engineering, Faculty of Engineering, University of Porto, Rua Dr. Roberto Frias, 4200-465 Porto, Portugal*
up201503607@edu.fe.up.pt, aferreir@fe.up.pt, arodrig@fe.up.pt, apeixoto@fe.up.pt

1. Introduction – Hydrogen, which is the most promising carbon-free clean fuel to be used in the energy generation sector, especially for fuel cell applications or as a feedstock in manufacturing chemicals like ammonia and methanol, is economically most efficiently produced at an industrial scale utilizing natural gas as the raw material in a steam methane reforming (SMR) unit combined with two water gas-shift reactors for high- and low-temperature operation [1]. The SMR off-gases typically comprise 70-80 % of H_2, 15-25 % of CO_2, 3-6 % of CH_4, and 1-3 % of CO, and are saturated with water. If the CH_4 source employed in the SMR reactor contains N_2, then the off-gases will have traces of this compound [2]. To obtain high-purity H_2, the contaminants can be removed using adsorption, absorption, membranes, or cryogenic processes. According to the specifications of the ISO 14687-2 standard [3], H_2 with 99.97+ % purity is required for fuel cells. Still, it also needs to comply with the maximum acceptable content of impurities (CO_2 – 2 ppm; CH_4 – 2 ppm; CO – 0.2 ppm; N_2 – 100 ppm; H_2O - 5 ppm).
Currently, the pressure swing adsorption (PSA) technology is the most used in the industry for hydrogen purification. Nowadays, hydrogen purification in PSA units is normally done in heterogeneous fixed beds composed of activated carbon and zeolite layers. In general, the activated carbon layer selectively removes carbon dioxide and methane, while the zeolite layer selectively adsorbs carbon monoxide and nitrogen. The water contained in the output stream of the reforming process can be pre-removed in a separation process upstream of the PSA hydrogen purification unit or may be removed in the PSA hydrogen purification unit using an initial layer of alumina (or silica gel) or the activated carbon layer in which carbon dioxide and methane are also adsorbed. Moreover, an additional separation unit can capture and recover carbon dioxide upstream or downstream of the hydrogen purification PSA unit [4].
The main objective of this work, which was carried out within the scope of the Research Project "Move2LowC – Combustíveis de Base Biológica", was to design, simulate, and optimize an industrial PSA process capable of obtaining renewable hydrogen from SMR to be used in electric vehicles powered by fuel cells. For this purpose, a PSA process fed with a mixture of 76.59 % H_2, 15.93 % CO_2, 2.89 % CH_4, 3.98 % CO, 0.28 % N_2, and saturated water vapor at 308 K and 17 bar and packed with commercial activated carbon (Norit R2030) was developed.

2. Results and Discussion – The adsorption equilibrium information is crucial in the design of any adsorption process like the PSA. So, firstly, the single-adsorption equilibrium data of the six components of the mixture on the commercial activated carbon was taken from the literature [5, 6]. The single-component adsorption equilibrium behavior of H_2, CO_2, CH_4, CO, and N_2 is well described by the Dual Site Langmuir (DSL) model, and of H_2O is fitted by the Cooperative Multimolecular Sorption (CMMS) model. Even though the feed stream is typically saturated with water, most studies do not account for its presence. However, it is crucial to consider the presence of water since it adsorbs much more strongly in activated carbon than the other adsorbates and also presents a different adsorption behavior from the rest of the components of this study; water vapor has a Type V isotherm shape according to IUPAC classification, while the other components present a Type I isotherm shape. Therefore, in this work, the multicomponent adsorption equilibrium data was predicted using the Ideal Adsorbed Solution Theory (IAST), which assumes that all adsorbates have the same available surface area, the adsorbent is inert, and that the multi-component mixture behaves as an ideal solution at constant pressure and temperature. The IAST prediction is made using the pure-component adsorption equilibrium models and equalizing the spreading pressures for the six considered components.
After the multicomponent adsorption equilibrium model is defined, it is then possible to develop the mathematical model that describes the proposed industrial PSA process composed of four columns with a 7 m length and a 1.81 m diameter and capable of producing H_2 above 99.97 % while also considering CO_2 valorization. This model includes mass, energy, and momentum balances. The mathematical model of this process, in which IAST equations were incorporated, was solved through the gPROMs® ModelBuilder, using the orthogonal collocation in finite elements method until the cyclic steady state is reached. Three different PSA cycles were studied and compared, and a parametric study was conducted for each distinct cycle design. The first analyzed PSA cycle comprises the following steps: feed, pressure equalization-

depressurization, blowdown, purge, pressure equalization-pressurization, and pressurization. The extension of the cycle proposed for a four-column unit with continuous feed consumption, which is schematized in **Figure 1 a)**, imposes some restrictions on the step times; namely, the total cycle duration needs to be four times the duration of the feed step. For this PSA unit, the step times presented in the figure (namely feed time of 1150 s) were the ones that resulted in a better overall process performance. This PSA cycle allows the H_2 production with a purity of 99.997 % for a recovery of 78.2 %. The PSA cycle of **Figure 1b)** differs from the abovementioned cycle because instead of having only one pressure equalization, it has two. This PSA cycle with the step times shown in the figure, such as feed time of 950 s, leads to the best performance results, *i.e.*, an H_2 product with a purity of 99.992 % for a recovery of 80.4 %. On the other hand, the third PSA cycle studied and shown in **Figure 1 c)** is the same as the first case presented but contains an extra adsorption step: the rinse step. With this PSA cycle, obtaining H_2 with a purity of 99.996 % and a recovery of 81.2 % is possible using the step times presented in the figure.

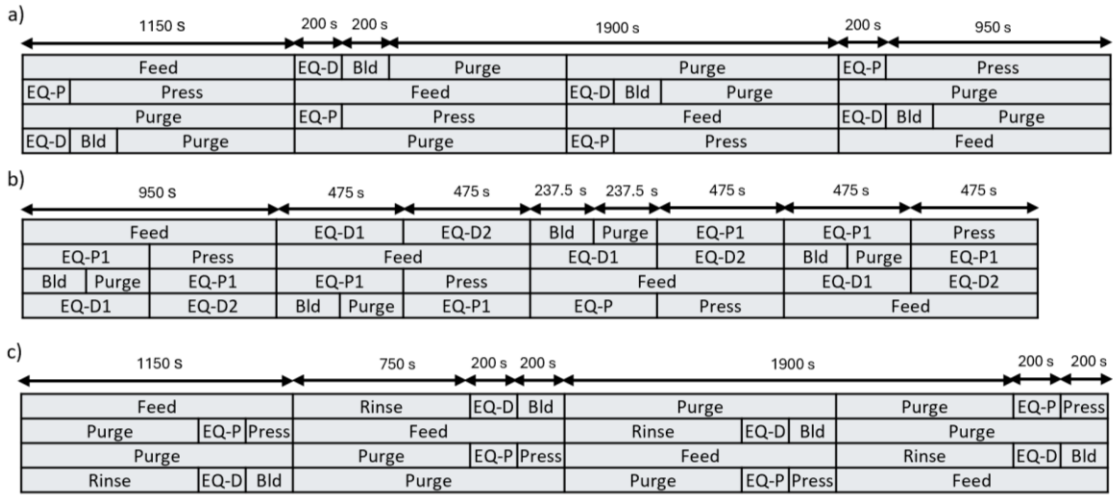

Figure 2 – PSA cycle containing a) one equalization step, b) two equalization steps, c) one pressure equalization, and a rinse step.

3. Conclusions – In this work, a PSA process for H_2 purification from a humid feed was designed, simulated, and optimized using the IAST model to predict the multicomponent adsorption equilibrium and commercial activated carbon (Norit R2030) as the adsorbent. The simulation results showed that the proposed PSA process that presents the best performance contains one rinse step and one pressure equalization step, being capable of obtaining H_2 with a purity of 99.996 % and recovery of 81.2 %.

4. Acknowledgement

This work was supported by national funds through FCT/MCTES (PIDDAC): LSRE-LCM, UIDB/50020/2020 (DOI: 10.54499/UIDB/50020/2020) and UIDP/50020/2020 (DOI: 10.54499/UIDP/50020/2020); and ALiCE, LA/P/0045/2020 (DOI: 10.54499/LA/P/0045/2020). Mariana Bessa acknowledges her Ph.D. scholarship 2022.10166.BD funded by FEDER funds through NORTE 2020 and by national funds through FCT/MCTES.

5. References

[1] A. Hajizadeh, et al., Applied Energy, 309 (2022).
[2] K. Liu, et al., John Wiley & Sons, Hoboken, 2010.
[3] T. Bacquart, et al., International Journal of Hydrogen Energy, 43 (2018) 11872-11883.
[4] P. Brea, et al., Microporous and Mesoporous Materials, 286 (2019) 187-198.
[5] I. Durán, et al., Energies, 10 (2017).
[6] F.V.S. Lopes, Ph.D. Thesis, University of Porto, 2010.

O25: Simulating the separation of flue gas components in TAMOF-1

S. Gooijer [(1)], J.M. Vicent-Luna [(1)], S. Giancola[(2)], D. Dubbeldam[(3)], S. Capelo-Avilés [(4)], J. R. Galán-Mascaros [(4,5)], S. Calero[(1)]

[(1)]*Materials Simulation and Modelling, Department of Applied Physics and Science Education, Eindhoven University of Technology, PO Box 513, 5600MB Eindhoven, The Netherlands.*
[(2)]*Orchestra Scientific SL, Av. Països Catalans 16, Tarragona, 43007, Spain.*
[(3)]*Van't Hoff Institute for Molecular Sciences, University of Amsterdam, Amsterdam, Netherlands.*
[(4)]*Institute of Chemical Research of Catalonia (ICIQ-CERCA), the Barcelona Institute of Science and Technology (BIST), Av. Països Catalans 16, Tarragona 43007, Spain.*
[(5)]*Catalan Institution for Research and Advanced Studies (ICREA), Passeig Lluís Companys 16, Barcelona, 08007, Spain,*
s.a.gooijer@tue.nl, j.vicent.luna@tue.nl, sgiancola@orchestrasci.com, d.dubbeldam@uva.nl, jrgalan@iciq.es, scapelo@iciq.es, s.calero@tue.nl

1. **Introduction –** Flue gases emitted by industries and power plants are major contributors to both CO_2 and NO_x emissions. Reducing these emissions is vital for a multitude of reasons. CO_2 is considered to be the main greenhouse gas and NO_x compounds are hazardous and highly reactive in nature, resulting in health and environmental issues. [1,2] Being able to capture and separate these gases will reduce emissionsand creates possibilities to convert them into more valuable compounds.
   TAMOF-1, a Metal Organic Framework with high chemical and hydro-thermal stability, has been shown to be able to effectively separate CO_2 from several gases (N_2, O_2, CH_4, H_2) and is therefore considered as apromising agent for carbon capture. The effect of the presence of NO_x compounds has however not been studied yet.
   The goal of this work is to a priori assess the adsorption of NO_x compounds in TAMOF-1 and its effect onCO_2 adsorption. To this end, adsorption isotherms of the pure components were simulated, as well as mixture isotherms and breakthrough curves.

2. **Experimental -** To simulate adsorption isotherms, Monte Carlo simulations in the grand-canonical ensemble were performed as implemented in the RASPA software package. [3] The TAMOF-1 framework was kept rigid. To describe the interactions between the framework and the adsorbed species, a forcefield consisting of Coulombic and Lennard-Jones potentials was used. To simulate the mixture isotherms and breakthrough curves, the RUPTURA package was used. [4]

3. **Results and Discussion -** The adsorption isotherms of CO_2 and flue gas impurities in TAMOF-1 are shown in Figure 1. CO_2 clearly adsorbs preferentially to NO and NO_2, with higher loadings over the whole pressure range. N_2O has been known to exhibit similar behavior to CO_2, which is also expressed in the adsorption isotherms which are almost equal. Of all the evaluated flue gas impurities, SO_2 showed the highest uptake, as it is the most polar of the compounds. Prior removal of SO_2 from exhaust flue gas mixtures is therefore preferable, as it is commonly practiced, to prevent hindrance to CO_2 adsorption.
   Calculated mixture isotherms of a flue gas mixture containing small amounts of NO and NO_2 show NO and NO_2 are barely adsorbed with loadings under 0.5 mol/kg, while the loading of CO_2 increased to 3 mol/kg at 1000 kPa. The simulated breakthrough curves show a similar picture, with CO2 being retained by TAMOF-1 the longest, therefore making a separation with the NOx compounds possible.

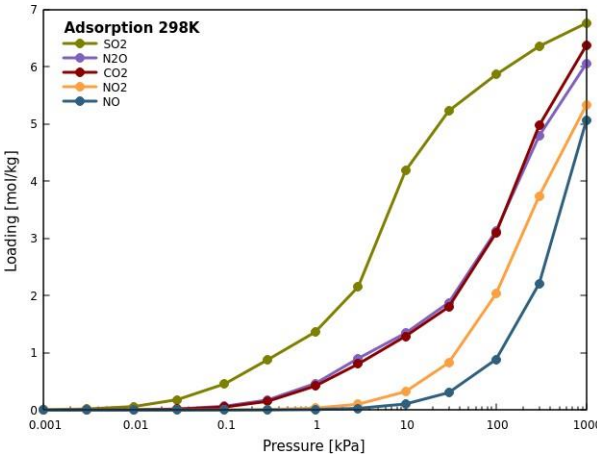

Figure 1: Pure component adsorption isotherms of flue gas components in TAMOF-1

4. Conclusions - Simulated adsorption isotherms of pure flue components, as well as flue gas mixtures, show TAMOF-1 is able to selectively adsorb CO_2 over NO_x compounds, making CO_2 capture and separation from NO_x compounds possible.

5. References

[1] https://www.eea.europa.eu/ims/global-and-european-temperatures
[2] Lin, J. et al.;. *Small*, 18, 1–23 (2022). DOI: 10.1002/smll.202105484
[3] D. Dubbeldam. et al; *Molecular Simulation*, 42, 81–101 (2016). DOI:10.1080/08927022.2015.1010082
[4] Sharma, S.,et al; *Molecular Simulation*, 49, 893–953 (2023). DOI: 10.1080/08927022.2023.2202757

O26: *In silico* study of the interactions of maqui anthocyanin extracts with biological receptors. Implications in Crohn's disease and colon cancer

P.J. Merkling [(1)], I. García Esteban [(1,2)], M. de Miguel [(2)], A.P. Zaderenko [(1)]

[(1)] *Departamento de Sistemas Físicos, Químicos y Naturales, Universidad Pablo de Olavide, 41013 Sevilla, Spain. pjmerx@upo.es*
[(2)] *Departamento de Citología e Histología Normal y Patológica. Facultad de Medicina. Universidad de Sevilla, 41009 Sevilla, Spain*

1. Introduction – Maqui berries are a natural source of significant amounts of anthocyanins that are known to have an antioxidant and anti-inflammatory effect. As such, they show promise in the prevention and treatment of Inflammatory Bowel Disease (IBD) such as Crohn's Disease (CD). This is especially relevant given that these diseases are on the rise worldwide and are often a first stage towards colon cancer. Therefore, it would be especially interesting to identify those molecules that also inhibit receptors responsible for the progress of cancer. In this sense, some polyphenols are especially interesting given that in addition to their antioxidant activity, they have been found to interact with receptors involved in the tumour genesis and growth. One of the most relevant receptors is the family known as Epidermal Growth Factor Receptor (EGFR) [1].

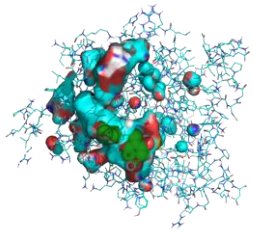

Image 1. Delphinidin physically adsorbed on an EGFR

In this work, we encapsulate the active components of maqui in a polyphenol nanoparticle (TAMA) made of tannic acid (TA), which has been shown to encapsulate active agents and enable their cellular intake [2], and maqui (MA) extract. We examine the effectiveness of TA, MA and TAMA in the treatment of CD in a murine model. In a further development, we study *in silico* the ability of the active compounds to bind to EGFR members and inhibit cell proliferation.

2. Experimental – TAMA nanoparticles were synthesized by a co-precipitation method developed in our group [2] and characterized by DLS, FTIR and SEM. Balb/c was used as murine model. The adsorption onto several types of EGFR (specifically HER1 and HER2) of the following delphinidin derivatives have been examined by molecular docking: Delphinidin (del), myrtillin or delphinidin-3-glucoside (del-3-glu), delphinidin-3,5-diglucoside (del-3,5-diglu), and delphinidin-3-sambudioside-5-glucoside (del-3-sa-5-glu).

3. Results and Discussion – Our results show that TA can form TAMA nanoparticles whose properties (hydrodynamic diameter, zeta potential, loading capacity and loading efficiency) are suitable for biomedical applications. The results in the murine model show that there is a synergy between TA and MA so that the TAMA nanoparticles are more effective than TA or MA alone. The strength of the interaction between TA or MA and EGFR receptors is comparable to current clinical first-line drugs. As can be seen in Image 1 for del, the ligand fits very well in the receptor cavity formed by the tyrosine kinase domain. In general terms, whereas TA shows a stronger affinity for the HER1 family of EGFR, the compounds of MA extract show a stronger affinity for HER2.

4. Conclusions - In the *in vivo* assays, TAMA nanoparticles show an improved effect over their individual components. As found in the *in silico* study, TAMA nanoparticles have the advantage of targeting two members of the EGFR family (HER1 and HER2), so that should a resistance to one of the compounds evolve, the other would still remain an effective tumour growth inhibitor.

5. References

[1] I. de Lavera, P.J. Merkling, J. M. Oliva, M.J. Sayagués, D. Cotán, J.A. Sánchez-Alcázar, J.J. Infante, A.P. Zaderenko. EGFR-targeting antitumor therapy: Neuregulins or antibodies? *Eur J Pharm Sci.* **158**, (2021) 105678, doi: 10.1016/j.ejps.2020.105678.

[2] J.R. Aguilera, V. Venegas, J.M. Oliva, M.J. Sayagués, M. de Miguel, J.A. Sánchez-Alcázar, M. Arévalo-Rodríguez, A.P. Zaderenko. Targeted multifunctional tannic acid nanoparticles *RSC Advances*. **6** (2016), p. 7279-7287.

O27: One MOF to find them ALL, one MOF to separate them and enrich methane streams

E. Andrés-García [(1)], G. Mínguez Espallargas [(1)]

[(1)] Crytal Engineering Lab (CEL), Instituto de Ciencia Molecular (ICMol); Universitat de València, Paterna, Spaineduardo.andres@uv.es

1. **Introduction -** The evolution of global energy demand shows an average annual growth of 1.7%. In the short term, fossil fuels will continue to be fundamental in the multidisciplinary field of energy. In this scenario, the importance of separation processes has been globally recognized. Industrial separation is not only crucial for production requirements but also in terms of investment and operation costs. Nowadays, almost 70% of the energy costs in a typical chemical plant derived from separation processes, what, consequently, derives in up to 10% of world energy consumption. The implementation of novel knowledge in industry brings tremendously advantageous impacts: i) economic benefit, reporting larger budgets; and ii) transfer benefit, reaching a wider public.
   Adsorption appears to be the most promising alternative. due to its low energy requirements, convenient regeneration and vast material availability. Pressure Swing Adsorption (PSA) is the most common and efficient industrial application based on adsorption. The major problem in the industrial development of thermochemical processes, is the production of contaminants. The typical flue gas contains many trace contaminants, such as metal derivatives, light hydrocarbons, secondary combustion products and, obviously, CO_2 and water. These contaminants have disadvantageous synergistic effects. Despite the importance of these operating conditions, they are often neglected in literature.
   The tunability of Metal-Organic Frameworks (MOFs) places them as the most promising available adsorbents. These hybrid networks are formed by multiple metal-ligand bonds, allowing almost infinite possible combinations: this adaptability places them as the most interesting available adsorbent. In addition, pore post-modification can complement their tunability, by creating larger mesopores through framework "*defects"*. Indeed, many MOFs have been already reported efficient for diverse gas separation, usually with some limitation in the operation conditions, and mostly for binary/ternary mixtures.

2. **Experimental -** For textural characterization, low-pressure N_2 and CO_2 volumetric isotherms were carried out in a Tristar II Plus Micromeritics sorptometer, at 77 K and 273 K, respectively. Activation, overnight and under vacuum condition, was set in a range from 373 to 423 K.
   If necessary, high-pressure gravimetric adsorption isotherms were measured at different temperatures, ranging from 283 to 333 K, in an IGA-100 gas sorption analyser (Hiden Isochema). Equilibrium conditions corresponded to 600 s interval, and 0.001 mg min^{-1} tolerance.
   Dynamic adsorption experiments were performed on an ABR (HIDEN Isochema) instrument. It is a *breakthrough* setup based on a fixed-bed adsorption column. In a typical experiment, pressure, temperature, and inlet composition are set and controlled, and the outlet composition was analysed, by an integrated mass spectrometer (HPR-20 QIC). The column was filled with different samples. Before every measurement, each sample was regenerated at atmospheric temperature and pressure in 15 mL min^{-1} Ar flow for 20 min. Operation conditions ranged from 283 to 333 K, and from 1 to 10 bar. The inlet gases mixtures consisted of a 15 mL min^{-1} dilution of CO_2, and C2-C4 hydrocarbons in methane, resembling expected industrial compositions. Time zero, in the analysis, is set with the first detection of helium due toits use as a tracer (1 mL min^{-1} of He in the feed flow). When using moisture condition, to arrange wet-gasinlet flows, a bubbler was installed in the setup upstream the column.

3. **Results and Discussion** - In order to achieve an enriched methane outlet stream, diverse (both novel, and reported) materials have been tested in our setups, under the previously described operation conditions. Light hydrocarbons inlet mixtures derived in different *breakthrough* profiles, depending on the variety of MOF structures. Some of them manage to separate all the hydrocarbon impurities from a methane (natural gas) stream, and a few group is even able to order by size all hydrocarbons from C2 to C4.
   The influence of carbon dioxide and water in the inlet stream (common industrial contaminants) was studied to evidence the potential of these adsorbents, and to reject the candidate with low moisture stability.
   Although kinetics displays a mayor role in these complex separation processes, thermodynamics effect increases the adsorption potential, providing a larger (and purer) methane outlet flow.

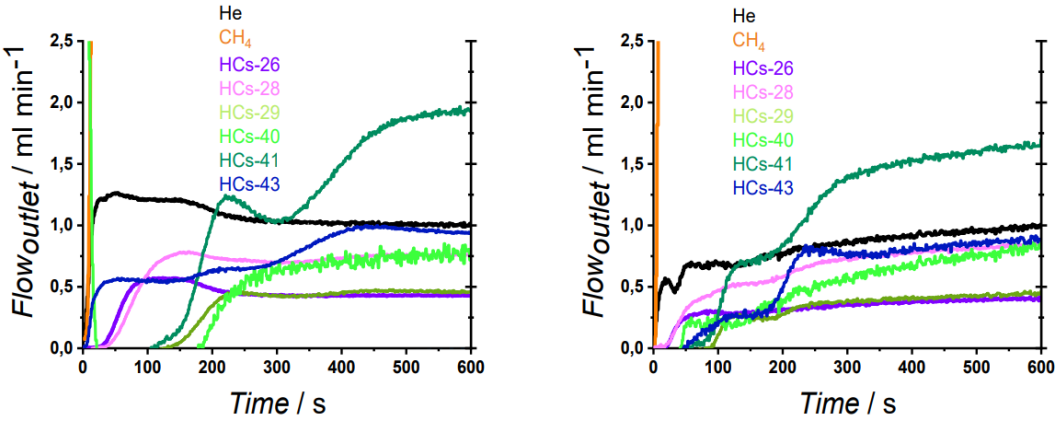

Image 1. Breakthrough exit flow rates at 298 K and 1 bar, for C1-C4 hydrocarbons inlet mixture, on: *right*) reported microporous MOF; *left*) novel mesoporous-induced structure, for the previously reported MOF.

4. Conclusions - In order to promote their future application in diverse industrial separation processes, one single MOF is able to separate gases from a mixture above 10 components. In the first time than such a complete mixture is studied in gas separation measurements. The effect of carbon dioxide and water (moisture) presence in the mixture is also evaluated for the most promising materials, reaching a completeseparation analysis of 15-gases inlet streams.

By combining thermodynamic and kinetic mechanisms, we manage to complete this challenging procedure,obtaining a profitable clean methane outlet flow.

5. References

[1] Chatterjee, A. K.; Morgan, J. P.; Scholl, M.; Grubbs, R. H. *J. Am. Chem. Soc.*, **122**, (2000) p. 3783.
[2] Wankat, P. C. *Separation Process Engineering* (4th ed.). Prentice Hall, 2017.
[3] Sholl, D. S. & Lively, R. P. *Nature*, **532**, (2016) p. 435.
[4] Alonso-Vicario, A. et al. *Microporous Mesoporous Mater.*, **134**, (2010) p. 100.
[5] Zhou, H.-C., Long, J. R. & Yaghi, O. M. *Chem. Rev.*, **112**, (2012) p. 673.
[6] Gan, L., et al. *ACS Appl. Mater. Interfaces*, **15**, (2023) p. 5309.

RIA 43
XLIII Reunião Ibérica de Adsorção
Porto, Portugal
1-4 September 2024

O28: Advancing Sustainability through Gas Adsorption and Reaction Technologies

Patrick S. Bárcia, M. Salomé Macedo

Rua do Comendador Brandão 461, 4495-375 Póvoa de Varzim, Portugal
patrick.barcia@sysadvance.com
salome.macedo@sysadvance.com

1. Introduction

SYSADVANCE was founded in Porto (Portugal) in 2002 as an academic spin-off of the Chemical Engineering Department of the Faculty of Engineering of University of Porto.

Over the last two decades, SYSADVANCE has become a leading innovator in applying the principles of adsorption science and technology to develop industrial processes either for onsite production of N_2 and O_2 (including Medical Oxygen93), or for renewable gases purification such as biogas (from anaerobic digestion of landfill gas), helium (He) or hydrogen (H_2) from photovoltaic solar or synthetic gas.

Image 1. Sysadvance headquarter in Póvoa de Varzim (Portugal).

Since its foundation, the company has experienced significant and continuous growth as result of its customer-centric strategy, its highly qualified technical personnel and strong R&D culture, as well as its superior technology and reliability proven with +5000 PSA systems operating in more than 50 countries.

The SYSADVANCE's comprehensive technology portfolio has transformed the gas production landscape by significantly reducing energy consumption, carbon footprint, and enhancing industrial gas and energy supply autonomy.

2. Adsorption Technology

Microporous adsorbents are the core of SYSADVANCE's gas purification technologies. The proper selection of adsorbents is a key step to increase productivity, extend separation media lifetime, or improve process energy efficiency.

Vacuum pressure swing adsorption (VPSA) can be designed with different adsorbents, or combinations of those (mixed or layered), depending on the major contaminants present in the gas and on the product gas specifications. This feature represents a strong advantage of the adsorption-based technology as it allows process integration by properly combining, in a single separation step, several adsorbents exhibiting different separation mechanisms (*e.g.*, equilibrium and kinetic selectivity).

3. Technology Portfolio

The current geopolitical situation has highlighted the vulnerability of EU's energy system in regards to autonomy and safety. Making our energy use more efficient is one of the most achievable steps we can take towards decarbonization and improving energy security.

Onsite production of industrial gas

Within this frame, Sysadvance deploys a portfolio of adsorptive technologies for gas purification with significant energy saving potential for both industry and medical sectors. The main driver is the decentralization of industrial gas production (O_2 and N_2) combined with a judicious adjustment of the quality grade based on the particular requirements of each application. As an example, tank blanketing operations (often requiring large volumes of N_2 with 98.0 vol.% grade) can be supplied by on-site N_2 production plants with a reduction of 75% on the specific power consumption when compared for instance to a pharmaceutical application which generally request higher N_2 purity grade (usually ≥ 99.999 vol.%). Decentralized production helps to abate CO_2 emissions associated not only with the production but specially with the gas distribution logistics from the Air Separation Units (ASU) to the final consumption point, improving the sustainability of the industry sector.

Biogas upgrading

Reducing the global economy energy intensity through energetic efficiency is only the first step to achieve the sustainability targets. As the energy transition takes place, it is fundamental to implement and scale-up

renewable alternatives that can substitute fossil fuel. The heating value of biomethane is similar to natural gas (HHV > 10.7 kWh/Nm^3), being at the same time a fundamental vector of development for a profitable waste valorisation chain. *METHAGEN AD* is a cyclic adsorption process developed by Sysadvance for the production of biomethane from biogas. Its new VPSA scheme is able to recycle a major fraction of the CH_4 content from the tail-gas increasing then the CH_4 recovery rate. This upgrade allows *METHAGEN AD* to meet the stringent CH_4 emission regulations expected to enter in force by 2025 in some territories like France.

Image 2. (Left) *METHAGEN AD* for agricultural waste biogas in Premery, France: biomethane for grid injection; (right) *METHAGEN AD* upgrading biogas produced from chicken manure in Iecava, Latvia: biomethane for grid injection.

Biogenic CO_2 is the tail gas released during the regeneration step of *METHAGEN AD* with an average concentration of 96 vol.%. This by-product can be stored or purified for either food & beverage sector, greenhouse production or for a variety of industrial applications. An alternative valorisation pathway for CO_2 consists on its use for renewable energy storage. Sysadvance *e-METHAGEN* process (currently in final stage of development) promotes the reaction of CO_2 with green H_2, via catalytic methanation. CO_2 reacts at 350 °C with H_2 to be converted into CH_4 and H_2O through exothermic reaction. The product is then dried by a thermal regeneration adsorber producing synthetic CH_4 (*e*-GAS) which can be stored in the grid.

Hydrogen production from syngas and electrolysis

As biomethane, H_2 is also a clean and versatile energy carrier that can help in reducing our reliance on fossil fuels and transition to a low-carbon economy. *METHAGEN Pure* is a VPSA process highly efficient process for purifying H_2 from syngas, and it is used in a variety of applications, including fuel cells, metal treatment, and chemical synthesis. In the VPSA packed bed, strongly adsorbed molecules like carbon monoxide, CO_2, water (H_2O) and methane (CH_4) are trapped in solid phase micropores while the weakly adsorbed H_2 pass through the bed being obtained as high purity grade product. Once saturated, the adsorbent undergoes a regeneration step either by reducing pressure, applying vacuum or performing counter-current purge with a fraction of the raffinate.

Image 3. H_2 deoxidation and drying system.

Electrolytic H_2, by its turn, is typically saturated with H_2O containing as well residual O_2 which makes it unsuitable for direct use in fuel cells. To overcome this, SYSADVANCE launched recently in the market the *METHAGEN Pure* C which combines catalytic deoxidation and H_2O adsorption steps to produce high purity grade H_2 complying with fuel quality standard SAE J2719:2020 and ISO 14687:2019.

4. Conclusions

Relying on gas adsorption and reaction science and technologies SYSADVANCE's processes portfolio has meaningfully contributed over the last two decades for the transition towards a more sustainable world by transforming gas production and purification industry landscape.

RIA 43
XLIII Reunião Ibérica de Adsorção
Porto, Portugal
1-4 September 2024

O29: Optimizing CO_2 capture in pressure swing adsorption units: A deep neural network approach with optimality evaluation and operating maps for decision-making

Carine Menezes Rebello[(1)], Idelfonso B.R. Nogueira[(1)]
[(1)] *NTNU*
Principal Author's e-mail: carine.m.rebello@ntnu.no

Abstract – This study presents a methodology for surrogate optimization of cyclic adsorption processes, focusing on enhancing pressure swing adsorption units for carbon dioxide (CO_2) capture. We developed and implemented a multiple-input, single-output (MISO) framework comprising two deep neural network (DNN) models, predicting key process performance indicators. These models were then integrated into an optimization framework, leveraging particle swarm optimization (PSO) and statistical analysis to generate a comprehensive Pareto front representation. This approach delineated feasible operational regions (FORs) and highlighted the spectrum of optimal decision-making scenarios. A key aspect of our methodology was the evaluation of optimization effectiveness. This was accomplished by testing decision variables derived from the Pareto front against a phenomenological model, affirming the surrogate model's reliability. Subsequently, the study delved into analyzing the feasible operational domains of these decision variables. A detailed correlation map was constructed to elucidate the interplay between these variables, thereby uncovering the most impactful factors influencing process behavior. The study offers a practical, insightful operational map that aids operators in pinpointing the optimal process location and prioritizing specific operational goals.

O30: Exploring the development of hydrochars from wet olive cake biomass as adsorbents for pharmaceutical compounds

Esperanza Romero[1*], Adriana Moral-Rodríguez[1], Celia Cifuentes Urien[1], Rogelio Nogales[1], Ana Sofía Mestre[2]

(1) Estación Experimental del Zaidín, Agencia Estatal del Consejo Superior de Investigaciones Científicas (EEZ-CSIC), C/ Profesor Albareda 1, 18008 Granada, España
(2) Centro de Química Estrutural, Institute of Molecular Sciences, Faculdade de Ciências, Universidade de Lisboa, Campo Grande, 1749-016 Lisboa, Portugal
**Esperanza.romero@eez.csic.es.*

1. Introduction – Wet olive cake (WOC in Spain known as *alperujo*) is a solid by-product generated during the two-phase extraction of olive oil (Image I) and contains a high amount of water (65-70%). Previous studies have shown that hydrothermal carbonization (HTC), a process that does not require pre-drying and consumes low energy compared to pyrolysis, can be a promising method to convert this biomass into a value-added carbon material capable of removing pharmaceutical compounds [1]. In this study, we explore two options to enhance the adsorption capacity of these hydrochars by employing direct steam activation or acid-mediated carbonization (AMC) followed by steam activation. The two newly synthesized materials were characterized physically and chemically, and tested as adsorbents for the removal of diclofenac (DCF) and iopamidol (IOP) from aqueous solutions.

Figure 1. Wet olive cake or *alperujo* from two-phase extraction of olive-oil

2. Experimental –A sample of WOC was subjected to hydrothermal carbonization (HTC) at a combustion temperature of 190 °C under autogenous pressure for 6 hours. After the HTC process, one fraction was washed with water and sieved (149µm) yielding the hydrochar. The other fraction was treated with sulphuric acid 13.5 M for 6 hours at 90°C (AMC), as described by Mestre et al., 2019 [2], yielding the acid-char. Subsequently, hydrochar and acid-char were steam activated under nitrogen stream at 900ºC for 1 hour (HSAc and ASAc, respectively) following the methodology described by Mestre et al. 2022 [3]. The nanoporous carbon materials obtained were characterized by N2 adsorption at -196 °C, pH at the point of zero charge (pHpzc) and apparent density.
Sodium diclofenac (DCF) and iopamidol (IOP) were used as target pharmaceutical compounds. Single-solution adsorption tests were conducted using adsorbent concentrations of 0.3 and 0.15 g/L. The adsorption kinetics were performed with pharmaceutical concentration of 90 mg/L for HSAc and 180 mg/L for ASAc. In all suspensions, the pH values of the initial concentrations were adjusted to pH 7, which is close to the measured pH value of 6.9 in effluent from the WWTP of Emasagra (Granada). The suspensions were shaken in a thermostatic chamber at 25±1°C for 0.16, 0.33, 1, 3, 6, 9, 12, 24 and 48 hours. All samples were filtered through 0.22 µm PTFE filter and analysed in a UV-vis spectrophotometer at appropriate wavelengths. Adsorption isotherms were carried out at pharmaceutical concentration ranging from 10 to 120 mg/L for HSAc and from 60 to 300 mg/L for ASAc following the procedure described for the kinetics experiments. The experimental data were fitted to the pseudo-first and pesdudo-second order kinetic models and to the Langmuir and Freundlich isotherm equations. A commercial activated carbon, Norit SAE- SUPER, was used for benchmarking.

Table I. Activated yield, textural parameters, apparent density and pHpzc of hydrochar derived (HSAc) and acid-char derived (ASAc) steam activated carbons

Materials	Yield (wt %)	S_{BET} ($m^2\ g^{-1}$)	W_0[a] ($cm^3 g^{-1}$)	L_0[b] (nm)	$V_{0.97}$[c] ($cm^3 g^{-1}$)	V_{meso}[d] ($cm^3 g^{-1}$)	App. Density ($Kg\ m^{-3}$)	pHpzc
HSAc	16	596	0.23	1.26	0.58	0.35	178	11
ASAc	22	1180	0.45	1.22	0.64	0.19	294	9

3. Results and Discussion – The N_2 adsorption isotherms and textural parameters, along with apparent density and pH at the point of zero charge (pHpzc) of the samples, are presented in figure 1a and Table I.
Both activated carbons exhibited a type I+IV isotherm (Figure 1a) characteristic of micro-mesoporous materials. The upward deviation along the whole p/p0 range is more pronounced for the hydrochar-derived material (HSAc) pointing for a larger volume of mesopores, the acid-char derived activated carbon presents a relative lower

volume of micropores (Figure 1 and Table I). The acid-mediated carbonization of the hydrochar followed by the steam activation allowed to increase the BET surface areas from 596 m2 g-1 in the hydrochar-derived activated carbon to 1180 m2 g-1, at no expenses of the activation yield that is similar.

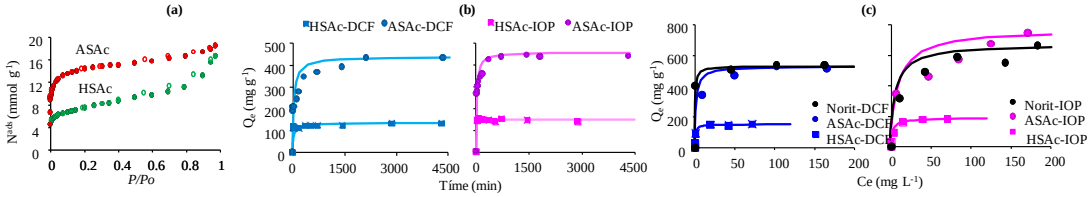

Figure 2. N_2 adsorption isotherms for HSAc) and ASAc (a). Adsorption kinetics for DCF and IOP (b), and adsorption isotherms for commercial Norit SAE-SUPER activated carbon as well as for the lab-made activated carbons (c). The symbols are experimental data, and the lines are the pseudo-second order kinetic equation or Langmuir isotherms.

The pseudo-second order adsorption kinetic fit model well the experimental data obtained for HSAc y ASAc (Fig. 1b and Table II). The adsorption rate constant (K_2) of DCF and IOP for the HSAc is, respectively, 3 and 33 times greater than that of ASAc, in line with its higher mesopore volume (Table I). Although the initial concentration of DCF and IOP was twice as high for the assay with ASAc, the adsorbed percentages in both cases were ~ 40 %. of DCF was adsorbed on HSAc in half an hour, and IOP in even less time.

Table II. Fitting parameters of the pseudo-order kinetic

Parameter	Unit	HSAc		ASAc	
		DCF	IOP	DCF	IOP
Ci	mg L^{-1}	90		180	
q_e	mg g^{-1}	133	147	435	455
K_2 x 10^{-5}	mg g^{-1} min^{-1}	22	382	3.6	11.4
R^2		0.99	0.99	0.99	0.99
Ads	%	44	46	39	40
$t_{1/2}$	min	34	2	64	19

The adsorption isotherms (Fig. 1c) revealed a higher maximum adsorption capacity (Table III) for ASAc of DCF and IOP in accordance with the higher volume of micropores (Table I). The adsorption performance of ASAc is comparable to that of commercial Norit materials, in the case of DCF and even superior for IOP.

Table III. Fitting parameters of the Langmuir isotherm

Parameter	Unit	HSAc		ASAc		Norit	
		DCF	IOP	DCF	IOP	DCF	IOP
q_m	mg g^{-1}	151	189	526	769	526	667
K_L	mL mg^{-1}	1.12	0.34	0.40	0.07	1.19	0.10
R^2		0.999	0.997	0.999	0.966	0.998	0.979

Given that both carbons have pHpzc values greater than 9, at pH 7 of the suspension they will present positively charged surfaces, favouring electrostatic interactions with diclofenac anion. IOP, with a pKa of 10.7, is in molecular form at pH 7, and its main adsorption mechanism would be through π-π interactions or hydrogen bonding (e.g. carboxyl/carbonyl group of IOP and the -OH group of the materials.

4. Conclusions – Steam activation of hydrochar and acid-char synthetized from WOC allows to obtain activated carbons with well-developed but different pore structure: higher abundance of micropores and larger apparent surface area for acid-char derived material (ASAc) while hydrochar-derived activated carbon (HSAc) has the highest mesopore volume. The size of the micropores does not hinder the adsorption of IOP (the most voluminous compound) but requires longer equilibrium times than in the case of DCF.

Acknowledgements – E. Romero would like to thanks the Spanish Ministry of Universities for funding a stay for teaching staff and/or senior researchers in foreign centres (PX22/00265) and to the project PID2020-116210RB-I00 (MCIU, AEI, FEDER). Centro de Química Estrutural is a Research Unit funded by Fundação para a Ciência e Tecnologia (FCT) through projects UIDB/00100/2020 and UIDP/00100/2020 (DOI 10.54499/UIDB/00100/2020 and 10.54499/UIDP/00100/2020). Institute of Molecular Sciences is an Associate Laboratory funded by FCT through project LA/P/0056/2020 (DOI 10.54499/LA/P/0056/2020). ASM thanks FCT for the Assistant Researcher contract (DOI 10.54499/PTDC/EQU-EQU/6024/2020).

5. References

[1] L. Delgado-Moreno, S. Bazhari, G. Gasco, A. Méndez, M. El Azzouzi, E. Romero, *Sci Total environ*. 752, (2021) p. 141838.
[2] A.S. Mestre, F. Hesse, C. Freire, C.O. Ania, A.P. Carvalho, *J Colloid Interface Sci* 536 (2019) 681-693.
[3] T.S. Hubetska, A.S. Mestre, N.G. Kobylinska, A.P. Carvalho, *Nanomaterials* 12 (2022) 3480.

O31: Unravelling the water adsorption mechanism of a luminescent optical fibre sensor silica xerogel membrane

Guillermo Cruz-Quesada [(1)(2)], Beatriz Rosales-Reina [(2)], Diego López-Torres [(3)], Santiago Reinoso [(2)], María Victoria López-Ramón [(4)], Gurutze Arzamendi [(2)], César Elosua [(3)], Maialen-Espinal Viguri [(2)], Julián J. Garrido [(2)].

[(1)] *guillermo.cruz@unavarra.es*
[(2)] *Institute for Advanced Materials and Mathematics (INAMAT²) & Departamento de Ciencias, Public University of Navarre (UPNA), Campus de Arrosadía, 31006, Pamplona, Spain.*
[(3)] *Institute of Smart Cities (ISC) & Departamento de Ingeniería Eléctrica, Electrónica y de Comunicación, Public University of Navarre (UPNA), Campus de Arrosadía,31006 Pamplona, Spain.*
[(4)] *Departamento de Química Inorgánica y Orgánica, Facultad de Ciencias Experimentales, University of Jaén, 23071 Jaén, Spain.*

1. Introduction – Porous silica xerogels (XGs) are known for their easy sol-gel synthesis and customised chemical and textural properties. In fact, due to their structural and thermochemical stability, they can also be used as matrices to host a variety of functional substances, such as lanthanide ions (Ln) with an antenna ligand (AL) that endows luminescence to these materials. Beyond these characteristics, XGs show additional features suitable to develop coatings for optical fibre sensors (OFS), such as a refractive index analogous to that of optical fibres and transparency in a wide wavelength range. Therefore, since luminescence can be used as the transduction mechanisms in an OFS coated with a lanthanide doped XG film, since its response decreases when it is exposed to gases or vapours containing luminescence quenching molecules, such as water or alcohols. On this ground, this work was conceived to explore the correlation between the response of a water-vapour OFS and the textural properties of the luminescent XG used as the sensitive coating. For this purpose, the isosteric heat of adsorption (ΔH_{ads}) of water vapour of two systems containing Tb^{III} and a tridentate chelate as the antenna ligand (PB) (Image I): a XG monolith (Tb-PB) and an OFS coated with a XG film (OFSTb-PB), was determined and compared.

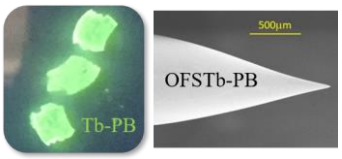

Image I. Tb-PB monolith and scanning electron micrograph of OFSTb-PB.

2. Experimental - Ln-PB was obtained as monoliths using $Tb(NO_3)_3{\cdot}6H_2O$ and following a sol-gel approach adapted from our previous works [1]. The non-commercial antenna ligand PB (2,2′-(4-(2-Ethoxyethoxy)pyridine-2,6-diyl)bis(4,5-dihydrooxazole)) was synthesised following the procedure described in the literature [2]. To prepare the sensor, the Ln-PB film was deposited onto the tip of a tapered fibre by dip-coating into sol-gel mixture at 75% of the gelation time. $H_2O_{(v)}$ adsorption isotherms of Tb-PB were obtained using the vapour kit of a Micrometrics ASAP2020 volumetric adsorption system, while the OFSTB-PB response toward 10 increasing and decreasing cycles of 20–90% relative humidity was recorded using a photonic experimental set-up that is described in the literature [3]. The isotherms and the sensor response were both recorded at three different temperatures (298 K, 303 K, and 308 K).

3. Results and Discussion - The variation of the OFSTb-PB response ($-\Delta I/I_{ref}$) increases linearly with the concentration of water vapour (C_{H2O}) due to the quenching of luminescence by water molecules, and it follows the C_{H2O} setpoint in all cycles. However, in the adsorption branch, when a certain value of C_{H2O} is reached, the response deviates abruptly from linearity to a third-grade polynomial tendency. Furthermore, the differences between the adsorption and desorption branches give rise to significant hysteresis loops, which widen as the temperature increases and relate to the retention of water molecules within the coating. On the other hand, although Tb-PB was found to be mainly microporous using the standard adsorbate N_2, it was mesoporous for H_2O since water molecules are smaller, more polar, and have higher kinetic energy in the adsorption process. Like in the OFSTb-PB response, water molecules are adsorbed in Tb-PB following a linear trend at low partial pressures, but this behaviour changes when certain p/p_0 values are reached and the capillary condensation begins in the mesopores. To demonstrate that the deviation of the OFSTb-PB response is indeed due to the capillary condensation of water in the mesopores of the xerogel film, the sensor response towards humidity could be explained in terms of analyte-adsorbent interactions by a mere comparison between ΔH_{ads} of the Tb-PB monolith and that of the sensor XG coating. Image II

shows the evolution of ΔH_{ads} values, calculated using the Clausius-Clapeyron equation, for both systems. The graph on the left indicates that in the sensor ΔH_{ads} becomes less negative with increasing $-\Delta I/I_{ref}$ until reaching a plateau at −34.5 kJ·mol^{-1}, which is consistent with a less exothermic process as more water molecules are adsorbed. Values higher than the theoretical one corresponding to water condensation ($\Delta Hcond$ = −40.7 kJ·mol^{-1}) agree with the predominance of condensation over adsorption. In close analogy to what has been commented for the sensor, the graph on the right depicts that ΔH_{ads} gradually increases with the amount of physiosorbed water (n_a) in Tb-PB until a plateau is reached at n_a 7.5–8.0 mmol·g^{-1}, which is a value similar to those calculated for the monolayer capacities of the monolith. Therefore, in both cases ΔH_{ads} increment until reaching the plateau, finally confirming that the loss of linearity in the OFSTb-PB response originates from the beginning of capillary water condensation in the mesopores.

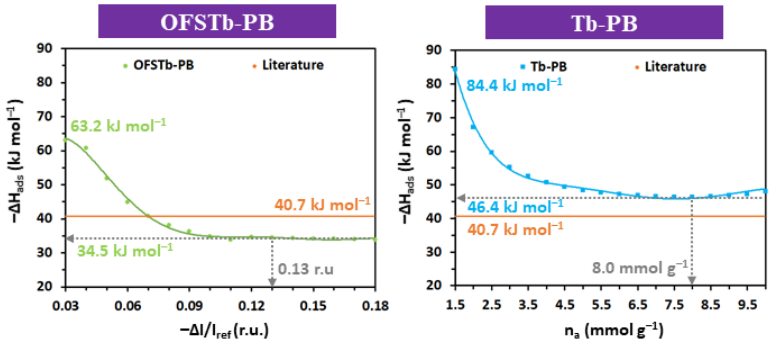

Image II. Evolution of the Isosteric enthalpies of adsorption

4. Conclusions - This work has established a correlation between the response of a luminescent probe and its textural properties, and proposes a plausible adsorption mechanism to explain the non-linear response of the sensor based on capillary condensation within mesopores.

5. References

[1] J. Estella, J.C. Echeverría, M. Laguna, and J.J. Garrido, *J. Non Cryst. Solids*, **353**, (2007) p. 286–294.
[2] A. de Bettencourt-Dias, P.S. Barber, S. Bauer, *J. Am. Chem. Soc.* **134** (2012) p. 6987–6994.
[3] G. Cruz-Quesada, B. Rosales-reina, D. López-Torres, S. Reinoso, M.V. López-Ramón, G. Arzamendi, M. Espinal-Viguri, and J.J. Garrido, *Sens. and Actuators B Chem*. **406** (2024) p. 135369.

O32: Adsorption of small molecules on zeolite SSZ-45

Alberto Barros, José Valero, Susana Valencia, Fernando Rey

Instituto de Tecnología Química, Universitat Politècnica de València – Consejo Superior de Investigaciones Científicas (UPV-CSIC), 46022 Valencia (Spain)
abarpar@itq.upv.es
jovaji2@upvnet.upv.es, svalenci@itq.upv.es, frey@itq.upv.es

1. Introduction – The increasing global demand for energy, driven by technological advancements and population growth, poses a significant challenge. According to the Energy Information Administration (EIA) in 2007, there is a projected 57 % increase in energy demand from 2004 to 2030 [1]. A substantial portion of the world's energy consumption, ranging from 10 to 15%, is attributed to separation processes of various chemical compounds. These separations involve processes such as cryogenic distillations, amine scrubbing or extraction-evaporation-distillation that could be replaced by separation units based on the use of porous materials as selective adsorbents. Crystalline porous materials have been extensively studied as exceptional adsorbents for selective gas separation due to their high versatility in pore engineering [2].

Small-pore zeolites are of particular interest for molecules separations due to their large pore volume and preferential guest molecule size exclusion [3]. In particular, high-silica small-pore zeolites combine fine molecular sieving and high thermal stability resulting in appropriate candidates for small molecules separations.

This study is focused on the high silica zeolite SSZ-45 that belongs to this category and consists of a one-dimensional pore system of 8R channels with large side pockets [4]. In the present work, the adsorption properties of zeolite SSZ-45 have been studied by single component adsorption isotherms of small molecules to evaluate its capability for different separations.

2. Experimental - Zeolite SSZ-45 was synthesized according to a reported recipe [4] and characterized by using different techniques, such as powder X-ray diffraction (XRD), scanning electron microscopy (SEM), solid state NMR, and determination of textural properties by N_2 and CO_2 adsorption. The adsorption capacities of different gases (CO_2, CH_4, C_2H_6 and C_2H_4) were measured in a volumetric adsorption instrument (iSorb HP, Quantachrome) at high pressure and different temperatures for studying the adsorption behaviour by means of the corresponding thermodynamic and kinetic parameters.

3. Results and Discussion - The zeolite SSZ-45 was successfully synthesized as confirmed by its characterization using XRD, SEM and textural properties determination. The high pressure adsorption measurements revealed that CO_2 exhibits the highest uptake, followed by C_2H_4 and C_2H_6, with CH_4 showing the lowest below 200 kPa (Figure 1). Above this pressure, C_2H_6 is the least adsorbed molecule, which may be related to the nature of SSZ-45 being a small pore zeolite with a narrow aperture and the limitations for molecules whose size and shape prevent entry into the cavities can lead to diffusional restrictions.

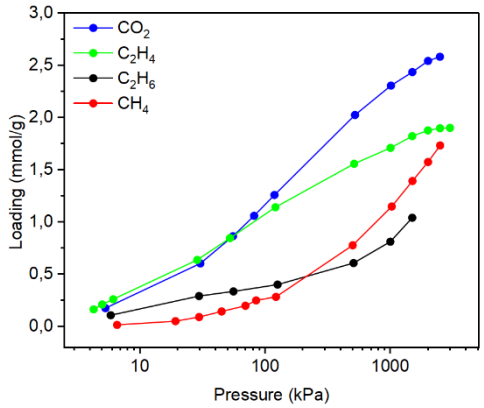

Figure 1. Adsorption Isotherms of different adsorbates on zeolite SSZ-45 at 298 K.

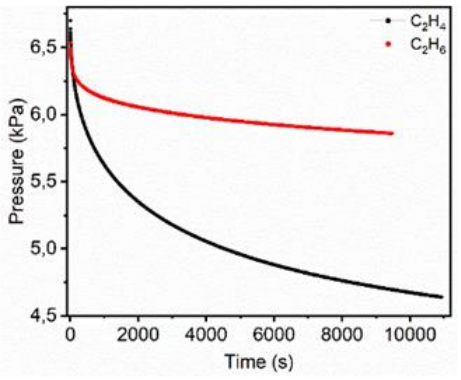

Figure 2. Kinetic study of C_2H_4 (black) and C_2H_6 (red) adsorption on SSZ-45 at 298 K.

As can be seen in Figure 1, CH_4 adsorption follows a type I isotherm tendency, but less squared that CO_2, which means that CH_4 molecules interact less strongly than CO_2 ones with the solid. This suggests that CO_2 and CH_4 could be thermodynamically separated using this zeolite.

Only C_2H_4, CH_4 and CO_2 reached thermodynamic equilibrium, confirming the diffusional restrictions for C_2H_6. In the case of the adsorption of the C_2H_6 and C_2H_4, the difference in the diffusion rates between the olefin (C_2H_4) and the paraffin (C_2H_6) could be the reason for the different adsorption behaviour, allowing a possible kinetic separation of both adsorbates. Figure 2 shows the pressure drop in the measuring cell caused by the adsorption of the C_2H_6 and C_2H_4 by the zeolite. As deeper is the pressure drop, higher is the diffusion of this component within zeolite microporores. Therefore, it is clearly seen that C_2H_4 is the fasted adsorbed molecule instead of its corresponding paraffin. Thus, zeolite SSZ-45 shows a promising kinetic separation mechanism, wherein the olefin exhibits greater adsorption compared to the paraffin. This suggests the potential for a less energy-intensive process to selectively separate one over the other based on SSZ-45's distinctive kinetic separation properties.

The calculation of isosteric heats of adsorption of the different adsorbates studied is shown in Figure 3. As can be seen in the figure, CH_4 is the molecule less strongly adsorbed on SSZ-45 zeolite with significant difference from CO_2, which interacts much more strongly, allowing a possible thermodynamic separation of CO_2 from CH_4 with this zeolite, as was also suggested by the isotherms shown in Figure 1.

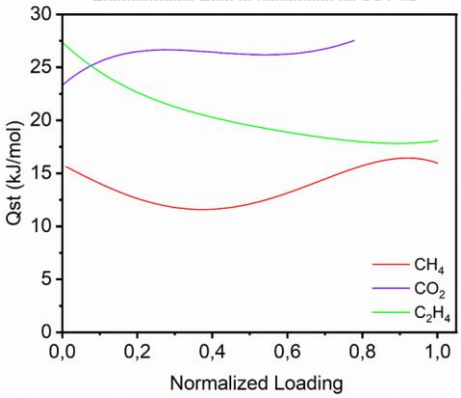

Figure 3. Isosteric heat of adsorption of CH_4 (red), CO_2 (blue), and C_2H_4 (green) on zeolite SSZ-45.

4. Conclusions - Zeolite SSZ-45 shows a promising kinetic separation mechanism, wherein the olefin exhibits greater adsorption compared to the paraffin. This suggests the potential for a less energy-intensive process to selectively separate one over the other based on SSZ-45's distinctive separation properties.

5. References

[1] H. Yang, Z. Xu , M. Fan, R. Gupta, R.B. Slimane, A.E. Bland, I. Wright, *J. Environ. Sci*. **20** (2008), 14–27.
[2] M. Dusselier, M.E. Davis, *Chem. Rev*. **118** (2018), 5265–5329.
[3] E. Pérez-Botella, S. Valencia, F. Rey, *Chem. Rev*. **122** (2022), 17647−17695.
[4] S. Smeets, D. Xie, L. B. McCusker, *Chem. Mater*. **26** (2014), 3909−3913.

O33: Mercury adsorption from water using activated carbons developed from lignocellulosic biomass

A. Arencibia [(1)], N. Izquierdo[(1)], G. Gómez-Pozuelo[(2)], M.J. López-Muñoz[(2,3)]

[(1)] Departamento de Tecnología Química, Energética y Mecánica, ESCET, Universidad Rey Juan Carlos, C/Tulipán s/n, 28933 Móstoles, Madrid, Spain.
[(2)] Departamento de Tecnología Química y Ambiental, ESCET, Universidad Rey Juan Carlos, C/Tulipán s/n, 28933 Móstoles, Madrid, Spain.
[(3)] Instituto de Tecnologías para la Sostenibilidad, Universidad Rey Juan Carlos, C/Tulipán s/n 28933 Móstoles, Spain
amaya.arencibia@urjc.es

1. Introduction

Water pollution is one of the global problems to address nowadays aiming to improve water quality and reduce human and ecosystem health impacts. Among the different types of water pollutants, heavy metals and semimetals are of concern because of their high toxicity [1]. Mercury stands out among them since it is naturally present in the environment and still used in some industrial processes, it can produce negative health effects at very low concentrations, such as respiratory problems or neurodegenerative disorders, and it is highly bioaccumulated and biomagnificated. Thus, the goal is to achieve the efficient reduction of mercury level in water as much as possible to match with the international regulation rules [2].

There are several adsorbents proposed and used as mercury adsorbents, with activated carbons being efficient and cost-effective of production. They can be produced from carbonaceous materials derived from petroleum, coal, tar, or polymers and, also, from wood or biomass. In the last decades, the valorization of carbonaceous materials has attracted the interest of many researchers due to the possibility of the conversion of biomass waste by carbonization into activated carbons with suitable properties as adsorbents. This approach simultaneously achieves the environmental waste management of bio-wastes and the reduction costs of carbon feedstock as an alternative to coal. Biomass has been presented as a key to sustainable development due to its recyclable properties and its abundant presence across the world. Moreover, many types of lignocellulosic biomass are always discarded or burned, which leads to an increase in the environmental pollution. Therefore, the use of this abundant biomass for producing activated carbon constitutes a challenge for developing low cost, environmentally friendly, and sustainable adsorbents. In this line, the aim of this work has been to develop activated carbon materials prepared from different types of agroforestry lignocellulosic biomass and analyse their properties for mercury adsorption from water.

2. Experimental

Three types of lignocellulosic biomass from agriculture, forestry, and food processing wastes, produced in Spain, were selected to be used as raw materials: rice husk (RH), eucalyptus leaves (EL), and spent coffee grounds (SC). All the biomass samples were widely characterised following the European Standards to obtain proximate (moisture, ash, volatile matter contents) and ultimate analyses (carbon, hydrogen, nitrogen, and oxygen proportions).
Before the thermal and chemical treatments, all the samples were washed, dried, crushed into a centrifugal mill, and sieved until the desired size (180-250 μm). Then, the powders so-obtained were thermally pyrolyzed under a nitrogen atmosphere to obtain the corresponding biochar samples, which were chemically activated. The role of the activating agent employed ($ZnCl_2$, KOH, and H_3PO_4) and the pyrolysis temperature (600-800 ºC) on the properties of the char was evaluated and related to the aqueous mercury adsorption behaviour. The activated carbons (AC) were characterized by thermogravimetric analysis, N_2 adsorption-desorption analysis, elemental analysis, Scanning Electron Microscopy (SEM), and FTIR spectroscopy.

Mercury adsorption experiments were carried out in batch mode to obtain the equilibrium adsorption isotherms of the prepared activated carbons as well as to study the kinetic performance. Mercury chloride was used as mercury source and the Hg(II) aqueous concentration varied from 5 to 150 mg/L. Mercury concentration in aqueous solution was determined by atomic Fluorescence spectroscopy (CV-AFS).

3. Results and Discussion

The results showed that the prepared activated carbons are microporous, with moderate values of BET surface areas. A significant effect of the type of activating agent on the textural properties of activated

carbons was found. In general, the activation of biochar with a highly concentrated solution of KOH produced carbonaceous materials with higher porosity compared to the activation with phosphoric acid, in agreement with the literature [4]. Besides, this activating agent leads to a high number of oxygenated groups on the carbon surface which are prone to adsorb mercury.

The study of mercury adsorption from aqueous solution has shown interesting results regarding the comparison of activated carbons prepared from different biomasses as precursors. Table I displays some physicochemical properties of KOH-activated carbons obtained from rice husk, eucalyptus leaves and coffee waste, along with the results of fitting of Hg(II) adsorption isotherms with Langmuir model, which described well their behaviour.

Table I. Activated carbons characterization and Hg(II) adsorption parameters of Langmuir model

Adsorbent	S_{BET} (m^2/g)	C (wt.%)	rem (wt.%)*	Q_o (mg/g)	K_L (L/mg)
CRH-700	148	59.3	31.4	**90**	0.13
CRH-KOH	128	62.3	27.6	**105**	0.19
CSC-KOH	100	76.6	9.84	**75**	0.04
CEL-KOH	48	83.3	5.40	**57**	0.33

*** remaining weight percent after heating in air**

As can be seen, the mercury adsorption capacity of activated carbons increased in the order EL< SC < RH achieving values for the latter as high as 105 mg/g, which exceeds other capacities reported in literature for similar samples [3]. The differences found in mercury adsorption capacity could be related with the porous properties of AC since mercury loading was increased as BET surface area of activated carbons increased (EL< SC < RH). However, it could be also related to the elemental analysis of activated carbons which is influenced by the chemical composition of the biomass source. For example, AC obtained from rice husk contains the lowest amount of carbon percentage and the largest amount of inorganic residue estimated by thermogravimetric analysis under air (Table I). Moreover, the ash content of rice husk biomass (related to alkaline, alkaline-earth metal oxides, and silica inherent to lignocellulosic biomass) is high (11.6%) compared to 0.7% and 2.6% obtained for spent coffee waste and eucalyptus leaves, respectively, that could explain the observed adsorption capacity for carbonized rice husk at 700 ºC (CRH-700) even without any chemical activation (Table I).

4. Conclusions

The mercury adsorption capacity of activated carbons prepared from the studied biomass residues was significant, especially for the AC obtained with rice husk. The distinctive behaviour of the activated carbons was related with their textural properties as well as the composition of lignocellulosic biomass employed to prepare the biochar.

Acknowledgments

The authors acknowledge the financial support to the Agencia Estatal de Investigación (Ministerio de Ciencia e Innovación, Spain) through the Projects TED2021-131144B-I0 and PID2021-126400OB-C32 and to the European Union's Horizon 2020 Research and Innovation Program, project SusWater H2020-MSCA-RISE-2020 under the Marie Skłodowska-Curie grant agreement No 101007578.

5. References

[1] C. Zamora-Ledezma, *Environ. Technol. Inn*, **22**, (2021) p. 101504.
[2] WHO, https://www.who.int/news-room/fact-sheets/detail/mercury-and-health.
[3] Z. Liu, *ACS Omega*, **5**(45) (2020), p. 29231.

O34: A glucose biosensor based on the adsorption of glucose oxidase onto graphitic carbon nitride

R. A. M. Barros [1,2], R. O. Cristóvão [1,2], C. G. Silva [1,2], J. L. Faria [1,2]

[1] *LSRE-LCM – Laboratory of Separation and Reaction Engineering – Laboratory of Catalysis and Materials, Faculty of Engineering, University of Porto, Rua Dr. Roberto Frias, 4200-465 Porto, Portugal*
[2] *ALiCE – Associate Laboratory in Chemical Engineering, Faculty of Engineering, University of Porto, Rua Dr. Roberto Frias, 4200-465 Porto, Portugal*
up201604653@edu.fe.up.pt
roc@fe.up.pt
cgsilva@fe.up.pt
jlfaria@fe.up.pt

1. Introduction – Glucose electrochemical sensors are one the most used biosensors in the fields of clinical detection, biological analysis, environmental monitoring, and food processing industries [1]. Due to its stability and great sensitivity to glucose, the enzyme glucose oxidase (GOx) is widely used in most glucose biosensors. GOx is an oxidoreductase that catalyses glucose oxidation to gluconic acid and H_2O_2. Measuring the current generated by the electrochemical reaction of H_2O_2 allows for the easy determination of the glucose concentration since the amount of glucose consumed is proportional to that of H_2O_2 produced (Image 1) [2]. However, direct adsorption of GOx on bare solid electrodes is difficult since the redox active sites of GOx are deeply buried inside the enzyme, limiting its activity and stability. Therefore, biosensor design requires synthesising and immobilising functional materials on the electrode surfaces that can support biomolecules and retain high activity and stability. Since carbon nanomaterials have excellent mechanical, surface area, and conductivity qualities, they are widely used as candidates in the field of glucose sensors. Synthesised by earth-abundant elements (i.e., C, N, and H), graphitic carbon nitride (GCN) has outstanding biocompatibility, stability, photocatalytic activity, and tuneable functionalisation, all of which provide a unique set of interesting properties for its use in various fields [3]. In this sense, this work aims to develop a versatile glucose biosensor based on the immobilisation of GOx onto thermally exfoliated GCN (GCN-T).

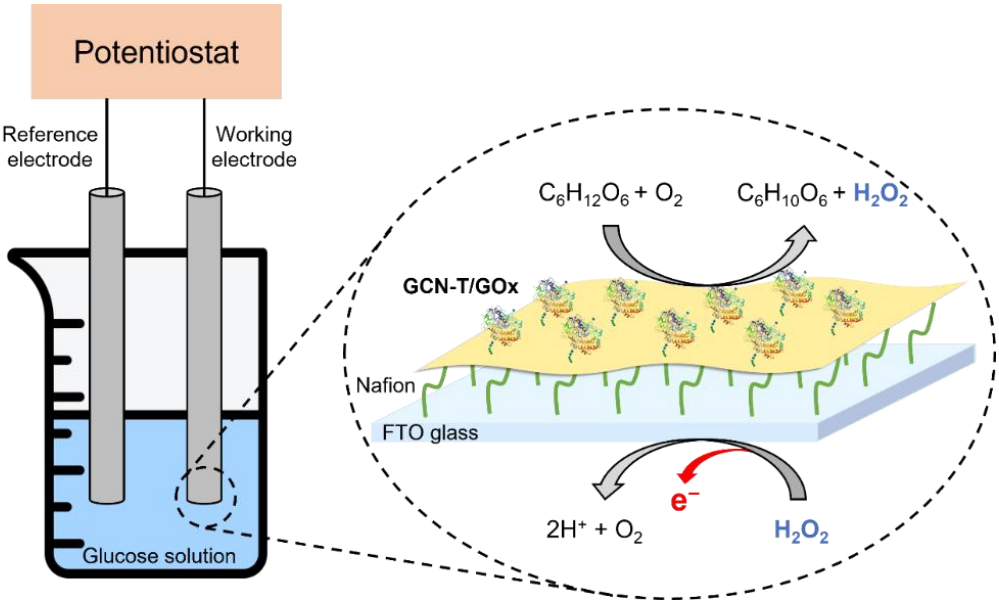

Image 1. GCN-T/GOx biosensor for the determination of glucose concentration.

2. Experimental – The immobilisation of GOx by physical adsorption was studied by adding 200 µL of GOx solution, prepared in citrate/phosphate buffer, to 2 mg of GCN-T. The immobilisation was performed by stirring the mixtures at 50 rpm in a vertical mini rotator. The experimental conditions (GOx

concentration, pH, and immobilisation time) were studied and optimised to maximise the activity of GOx and immobilisation yield. The bioconjugate GCN-T/GOx was adsorbed onto a fluorine-doped tin oxide-coated (FTO) glass to fabricate the working electrode. A mixture containing 10 mg of GCN-T/GOx, 50 μL of 5 wt% Nafion solution, and 1 mL of distilled water was prepared. The mixture was submitted to ultrasounds for 10 min to obtain a homogeneous suspension, then deposited on the working electrode by a drop-casting method (drying step at 80 ºC).

3. Results and Discussion – The results demonstrate the excellent performance of the GCN-T as support of GOx with immobilisation yields of 90%. GCN-T/GOx was then adsorbed onto the FTO glass, and its capacity for glucose degradation was evaluated. After 2 h of reaction, the bioconjugate was able to degrade 58% of the glucose in the solution, confirming the enzymatic activity of GOx when immobilised. Afterwards, the prepared FTO/GCN-T/GOx electrode was immersed in glucose solutions of various concentrations. The electrochemical behaviour of the prepared electrode was studied and compared with respect to the reference electrode.

4. Conclusions – The immobilisation of commercial GOx on GCN-T was successfully achieved by a simple and cost-effective physical adsorption mechanism. The efficient oxidation of glucose on the surface of the prepared FTO/GCN-T/GOx electrode showed the suitability of GCN-T as an excellent interface between GOx active sites and the electrode, effectively creating a glucose biosensor.

5. Acknowledgments
This work was supported by national funds through FCT/MCTES (PIDDAC): LSRE-LCM, UIDB/50020/2020 (DOI: 10.54499/UIDB/50020/2020) and UIDP/50020/2020 (DOI: 10.54499/UIDP/50020/2020); and ALiCE, LA/P/0045/2020 (DOI: 10.54499/LA/P/0045/2020). RAMB acknowledges FCT for her PhD grant 2022.12055.BD.

6. References
[1] Fang, B.; Zhang, C.; Wang, G.; Wang, M.; Ji, Y.; Sensors and Actuators B: Chemical, 2011, 155, 304-310.
[2] Khan, A. Y.; Noronha, S. B.; Bandyopadhyaya, R.; Biochemical Engineering Journal, 2015, 91, 78-85.
[3] Liu, J.; Wang, H.; Antonietti, M.; Chem. Soc. Rev., 2016, 45, 2308-2326.

O35: Batch Adsorption of Copper and Lead by an Agar-Graphene Oxide Hydrogel in a Single-Component System

N. B. V. Serafim [(1)], C. M. B. Araujo [(2)], A. F. P. Ferreira [(3)], M. A. Motta Sobrinho [(1)], J. V. F. L. Cavalcanti [(1)]

[(1)] *Federal University of Pernambuco, Chemical Engineering Department, Recife, Pernambuco, Brazil. nickolly.bukkyo@ufpe.br, jorge.cavalc@ufpe.br, mauricio.motta@ufpe.br*

[(2)] *University of Minho, R. da Universidade, 4710-057 Braga, Portugal. caroline.maria@ufpe.br*

[(3)] *University of Porto, Faculty of Engineering, Department of Chemical Engineering, Porto, Portugal. aferreir@fe.up.pt*

1. Introduction – Heavy metals are highly toxic substances that can accumulate in ecosystems, causing severe damage and exposing the population to contamination levels exceeding those deemed safe by the WHO. Adsorption has emerged as a sustainable and economically viable alternative for removing these contaminants from aqueous environments, driving research towards the development of new adsorbents. In this context, graphene oxide-based polymer nanocomposites stand out due to their ability to combine the properties of graphene oxide, such as high surface area and chemical stability, with a polymeric structure. Among polymer matrices, biopolymers are recognized for their ability to decompose after their useful life, thereby preventing future environmental problems. In this study, an agar and graphene oxide hydrogel was used for the adsorption of lead and copper in an aqueous medium.

2. Experimental - The hydrogel is obtained by incorporating a graphene oxide suspension during the production of agar gel. After homogenizing the mixture, it is transferred to a Petri dish where gelation occurs at room temperature. The material is then manually cut with a spatula to obtain particles approximately 2 mm thick. The influence of pH on adsorption was studied, varying between pH 2 and 5, a range in which the metals remain in suspension. The influence of ionic strength was also analyzed, conducting the process in media with salt concentrations between 0.05 and 0.10 M. In addition to these tests, kinetic and equilibrium batch assays were performed using a single-component system. The kinetic data were fitted using the LDF and QDF models, as well as Fick's diffusion equation. For the equilibrium data, the Langmuir, anti-Langmuir, and Freundlich isotherm models were used to perform the necessary adjustments.

3. Results and Discussion - The results obtained from the tests on the influence of initial pH and ionic strength are presented in Tables I and II. It is observed that the adsorption capacity decreases as the initial pH of the solution is lowered for both metals (Table I). This occurs due to the higher concentration of H^+ ions at lower pHs, which compete with the adsorbate cations, hindering the removal of contaminants. This trend is related to the charge equilibrium on the surface of the adsorbent, which possesses a negative charge. Regarding the influence of ionic strength on the process, it is found that the adsorption of Cu^{2+} is not affected by increased salinity in the medium, while the adsorption capacity for Pb^{2+} decreases significantly (Table II). This result suggests that weak interactions associated with physisorption predominate in the adsorption of Pb^{2+}, whereas the adsorption of Cu^{2+} may involve the formation of complexes on the adsorbent surface.

Table I. Adsorptive capacity of the GO-agar hydrogel for the removal of Cu^{2+} and Pb^{2+} in single-component systems as a function of the initial solution pH. Experimental conditions: $[Cu^{2+}]$ = 23,1 mg.L^{-1}; $[Pb^{2+}]$ = 19,4 mg.L^{-1}; m/V (wet basis) = 12 g.L^{-1}; 200 rpm; 180 min; 298 K.

	Cu^{2+}	Pb^{2+}
pH	**q (mg.g^{-1})**	
2	0,1	0,1
3	9,2	6,7
4	11,6	15,8
5	18,8	37,5

Table II. Adsorptive capacity of the GO-agar hydrogel for the removal of Cu^{2+} and Pb^{2+} in single-component systems as a function of NaCl concentration. Experimental conditions: $[Cu^{2+}]$ = 23,1 mg.L^{-1}; $[Pb^{2+}]$ = 19,2 mg.L^{-1}; m/V (wet basis) = 12 g.L^{-1}; 200 rpm; 180 min; 298 K.

	Cu^{2+}	Pb^{2+}
NaCl	**q (mg.g^{-1})**	
0,00 M	20,7	40,8
0,05 M	23,5	4,8
0,07 M	21,7	7,3
0,10 M	22,1	5,2

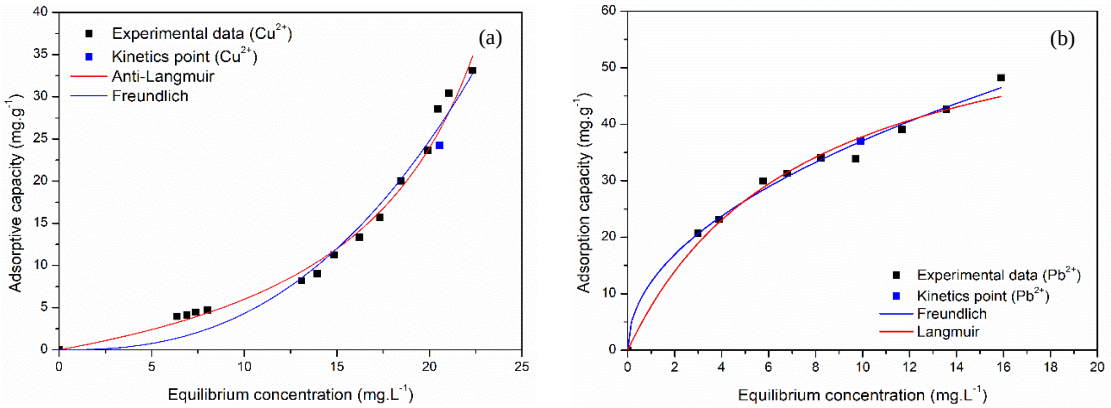

Image 1. Adsorption isotherms of the GO-agar hydrogel for the removal of (a) Cu^{2+} and (b) Pb^{2+} in single-component systems. Experimental conditions: [Cu^{2+}] = 23,8 mg.L^{-1}; [Pb^{2+}] = 16,9 mg.L^{-1}; m/V (wet basis) = 2 a 40 g.L^{-1}; 200 rpm; 180 min; 298 K.

Based on Image 1, a good fit of the models to the experimental data is observed. Additionally, the points corresponding to the kinetic assays are close to the equilibrium data, indicating good reproducibility of the experiments. Lead adsorption was best represented by the Freundlich model (R^2 = 0.99), suggesting the formation of multiple layers on the adsorbent surface or at heterogeneous sites. For copper adsorption, a good fit was observed with the anti-Langmuir isotherm (R^2 = 0.98). However, it is important to highlight the physical inconsistency of the anti-Langmuir model when applied to liquid-solid systems, as it predicts a vertical asymptote at a specific concentration of the metal in the mobile phase, which contradicts the concept of saturation capacity. In reality, the isotherm would have an "S" shape if higher equilibrium concentrations were investigated. The maximum adsorption capacity values in the equilibrium obtained experimentally for Cu^{2+} and Pb^{2+} were nearly 35 mg.g^{-1} and 50 mg.g^{-1}, respectively.

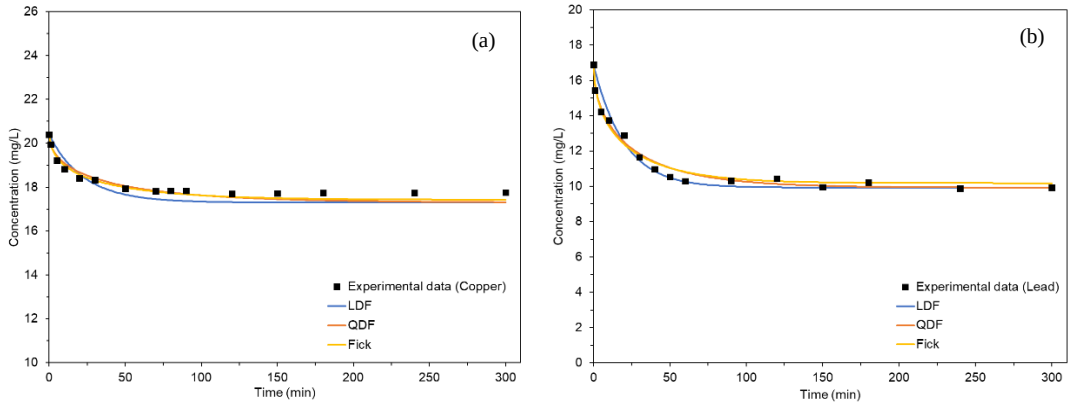

Image 2. Kinetic evolution of the adsorption of (a) Cu^{2+} and (b) Pb^{2+} on a GO-agar hydrogel in a single-component system. Experimental conditions: [Cu^{2+}] = 20,4 mg.L^{-1}; [Pb^{2+}] = 16,9 mg.L^{-1}; m/V (wet basis) = 12 g.L^{-1}; 200 rpm; 300 min; 298 K.

Observing Image 2, it is noted that approximately 50 minutes are required for the systems to reach equilibrium. Analyzing the parameters calculated from the model fittings, it is evident that all models fit the data well, with Fick's diffusion equation (R^2 = 0.97 for Cu^{2+}; R^2 = 0.99 for Pb^{2+}) and the QDF model (R^2 = 0.94 for Cu^{2+}; R^2 = 0.99 for Pb^{2+}) demonstrating the best fits for both metals.

4. Conclusions – Overall, the composite exhibited a great potential for applications as adsorbent to remove lead and copper ions from aquatic environments. In addition to the batch adsorption tests, in the future, fixed-bed adsorption experiments will also be performed using the GO-based hydrogel as adsorbent.

5. References

[1] G. Guiochon, D. G. Shirazi, A. Felinger Fundamentals of preparative and nonlinear chromatography. Academic Press (2006)

[2] F. Fayyazi et al. Synthesis of a three-dimensional reduced graphene oxide aerogel decorated with (Fe3O4@ SiO2–NH2)–COC2H4COOH for adsorption of heavy metal cations. Journal of Molecular Liquids (2023)

O36: High capacity zeolite laminates: enhancing gas separations beyond packed beds

M. H. B. Born [(1)], J. F. M. Denayer [(1)], T. R. C. Van Assche[(1)]

[(1)]*Department of Chemical Engineering, Vrije Universiteit Brussel, Pleinlaan 2, 1050 Brussels, Belgium.*
Mathijs.Hubert.Born@vub.be
joeri.denayer@vub.be
tom.van.assche@vub.be

1. Introduction

Packed beds have long been the standard for adsorption based separation processes. However, structured adsorbents have emerged as promising alternatives as they offer several key advantages such as a lower pressure drop and improved mass transfer kinetics [1]. Monoliths and coated structures such as honeycombs and foams have been investigated. However, these structures often exhibit a low volumetric adsorption capacity due to the presence of a support structure or a large bed void fraction [2,3]. Limited research has been done on laminates without support structure. In our work, self-standing adsorbent laminates were manufactured, assembled, and extensively tested for gas separation.

2. Experimental

Laminates containing 84 wt.% zeolite 13X were manufactured. The laminate shaping and drying process allows for adsorbent sheets with a highly controlled thickness. A novel method for assembly of the laminates was used to obtain adsorber devices containing up to 12 laminates. Three adsorber devices were assembled, employing laminates with thicknesses ranging between 0.5-1.2 mm and spacer distances between 0.4-0.8 mm (Figure 1). For comparison, an identical packed bed with pellets was manufactured.

3. Results and Discussion

Equilibrium measurements show that the composite materials retain approximately 81-84% of the pure zeolite 13X powder adsorption capacity. The laminate adsorbers and reference packed bed were tested in breakthrough experiments in which a CO_2/O_2 mixture was separated. All tests show sharp breakthrough fronts, indicating excellent flow distribution in the laminar adsorbers. The mass transfer kinetics in the laminate adsorbers match and even exceed the kinetics in the reference packed bed. Moreover, it was demonstrated that by reducing laminate thickness, mass transfer kinetics are improved. The laminate system also allows significant improvements in volume efficiency. A laminar adsorber with 0.4 mm spacing distance surpassed the reference packed bed, achieving a 19% larger volumetric capacity. In Figure 1, the volumetric capacities for the various laminate adsorbers and packed bed are shown. The significantly larger volumetric capacity in laminar adsorber LAM2 is caused by the high solid fraction, which cannot be achieved in packed beds. Furthermore, pressure drop measurements show a significantly lower pressure drop over the laminate adsorbers than over the reference packed bed already at low velocities. Pressure drop calculations show that this difference is even larger at higher velocities.

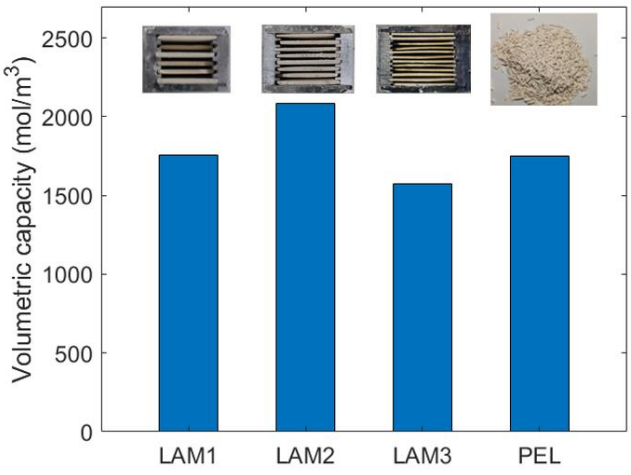

Figure 1: Volumetric capacities of the various laminate adsorbers (LAM1, LAM2, LAM3) and the reference packed bed (PEL).

4. Conclusions

The described method for laminate shaping and assembly allows for laminate adsorbers with excellent flow distribution. The laminate adsorbers outperform the reference packed bed in terms of pressure drop. By tailoring the laminate thickness and spacing, significantly larger volumetric capacities (+19%) are achieved. Furthermore, the laminates show fast uptake kinetics which are further improved by reducing laminate thickness. This research highlights the potential adsorbent laminates have towards enhancing gas separations.

5. References

[1] F. Razaei and P. Webley, *Sep. Purif. Technol*., **70**, (2010) 243-256.
[2] A. Mosca, J. Hedlund, P.A. Webley, M. Grahn, F. Rezaei, *Microporous Mesoporous Mater.* **130** (2010) 38–48.
[3] R. Sharma, D. Sürmeli, T.R.C. Van Assche, S. Tiriana, M.-P. Delplancke, G.V. Baron, J.F.M. Denayer, *Microporous Mesoporous Mater*. **343** (2022) 112146.

O37: Effect of Cations on the Ammonia Synthesis Reaction Under the Confinement in Zeolites

Botagoz Zhakisheva[(1)], Sofia Calero[(1)], and Juan José Gutiérrez-Sevillano[(2)]

[(1)] Department of Applied Physics and Science Education, Eindhoven University of Technology, 5600 MB Eindhoven, Netherlands
b.zhakisheva@tue.nl
[(2)] Center for Nanoscience and Sustainable Technologies (CNATS) - Universidad Pablo de Olavide, Seville, Spain s.calero@tue.nl, jjgutierrez@upo.es

1. Introduction – Ammonia is one of the most important molecules in the chemical industry[1,2] Its annual production accounts for million metric tons making the ammonia synthesis reaction the second largest production of synthetic chemicals. On a large scale, ammonia is mainly manufactured by the well-known Haber-Bosch process[6] in which hydrogen and nitrogen react in the presence of the commonly used iron catalyst to generate a dilute ammonia-gas stream. Produced ammonia needs to be purified and recovered from the reaction batch. In recent years, the study of confined reactions has emerged as an intriguing area of research,with the confinement reactions within nanoscale environments showing potential for enhancing reaction yieldsand altering reaction equilibria. In this study, we take into account the activity of alkali metals as catalystspromoters, the positive confinement effect on the ammonia reaction yield in all-silica zeolite, and the effect ofcations to increase the heat of adsorption of ammonia to investigate the influence of Na^+ cations in zeolites on the adsorption of reaction molecules (N_2, H_2, NH_3) and on reaction yield under the confinement in zeolites with various Si/Al ratios.

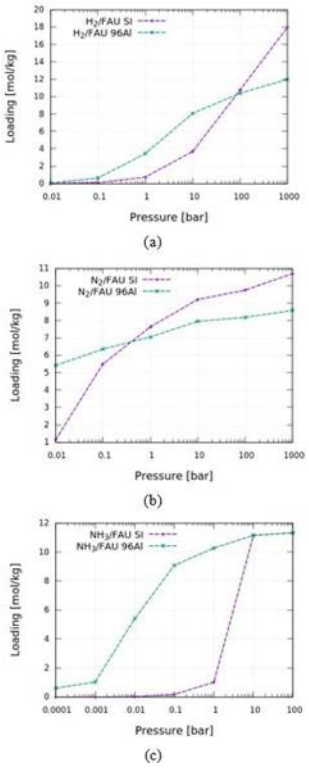

Image 1. Single component adsorptionof a) H2 at 120 K, b) N2 at 120 K, and

c) NH3 at 300K on all-silica zeolite (FAU SI) and zeolite with cations (FAU96Al).

2. Experimental - We performed simulations of adsorption and the ammonia synthesis reaction using the RASPA code [3]. We used the combination of Reactive ensemble Monte Carlo (RxMC) and Continuous Fractional Component Monte Carlo (CFCMC) methods. The reaction molecules and zeolite frameworks were modeled as rigid, i.e., bonding interactions were not considered. models for hydrogen[4], nitrogen [5], and ammonia [6] are rigid andtaken from the literature. Na+ cations were randomly distributed in the aluminum-substituted frameworks to compensate for the negative net charge and they wereable to freely move and adjust their positions depending on their interactions withadsorbates, other cations, and zeolite atoms.

3. Results and Discussion - To investigate how Na+ cations in zeolites affect the adsorption behavior of ammonia reaction molecules we simulated the adsorption isotherms of H2, N2 and NH3 in FAU type zeolite with Si/Al= ∞ and Si/Al = 1 and for mixtures. We obtain in the structure with cationsthat for mixtures, the maximum values of hydrogen and nitrogen are 0.0033 mol/kg and 0.0022 mol/kg respectively, whereas the maximum loading of ammonia was 12.45 mol/kg. In contrast to these values, at the same T and p conditions, the zeolite without cations presented the maximum loading of 0.086 mol/kg of H2, 0.7 mol/kg of N2 and 15.1 mol/kg of NH3. The loadingof hydrogen and nitrogen has decreased in zeolite with cations at allconditions. Thus, these results suggest that cations in zeolite promote the selectivity of ammonia adsorption, favouring the adsorption of ammonia molecules that prevents the adsorption of hydrogen and nitrogen. This impliespotential benefits for the confinement effect on the equilibrium of the reaction. Then, we performed simulations of the ammonia synthesis reaction at 873 Kand Si/Al ratios and as an initial reaction composition, we used the mole fractions of the components of the reaction at equilibrium obtained by the RxMC method in the bulk. As can be seen in Figure 2 the inclusion of even a small number of cations in the zeolite structure (Si/Al = 23,

corresponding to 8 Al substitutions and 8 Na^+ cations per unit cell) results in a slightenhancement of the confinement effect and, consequently, the ammonia mole fraction produced in the reaction. We completed the study by computing the ammonia mole fractions yielded in the reaction under the confinement of FAU at several temperatures and pressures and analysing the effects exertedby the cations.

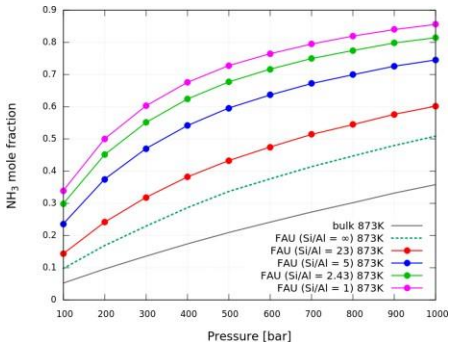

Image 1. Ammonia mole fractions from the reaction of N_2 and H_2 at 873 K in the bulk and under the confinement of FAU: grey solid line - reaction in the bulk, dashed lines - reaction under the confinement in all-silica FAU; solid lines

4. Conclusions - We found that the incorporation of cations into the zeolite structure significantly modified the adsorption behavior of ammonia, resulting in a gradual increase in ammonia density within the pores and preventing its phase transition. The adsorption of ammonia exhibited higher selectivity from the mixture of gases in the zeolite with cations as compared to all-silica zeolite. Based on that findings, the inclusion of Na^+ cations in the zeolite structure could have a beneficial impact on the production of ammonia in the reaction, leading to higher mole fractions obtained at all temperatures and pressures. The most significant improvement has been observed with the lowest Si/Al = 1, which comprises 96 Na^+ cations per unit cell of FAU. Our study suggests that the optimal conditions for the process can be achieved at 573 K and 10 bar, resulting in a high value of 0.93 for ammonia mole fraction adsorbed.

5. References

[1] Erisman, J. W.; Sutton, M. A.; Galloway, J.; Klimont, Z.; Winiwarter, W. *Nature Geoscience* **2008**, 1, 636–639.

[2] Glaeser, B. The Green Revolution revisited: Critique and alternatives. *The Green Revolution Revisited: Critique and Alternatives* **2010**, 1–170.

[3] Dubbeldam, D.; Calero, S.; Ellis, D. E.; Snurr, R. Q. *Molecular Simulation* **2016**, *42*, 81–101.

[4] Deeg, K. S.; Gutiérrez-Sevillano, J. J.; Bueno-P´erez, R.; Parra, J. B.; Ania, C. O.; Doblar´e, M.; Calero,S. Insights on the molecular mechanisms of hydrogen adsorption in zeolites. *Journal of Physical Chemistry C* **2013**, *117*, 14374–14380.

[5] Martın-Calvo, A.; Garcıa-Pérez, E.; Garcıa-Sánchez, A.; Bueno-Pérez, R.; Hamad, S.; Calero, S. *Physical Chemistry Chemical Physics* **2011**, *13*, 11165–11174.

[6] Zhang, L.; Siepmann, J. I. *Collection of Czechoslovak Chemical Communications* **2010**, *75*, 577–591

O38: The Impact of Metal Centers in the Metal-Organic Frameworks on Carbon Dioxide Hydrogenation to Formic Acid

Dominika O. Wasik[1,2], José Manuel Vicent-Luna[1], Shima Rezaie[3], Azahara Luna-Triguero[3,2], David Dubbeldam[4], Thijs J. H. Vlugt[5], Sofia Calero[1,2]

[1]Materials Simulation and Modelling, Department of Applied Physics, Eindhoven University of Technology, 5600MB Eindhoven, The Netherlands
[2]Eindhoven Institute for Renewable Energy Systems, Eindhoven University of Technology, PO Box 513, Eindhoven 5600 MB, The Netherlands
[3]Energy Technology, Department of Mechanical Engineering, Eindhoven University of Technology, 5600MB Eindhoven, The Netherlands
[4]Van't Hoff Institute for Molecular Sciences, University of Amsterdam, 1098XH Amsterdam, The Netherlands
[5]Engineering Thermodynamics, Process & Energy Department, Faculty of Mechanical, Maritime and Materials Engineering, Delft University of Technology, Leeghwaterstraat 39, Delft 2628CB, The Netherlands
Principal Author's e-mail: d.o.wasik@tue.nl

1. **Introduction** - The confinement effect of porous materials on the thermodynamical equilibrium of the reaction presents a cost-effective alternative to transition metal catalysts. This is due to the higher density of the pore phase compared to the gas phase by Le Chatelier's principle and the selective adsorption of favored components. A molecular simulation study on the thermodynamic confinement effects of MOFs on the CO_2 hydrogenation to HCOOH[1] showed that the type of metal center in MOFs has a greater impact on the enhancement of HCOOH production than the scale of confinement resulting from the pore size. Due to the presence of highly reactive open-metal sites, the M-MOF-74 series allows to fully investigate the dependence of HCOOH production enhancement on the type of metal center, minimizing the effect of pore size. We propose a non-polarizable CO_2, and H_2 force field for adsorption in M-MOF-74 (M = Ni, Cu, Co, Fe, Mn, Zn)[2], compatible with the HCOOH force field.

2. **Experimental** – The CO_2/H_2 force field is adjusted by scaling the Coulombic interactions of M-MOF-74 atoms, and Lennard-Jones interaction potentials between the center of mass of H_2 and the open-metal centers. To validate the force field, the experimental isotherms, enthalpy of adsorption, and the binding geometries were reproduced using GCMC simulations. The compatibility of the HCOOH force field with the proposed force field was confirmed by reproducing the binding geometries of HCOOH in M-MOF-74obtained from DFT. To study the thermodynamic confinement effects of M-MOF-74 on the CO_2 hydrogenation to HCOOH, GCMC simulations were performed in the frameworks, using gas-phase mole fractions of CO_2, H_2, and HCOOH at chemical equilibrium, obtained from Rx/CFCMC simulations.

3. **Results and Discussion** - The computed loadings, heats of CO_2 and H_2 adsorption, and binding geometries in M-MOF-74 are in very good agreement with the experimental data. DFT and Baker's minimization result in comparable equilibrium geometries of HCOOH in M-MOF-74. Depending on the metal center, the enhancement in HCOOH production decreases in the same order as its isosteric heat of adsorption: Ni > Co > Fe > Mn > Zn > Cu. The strongest host-guest interaction of HCOOH with Ni-MOF-74 causes the most significant influence on the CO_2 hydrogenation thermodynamics, enhancing HCOOH production by ca. 120,000 times compared to the gas phase at 298.15 K, 60 bar.

4. **Conclusions** - Ni-MOF-74 has the potential to be an alternative to transition metal catalysts for improving HCOOH production due to elimination of the high-cost temperature elevation, more valuable final product, and comparable final concentration of HCOOH to the reported concentrations of formate obtained using transition metal catalysts.

5. **References**

[1] Wasik, D. O., et al. *Chemical Engineering Journal* **467** (2023) p. 143432.
[2]Wasik, D. O., et al. *Separation and Purification Technology* **339** (2024) p. 126539.

O39: Kinetic separation of green hydrogen from natural gas grids by using vacuum pressure swing adsorption

L. F. A. S. Zafanelli [1,2,3,4], A. Henrique [1,2], E. Aly [1,2], A. E. Rodrigues [3,4], G. Mouchaham [5], J. A. C. Silva [1,2]

[1]*Centro de Investigação de Montanha (CIMO), Instituto Politécnico de Bragança, Campus Santa Apolónia, 5300-253 Bragança, Portugal*
[2]*Laboratório Associado para a Sustentabilidade e Tecnologia em Regiões de Montanha (SusTEC), Instituto Politécnico de Bragança, Campus de Santa Apolónia, 5300-253 Bragança, Portugal*
[3]*LSRE-LCM – Laboratory of Separation and Reaction Engineering - Laboratory of Catalysis and Materials, Faculty of Engineering, University of Porto, Rua Dr. Roberto Frias, 4200-465 Porto, Portugal*
[4]*ALiCE – Associate Laboratory in Chemical Engineering, Faculty of Engineering, University of Porto, Rua Dr. Roberto Frias, 4200-465 Porto, Portugal*
zafanelli@ipb.pt
[5]*Institut des Matériaux Poreux de Paris, Ecole Normale Supérieure de Paris, ESPCI Paris, CNRS, PSL University, 75005 Paris, France*
adriano_henrique@ipb.pt; ezzeldin@ipb.pt; arodrig@fe.up.pt; georges.mouchaham@ens.psl.eu; jsilva@ipb.pt

1. **Introduction –** Transitioning to renewable energy sources is crucial to mitigating climate change. In this scenario, green hydrogen (GH) is considered a promising energy carrier due to its high calorific value, versatility in applications, clean combustion, and potential for local generation in abundance [1]. As interest in GH grows, developing its distribution chain becomes crucial in facilitating its widespread use. The co- transporting GH into existing natural gas grids (NGG) emerges as a viable alternative, eliminating the need for significant infrastructure investments [2]. However, upon blending GH into the NGG, it becomes essential to de-blend and purify it to a high degree to enable, for instance, fuel cell applications (H2 > 99,97%). One problem concerning the separation and purification of GH from NGG relates to the H2 feed concentration (< 20%), which differs significantly from conventional H2 purification processes (> 70%). Moreover, the high CH4 concentration and its relatively weak adsorption affinity on commonly used adsorbents further complicate achieving high-purity H2 and high recovery rates through conventional approaches. In this work, we report a novel conceptual vacuum pressure swing adsorption (VPSA) process to separate H2 from CH4 by exploiting the kinetic selectivity of H2 over CH4 on CMS-3K-172, as shown in Figure 1.

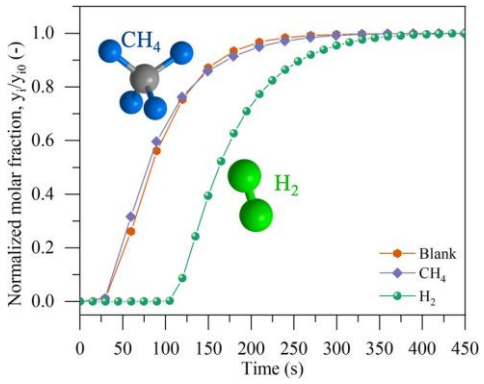

Figure 1. Experimental single breakthrough curves of H_2 and CH_4 on CMS-3K-172 compared to the blank experiment.

2. Experimental - To develop the conceptual VPSA cycle, a series of single and multicomponent breakthrough curves for H_2 and CH_4 were performed on CMS-3K-172 between 195 - 273 K and pressures up to 18 bar. These experiments were performed in a cryogenic fixed-bed adsorption unit designed to work at lower temperatures (until 77 K) [3].

3. Results and Discussion - Figure 1 shows the single breakthrough curves of H_2 and CH_4 on CMS-3K-172 compared to a blank experiment performed at 195 K and 12 bar, where a kinetic separation can be seen. CH_4 has a limited diffusion into the CMS-3K-172 structure, which results in its early breakthrough at the same time as the blank experiment. Conversely, H_2 is adsorbed on CMS-3K-172 as its breakthrough curve presents a delay compared to the blank experiment. The conceptual VPSA developed consists of 1 bed with 5 steps, namely (1) pressurization with feed, (2) feed, (3) H_2 purge, (4) cocurrent depressurization (COD), and (5) countercurrent vacuum blowdown. The H_2 purity and recovery were evaluated by changing the process variables such as step time, intermediate-to-high pressure ratio, purge-to-feed ratio, and VPSA type configuration. Figure 2 shows three simulated VPSA types: type I with the five steps mentioned above

type II without the COD step, and type III without the H_2 purge step. The H_2 purity-recover trade-off for the three VPSA types can be seen in Figure 3. From a feed of 20% H_2, the VPSA type II allows obtaining an H_2 purity of up to 68% with a recovery of up to 92%, and the best trade-off between purity and recovery was 83% and 85%, respectively.

4. Conclusions - This work shows for the first time that an adsorbent, which preferentially adsorbs H_2 and blocks CH_4 from entering its pores, can enrich H_2 from a low feed concentration. Moreover, this work provides insights for developing new materials with the same CMS characteristics but with higher H_2 capacity, which could be beneficial to improve the VPSA process. In conclusion, the developed VPSA process increases the H_2 molar fraction from 20% to 60 - 70% with a high recovery. We are currently working on a second stage to be incorporated into the VPSA process to purify H_2 for fuel cell applications (>99.97%).

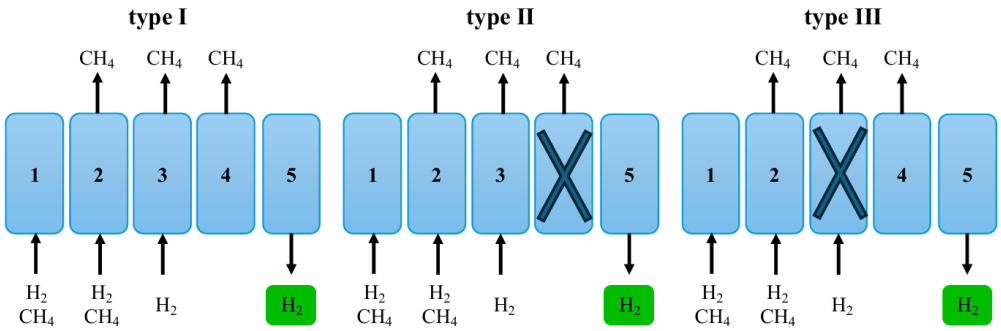

Figure 2. VPSA type configurations.

5. Acknowledgments The authors are grateful to the Foundation for Science and Technology (FCT, Portugal) for financial support: (1) under project PTDC/EQU-EPQ/0467/2020 (DOI: 10.54499/PTDC/EQU-EPQ/0467/2020), (2) through the national funds FCT/MCTES (PIDDAC) to CIMO (UIDB/00690/2020 and UIDP/00690/2020), and SusTEC (LA/P/0007/2020), (3) by the national funds through FCT/MCTES (PIDDAC): LSRE-LCM, UIDB/50020/2020 (DOI: 10.54499/UIDB/50020/2020) and UIDP/50020/2020 (DOI: 10.54499/UIDP/50020/2020); and ALiCE, LA/P/0045/2020 (DOI: 10.54499/LA/P/0045/2020).
Additionally, we thank national funding by FCT, Foundation for Science and Technology, through the individual research grant 2020.07925.BD (DOI: 10.54499/2020.07925.BD) of Lucas F. A. S. Zafanelli.
Moreover, the authors are grateful to Osaka Co. for kindly providing the CMS-3K-172 studied in this work.

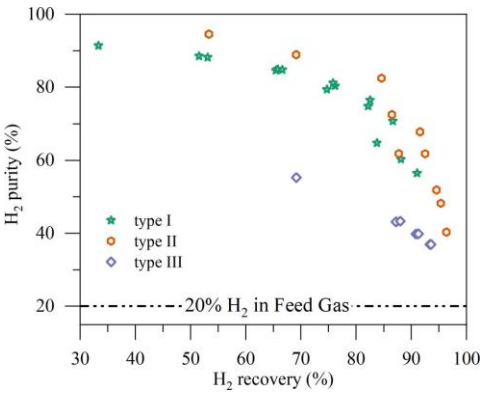

Figure 3. Trade-off between H2 purity and recovery for different VPSA types and sets of process variables.

6. References

[1] IRENA, International Renewable Energy Agency, 2022.
[2] L. Dehdari, I. Burgers, P. Xiao, K. G. Li, R. Singh, & P. A. Webley, *Sep. Purif. Technol.*, 282, (2022) 120094.
[3] L. F. A. S. Zafanelli, E. Aly, A. E. Rodrigues, & J. A. C. Silva, *Sep. Purif. Technol.*, *307*, (2023) 122824.
L. F. A. S. Zafanelli, E. Aly, A. Henrique, A. E. Rodrigues, G. Mouchaham, & J. A. C. Silva, *Ind. Eng. Chem. Res.*, **63**(14), (2024) 6333-634

RIA 43
XLIII Reunião Ibérica de Adsorção
Porto, Portugal
1-4 September 2024

O40: From forest to filter: A holist approach to pine bark's adsorption technology

Ricardo M. Ferreira, Pedro Gonçalves, Mariko Carneiro, Olivia Salomé Soares, Ariana Pintor, Manuel Fernando Pereira, Cidália Botelho

Laboratory of Separation and Reaction Engineering – Laboratory of Catalysis and Materials (LSRE-LCM), Department of Chemical Engineering, Faculty of Engineering, University of Porto, Rua Dr. Roberto Frias, 4200-465 Porto, Portugal.
ALiCE - Associate Laboratory in Chemical Engineering, Faculty of Engineering, University of Porto, Rua Dr. Roberto Frias, 4200-465 Porto, Portugal
rmmferreira@fe.up.pt
up202006707@edu.fe.up.pt; up201902701@edu.fe.up.pt; osgps@fe.up.pt; ampintor@fe.up.pt; fpereira@fe.up.pt; cbotelho@fe.up.pt

1. Introduction – Dyes are extensively used in the textile industry and released into the generated effluents. The discharge of these untreated wastewaters into the environment is extremely harmful to aquatic ecosystems. Therefore, the development of economically and environmentally sustainable treatment technologies is of utmost importance [1,2]. In the present study, bioadsorbents were produced from pine bark (*Pinus pinaster*), and their capacity to remove dye from a synthetic textile effluent was evaluated. Pine bark is an abundant by-product of the timber industry in Portugal, making it an excellent raw material for this purpose. Tannin-based adsorbents were produced through conventional solid-liquid extractions using distilled water as a solvent. The impact of extraction conditions—solid-liquid ratio, temperature, and duration—was tested across 12 trials, achieving a maximum extraction efficiency of 8.39% in the trial conducted with a solid-liquid ratio of 1:30 at 80 ºC for 60 min. The determination of total phenolic compounds (TPC) and condensed tannins (CT) in the extracts was performed, revealing that higher temperatures and solid-liquid ratios resulted in an increase in TPC and a decrease in CT content. The highest amounts of TPC and CT extracted were 0.9 ± 0.2 mg/g (1:10, 80 ºC, 20 min) and 1.13 ± 0.01 mg/g (1:30, 70 ºC, 20 min), respectively. The dried extraction residue produced different adsorbents, such as washed bark, and washed bark and activated pine bark, coated with iron and used for color removal assays. The dye removal capacity was evaluated by conducting adsorption tests using a synthetic effluent (80 mg/L) prepared with the dye Sirius Blue K-CFN (containing Direct Blue 85), sodium chloride (2.5 g/L), and sodium bicarbonate (1.0 g/L), to simulate real textile effluent conditions. The results revealed that increasing the amount of iron used in the adsorbent coating enhanced their dye removal capacity. The activated pine bark coated with 10% iron was the most promising adsorbent produced, removing 99.60 ± 0.04% of the dye from the solution after 24 h of treatment, and resulting in minimal iron release into the treated solution. Additionally, through the construction of kinetic curves, a maximum dye removal capacity of 16.00 ± 0.02 mg per gram of this activated pine bark was determined, with almost all the dye being removed within just 2 h of treatment.

2. Experimental - To produce tannic coagulants, solid-liquid extractions were performed using ethanol and distilled water as solvents. A three-level factor was used to optimize the recovery of condensed tannins (CT) and total phenolic content (TPC), considering extraction time (X_1), temperature (X_2), and solid-to-liquid ratio (X_3) based on single-factor tests [3]. After extraction, the suspensions were cooled and filtered using a glass filter (1.5 µm porosity) and a Welch MPC 090 E Vacuum Pump, then freeze-dried for analysis. Twelve experiments were conducted in randomized order. Then, the washed pine bark from the extractions was dried at 60°C and subjected to an iron coating process as described by Messele et al. [4]. Iron(III) chloride hexahydrate ($FeCl_3$•$6H_2O$) was dissolved to achieve 5% and 10% (wt.%) iron content in 2 g samples, by the incipient wetness impregnation method. The mixture was sonicated at room temperature for 90 min and part of the resulting iron-coated pine bark that was then converted to activated pine bark by heating in a furnace at 400°C with heating ramp of a 10°C/min.

The total polyphenolic content (TPC) and condensed tannin (CT) content were determined as reported by Tomasi et al. [5]. TPC of the extract was measured as gallic acid equivalent (GAE) per gram of dried extract ($g_{GAE}/100g_{extract}$) using the Folin-Ciocalteu method, while CT content was assessed using a modified acidified vanillin method, with results expressed as milligrams of catechin equivalent (CE) per gram of extract ($mg_{CE}/g_{extract}$).

3. Results and Discussion - Twelve tannin extracts were obtained through conventional solid-liquid extraction, achieving efficiencies ranging from 4.36% to 8.39%. Extraction efficiency benefited from

higher solid-liquid ratios, while slightly elevated temperatures contributed to an increase in total phenolic content. Pine bark demonstrated lower extraction efficiency compared to species such as acacia, attributed to its high molecular weight tannins and polymerization [5].

To assess effective color removal, adsorption tests were conducted using synthetic effluent. Results showed limited efficacy for washed pine bark and polymerized extract as adsorbents. Iron-coated bark at 10% exhibited high removal (88 ± 3%) after 24 h, contrasting with activated pine bark coated at 10% iron, which achieved nearly complete color removal (99.60 ± 0.04%).

Table 2 Average color removal percentages (%CR) recorded after 24 and 48 h treatments

Adsorbent	Color removal	
	24 h (%)	48 h (%)
Washed pine bark	2 ± 3	1 ± 2
Washed pine bark + Fe 5%	46 ± 11	23 ± 14
Washed pine bark + Fe 10%	88 ± 3	23 ± 16
Activated pine bark + Fe 5%	23 ± 4	20 ± 3
Activated pine bark + Fe 10%	99,60 ± 0.04	51,4 ± 0.2

To characterize color removal from promising adsorbents – 5% and 10% iron-coated washed pine bark, and 10% iron-coated activated pine bark – kinetic curves were constructed. Washed bark with 5% iron showed a max removal of 8 ± 2 mg/g after 24h, while 10% iron-coated bark had 14.4 ± 0.6 mg/g after 24 h. The activated pine bark with 10% iron reached 16.00 ± 0.02 mg/g, removing dye in 2 h. Considering the literature findings, the results suggest that the dye removal mechanism likely involves the complexation of the dye with iron, indicating a process of chemical adsorption [6].

4. Conclusions - The study found tannin extraction efficiencies from pine bark aligning with expectations from literature, with optimal conditions yielding up to 8.39% efficiency. Lower solid-liquid ratios and higher temperatures or durations marginally increased extraction. Elevated temperatures and ratios enhanced total phenolic content but reduced condensed tannins. Adsorption tests indicated limitations of washed pine bark and polymerized tannin extract for textile effluent treatment. Enhanced iron coating improved dye removal, notably achieving 99.60 ± 0.04% removal efficiency with minimal iron release in activated pine bark coated with 10% iron. This transformation highlighted activated pine bark's potential, swiftly and effectively removing dye pollutants from water systems.

5. References

1. Ghaly, AE.; Ananthashankar, R.; Alhattab, M.; Ramakrishnan, V. *Journal of Chemical Engineering & Process Technology* **2014**, *05*.
2. Santos, S.C.R.; Boaventura, R.A.R. *J Environ Chem Eng* **2016**, *4*, 1473–1483.
3. Ferreira, R.M.; Queffelec, J.; Flórez-Fernández, N.; Saraiva, J.A.; Torres, M.D.; Cardoso, S.M.; Domínguez, H. *Lwt* **2023**, *186*.
4. Messele, S.A.; Soares, O.S.G.P.; Órfão, J.J.M.; Stüber, F.; Bengoa, C.; Fortuny, A.; Fabregat, A.; Font, J. *Appl Catal B* **2014**, *154–155*, 329–338.
5. Vâzquez, G.; González-Alvarez, J.; Freire, S.; López-Suevos, F.; Antorrena, G. *European journal of wood and wood products*, **2001**, 59.
6. Ho, Y.S.; McKay, G. A. *Process Safety and Environmental Protection* **1998**, *76*, 332–340.

Poster Communications

P1: A novel dual-function material for CO_2 capture and conversion via low-temperature sunlight-assisted methanation

L. Paulista [(1)(2)], A. Ferreira [(1)(2)], A. Rodrigues [(1)(2)], R. Martins [(1)(2)], R. Boaventura [(1)(2)], V. Vilar [(1)(2)], T. Silva [(1)(2)]

[(1)] LSRE-LCM – Laboratory of Separation and Reaction Engineering - Laboratory of Catalysis and Materials, Faculty of Engineering, University of Porto, Rua Dr. Roberto Frias, 4200-465 Porto, Portugal.
[(2)] ALiCE – Associate Laboratory in Chemical Engineering, Faculty of Engineering, University of Porto, Rua Dr. Roberto Frias, 4200-465 Porto, Portugal

tania.silva@fe.up.pt
up201809110@edu.fe.up.pt, aferreir@fe.up.pt, arodrig@fe.up.pt, rjemartins@fe.up.pt, bventura@fe.up.pt, vilar@fe.up.pt

1. Introduction

Global warming, driven by unmitigated CO_2 emissions and other greenhouse gases primarily from modern industries, is becoming a severe environmental issue. Although several strategies have been developed to tackle this problem, they often require complex equipment and stringent reaction conditions. Recent advances in nanotechnology have brought new possibilities for efficiently recycle CO_2 under mild conditions by integrating adsorption (physical and/or chemical) and conversion (e.g., electrocatalysis and photocatalysis) processes. The use of nanomaterials to directly capture and convert CO_2 into valuable chemicals under mild conditions is emerging as an appealing strategy to reduce CO_2 levels [1].
Among various nanostructured catalysts used to promote photocatalytic CO_2 reduction into fuels, heterojunctions of wide bandgap semiconductors (such as TiO_2 and $SrTiO_3$) with metal oxides (such as RuO_2 and NiO) have been employed to boost electron flow and solar-to-fuel conversion efficiency [2]. Ruthenium (Ru)-based catalysts combined with thermo-photocatalysis have shown promise in conducting the Sabatier reaction ($CO_2 + 4H_2 \rightarrow CH_4 + 2H_2O$) at low temperatures (150 ºC) [3]. Zeolite 13X (Z13X), one of the best commercial adsorbents for carbon capture, can be functionalized with catalysts to improve conversion yields by attracting CO_2 to the catalyst active sites [4]. Hence, this study aimed to explore the use of Z13X adsorbent impregnated with RuO_2:TiO_2 photocatalyst as a dual-function material to foster solar-driven thermo-photocatalytic CO_2 methanation at low temperature.

2. Experimental

The RuO_2:TiO_2 photocatalyst was prepared by ethylene glycol-mediated synthesis, as reported elsewhere [5]. The Z13X adsorbent was functionalized with the optimal catalyst using wet (WIM) or solid-state (SIM) impregnation method (catalyst-to-adsorbent mass ratios of 1:10-5:10). The WIM procedure was as follows: (i) dispersion of Z13X (200 mg) in ultrapure water (10 mL) by sonication (5 min); (ii) slow evaporation (70 ºC) under stirring while gradually adding ultrapure water (5 mL) containing the catalyst; (iii) drying (1 h; 100 °C); and calcination (3 h; 350 °C). The SIM procedure was as follows: (i) manual mixing of the Z13X with the catalyst using a pestle and agate mortar (15 min); (ii) mechanical mixing/grinding using an RM100 Laboratory Mixer-Mortar-Grinder (30 min); and (iii) calcination (3 h; 350 °C).
Catalytic activity towards CO_2 methanation via thermo-photocatalysis was evaluated in a gas-phase batch quartz reactor (40 mL), equipped with heating (≤ 300 ºC) and pressure (≤ 4 bar) control systems, inside a sunlight simulator (Atlas, Suntest XLS+), as follows: (i) the RuO_2:TiO_2/Z13X composite (20-60 mg) was loaded into the photoreactor; (ii) the gas mixture were fed keeping the stoichiometric [H_2]:[CO_2] molar ratio of 4:1 up to a total pressure of 1.6 bar, after H_2-based purging; and (iii) heating system/illumination source was switched on at 0/10 min (temperature: 50-250 ºC; radiant power: 0.42-0.75 W), thus starting the reaction. Gas samples were directly withdrawn from reactor headspace to a gas chromatograph, fitted with two capillary columns (Carbon Plot, Agilent, and Mol Sieve 5A Plot, Supelco), and a micro-thermal conductivity detector (μTCD) followed by a flame ionization detector (FID), for reaction quantification.
The adsorption equilibrium isotherms of CO_2 and CH_4 gases on the RuO_2:TiO_2/Z13X samples were obtained from a magnetic suspension microbalance (MSB, Rubotherm) at 150, 200 and 250 ºC.

3. Results and Discussion

Initially, prior to the synthesis of the bifunctional material, photocatalyst composition was optimized. The highest thermo-photoactivity was obtained using a Ru:TiO_2 mass ratio of 2:10 (30 mg; 150 ºC; 0.75 W), leading to a 81% CO_2 conversion after 100 min and a specific CH_4 production rate of 9.2 mmol g^{-1}_{cat} h^{-1}.
Then, the best-performing $RuO_{2(13.4\%)}$:TiO_2 catalyst was impregnated into the Z13X using the SIM and WIM. The WIM hindered the catalytic activity for the same material composition, with higher CO_2 conversion rates in the absence Z13X for similar specific CH_4 productions (i.e., CH_4 generated per unit mass of RuO_2:TiO_2 catalyst). This behaviour was likely due to inadequate water removal during

drying/calcination steps of the preparation procedure, given the strong interaction between water and Z13X. The presence of water can negatively affect the sintering of Ru during calcination and may also compete with CO_2 for adsorption sites during the reaction. Conversely, the SIM improved the RuO_2:TiO_2/Z13X catalytic activity. The composite with 30% active catalyst achieved an 88% CO_2 conversion after 100 min, close to the photocatalyst alone, but with a specific CH_4 production rate ca. 3.2-fold higher (29.2 mmol g^1_{cat} h^{-1}). This performance can be attributed to the combined effect of adsorption and thermo-photocatalysis.

The photocatalytic activity of the $RuO_{2(4.0\%)}$:$TiO_{2(26.3\%)}$/Z13X composite was also affected by other factors, namely:

• Material amount: within the 40 mL batch reactor (150 ºC; 0.75 W of radiant power), catalyst masses above and below 30 mg led to lower CO_2 reduction rates and specific CH_4 production rates.

• Radiant power: the higher the photon flux, the higher the catalyst photo-responsiveness until a radiant power of 0.75 W.

• Temperature: the highest synergy between thermal catalysis (dark conditions) and photocatalysis (light conditions) was attained at 150 ºC, as can be verified by the kinetic constant for CO_2 reduction presented in Figure 1. No CH_4 was detected under dark conditions at lower temperatures, while some CH_4 production was observed under sunlight, underlining the significance of the photochemical reaction pathway. At higher temperatures, similar methanation performances were found for thermal catalysis and thermo-photocatalysis, indicating that solar photons did not significantly contribute to the reaction mechanism.

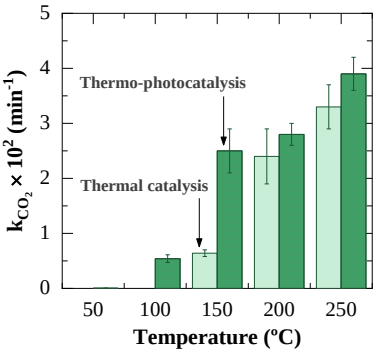

Figure 1. Pseudo-first-order kinetic constants for CO_2 reduction at different temperatures. Operating conditions: 30 mg of $RuO_{2(4.0\%)}$:$TiO_{2(26.3\%)}$/Z13X; RP = 0.75 ± 0.01 W (for thermo-photocatalysis).

Experimental adsorption equilibrium isotherms displayed higher CO_2 adsorption capacity for lower temperatures (see Table 1), in agreement with the results of thermo-photocatalytic tests. The bifunctional material's adsorption was about 2.6-fold higher than the photocatalyst, favouring CH_4 production per mass of active photocatalyst. The high yield of CO_2 methanation at 150 ºC can be attributed to the simultaneous contribution of adsorption and thermo-photocatalytic processes.

Table 1. Adsorption capacity of each material for CO_2 at initial conditions of the methanation reaction.

Material	Condition	q_{CO_2} (mol kg^{-1})
$RuO_{2(13.4\%)}$:TiO_2	150 ºC /2.3 bar	0.088
	200 ºC /2.6 bar	0.031
	250 ºC /2.9 bar	0.011
$RuO_{2(4.0\%)}$:$TiO_{2(26.3\%)}$/Z13X	150 ºC /2.3 bar	0.232
	200 ºC /2.6 bar	0.086
	250 ºC /2.9 bar	0.034

4. Conclusions

The novel dual-function material, obtained from the solid-state impregnation of Z13X adsorbent with RuO_2:TiO_2 photocatalyst (26.3% TiO_2; 4.0% RuO_2), was effectively able to promote simultaneous CO_2 adsorption/thermo-photoconversion (88 %), resulting in a CH_4 production of 29.2 mmol g^{-1}_{cat} h^{-1} at 150 ºC.

5. References

[1] C. Lu, X. Shi, Y. Liu, H. Xiao, J. Li, y X. Chen, *Mater. Today*, **50**, (2021) p. 385.
[2] W. Tu, Y. Zhou, Z. Zou, *Adv. Mater.*, **26**(27), (2014) 4607.
[3] D. Mateo, J. Albero, H. García, *Joule*, **3** (2019) 1949.
[4] G. Li, P. Xiao, P. Webley, J. Zhang, R. Singh, *Energy Procedia*, **1**(1), (2009) 1123.
[5] L. Paulista, A. Ferreira, B. Castanheira, M. Đolić, R. Martins, R. Boaventura, V. Vilar, T. Silva, *Appl. Catal. B: Environ.*, **340**, (2024) 123232.

Acknowledgments

This work was supported by sources provided by FCT/MCTES (PIDDAC), under Project CO2-to-CH4, 2022.01176.PTDC (DOI: 10.54499/2022.01176.PTDC). This research was also funded by FCT/MCTES (PIDDAC): LSRE-LCM - UIDB/50020/2020 (DOI: 10.54499/UIDB/50020/2020) and UIDP/50020/2020 (DOI: 10.54499/UIDP/50020/2020); and ALiCE - LA/P/0045/2020 (DOI: 10.54499/LA/P/0045/2020). L. Paulista, T. Silva, and V. Vilar acknowledge their fellowship/contracts granted by FCT (SFRH/BD/137639/2018, CEECIND/01386/2017, and CEECIND/01317/2017, respectively).

P2: Biochar modificado com enxofre orgânico: um adsorvente verde eficaz para remover espécies metálicas em sistemas aquáticos

J. C. A. Macedo [(1)], P.S. Tonello[(2)], A. H. Rosa [(3)]

[(1)] Departamento de Química, Física y Ciencias Ambientales y del Suelo, Universitat de Lleida y AGROTECNIO, Rovira Roure 191, 25198 Lleida, Spain.
joaocarlosalvesmacedo@hotmail.com
[(2,3)] UNESP Instituto de Ciência e Tecnologia – Campus Sorocaba, Sorocaba CEP: 18087-180, Brasil
[(2)]paulo.tonello@unesp.br, [(3)]andre.rosa@unesp.br

1. Introdução – A poluição ambiental causada pela contaminação de metais potencialmente tóxicos é um dos problemas do mundo que vem recebendo atenção crescente da comunidade científica, sendo estes os principais poluentes inorgânicos presentes nos rios e lagos, afetados especialmente por efluentes industriais [1]. Atualmente, a modificação do biochar (BC), um adsorvente verde, subproduto da pirólise da biomassa, apresenta-se como uma alternativa para o desenvolvimento de um material eficiente e sustentável na remoção de contaminantes inorgânicos [1]. Apesar de todas as vantagens dos BCs brutos (não modificados), sua eficiência de remoção de metal é geralmente inferior à eficiência dos métodos convencionais de adsorção. Como resultado, a modificação dos BCs brutos surgiu como uma alternativa para aumentar a capacidade de adsorção e seletividade do BC para remoção de metais por meio da formação de novos grupos funcionais em sua superfície. Embora existam vários estudos sobre modificação química de BCs, poucos deles investigam as contribuições da modificação de BCs por componentes enxofre-nitrogênio para a adsorção de metais, especialmente em sistemas multielementares. O objetivo deste estudo foi investigar o desempenho e a seletividade dos BCs (produzidos a partir de bagaço de cana-de-açúcar) modificados com enxofre orgânico, em uma rota sintética de etapa única, para remoção de Cd^{2+}, Ni^{2+}, Pb^{2+} e Cr^{3+} de soluções aquosas mono e multielementares.

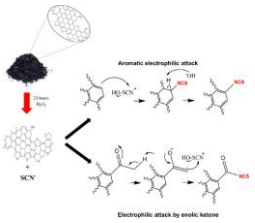

Imagem 1. Mecanismos de reação do biochar com íon tiocianato.

2. Experimental - A adição de compostos organossulfurados no biochar pirolisado a 700ºC foi preparado pela reação entre o biochar e o tiocianato de potássio catalisado com H_2O_2 a 25ºC (BC_{SCN700} e BC_{700}, para amostra modificada e não modificada, respectivamente). Os materiais foram caracterizados por espectroscopia no infravermelho com transformada de Fourier (FTIR), espectroscopia de fotoelétrons de raios X (XPS), espectroscopia de energia dispersiva (EDS) e pirólise acoplada a cromatografia gasosa-espectrometria de massa (Py-GC-MS). Os biochars antes e depois da modificação foram testados em sua eficiência de remoção na adsorção dos íons Cd^{2+}, Cr^{3+}, Ni^{2+} e Pb^{2+} em pH 6

3. Resultados e discussões – O espectro de infravermelho de BC_{SCN700} revelaram bandas em 2000 e 2100 cm^{-1} atribuídas a estiramento do grupo isotiocianato. Os pirograma obtido da técnica de Pi-CG-EM apresentou picos de compostos derivados da modificação (guanidina, dissulfeto de carbono, isotiocianato de metila, ciclohexassulfeto, 6-(1,1-dimetil-tioureido)benzotiazol-2(3H)-tiona e enxofre octatômico cíclico), confirmando a presença de grupos sulfônicos na estrutura do biochar modificado. Os resultados do ajuste XPS confirmaram que a modificação $KSCN/H_2O_2$ aumentou o número de átomos de S e N, como corroborado com os resultados de EDS. Isto é observado pelos picos maiores e mais intensos dos átomos de S e N nos espectros do BC_{SCN700} quando comparado com BC_{700}, implicando num aumento dos sítios de adsorção.

A partir do ajuste ao modelo teórico de Langmuir-Freundlich (Sips), a adsorção pelo biochar modificado apresentou a seguinte ordem para os valores de $Q_{máx}$ os resultados indicaram que a remoção de íons metálicos por BC_{SCN700} segue a ordem $Pb^{2+} > Cr^{3+} > Cd^{2+} \cong Ni^{2+}$ e $Cd^{2+} > Pb^{2+} > Ni^{2+} \cong Cr^{3+}$ para mono-sistemas de elementos e multielementos, respectivamente. A sequência de adsorção de metal no BC_{700} (Cr^{3+} (40,29 mg g^{-1}) > Pb^{2+} (35,6 mg g^{-1}) > Ni^{2+} (20,3 mg g^{-1}) > Cd^{2+} (11,9 mg g^{-1})) seguiu a mesma ordem de dureza dos metais: Cr^{3+} (0,147) > Pb^{2+} (0,131) > Ni^{2+} (0,126) > Cd^{2+} (0,081). Além disso, a sequência de adsorção de multielementar no BC_{SCN700} seguiu aproximadamente a ordem de maciez dos metais: Pb^{2+} (3,58) > Cd^{2+} (3,04) > Ni^{2+} (2,82) > Cr^{3+} (2,70). O aumento de átomos de enxofre contido no grupo isotiocianato, promoveu um aumento na adsorção principalmente de Cd^{2+} e Ni^{2+}, devido a teoria de ácidos/bases mole/dura (HSAB), onde sendo o enxofre uma base mole, tende a ter uma maior interação com o Cd^{2+} e Ni^{2+} considerados ácidos moles [2].

A presença de outros metais no sistema multielementar causou um efeito sinérgico e antagônico na adsorção para ambas as amostras de BC, conforme descrito pelo efeito dos valores de interação iônica.

Os mecanismos envolvidos na adsorção foram fisissorção , quimissorção , complexação, precipitação e troca iônica.

4. Conclusões - O biochar modificado preparado por pirólise a 700°C teve o melhor desempenho de adsorção, principalmente nos experimentos em pH 6. Além disso, a adsorção de Cd^{2+}, Ni^{2+}, Pb^{2+} e Cr^{3+} no sistema multielementar causaram efeito sinérgico na adsorção de Cr^{3+}, Ni^{2+} e Cd^{2+} e efeito antagônico na adsorção de Pb^{2+} em BC_{SB700} e BC_{SCN700}. Complexação superficial, co-precipitação com PO_4^{3-} e troca iônica com Ca^{2+}, K^+ e Mg^{2+} foram os mecanismos na remoção de Cd^{2+}, Ni^{2+}, Pb^{2+} e Cr^{3+} por BC_{SB} e BC_{SCN}. Embora a eletronegatividade possa ter controlado a adsorção dos metais nos sistemas monoelementares, a suavidade e a dureza dos metais podem ter afetado a adsorção nos sistemas multielementares. A modificação do BC_{SB700} obteve bons resultados, o que pode levar ao desenvolvimento de um material de sorção eficaz para remover Cd^{2+}, Ni^{2+} , Pb^{2+} e Cr^{3+} de fluxos de água e efluentes industriais.

Agradecimento
Os autores agradecem ao CNPq, Capes, Finep e Fapesp (Proc. 2016/08215-4; 2018/20326-1; 2023/15847-0) por bolsas e suporte financeiro

5. Referencias
[1] Shakoor, M. B. et al.,2013. **Journal of Biodiversity and Environmental Sciences**, v. 3, p. 12-20, 2013.
[2] MISONO, M. et al., 1967. **J. Inorg, Nucl. Chem.**, v. 29, p. 2685 – 2691
[3] Macedo, J.C.A. et al.,2021. **Surfance and Interface**., v 22, 100822

RIA 43
XLIII Reunião Ibérica de Adsorção
Porto, Portugal
1-4 September 2024

P3: Remoção de mercúrio de soluções aquosas a partir de bagaço de cana modificado com plasma

A.P. Santacruz-Salas [(1)], M. L. P. Antunes [(2)], E. C. Rangel [(3)],

C. H. Watanabe [(4)], A. H. Rosa [(5)]

Universidade Estadual Paulista (UNESP), Instituto de Ciência e Tecnologia, Câmpus Sorocaba, Brasil.
paola.santacruz@unesp.br
[(2)]pereira.antunes@unesp.br, [(3)]claudia.watanabe@unesp.br, [(4)]elidiane.rangel@unesp.br, [(5)]andre.rosa@unesp.br

1.Introdução – De acordo com a Organização Mundial da Saúde, o mercúrio é classificado como um metal potencialmente toxico devido a sua capacidade de bioacumulação e biomagnificação ao longo da cadeia alimentar, representando um risco significativo tanto para a saúde humana como para o meio ambiente [1]. Diante essa problemática, a adsorção tem sido reconhecida como uma técnica simples, rápida, eficaz e econômica em comparação com outros tipos de tratamento, na que é possível o reaproveitamento de outros materiais como os resíduos agrícolas [2].
No entanto, para alcançar uma maior eficiência de remoção é necessário modificar a biomassa para melhorar suas características físicas e químicas, processos que geralmente exigem de longos tempos de tratamento, altas temperaturas e podem geram contaminação secundário [3,4]. Nesse contexto, a tecnologia de plasma surge como uma ferramenta promissora para a modificação dos materiais, sendo eficiente em termos energéticos e mais amigável com o meio ambiente, pois não gera resíduos ou emissões atmosféricas consideráveis [5]. O tratamento com plasma é eficaz para a funcionalização da superfície, ao mesmo tempo que mantém as propriedades físicas e químicas do material [6]. Em adsorventes como o biochar se tem encontrado que o tratamento com plasma pode melhorar a estrutura porosa e aumentar a concentração de grupos funcionais ativos [4,6,7]
Com base nisso, este trabalho teve como objetivo avaliar a incorporação de um elemento eletronegativo, como o flúor, na estrutura do bagaço de cana-de-açúcar (SB) por meio da tecnologia de plasma de baixa temperatura, para a remoção de mercúrio de soluções aquosas. Até o momento não há relatos na literatura sobre o uso de tratamentos com plasma de hexafluoreto de enxofre (SF_6) de baixa pressão em resíduos agrícolas como o SB para a adsorção de contaminantes inorgânicos de efluentes líquidos.

2. Metodologia - O SB obtido na região de São Paulo (Brasil) foi previamente lavado, seco na estufa a 80°C por 12 horas e resfriado. Em seguida, foi pulverizado em um moinho e peneirado em uma malha de 35 mesh para padronizar o tamanho das partículas. A modificação por plasma foi feita usando um reator de aço inoxidável, no qual o eletrodo inferior foi ligado a radiofrequência e o superior foi aterrado. O SB foi tratado com plasma de baixa temperatura com hexafluoreto de enxofre (SF_6) como gás de trabalho, variando os tempos de tratamento (2, 30 e 60 minutos) e as potências fixadas (80, 190 e 300 W) em uma pressão final de 16 Pa.
Os efeitos das modificações foram avaliados com microscopia eletrônica de varredura (MEV), espectroscopia de energia dispersiva de raios X (EDS/MEV), infravermelho por transformação de Fourier (FTIR) e ponto de carga zero (pHpzc). Foi feito um estudo preliminar com todos os adsorventes desenvolvidos. Para o adsorvente que apresentou a maior porcentagem de remoção, foram calculadas as cinéticas de adsorção de primeira e de segunda ordem, assim como os modelos de isotermas de adsorção propostos por Langmuir e Freundlich.

3. Resultados e discussão - Os resultados da caracterização indicam que o plasma de baixa temperatura induz efetivamente modificações nos adsorventes, preservando sua estrutura principal intacta. Nota-se um aumento na estrutura porosa à medida que o tempo de tratamento aumentou. Além disso, a análise EDS/MEV demonstrou a incorporação de flúor em todos os materiais, enquanto o enxofre só foi detectado em algumas amostras. O teor de carbono aumentou com o aumento do tempo de tratamento, enquanto o flúor apresentou um efeito inverso, possivelmente ligado à formação de HF.
Entre as condições testadas, como se observa na tabela 1, o SB tratado com 300 W por 60 minutos demonstrou a maior eficiência de remoção de mercúrio, alcançando uma elevada taxa de remoção de 83,67% em comparação com o SB não tratado, que apresentou cerca de 57,95%. O mecanismo de adsorção indicou um comportamento físico e químico, sendo a quimissorção o processo dominante. O modelo de Freundlich forneceu o melhor ajuste aos dados experimentais, com um valor R^2 de 0,97.

Tabela 1. Porcentagens de remoção dos adsorventes tratados em 60 minutos

Adsorvente	% remoção
SB sem tratamento	57,95 ± 6,55
SB 80 W 60 min	63,35 ± 1,55
SB 190 W 60 min	71,47 ± 2,55
SB 300 W 60 min	83,67 ± 1,04

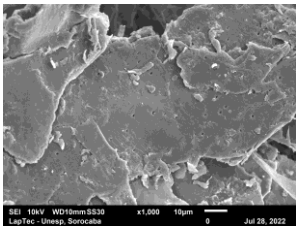

Figura 1. MEV x1000 do SB tratado com 300 W durante 60 Min

4. Conclusões – Com base nos resultados deste estudo, conclui-se que a técnica de plasma de baixa temperatura com SF_6 é um método eficaz para melhorar as características do SB, facilitando a adsorção de íons de mercúrio em soluções aquosas, especialmente com o pH ajustado para 7. Portanto, essa técnica pode abrir novas perspectivas para a produção de adsorventes inovadores e eficazes no tratamento de água para a remoção de contaminantes inorgânicos, dado que permite modificar e funcionalizar as propriedades físico-químicas de resíduos agroindustriais como o bagaço de cana sem afetar sua estrutura principal.

Agradecimento
Os autores agradecem ao BECATE Narino - Fundacion Ceiba, CNPq, , Capes, Finep e Fapesp (Proc. 2016/08215-4; 2018/20326-1; 2023/15847-0) por bolsas e suporte financeiro

5. Referências bibliográficas

[1] C. da Silva Montes, M. Ferreira, T. Giarrizzo, LL. Amado e R. Rocha. Chemosphere, **287**, (2022) p. 132263.
[2] M. Shahabi Nejad e H. Sheibani. Journal of Environmental Chemical Engineering **10**, (2022), p. 107363.
[3] M. Khan, A. Khan, H. Bhatti, M. Zahid, S. Alissa e Y. El-Badry. Journal of Materials Research and Technology **15**, (2021), p. 2016 - 2025
[4] X. Zhang, Y. Chu, X. Yu, C. Yan, Y. Yang, J. Liu, G. Shen, X Wang, S. Tao e X. Wang. Journal of Hazardous Materials **424**, (2022), p. 127438
[5] Z. Mohammed, S. Jeelani, V. Rangari. Materials Letters **292**, (2021), p. 129678.
[6] R. Hu, J. Xiao, T. Wang, Y. Gong, G. Chen, L Chen e X Tian. Carbon **168**, (2020), p. 515–527.
[7] H. Zhang, T. Wang, A. Sui, Y. Zhang, B. Sun e W-P. Fuel **253**, (2019), p. 703–712

P4: Ionic dyes adsorption on bone char

S. Aguirre-Contreras [(1)], M.V. López-Ramón [(2)], I. Velo-Gala[(3)], M.A. Álvarez[(2)], R.Ocampo-Pérez [(1)].

*[(1)] Universidad Autónoma de San Luis Potosí, San Luis Potosí 78260, México*a237074@alumnos.uaslp.mx
[(2)] Universidad de Jaén, Jaén 23071, España
[(3)] Universidad de Granada, Granada 18071, España
mvlro@ujaen.es, invega@ugr.es, *malvarez@ujaen.es*, *raul.ocampo@uaslp.mx*

1. Introduction – It is well known that industrial dyes are an environmental problem due to their harmful effects on human and the environment. About 10,000 tons of industrial dyes are produced annually, and about 100 tons are discharged into wastewater [1]. Among the treatment methods, adsorption with low-cost materials is an affordable option due to easy operation, low energy consumption, and high efficiency even at low concentrations. Recently, bone char has been considered as an adsorbent material with low environmental impact, easy regeneration and low cost [2]. For these reasons, the objectives of this work are to evaluate the adsorption capacity of ionic dyes on commercial bone char, as well as the adsorption kinetics.

2. Experimental – The dyes used in this work were IndigoCarmine (IC) and Congo Red (CR). The concentration in aqueous solution was determined by UV-vis spectroscopy. The bone char (BC) used is commercialized under the brandname BRIMAC®. The equilibrium and kinetic adsorption experiments were carried out at neutral pH, varying the initial concentration, in a batch reactor. The adsorption equilibrium data were interpreted by Langmuir, Freundlichand Prausnitz-Radke isotherms. The kinetic experiments were mathematically modeled considering diffusive phenomena, using the PVSDM model [3].

Results and Discussion - The adsorption equilibrium ofIC and CR on BC was favorable (see Image 1 and 2), presenting adsorption capacities greater than 30 mg g^{-1} at very low concentrations for both contaminants. This behavior is typical of a high affinity system. The adsorptionmechanism could be attributed to electrostatic interactionsbetween the negative charges contributed by the sulfonate groups of the dyes and the protonated hydroxyl groups of the hydroxyapatite of the BC. On the other hand, the carbon content of BC is low (8-11%), however, because that the ICand CR molecules are organic compounds, with relatively high octanol-water partition coefficients (3.57 and 2.63, respectively), some affinity is to be expected. Themaximum adsorption capacities obtained were 57 and 257 mg g^{-1} for IC and CR, respectively. The Freundlich adsorption isotherm interpreted the equilibrium data for IC with a percentage deviation of 4.3%, while the Prausnitz-Radke isotherm with 1.6% for CR.

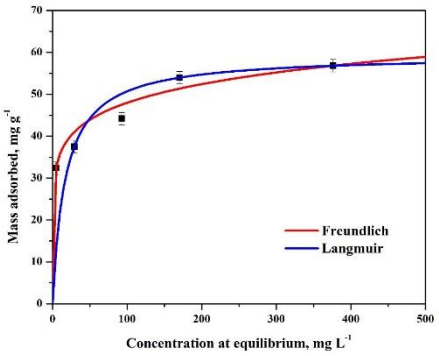

Image 1. Equilibrium data for IC adsorption on BC

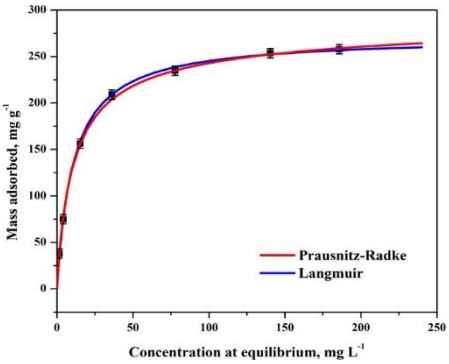

Image 2. Equilibrium data for RC adsorption on BC

The adsorption equilibrium was reached in 1000 minutes for IC, while for CR it took 3000 minutes (see Image 3 and 4). This could be explained by the molecular difference, CR having a molecular weight 1.5 times larger than IC. The PVSDM interpreted the decay curves adequately, with low percentage deviations. Since the model is based on intraparticle diffusive processes, a good interpretation of the experimental data reveals that intraparticle transport controls the adsorption rate. This is important because diffusive processes may involve an extensive mass transfer zone in dynamic adsorption.

3. Conclusions – Based on the high adsorption capacities obtained, BC is a favorable material for the removal of industrial dyes from wastewater. In addition, BC has advantages over other adsorbents such as low cost and lower environmental impact, which makes it a suitable material for use inwastewater treatment. On the other hand, the adsorption rate study revealed that intraparticle diffusion phenomena are important, and that the adsorption rate depends on the molecular weight of thepollutant, which should be take into account for dynamic adsorption.

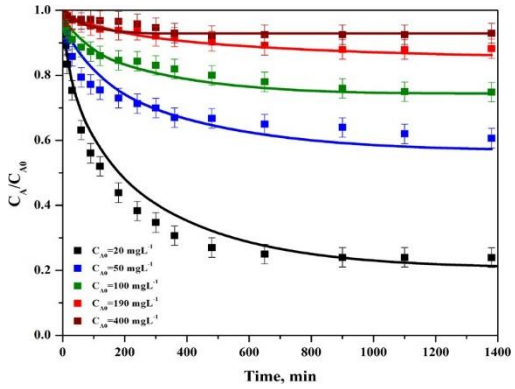

Image 3. Concentration curves decay for IC on BC at several operation conditions. The lines represent the solution of the PVSDM.

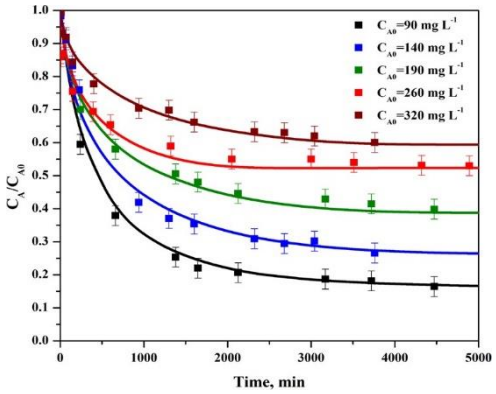

Image 4. Concentration curves decay for CR on BC at several operation conditions. The lines represent the solution of the PVSDM.

4. References

[1] P. Semeraro, et. al., *Dyes and Pigments*, 119,(2015) p. 84-94.
[2] N.A. Medellín-Castillo, et. al., *Journal Analyticaland Applied Pyrolysis* 175 (2023) p. 106161.
[3] S. Aguirre-Contreras, et. al., *Journal of WaterProcess Engineering* 54 (2023) p. 103967

P5: Extremum Seeking Control for Pressure Swing Adsorption units

Beatriz C. Silva [(1), (2)], Ana M. Ribeiro [(1), (2)], Diogo Rodrigues [(1), (2)], Alexandre F.P. Ferreira [(1), (2)], Idelfonso B.R. Nogueira [(3)]

[(1)] *Laboratory of Separation and Reaction Engineering−Laboratory of Catalysis and Materials (LSRE-LCM), Department of Chemical Engineering, University of Porto, Porto, 4200-465, Portugal*

[(2)] *ALiCE−Associate Laboratory in Chemical Engineering, Faculty of Engineering, University of Porto, Porto, 4200-465, Portugal*

[(3)] *Chemical Engineering Department, Norwegian University of Science and Technology, Sem Sælandsvei 4, Kjemiblokk 5, Trondheim, 793101, Norway*

e-mail: up201707213@edu.fe.up.pt , apeixoto@fe.up.pt , dfrodrigues@fe.up.pt , aferreir@fe.up.pt , idelfonso.b.d.r.nogueira@ntnu.no

1. Introduction

Real-time optimization (RTO) has emerged in the last 30 years to overcome some of the optimization's weak points when applied to the industry [1]. Whereas simple optimization relies on mathematical models that are not always representative of the industrial plant operation, RTO ensures a better representation of the plant and continuous optimization to improve process performance autonomously [2].

The application of RTO to dynamic operations is challenging due to the complexity of the nonlinear problems involved, making it difficult to achieve robust solutions [3]. Regarding cyclic adsorption processes, particularly Pressure Swing Adsorption (PSA) and Temperature Swing Adsorption (TSA), the control of the process in real-time is essential to maintain or increase productivity.

The literature on Real-time Optimization in PSA units relies on Model Predictive Control (MPC) and Economic Model Predictive Control (EMPC). Given the importance of PSA and TSA systems on multiple separation operations, establishing alternatives for control and optimization in real-time is in order.

With that in mind, this work aimed to explore an alternative real-time optimization technique, Extremum Seeking Control. The chosen case study was Syngas Upgrading. Syngas upgrading is gaining relevance due to the Fischer-Tropsch reactions and their role in enabling an alternative to fossil fuels, with the possibility of also providing H_2 for ammonia production and capturing CO_2 to avoid its release into the atmosphere.

2. Experimental

The operation of the PSA unit for syngas upgrading used in this work was discussed in the work of Regufe et al. [4].

The objective function defined in this work was CO_2 productivity, presented in Equation 1.

$$CO_2\ Productivity\ (mol_{CO_2} kg^{-1} h^{-1}) = \frac{\left[\int_0^{t_{blow}} C_{CO_2} u_0|_{z=0}\, dt + \int_0^{t_{purge}} C_{CO_2} u_0|_{z=0}\, dt - \int_0^{t_{rinse}} C_{CO_2} u_0|_{z=0}\, dt\right] A_{bed}}{t_{cycle} m_{dry\ adsorbent}} \quad (1)$$

Extremum-seeking control (ESC) is a method that aims to control the process by moving an objective's gradient towards zero and estimating that gradient based on persistent perturbations. The corresponding block diagram is presented in Image 1. High-pass Filter (HF) eliminates the signal's DC component to get a clearer response to the changes in the system. The input variable u is continually disrupted by a sinusoidal wave, which helps assess the evolution of the objective function by keeping the system in a state of constant perturbation. The integration will determine the necessary adjustment in u to bring the objective function closer to its optimum. This adjustment is often scaled by a gain K to accelerate convergence.

The model was implemented in gPROMS with communication with MATLAB and Simulink, where the ESC was implemented.

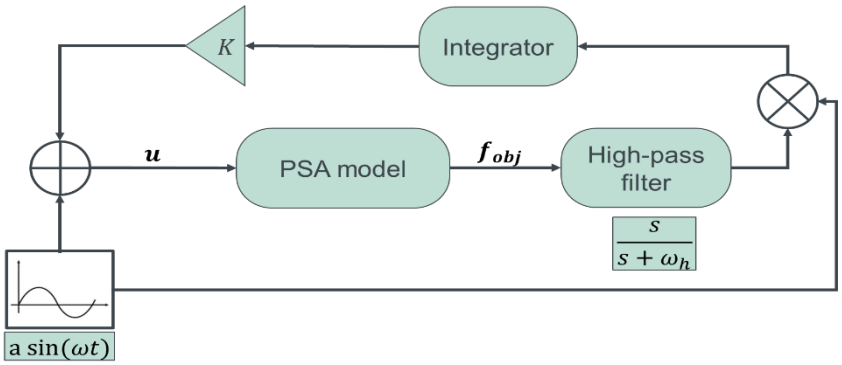

Image 1. Extremum Seeking Control block diagram

3. Results and Discussion

The parameters used in the results presented in this abstract are summarized in Table I. The results are presented in Image 2.

Table III. Parameters used in the case presented

Parameter		Parameter		Parameter		Parameter	
a	1	Number of cycles per parameter update	1	K	15000	Simulation time (s)	10
ω	20	Initial t_{feed} (s)	330	ω_h	15	Running time (s)	868

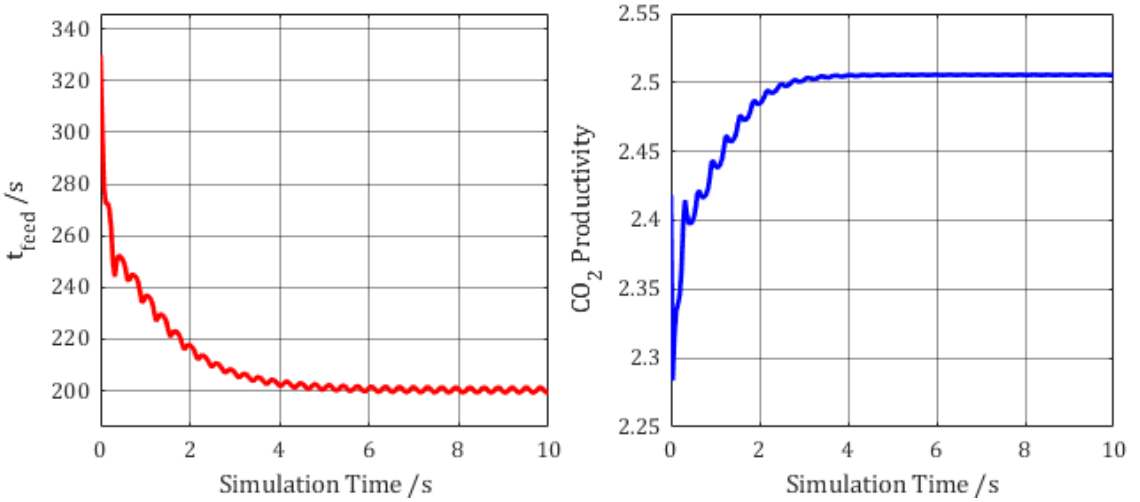

Image 1. ESC action on time of feed value and effect on the objective function, the productivity of CO_2

4. Conclusions

Extremum Seeking Control successfully optimised the CO_2 Productivity in PSA units for syngas upgrading/ H2 purification. This proves that ESC can be a valuable tool in optimizing and controlling PSA processes, and it does not require the unit to reach a Cyclic Steady State to adjust the operation.

5. References

[1] D. Bonvin, "Special Issue 'Real-Time Optimization' of Processes," *Processes*, vol. 5, no. 2, 2017
[2] G. Pfaff, J. Fraser Forbes, and P. James McLellan, "Generating information for real-time optimization," *Asia-Pacific Journal of Chemical Engineering*, vol. 1, no. 1–2, pp. 32–43, 2006
[3] S. Kameswaran and L. T. Biegler, "Simultaneous dynamic optimization strategies: Recent advances and challenges," *Comput Chem Eng*, vol. 30, no. 10, pp. 1560–1575, 2006
[4] M. J. Regufe *et al.*, "Syngas Purification by Porous Amino-Functionalized Titanium Terephthalate MIL-125," *Energy & Fuels*, vol. 29, no. 7, pp. 4654–4664, Jul. 2015

RIA 43
XLIII Reunião Ibérica de Adsorção
Porto, Portugal
1-4 September 2024

P6: Desenvolvimento de monolito Sílica/HKUST-1 para Captura de CO_2

K.C. Santos [(1)], M.R. Oliveira [(2)], T.L. Silva [(1)], T.R. Menezes [(1)], K.S. Santos [(2)], G.R. Borges [(1,2)], C. Dariva [(1,2)], E. Franceschi [(1,2)], S.M. Egues [(1,2)], J.F. De Conto [*(1,2)]

[(1)] *Programa de Pós-Graduação em Engenharia de Processos (PEP)/ Universidade Tiradentes (UNIT), Aracaju, SE Brasil. e-mail: jfconto@gmail.com*

[(2)] *Laboratório de Síntese de Materiais e Cromatografia (LSINCROM), Núcleo de Estudos em Sistemas Coloidais (NUESC)/Instituto de Tecnologia e Pesquisa (ITP), Aracaju, SE, Brasil.*

1. Introdução – O aquecimento global tem impulsionado extensas pesquisas para a captura de dióxido de carbono (CO_2) com o objetivo de atingir emissões líquidas zero de gases de efeito estufa até 2050, em conformidade com o Acordo de Paris. Essa iniciativa é especialmente relevante em diversos sistemas, incluindo desde a remoção de CO_2 do ar até a captura de CO_2 do gás natural (GN). Dentre os métodos existentes, a captura de CO_2 por adsorção destaca-se devido à sua alta capacidade de remoção, utilização em sistemas com condições distintas de operação e à simplicidade econômica do processo. No entanto, a eficiência desse método depende do desenvolvimento de adsorventes adequados, que possuam elevada seletividade e capacidade de adsorção de CO_2, além de serem economicamente viáveis e estáveis em distintas condições de operação [1]. Assim, as redes metalorgânicas (MOFs) surgem como uma classe de adsorventes promissores para a captura de CO_2, pois possuem tais propriedades desejáveis e resultados notáveis na adsorção de diferentes gases. Todavia, a estabilidade mecânica e o custo da MOF ainda são lacunas que podem ser melhoradas, assim a junção de MOFs com a sílica, é uma alternativa bastante promissora, pois além de melhorar a estabilidade mecânica das MOFs, reduz o custo do material adsorvente. Desta forma, este trabalho teve como objetivo a síntese de um monolito de sílica/HKUST-1 através de secagem supercrítica, para avaliar suas propriedades estruturais e capacidade de adsorção de CO_2.

2. Experimental – Neste trabalho, uma nova rota de síntese foi implementada para a construção do monólito, baseada nos estudos de Ulker [2], utilizando uma mistura de TEOS e etanol, seguida pela adição de água e HCl 37% para ajuste do pH. Depois, 10% de MOF HKUST-1 (Sigma-Aldrich) foram incorporados à mistura. Com agitação vigorosa, observou-se o pó do MOF HKUST-1 se dispersando na mistura, conferindo-lhe uma coloração azul. Após 2 h, foi adicionada amônia aquosa a 25% para acelerar a reação de condensação, levando à gelificação em condições neutras. Posteriormente, a solução foi vertida em uma coluna de aço inoxidável de 10 mL, e a etapa de envelhecimento continuou por 24 h a 40 °C em estufa. A etapa seguinte foi a secagem supercrítica (Figura 1), a 90 bar e 40°C, por aproximadamente 5 h para o monólito de sílica e cerca de 3 h para o monólito de sílica/HKUST-1. Vale destacar que a síntese do monólito de sílica foi realizada de maneira idêntica, mas sem a adição da HKUST-1. Na Figura 2, observa-se os monólitos após a secagem com CO_2 supercrítico. As análises dos materiais e monolitos foram feitas por DRX, FTIR e isoterma de adsorção/dessorção de N_2. As isotermas de CO_2 foram coletadas nas temperaturas de 30, 40 e 50 °C usando um analisador de adsorção de gás *Micromeritics 3Flex*.

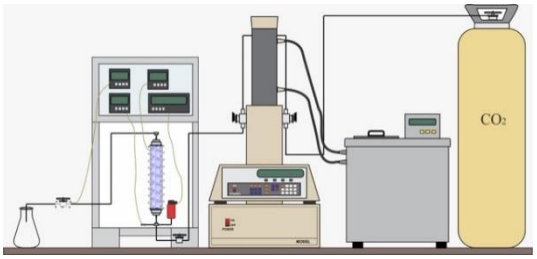

Figura 1: Unidade experimental para secagem de materiais com CO_2 supercrítico.

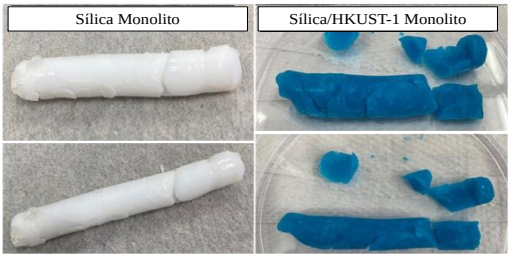

Figura 2: Monolito de sílica e sílica/MOF depois da secagem com CO_2 supercrítico.

3. Resultados e Discussão – O difratograma DRX do pó da HKUST-1 comercial, do monólito de sílica e do monólito de sílica/HKUST-1 após secagem com CO_2 estão apresentados na Figura 3. O monólito de sílica exibiu dois picos indicando sua natureza amorfa, enquanto os picos da HKUST-1 comercial foram preservados no monólito sílica/HKUST-1, confirmando a integridade estrutural. A Figura 4 destaca as bandas características da sílica na região de 790, 1054 e 945 cm^{-1} referentes ao grupo Si-O-Si e Si-OH e as bandas da HKUST-1 na região de 1700-1500, 1500-1300 e 710-758 cm^{-1} as quais são atribuídas aos estiramentos assimétricos e simétricos dos grupos $–COO^-$ e vibrações fora do plano C–H do anel de benzeno [3]. Outra evidência da formação da HKUST-1, está relacionada com o estiramento característico da ligação Cu-O em torno de 760 cm^{-1}, verificados para a MOF HKUST-1 e seu compósito.

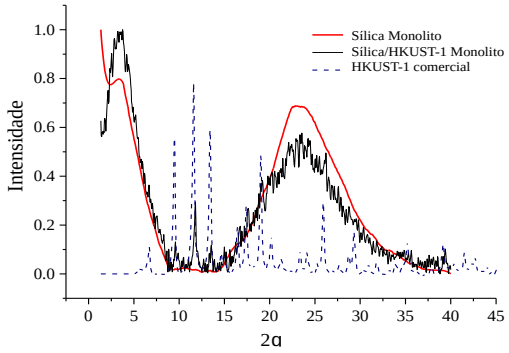

Figura 3: DRX da HKUST-1 comercial, sílica monolito e sílica/HKUST-1 monolito seco com CO_2 supercrítico.

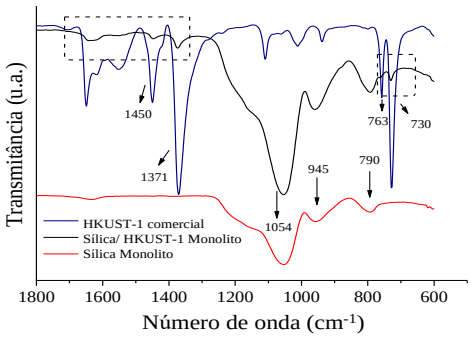

Figura 4: FTIR da HKUST-1 comercial, sílica monolito e sílica/HKUST-1 monolito seco com CO_2 supercrítico.

Além disso, este trabalho otimizou o tempo de secagem de 12 h, utilizado por Ulker [2], para aproximadamente 5 h para o monólito de sílica e 3 h para o monólito de sílica/HKUST-1, reduzindo o consumo energético e mantendo áreas superficiais elevadas: 943 e 906 $m^2 g^{-1}$ para o monolito de sílica e monolito de sílica/HKUST-1, respectivamente. Quanto aos experimentos de adsorção de CO_2, verifica-se na Figura 5 que as isotermas de adsorção se comportam de forma linear em baixas pressões. Observou-se que a quantidade de CO_2 adsorvida aumenta com a diminuição da temperatura, demonstrando uma adsorção exotérmica e espontânea. A sílica adsorveu 0,78 mmol g^{-1} a 30 °C e a sílica/HKUST-1 adsorveu 1,03 mmol g^{-1} a 30 °C. Nenhuma das amostras atingiu a capacidade máxima de adsorção nas temperaturas estudadas, sugerindo que maior tempo e/ou pressão poderiam levar a saturação do adsorvente.

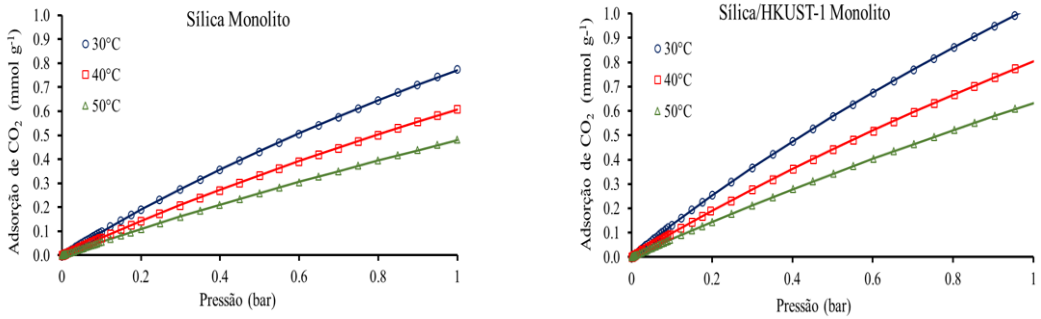

Figura 5: Isotermas de adsorção de CO_2 dos monolitos de sílica e sílica/HKUST-1 até 1 bar nas temperaturas de 30 °C, 40 °C e 50 °C.

Nota-se que a adição de 10% de HKUST-1 à sílica aumentou a capacidade de adsorção de CO_2 em 0,25 mmol g^{-1} em comparação com a sílica pura, isso é devido a presença de sítios energéticos de adsorção na HKUST-1, que são ativados pela remoção de moléculas de solvente ligadas aos centros metálicos de Cu^{2+}, favorecendo a adsorção. Além disso, a capacidade de adsorção diminui com o aumento da temperatura, o que se explica pelos fatores termodinâmicos que favorecem o estado gasoso livre do CO_2, reduzindo a interação molecular entre adsorvente e adsorvato [4]. Este comportamento foi observado para a sílica (0,60 e 0,47 mmol g^{-1} para 40 e 50 °C) e para a sílica/HKUST-1 (0,80 e 0,63 mmol g^{-1} para 40 e 50 °C).

4. Conclusão - Os resultados comprovaram a eficácia dos monolitos na melhora da estabilidade estrutural da HKUST-1 sem a perda de suas qualidades texturais e estruturais, contribuindo para o desenvolvimento de um novo monolito híbrido sílica/HKUST-1, potencializando suas aplicações e tornando os materiais promissores. Os testes de adsorção de CO_2 mostraram que os monolitos de sílica com adição de 10% de HKUST-1 forneceram uma maior capacidade de adsorção quando comparada às sílicas, supondo assim, que com maior concentração desses MOFs os novos monolitos poderiam obter resultados melhores.

5. Referências

[1] K. Santos et al., *Separation and Purification Technology*, **271**, (2021) p. 119409.
[2] Z. Ulker et al., *Microporous and Mesoporous Materials*, **170**, (2013) p. 352-358.
[3] A.L. Nuzhdin et al., *The Royal Society of Chemistry*, v. **6**, (2016) p. 62501-62507.
[4] M.R. Oliveira et al., *Journal of Sol-Gel Science and Technology*, **105**, (2023) p. 370–387
.

P7: Tailoring activated carbon supported on 3D alumina macrospheres for micropollutant adsorption

A. Torres-Pinto[(1,2)*], J.J.M. Dele[(1,2)], A.M. Chávez[(3)], A.M.T. Silva[(1,2)]

[(1)] LSRE-LCM – Laboratory of Separation and Reaction Engineering - Laboratory of Catalysis and Materials, Faculty of Engineering, University of Porto, Rua Dr. Roberto Frias, 4200-465 Porto, Portugal
[(2)] ALiCE – Associate Laboratory in Chemical Engineering, Faculty of Engineering, University of Porto, Rua Dr. Roberto Frias, 4200-465 Porto, Portugal
[(3)] Departamento de Ingeniería Química y Química Física, Instituto Universitario del Agua, Cambio Climático y Sostenibilidad (IACYS), Universidad de Extremadura, 06006 Badajoz, Spain
** andretp@fe.up.pt*

1. Introduction – Human activities have caused the presence of organic micropollutants in drinking water sources. Therefore, according to their risk to human health and the threat of exposure there is a growing concern for the drinking water decontamination. In this sense, sophisticated technologies, such as adsorption, are being explored for the removal of micropollutants from water. The application of activated carbon (AC) has been proven to be efficient for the adsorption of several contaminants [1]. In this work, we aimed to modify a carbon material with nitrogen groups to allow its self-immobilisation onto three-dimensional alumina spheres according to our previous work [2]. The functionalised AC successfully adhered to the 3D support and was investigated for the removal of venlafaxine (VFX) from simulated mineral waters.

2. Experimental – AC materials were prepared by calcination of the precursors dissolved in an aqueous solution on a microwave muffle furnace under air atmosphere. For the immobilisation step, alumina spheres were submerged in the mixture and followed the same calcination procedure. The final 3D structures were sonicated, thoroughly rinsed and dried. The powder materials were tested in batch conditions, while the spheres were transferred to a column reactor and used for the adsorption of VFX in continuous mode. The concentration of the pharmaceuticals was followed by high-performance liquid chromatography. The prepared materials were characterised before and after use different techniques.

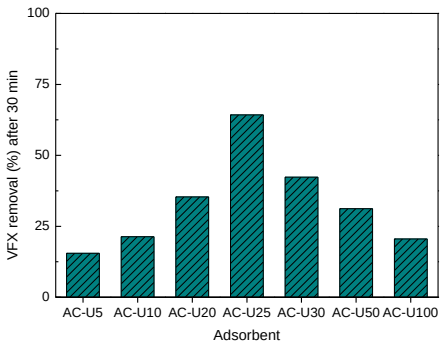

Figure 1. Removal of VFX in mineral water by adsorption

3. Results and Discussion – Preliminary assays were carried out using the prepared adsorbents in powder form. Different reaction conditions were optimised, such as precursor concentration, adsorbent load and pH level. Then, the prepared immobilised adsorbents were placed in a packed-bed reactor and operated in continuous mode for the removal of VFX at a flow rate of 0.25 mL min^{-1}. The self-immobilisation does not occur for bare AC, therefore only the results for functionalised materials are shown (Figure 1). The optimal material was prepared by using 25 g of urea per 0.5 g of AC (AC-U25) allowing for >64% removal of VFX in 30 min of contact time (Figure 1). Moreover, the spent adsorbents were recovered by catalytic wet peroxide oxidation, since the functionalised materials showed improved catalytic activity.

4. Conclusions – The functionalisation and self-immobilisation processes of AC onto 3D alumina spheres was successful, creating an adsorbent macrostructure to operate under continuous mode. This system, in a packed-bed reactor with a constant inlet of contaminated mineral water, allowed for a removal of 64% of VFX in 30 min. Furthermore, by addition of hydrogen peroxide is possible to effectively recover the spent adsorbents.

5. References

[1] D.A. Gkika, A.C. Mitropoulos, G.Z. Kyzas, *Sci. Total Environ. Eng.*, **822**, (2002) 153612.
[2] A.M. Chávez, A. Torres-Pinto, P.M. Álvarez, J.L. Faria, C.G. Silva, A.M.T. Silva, *Chem. Eng. J.*, **481** (2024) 148141.

RIA43
XLIII Reunião Ibérica de Adsorção
Porto, Portugal
1-4 September 2024

P8: The impacts of adsorption in the production and purification of green hydrogen

D. Miscenco, M.J. Beira, K.V. Petrov, D.G. Jammal, C.M. Cordas, R.P.P.L. Ribeiro

HyLab – Green Hydrogen Collaborative Laboratory, Estrada Nacional 120-1, Central Termoeléctrica, 7520-089 Sines, Portugal
rui.ribeiro@hylab.pt

1. Introduction – Hydrogen (H_2) is an energy vector of paramount importance in the much-needed change of paradigm in the energy field. It is urgent to move from fossil fuels to sustainable energy sources and H_2 can produce energy cleanly – i.e. without carbon emissions – which makes it greatly interesting for hard to decarbonize sectors. Furthermore, H_2 is much needed to produce ammonia, methanol, and other valuable energy carriers and products [1].

Hydrogen is a versatile species that can be obtained from various sources. Around 47% of the produced H_2 is obtained from natural gas, 30% from oil, 18% from coal, and only 4% from water electrolysis [2]. The production of H_2 by electrolysis is a flexible approach that can allow storing excess electricity generated from intermittent renewable energy sources, such as wind and solar, enhancing grid stability. This approach is identified as green H_2 production.
The production of high purity green hydrogen streams involves a complex combination of systems and unit operations. Besides the electrolyser itself, which can be based in different technologies (alkaline, PEM), several other peripheric components are needed to guarantee the operation of the electrolysis systems. Considering the overall green H_2 production system, adsorption phenomena play a major role in it – both in electrochemical process for H_2 generation and in its purification process.

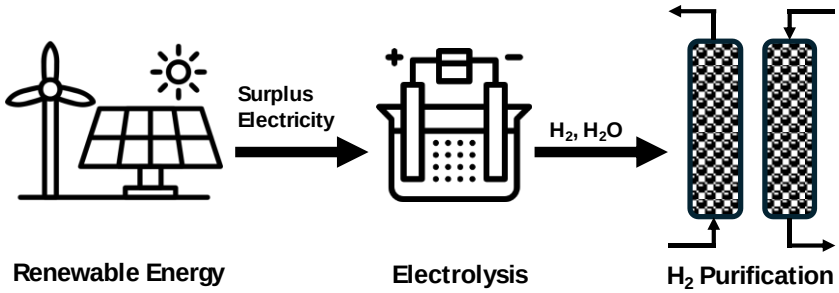

Figure 1. Scheme of the green hydrogen production pathway by electrolysis

In this work, we dive into the impact of adsorption phenomena at the catalytic surfaces in the electrolyser and at the use of adsorbents (zeolites and alumina) for the drying of hydrogen streams obtained, supported by numerical simulations and experimental work.

2. Results and Discussion – The performance of several materials is evaluated, regarding its adsorption-desorption properties. Electrochemistry techniques, namely cyclic voltammetry, are employed to study the adsorption-desorption behaviour in different surfaces used as electrodes (including catalysts) in water electrolysis using the PEM (proton exchange membrane) electrolysis technology. The adsorption phenomena by the produced H_2 in the cathode as the oxides that are formed on the anode influence the efficiency of the overall process.

The electrolyser outlet stream is rich in H_2 but saturated in water and generally presents oxygen (O_2) contamination between 2000 and 6000 ppm. Since the H_2 quality defined by the ISO 14687:2019 is 5 ppm of each of the referred contaminants (O_2 and H_2O), the stream exiting the electrolyser must be conditioned. The O_2 is removed by catalytic conversion and the water vapour is removed by adsorption [3]. In this work, we simulate the performance of different fixed-beds packed with various commercially available adsorbents (zeolites 4A, 13X and alumina). Although the capacity of the adsorbent is of great importance for the drying process, the regenerability is critical to allow reaching a process with suitable performance and reduced energy consumption. Therefore, we explore the potential of regenerating the adsorbent by temperature

increase and compare it with the use of a pressure swing approach. The simulations are performed using gPROMS (Siemens, UK) software.

3. Conclusions – This work illustrates the importance of adsorption phenomena in different stages and scales of the green hydrogen production by electrolysis. The importance of suitable adsorption-desorption dynamics at the catalyst surfaces for efficient establishment of the electrochemical reactions is demonstrated. Also, on a different level and approach, the importance of adsorption-based processes is for the purification of green H_2 and the performance of systems using different adsorbents is demonstrated.

4. References

[1] IRENA, Green Hydrogen Cost Reduction: Scaling up Electrolysers to Meet the 1.5ºC Climate Goal, International Renewable Energy Agency, Abu Dhabi, 2020.
[2] P.-A. Le, V.D. Trung, P.L. Nguyen, T.V.B. Phung, J. Natsukicd and T. Natsuki, *RSC Adv.*, **13**, (2023) p. 28262.
[3] Y. Ligen, H. Vrubel and H. Girault, Int. J. Hydrogen Energ., **45**, (2020) p. 10639.

P9: Tannic acid-doxorubicin nanoparticles in cancer therapy

A. P. Zaderenko [(1)], O. Garzo-Sánchez [(1,2)], M. Llana Ruiz [(2)], S. Maisanaba [(2)], G. Repetto[(2)] and P. J. Merkling [(1)]

[(1)] Departamento de Sistemas Físicos, Químicos y Naturales and [(2)] Departamento de Biología Molecular e Ingeniería Bioquímica. Universidad Pablo de Olavide. 41807- Seville, Spain. apzadpar@upo.es

1. Introduction – Breast cancer (BC) is the most common cancer in women. Unfortunately, first-line chemotherapeutic treatments against BC, such as doxorubicin (DOX), suffer from lack of selectivity towards tumour cells, which is why they exhibit numerous side effects that can even cause the death of the patient. Our study focuses on the encapsulation of DOX in tannic acid (TA) nanoparticles (NPs). The choice of TA is because preliminary results obtained by our group [1] show it as an excellent candidate to form nanoparticles with DOX. Furthermore, TA has antitumor activity, so beyond being a mere encapsulating agent, it can be expected to increase antitumor activity compared to the administration of DOX only. Another factor to take into account is that the encapsulation of chemotherapeutic agents in NPs allows their passive and active targeting. Finally, TA exerts its antitumor activity through multiple mechanisms, a fact that can offer enormous benefits in terms of the development of acquired resistance, the main cause of death for this disease. It is also worth noting that some of these mechanisms involve receptors whose expression is increased in certain tumour types, giving TA treatment a certain intrinsic selectivity. Our work also focuses on the *in silico* study of DOX and TA, with the aim of establishing a possible correlation between the results obtained in cultures of several BC lines and the capacity of these compounds to act as tyrosine kinase inhibitors of receptors involved in tumour proliferation.

2. Experimental – Two co-precipitation protocols have been developed to synthesize DOX/TA NPs (TADOX), and the obtained NPs were characterized by DLS, UV-Vis, FTIR and EM techniques. The effect of both NPs and their components has been studied on two BC cell lines: MCF-7 (ER^+) and MDA-MB-231 (triple negative; $EGFR^+$). For this, cell viability and oxidative stress assays were made. The *in silico* Molecular Docking (MD) studies were carried out on fragments of the receptors of interest (EGFR and ER) using Autodock Vina.

3. Results and Discussion – We have obtained two TADOX NPs with different DOX:TA molar ratios. Both NPs showed physicochemical characteristics (surface charge, hydrodynamic diameter, stability, etc.) that made them suitable for the cellular assays. Breast cancer cells, MCF7 and MDA-MB-231, showed different sensitivity to DOX, TA and their mixtures, as well as TADOX NPs, and DOX/TA synergy was observed only for MCF7. Contrary to what happens with TA, which has a marked antioxidant character, DOX fails to protect cells against oxidative stress. This effect is especially noticeable in MDA, where the levels of stress even exceed those obtained for the positive control in all the conditions tested. The comparison of the MD data of TA and DOX with the native ligands or clinical TKIs to the receptors suggest that TA adsorbs on both ER and EGFR, which is in agreement with experimental observations. Our preliminary results suggest that DOX also adsorbs rather strongly on ER and EGFR.

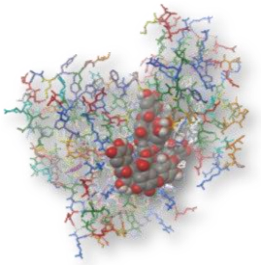

Image 1. MD of TA/EGFR.

4. Conclusions – The complex mixture of mechanisms that make up the antitumor action of both DOX and TA makes it difficult to understand their joint action. The interactions with different receptors involved in cancer pathogenesis and evolution that have been studied by MD do not show a straightforward correlation.

5. References

[1] Aguilera, J.R., Venegas, V., Oliva, J.M., Sayagués de Vega, M.J., de Miguel, M., Sánchez-Alcázar, J.A. and Zaderenko Partida, A.P. (2016). Targeted multifunctional tannic acid nanoparticles. RSC Advances, 6 (9), 7279-7287.

P10: Adsorption-based separation of Dicyclohexylamine from aniline production streams

D. Miscenco [(1), (*)], N. M. C. Oliveira [(1)], A. E. Rodrigues [(2)], D. C. M. Silva [(3)]

[(1)] *CERES, DEQ-FCTUC, Rua Sílvio Lima, 3030-790 Coimbra, Portugal.dorinmish@gmail.com*
[(2)] *LSRE-LCM, FEUP, Rua Dr. Roberto Frias, 4200-465 Porto.*
[(3)] *Bondalti Chemicals, Rua do Amoníaco Português nº10, 3860-680 Estarreja.*
[(*)] *Current affiliation: HyLab, Central Termoeléctrica, Estr. Nacional 120-1, 7520-089 Sines*

1. Introduction – During the nitrobenzene hydrogenation that occurs in aniline production, several byproducts originate that need to be separated from the main reaction product. Among these byproducts, dicyclohexylamine (DICHA) and cyclohexanone (CHONA) are the most difficult to remove by conventional distillation from the liquid aniline streams, due to the proximity of their boiling points at traceconcentrations. Here adsorption processes are relevant alternatives to purification via distillation, potentially allowing significant reductions in the energy footprint of this process. This work evaluates the use of a liquid adsorption system for the removal of trace amounts of DICHA from the liquid aniline streams, as a finalpolishing stage after the main distillation sequence. Given that the involved byproducts have distinct acid strengths (Table I) and different molecular sizes,it is possible to selectively remove DICHA from aniline streams by employingzeolite adsorbents with appropriate morphology and active sites. Preliminary batch experiments were performed to evaluate the adsorption equilibrium parameters and the regeneration possibilities of the tested zeolite adsorbent. Later, fixed-bed isothermal experiments were performed to find suitable parameters for the Linear Driving Force (LDF) model, proposed by Glueckauf [1]; this was later used for the simulation of a scaled-up adsorption process to be implemented at theBondalti aniline plant in Estarreja, followed by an economic evaluation of the proposed configuration.

Table I. Acidic strength of byproducts from aniline streams.

Component	pKa
CHOL	16
CHONA	11.3
CHA	10.6
DICHA	10.4
Aniline	4.6

2. Experimental – In the present work, a FAU-type zeolite (CBV-720 from Zeolyst) was identified as a suitable commercial candidate for DICHA adsorption from aniline. As summarized in Image I, batch adsorption experiments were performed using powder zeolite samples, mixed at variable zeolite concentrations with prepared aniline feeds containing excess DICHA. The batch tests were repeated for 3 different DICHA concentrations in the feed,using adsorption times of up to 2 h. Regenerationtests were performed 27 times with a solution ofdiluted sulfuric acid to remove the adsorbed DICHA and replenish the active acid sites with fresh protons.
The fixed-bed adsorption tests were performed using a laboratory glass condenser with the zeolite pellet bed inside the inner tube and warm water passing through the external tube for temperature control. Prepared aniline samples were fed using an analytic pump at a flowrate of5 ml/min and a hydraulic residence time of about1 min. The tests were continued until the outlet concentration became equal to the feed concentration; then the bed was washed with a small amount of water to remove the remaining aniline, and the adsorbent was regenerated with a certain amount of dilutedacid solution. Due to analytical limitations, the DICHA concentration in the acid regeneration outlet couldnot be quantified directly and the regeneration efficiency was estimated from the mass balances of two consecutive adsorption tests.concentration became equal to the feed concentration; then the bed was washed with a small amount of water to remove the remaining aniline, and the adsorbent was regenerated with a certain amount of dilutedacid solution. Due to analytical limitations, the DICHA concentration in the acid regeneration outlet couldnot be quantified directly and the regeneration efficiency was estimated from the mass balances of two consecutive adsorption tests.

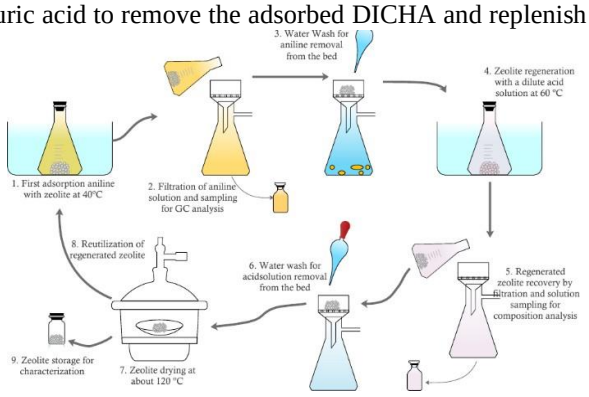

Image 1. Experimental procedure for the batch experiments.

3. Results and Discussion – The batch experiments allowed the identification of the required zeolite concentration, the minimum duration of the adsorption stage and the Langmuir isotherm parameters q_m

and K_L. Two zeolite powder samples were tested, and the adsorbed capacity obtained is shown in Image 3.

The 30 minutes adsorption tests showed that up to 20 mg of DICHA/g of adsorbent can be achieved. It wasalso shown that the Langmuir isotherm adjusted the experimental data sufficiently well for the relevant concentration range, whereas multiple layer adsorption can happen for larger DICHA concentrations. Theregeneration tests (Image 3) indicate a good overall efficiency for the tested 27 adsorption cycles. After removing the outliers, an average regeneration efficiency of 95.2 % was obtained with an 18.9% standard deviation.

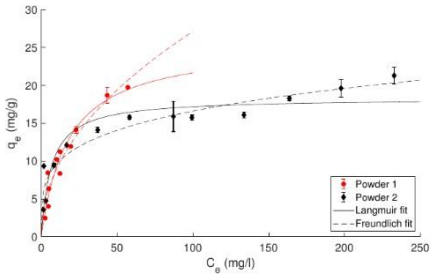

Image 3. Adsorption capacity for the 30-minutes batch experiments.

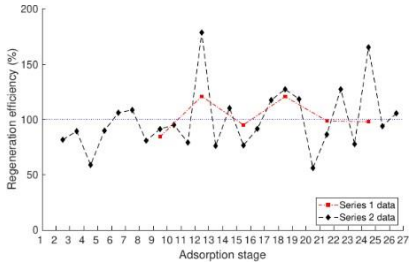

Image 3. Calculated regeneration efficiency for thebatch experiments.

Fresh and regenerated fixed-bed results (Image 4) were used to estimate the LDF model parameters by fitting a simulation developed in Aspen Adsorption V11 to the obtained experimental data. The isotherm and mass transfer parameters obtained for the three tested adsorptions cycles are given in Table II. The simulation assumed a linear lumped resistance with constant parameters; these were later used to develop a full-size process simulation. Several configurations were simulated to identify the optimal cycle time, thebed size and the number of columns required. Assuming that the bed can be effectively regenerated 50 times, an optimal configuration with just 2 columns would have a 1-week operation cycle (~170 h) and costabout 200 k€ in capital investment. Furthermore, considering a zeolite price of 3 €/kg, the adsorption treatment can cost less than 1€ per metric tonne of aniline. In the proposed process configuration, the reduction in distillation heat duty can amount to savings of up to 2.5 € per tonne of produced off-spec concentration, which is significant considering the monthly output of the plant.

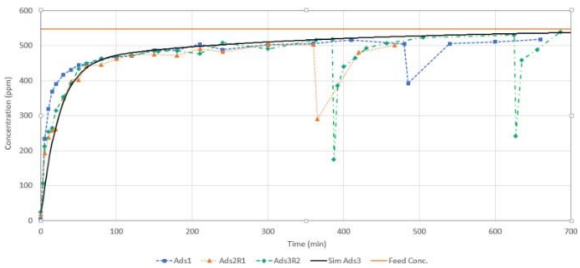

Image 4. Experimental and simulation results for fixed-bed experiments with fresh and regenerated adsorbent.

Table II. Adjusted operating parameters for the fixed-bed experiments.

Parameter	Fresh	2nd adsorption	3rd adsorption
q_m (mg/g)	64.4	64.5	58.02
K_L (l/mg)	0.152	0.077	0.077
D_L (m^2/s)	1.6e-3	1.3e-3	1.3e-3
k_p (s^{-1})	2.0e-3	2.8e-3	2.8e-3
Regen. Efficiency (%)	-	130	96

4. Conclusions – The results obtained show that zeolite adsorption can be effectively used to offset the distillation operating costs for aniline feeds containing large amounts of DICHA, with the added benefit ofalso reducing the final CHONA amount. To the best of our knowledge, this is first time the liquid adsorption was reported in the context of aniline purification systems. Further studies are required to insure economicviability across long-term operation in industrial context. In this sense, further optimization of the operatingconditions, testing of different zeolites and additional fixed-bed regeneration tests are required to insure consistent operation in the industrial setting. Evidently, pilot-scale experiment would also be beneficial before full-scale implementation in aniline production plants.

5. Acknowledgments – This work was financially supported by Fundação para a Ciência e a Tecnologia (FCT) and Bondalti Chemicals S.A. under the Doctoral Program in Refining, Petrochemical and ChemicalEngineering (PD/BDE/128613/2017).

6. References

[1] E. Glueckauf and J. I. Coates, *Journal of the Chemical Society, 241*, (1947) p. 1315-1321.

RIA 43
XLIII Reunião Ibérica de Adsorção
Porto, Portugal
1-4 September 2024

P11: Bovine Serum Albumin and Myoglobin separation on HAp

Albertina G. Rios [(1,2)*], Ana M. Ribeiro[(1,2)], Alírio E. Rodrigues[(1,2)], Alexandre F. P. Ferreira[(1,2)]

[(1)] *LSRE-LCM – Laboratory of Separation and Reaction Engineering - Laboratory of Catalysis and Materials, Faculty of Engineering, University of Porto, Rua Dr. Roberto Frias, 4200-465 Porto, Portugal*

[(2)] *ALiCE – Associate Laboratory in Chemical Engineering, Faculty of Engineering, University of Porto, Rua Dr. Roberto Frias, 4200-465 Porto, Portugal*

*arios@fe.up.pt

1. Introduction – Separation by chromatography is one of the most relevant processes for purifying biological molecules, such as proteins. Hydroxyapatite (HAp) has been successfully used as adsorbent for protein separation and it is characterized by its dual adsorption sites. The C-site, characterized by the Ca^{2+}groups of the material, work as an anion exchanger and metal affinity site, which is a strong interaction, and it is crucial for adsorbing the carboxylic groups of proteins. Acidic proteins selectively bind on this site being then eluted using high concentrations of sodium phosphate solutions [1, 2]. Conversely, the P-site, characterized by the PO_4^{3-}group works as a cation exchanger, so the binding is based on electrostatic interactions and is responsible for the adsorption of amino groups of the protein. Consequently, HAp can be considered a mixed-mode medium for protein separations.
Simulated moving bed (SMB) chromatography is a continuous process where counter current operation increases the productivity and reduces eluent consumption. SMB is characterized by having two inlet streams, the feed, the eluent, and two outlet streams, the extract (where the component with higher affinity with the solid phase is obtained), and the raffinate (containing the species that interact less with the solid) [3].

2. Experimental - BSA and Mb are the selected proteins, which are two model proteins with different isoelectric points. BSA carried negative charge at physiologic pH due to its isoeletric point of 4.7. In its turn, Mb isoelectric point is 7.4.
Since HAp was provided in powder, it was necessary to shape it into a granular form. Therefore, a lab extruder was used to shape the granules.
The adsorption equilibrium of BSA and Mb was determined through batch experiments conducted at pH 7, and different phosphate buffer (PBS) concentrations. Subsequently, fixed bed experiments were conducted for both proteins using the same buffer concentration. Afterwards, the FlexSMB-LSRE unit with six interconnected stainless-steel columns, was used to perform SMB experiments in the configuration of 1-2-2-1 with an equimolar mixture of the two proteins. The main objective is to separate these two proteins, and a buffer step-elution gradient was applied in the system by selecting a different buffer concentration in the feed and eluent streams.

3. Results and Discussion - Batch and fixed bed experiments were performed for BSA and Mb at pH7 and 0.01 M, 0.05 M, 0.1 M, and 0.4 M of PBS buffer. Adsorption capacity increases with the decrease of PBS concentration for both proteins, Mb and BSA. The adsorbed amounts are considered negligible when using buffer solutions with 0.4 M concentration of PBS. Consequently, this higher concentration of buffer was utilized as the elution medium.
Breakthrough curves were obtained for the different PBS concentrations for both proteins. Elution was performed using 0.4 M of PBS concentration.
Then, a phenomenological mathematical model, i.e., the general rate model coupled with steric mass action equilibrium, was used and validated against fixed bed dynamic adsorption experiments at different buffer concentrations.
To operate the SMB unit, the selection of a suitable operating point was required. Firstly, an appropriate switching time was selected, which was 20 minutes. Then, flow rates in section I and IV were selected, and a separation region was computed, considering a purity requirement of 95% in the extract and raffinate streams.
Based on the separation region obtained, an operating point was selected and experimentally verified, and purity, recovery, and productivity of Mb on the extract were 92%, 87% and 1.04×10^{-3} $mol_{protein} \cdot kg_{ads}^{-1} \cdot day^{-1}$, and for BSA on the raffinate were 95%, 98%, and 1.24×10^{-3} $mol_{protein} \cdot kg_{ads}^{-1} \cdot day^{-1}$, respectively.

The concentration histories of BSA and Mb on both streams are presented in Figure 1.

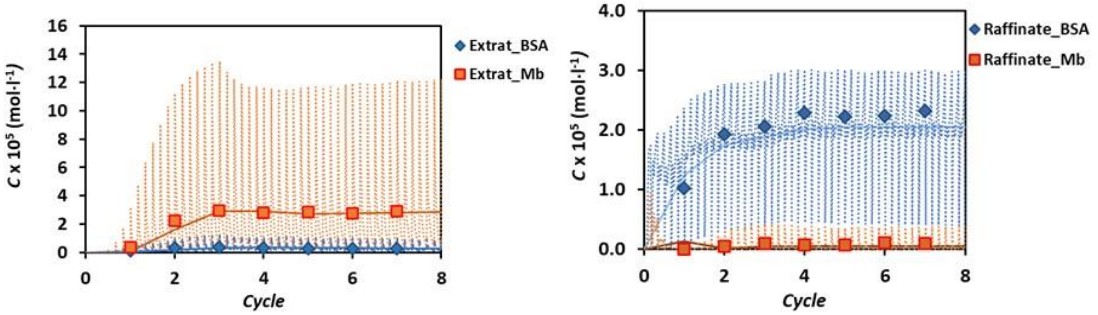

Figure 1 - Extract (a) and Raffinate (b) concentration histories.

4. Conclusions - In this work, the two proteins were separated by a simulated moving bed process using HAp as an adsorbent. This ceramic material was provided in powder form, so it was necessary to develop a procedure for its shaping and obtain granules that could be used in chromatographic experiments. Granules were produced in a lab extruder, binder-free. Thus, adsorption equilibrium data was obtained using pH 7 at different buffer concentrations. Then, fixed bed experiments were also obtained for both proteins using the same buffer concentration. A mathematical model was proposed and implemented in the software gPROMS to simulate the obtained breakthrough curves. This way, it was possible to determine a separation region and select appropriate conditions to operate the SMB unit using a buffer gradient mode. The SMB experiment was performed and purity, recovery, and productivity of Mb on the extract were 92%, 87% and 1.04×10^{-3} $mol_{protein} \cdot kg_{ads}^{-1} \cdot day^{-1}$, and for BSA on the raffinate were 95%, 98%, and 1.24×10^{-3} $mol_{protein} \cdot kg_{ads}^{-1} \cdot day^{-1}$, respectively.

Acknowledgements
This work was supported by national funds through FCT/MCTES (PIDDAC): LSRE-LCM, UIDB/50020/2020 (DOI: 10.54499/UIDB/50020/2020) and UIDP/50020/2020 (DOI: 10.54499/UIDP/50020/2020); and ALiCE, LA/P/0045/2020 (DOI: 10.54499/LA/P/0045/2020). Albertina Rios also acknowledges her Ph.D. research grant awarded by the Foundation of Science and Technology of Portugal (FCT) under SFRH/BD/137891/2018 project.

5. References

1. Gorbunoff, M.J., *The interaction of proteins with hydroxyapatite: II. Role of acidic and basic groups.* Analytical Biochemistry, 1984. **136**(2): p. 433-439.DOI: https://doi.org/10.1016/0003-2697(84)90240-9.
2. Cummings, L.J., M.A. Snyder, and K. Brisack, *Chapter 24 Protein Chromatography on Hydroxyapatite Columns*, in *Methods in Enzymology*, R.R. Burgess and M.P. Deutscher, Editors. 2009, Academic Press. p. 387-404.
3. Rodrigues, A.E., C. Pereira, M. Minceva, L.S. Pais, A.M. Ribeiro, A. Ribeiro, M. Silva, N. Graça, and J.C. Santos, *Principles of Simulated Moving Bed*, in *Simulated Moving Bed Technology*. 2015. p. 1-30.

Synthesis of Graphene Oxide/Sodium Alginate and Cotton Fibers Composite Hydrogel via 3D Printing and Its Application as Chloroquine Adsorbent in Water

N. B. V. Serafim [(1)], C. M. B. Araújo [(2)], A. F. P. Ferreira [(3)], M. A. Motta Sobrinho [(1)], M. S. C. A. Brito [(3)], Y. A. Manrique [(3)]

[(1)] *Federal University of Pernambuco, Chemical Engineering Department, Recife, Pernambuco, Brazil. nickolly.bukkyo@ufpe.br, mauricio.motta@ufpe.br*
[(2)] *University of Minho, R. da Universidade, 4710-057 Braga, Portugal. caroline.maria@ufpe.br*
[(3)] *University of Porto, Faculty of Engineering, Department of Chemical Engineering, Porto, Portugal. aferreir@fe.up.pt, mbrito@fe.up.pt, yjam@fe.up.pt*

1. Introduction – With the development of 3D printing technology, it has become possible to produce adsorbents with complex geometries and low production costs that can optimize mass and heat transfer during the adsorption process. In this context, the use of cellulose in the structure of these adsorbents has emerged as a promising option due to its biodegradability and abundance of hydroxyl groups. Sodium alginate is widely used to adjust the rheological properties of the cellulose paste, enabling its use as a 3D printing paste. The incorporation of graphene oxide (GO) into the adsorbent structure adds interesting properties to the adsorbent, such as a larger surface area and chemical stability. Furthermore, the abundance of functional groups on the surface of GO enhances the adsorption of organic compounds [1].
Thus, the present work aims to synthesize a biocomposite hydrogel based on graphene oxide, sodium alginate, and cotton fibers using 3D printing, and to explore its application as a potential adsorbent for the removal of an emerging contaminant in an aqueous medium. In this case, the chosen contaminant is chloroquine diphosphate, a drug commonly used for malaria treatment [2].

2. Experimental – A composite was produced with cotton fibers and sodium alginate, into which graphene oxide was incorporated to obtain the hydrogel (alginate-GO). For this, 1.64 g of alginate, 0.85 g of cellulose fibers, and only 0.095 g of graphene oxide were used. Image 1 shows the 3D printing scheme and one of the produced pieces. The syringe system of the 3D printer was loaded with the material for the subsequent extrusion of the adsorbent pieces. Printing was done for 4 layers (Image 2a) and 12 layers (Image 2b). After printing, the pieces were submerged in a 10% KCl solution and then in a 3% $CaCl_2$ solution for curing. The samples were stored at 4°C in sealed containers to preserve their shapes and moisture content.

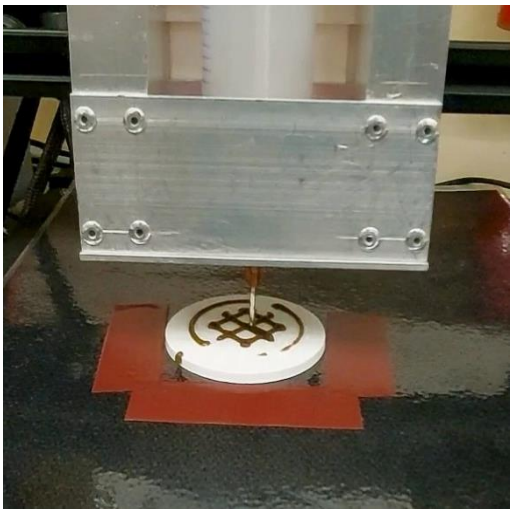

Image 1. 3D printing scheme for obtaining the adsorbent pieces

Adsorption tests were conducted to remove chloroquine diphosphate from an aqueous medium, starting with an initial concentration of 21.8 $mg.L^{-1}$, a solution volume of 100 mL, under constant agitation at 200 rpm at 298 K.
The quantification of the drug in the aqueous medium was carried out using spectrophotometry, employing a UV-Visible spectrophotometer (Jasco) at 343 nm [2]. Batch adsorption tests were performed in duplicate for the samples produced with different layers.

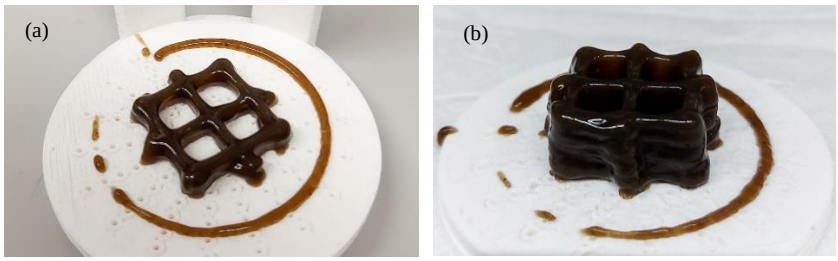

Image 2. Pieces of Alginate-Cellulose-GO Hydrogel Obtained on the 3D Printer with 4 Layers (a) and 12 Layers (b)

3. Results and Discussion – The experimental data obtained from the adsorption tests are presented in Image 3. It can be observed that the system reaches equilibrium after approximately 360 min for the adsorbents with 4 layers and after 1500 min for the adsorbents with 12 layers. The difference in the equilibrium times can be attributed to the thickness of the 12-layer structure. It appears that the presence of a greater number of layers in the material slows down the diffusion process of the contaminant, making it more time-consuming for the contaminant to access the active sites of the produced adsorbent.

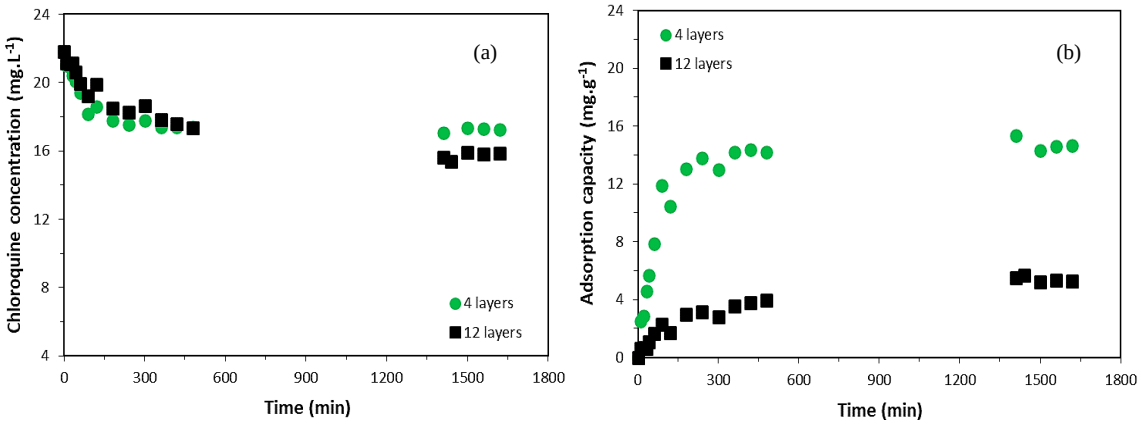

Image 3 Kinetic evolution of chloroquine adsorption in relation to concentration (a) and adsorptive capacity (b) in an alginate-cellulose-GO hydrogel. Experimental condition: C_0 = 21,8 mg.L^{-1}, 200 rpm, 298 K, 100 mL

It is observed that at the end of the experiment (t ~1800 min), the composite produced with 4 layers achieved an adsorptive capacity of approximately 15 mg.g^{-1}, while the composite with 12 layers showed an adsorptive capacity of about 5.5 mg.g^{-1}. Considering that the composite hydrogel contained only approximately 3% GO on a dry weight basis, the preliminary results are promising for the removal of chloroquine from water.

Previously, Araujo et al. [2] evaluated the production and use of a composite hydrogel based on GO and agar for the removal of chloroquine diphosphate by adsorption. In this case, an adsorptive capacity of over 50 mg.g^{-1} was experimentally observed. However, the material produced contained 20% GO on a dry weight basis, which is over six times the amount of GO used in the present work.

4. Conclusion – The composite hydrogel produced from graphene oxide, sodium alginate, and cotton fibers via 3D printing has shown promising preliminary results regarding the removal of chloroquine from aqueous solutions. Future studies will include characterization analyses to evaluate the morphological and structural properties of the produced composites. Additionally, tests will be conducted by increasing the proportion of GO in the composites, on a dry weight basis, to assess the effects of this variable on the adsorptive capacity for chloroquine diphosphate in aqueous media.

5. References

[1] J. Yuan et al. *ACS Applied Polymer Materials*, (2021) p. 699-709. DOI: 10.1021/acsapm.0c01002.

[2] C. M. B. Araujo, G. Wernke, M. G. Ghislandi, A. Diório, A., M. F. Vieira, R. Bergamasco, M. A. Motta Sobrinho, A. E. Rodrigues. *Environmental Research*, ***216***, (2023) p. 114425. DOI: 10.1016/j.envres.2022.114425

P13: Investigating the role of the metal on NO-adsorption in M-MOF 74

S. Gooijer [(1)], J.M. Vicent-Luna [(1)], A. Luna-Triguero[(2)], D. Dubbeldam[(3)], S. Calero[(1)]

[(1)]*Materials Simulation and Modelling, Department of Applied Physics and Science Education, Eindhoven Universityof Technology, PO Box 513, 5600MB Eindhoven, The Netherlands.*
[(2)]*Energy Technology, Department of Mechanical Engineering, Eindhoven University of Technology, PO Box 513,5600MB Eindhoven, The Netherlands*
[(3)]*Van't Hoff Institute for Molecular Sciences, University of Amsterdam, Amsterdam, Netherlands.*
s.a.gooijer@tue.nl, j.vicent.luna@tue.nl, a.luna.triguero@tue.nl, d.dubbeldam@uva.nl, s.calero@tue.nl

1. Introduction – Nitric Oxide (NO) is involved in many biological processes, among which the prevention of blood platelet aggregation and the immune response to bacteria. [1,2] Developing NO-releasing medical therapies would therefore have many benefits. The nature of this delivery is then of vital importance, as NO is a reactive molecule, which can cause side effects if not delivered to the targeted area. A possible NO-storing agent must therefore have a strong interaction with NO so it doesnot release when stored. The frameworks of the M-MOF-74 series contain coordinatively unsaturated metal sites, which can be strong bonding sites. [3] NO adsorption in several of the M-MOF-74 analogues (M=Fe, Ni, Co, Zn and Mg) has been measured experimentally. The adsorption isotherms show large differences in NO-uptake, as it is three times as high in Fe compared to Mg near ambient conditions. [4,5]The goal of this work is to assess these differences in adsorption, by investigating the influence of the nature of the metal. To accomplish this, DFT-calculations of binding energies and geometries were performed and adsorption isotherms of NO in the M-MOF-74 series are modelled by introducing an additional potential to describe the bonding between the metal sites and NO.

2. Experimental – Periodic DFT-calculations of binding energies and geometries were performed using the CP2K-program. [6] To simulate adsorption isotherms, Monte Carlo simulations in the grand-canonical ensemble were performed as implemented in the RASPA software package. [7] Along with potentials to describe the electrostatic and van der Waals interactions between NO and the framework, an additional potential between M-N_{NO} was introduced to describe bonding. The parameters of this potential were fitted to reproduce the experimental isotherms, as well as the optimal calculated M-N_{NO} bond length.

3. Results and Discussion – The simulated adsorption isotherms in NO in the M-MOF- 74 series are shown in Figure 1. For Fe, Ni and Co-MOF-74, a two-step adsorption mechanism can be seen. The first stepcorresponds to the binding of NO to the open metal sites in the framework, as the numberof NO molecules adsorbed is equal to thenumber of metal atoms present in the unit cell. The second step is the filling of the rest of the pore with NO, which converges to the same amount for the whole series, as the poresizes are almost equivalent to each other. For Zn and Mg, the first step of adsorption is not present, and the heat of adsorptions are twice as low compared to Fe, Co and Ni. The interaction between the metal and NO is therefore much weaker, a picture which is supported by DFT-calculations, which show smaller binding energies and larger M-N_{NO} bond lengths for Zn and Mg compared to Fe, Co and Ni.

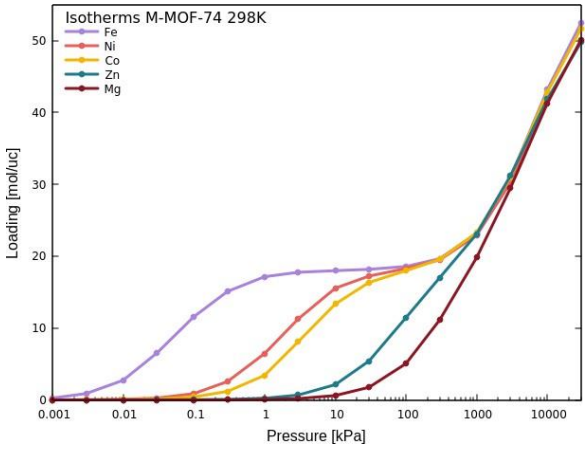

Figure 1: Simulated adsorption isotherms of NO in the M-MOF-74 series.

4. Conclusions – By introducing an additional potential to describe the bonding between NO and the metal in MOF-74, the total adsorption of NO in several MOF-74 frameworks could be modelled reproducing experimental isotherms. The modelled isotherms, as well as periodic DFT-calculations, showFe, Co and Ni exhibit the strongest bonding with NO in MOF-74, while Zn and Mg have much weaker interactions.

5. References

[1] Schairer, D.O. et al; The Potential of Nitric Oxide Releasing Therapies as Antimicrobial Agents. *Virulence* **2012**, *3* (3), 271–279. DOI:10.4161/viru.20328.

[2] Morris, R. E.; Wheatley, P. S. Gas Storage in Nanoporous Materials. *Angew. Chem. Int. Ed.* **2008**, *47* (27), 4966–4981. DOI:10.1002/anie.200703934.

[3] McKinlay, A. C. et al; Exceptional Behavior over the Whole Adsorption-storage-delivery Cycle for NO in Porous Metal Organic Frameworks. *J. Am. Chem. Soc.* **2008**, *130* (31), 10440–10444. DOI:10.1021/ja801997r.

[4] Bloch, E. D. et al; Gradual Release of Strongly Bound Nitric Oxide from $Fe_2(NO)_2$(dobdc). *J. Am. Chem. Soc.* **2015**, *137* (10), 3466–3469. DOI:10.1021/ja5132243.

[5] Cattaneo, D. et al; Water Based Scale-up of CPO-27 Synthesis for Nitric Oxide Delivery. *Dalton Trans*. **2016**, *45* (2), 618–629. DOI:10.1039/c5dt03955j.

[6] Kühne, T. D. et al; CP2K: An Electronic Structure and Molecular Dynamics Software Package - Quickstep: Efficient and Accurate Electronic Structure Calculations. *J. Chem. Phys*. **2020**, *152* (19). DOI:10.1063/5.0007045.

[7] D. Dubbeldam. et al; RASPA: molecular simulation software for adsorption and diffusion in flexible nanoporous materials *Mol Simul*. **2016,** *42*, 81–10. DOI:10.1080/08927022.2015.1010082.

P14: Adsorption of Clonazepam using Biochar from Wood Waste: Kinetics, Equilibrium, and Thermodynamics

N. B. V. Serafim [(1)], J. V. F. L. Cavalcanti [(1)], M. A. Motta Sobrinho [(1)]

[(1)] *Federal University of Pernambuco, Chemical Engineering Department, Recife, Pernambuco, Brazil*
nickolly.bukkyo@ufpe.br, jorge.cavalc@ufpe.br, mauricio.motta@ufpe.br

1. Introduction – The COVID-19 health crisis has led to increased social isolation, uncertainties, and restrictions, significantly impacting mental health and intensifying psychiatric disorders. According to the WHO, 2020 saw a 27.6% rise in depression and a 25.6% increase in anxiety cases globally. Treatment often involves anxiolytic medications like diazepam, alprazolam, lorazepam, and clonazepam, whose consumption has increased during the pandemic. However, these medications are not fully metabolized by the human body and are not entirely removed by conventional sewage treatment, leading to water contamination that poses risks to human health and aquatic life. To address this environmental issue, adsorption has been explored as an efficient treatment for drug-contaminated effluent. Using biomass-derived adsorbents promotes sustainability by adding value to waste materials and offering an alternative to fossil-origin commercial activated carbon. Materials like seaweed, wood waste, bark, and fruit seeds are potential sources. This study evaluated the effectiveness of biochars derived from wood chips in removing clonazepam from water.

2. Experimental - The adsorbent was obtained from a gasifier with an energy capacity of 8 kW, fed with wood waste in the form of chips from broken chairs and tree pruning on the campus of the Federal University of Paraíba (UFPB). The produced charcoal was ground to a 100 mesh size and used without further treatment. A stock solution of clonazepam was prepared at a concentration of 20 mg/L in a 9:1 volumetric ratio of water to methanol. Working solutions were made by diluting the stock solution in distilled water. Clonazepam quantification was performed using high-performance liquid chromatography (HPLC). All experiments were conducted with a volume of 50 mL, an agitation speed of 200 rpm, and a mass/volume ratio of 0.4 g/L. The kinetic study monitored the decrease in the concentration of the clonazepam solution over time in contact with the adsorbent. The experimental data were fitted to pseudo-first-order (PFO) and pseudo-second-order (PSO) kinetic models. The equilibrium study varied the concentration of clonazepam solutions (from 2 to 20 mg/L) while keeping the contact time fixed at 120 minutes and the temperature at 300K. The evaluated isotherm models were Freundlich, Langmuir, and Sips. For the thermodynamic study, the clonazepam solution was kept in contact with the adsorbent for 120 minutes at temperatures of 300K, 308K, and 316K, and the thermodynamic parameters were estimated.

3. Results and Discussion – Image 1a illustrates the kinetic adsorption curves of clonazepam using the gasification biochar, along with the fitting of the PFO and PSO models. The adsorption process is rapid, reaching equilibrium within 15 minutes, with an adsorptive capacity of 18 $mg.g^{-1}$. Image 1b illustrates the equilibrium adsorption isotherm, depicting the fitting of the theoretical models.

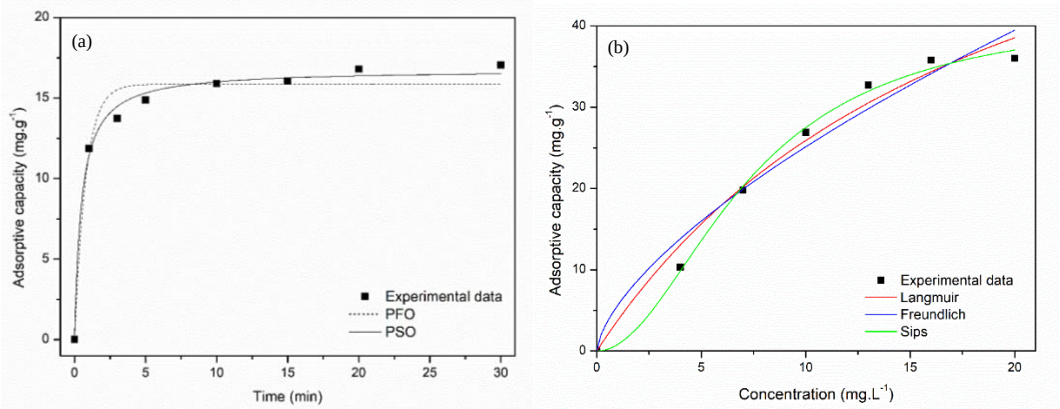

Image 1. Kinetics (a) and equilibrium (b) experimental data for clonazepam adsorption onto gasification biochar and theorical models

It can be observed from the parameters shown in Tables I and II that the pseudo-second order model best represents the process kinetics, while the Sips isotherm best indicates a heterogeneous system where active sites have different energies, combining Freundlich model behavior at low concentrations and Langmuir model behavior at higher concentrations.

Table I Parameters of empirical kinetic models for the adsorption of clonazepam onto gasification biochar

Parameters	Models	
	PFO	PSO
q_{eq} (mg g^{-1})	15.86 ± 0.44	16.77 ± 0.28
k_1 (min^{-1})	1.28 ± 0.25	0.13 ± 0.07
R^2	0.97	0.99
AIC	10.45	1.33

Table II Parameters of theorical isoterms models for adsorption of clonazepam onto gasification biochar

Model	Parameters	
Langmuir	$q_{m,l}$ ($mg.g^{-1}$)	75.29 ± 14.89
	K_L ($L.mg^{-1}$)	0.05 ± 0.02
	R^2	0.98
	AIC	21.97
Freundlich	K_F ($mg^{1-n}.g^{-1}.L^{1/n}$)	5.61 ± 1.48
	n_F	1.53 ± 0.24
	R^2	0.96
	AIC	25.94
Sips	$q_{m,s}$ ($mg.g^{-1}$)	41.92 ± 2.50
	K_s ($L.mg^{-1}.min^{-1}$)	0.019 ± 0.007
	n_s	0.50 ± 0.06
	R^2	0.99
	AIC	23.02

Table III presents the thermodynamic parameters calculated, The negative values of ΔG° indicate the process's spontaneity and the drug adsorption's feasibility. The positive values of ΔH° and ΔS° indicate, respectively, the occurrence of endothermic processes and the decrease in the system's order level. Based on these findings, it can be inferred that the adsorption process is predominantly physical. This is supported by the enthalpy variation being below 80 kJ, suggesting that adsorption occurs on the surface of the adsorbent through interactions such as pi-pi stacking of aromatic rings, dipole-dipole bonds, and electrostatic forces.

Table III Thermodynamic parameters for clonazepam adsorption on gasification biochar

T (K)	ΔG° ($kJ.mol^{-1}$)	ΔH° ($kJ.mol^{-1}$)	ΔS° ($kJ.mol^{-1}.K^{-1}$)
300	-0.05	14.55	51.04
308	-0.96		
316	-1.32		

4. Conclusions - This study utilized gasification biochar as a potential adsorbent for the removal of clonazepam from water. The maximum estimated adsorptive capacity was 38.94 $mg.g^{-1}$. The Sips isotherm provided the best fit to the experimental data, suggesting that the adsorption process occurs through a combination of Langmuir and Freundlich isotherms on a heterogeneous surface. The kinetic study showed that the PSO model accurately described the behavior of the experimental data. Furthermore, the thermodynamic study indicated that the adsorption process is endothermic, spontaneous, and predominantly physical.

5. References

[1] Mental health and COVID-19: early evidence of the pandemic's impact: scientific brief. World Health Organization, 2022

[2], B. Qiu et al. Application of biochar for the adsorption of organic pollutants from wastewater. *Separation and Purification Technology* (2022).

[3] E. C. LIMA et al. A critical review of the estimation of the thermodynamic parameters on adsorption equilibria. *Journal of molecular liquids* (2019).

P15: Synthesis of activated carbons from sewage sludge and their application to biogas purification

R. Calero-Berrocal [(1)], G. Pascual-Muñoz [(1)], V.I. Águeda [*(1)], J.A. Delgado [(1)]

[(1)] *Catalysis and Separation Processes Group (CyPS), Chemical and Materials Engineering Department, Universidad Complutense de Madrid, 28040 Madrid, Spain;*
[*]*viam@ucm.es*

1. Introduction – High purity biomethane is mainly produced from raw biogas through an upgrading process in which carbon dioxide and other contaminants are removed [1]. Pressure swing adsorption (PSA) has already proven to be an effective technology for biogas upgrading [2-3]. Carbon molecular sieves (CMS), and activated carbons have been used for this application [4]. The industry is looking for new sustainable precursors such as sewage sludge to obtain selective adsorbents and to increase the circularity of waste products. In this work, the performance of sewage sludge-based adsorbents has been studied in a PSA process to obtain biomethane from biogas.

2. Experimental – Activated carbons have been obtained from sewage sludge by means of pyrolysis. BPL activated carbon was supplied by Kuraray and used for comparison purposes. The adsorbents were characterized. Adsorption equilibrium isotherms of CO2 and CH4 were measured using a BELSORP MAX II volumetric equipment. Breakthrough curves were measured and the kinetic parameters were obtained using a mathematical model. A Pressure Swing Adsorption process was simulated using PSASIM® [5].

3. Results and Discussion – Three different activated carbons were obtained from sewage sludge using low temperature pyrolysis followed by chemical activation. Compared to commercial activated carbons widely used in gas separation processes, such as BPL, adsorbents based on sewage sludge showed lower surface areas, pore volumes (Table 1) and CO_2 and CH_4 adsorption capacities. However, the CH_4/CO_2 selectivities obtained are higher, which is an advantage in the performance of a PSA process.

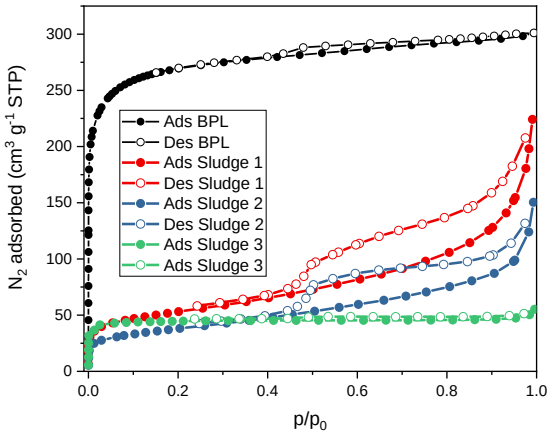

Image 1. N_2 adsorption – desorption isotherm at 77K

Table 1. Adsorbents characterization

Adsorbent	S_{BET}	V_{pore}
	$(m^2 \cdot g^{-1})$	$(cm^3 \cdot g^{-1})$
BPL	973	0.461
Sludge 1	182	0.342
Sludge 2	132	0.221
Sludge 3	134	0.082

Based on the experimental equilibrium and kinetic parameters of the four adsorbents, simulations of the PSA process were carried out with different cycle configurations to maximise productivity and methane recovery in the product. In all simulations, a high pressure of 1 bar and a low pressure of 0.1 bar were considered. Table 2 shows the results of the simulations with a 6-bed, 11-stage PSA process.
It is observed that, with the studied PSA configuration, high methane recoveries can be obtained in the product (> 90%), being higher when using Sludge1 as adsorbent. However, the productivity achieved in this case is lower due to its lower adsorption capacity. The energy consumption due to the compressor is similar.

Table 2. Performance of 6-bed, 11-step PSA cycle

Adsorbent	u_{feed}	y_{CH4} light product	y_{CO2} heavy product	CH_4 recovery	CH_4 productivity	Compressor energy
	(m s^{-1})			(%)	(mol $kg_{ads}^{-1}s^{-1}$)	(kJ mol^{-1})
BPL	0.0704	0.9803	0.8868	91.73	5.896E-04	9.687
Sludge 1	0.0280	0.9808	0.9029	93.03	2.814E-04	9.705
Sludge 2	0.0324	0.9803	0.9068	93.34	2.506E-04	9.656
Sludge 3	0.0398	0.9806	0.8113	84.88	2.841E-04	11.880

4. Conclusions - The sewage sludge-based adsorbents obtained are suitable for biomethane production from biogas. Higher CH_4 recovery can be obtained although much lower productivity than with commercial adsorbents. This study can contribute to the circular economy and to achieving the EU biomethane production targets.

Acknowledgements
Funding from the Centre for the Development of Industrial Technology (CDTI) through project MIG-20201034 (ShineFleet) and from the Spanish Ministry of Economy and Competitiveness through projects CTM2017-84033-R and PID2020-116478RB-100 is gratefully acknowledged.

5. References

[1] R. Kapoor et al., *Environmental Science and Pollution Research*, 26 (2019) 11631–11661.
[2] C. A. Grande, Chapter 3 in Biofuel's Engineering Process Technology, IntechOpen, 2011.
[3] A. Mersmann et al., *Chemical Engineering & Technology*, 23 (2000) 937–944.
[4] I. Durán et al., *Chemical Engineering Journal*, 428 (2022) 132564.
[5] J. A. Delgado, *Materiales en Adsorción y Catálisis*, 7 (2014) 15–29.

P16: Oxygen plasma-engineering of ZIF-67 nanomaterials

V. K. Abdelkader-Fernández, R. Vismara, F. J. López Garzón, J. A. Rodríguez-Navarro, M. Pérez-Mendoza[(1)]

Departamento de Química Inorgánica, Facultad de Ciencias, Universidad de Granada, C/ Severo Ochoa s/n, 18071, Granada
[(1)]mjperezm@ugr.es
victorkarim@ugr.es, rvismara@ugr.es, flopez@ugr.es, jarn@ugr.es

1. Introduction – Metal-organic networks (MOFs) present interesting properties, such as high crystallinity degrees, defined porosity, high surface areas, and great versatility in their structures and compositions. In addition, the metallic nodes that form the 3D networks —together with the organic linkers— are homogeneously distributed at the nanometre scale, offering numerous active centres for the (electro)catalysis of various energy processes. However, these promising nanomaterials have several drawbacks: limited accessibility to the active centres, low electrical conductivity, moderate stability under operando conditions, etc. In this context, advanced cold plasma treatments (systems out of thermal equilibrium and consequently highly reactive, formed from the partial ionization of a gas or mixture of gases) can be a very useful —and environmentally friendly— tool. To improve the electrocatalytic behaviour of MOFs, since they allow their nanostructures to be easily modified —via functionalization, nanoparticle formation, defect creation, etc.— with a very high degree of control over the above-described alterations.
Thus, recently, in our research group, we have begun to explore the compositional/structural modification of ZIF-67-based nanomaterials (a MOF formed by Co2+ ions and 2-methyl-imidazole ligands) with plasmas obtained from different precursors, observing that with short treatments —minutes— can significantly improve the electrocatalytic activity of these nanomaterials against the oxygen evolution process (OER), a key reaction for the production of green hydrogen in electrolyser devices.

2. Experimental – Two different ZIF-67 materials have been synthesized: a canonical polyhedral ZIF-67 (named as Z) and a nano-sized and more amorphized ZIF-67 sample (named as nZ). See the morphologies of these samples in Image I. Then, these pristine samples have been plasma-engineered by applying RF-generated plasmas composed by 100% O_2 gas with different durations: 30, 45 and 60 minutes. The resulting plasma-engineered samples have been tagged as Z(or nZ)-pX (where p stands for O_2 plasma, and X = 30, 45 or 60 min). These nanomaterials have been thoroughly characterized by using diverse characterization techniques: X-ray photoelectron spectroscopy (XPS), attenuated total reflection infrared spectroscopy (ATR-IR), powder X-ray diffraction (PXRD), N_2 adsorption, CO_2 adsorption, and scanning electronic microscopy (SEM). Finally, the effect of O_2 plasmas on the electrocatalytic activity of these ZIF-67 materials towards the strategic OER process in alkaline medium has been assessed by recording the corresponding cyclic and linear sweep voltammetries (CV and LSV, respectively) employing a standard potentiostat/three-electrode cell setup.

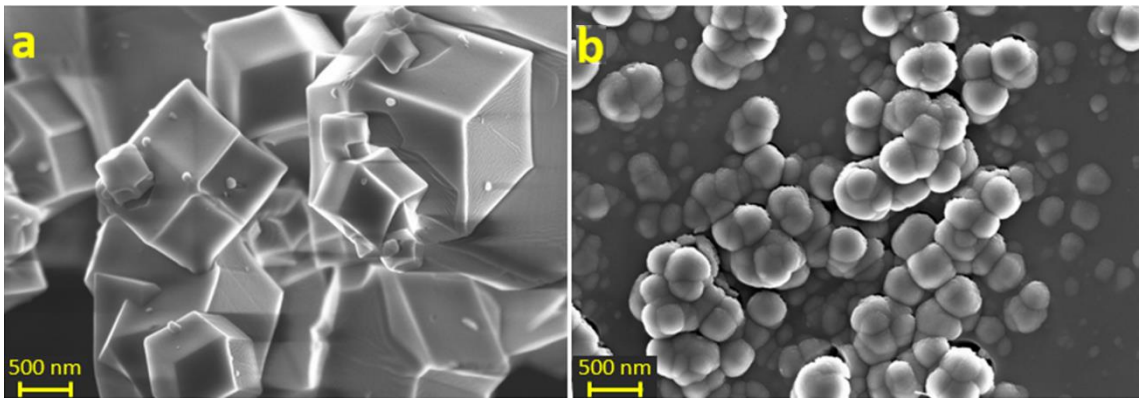

Image 1. SEM micrographs of the two pristine ZIF-67 nanmoaterilas: (a) Z and (b) nZ.

3. Results and Discussion -Various effects induced by O_2 plasmas on the composition/structure of ZIF-67 materials have been identified. These modifications can be classified into two groups: effects derived from the oxidative nature of the O_2 plasma and effects derived from "etching". The oxidation of ZIF-67 materials is evidenced by the formation of cobalt oxide (primarily) and the attachment of oxygenated functions on

the organic ligands (a minor effect). Additionally, the etching effect of the plasma results in the generation of structural defects due to the (partial) loss of organic ligands coordinated to the Co^{2+} metal nodes, as well as the generation of structural disorder (with a limited increase) in these nanostructures. This latter modification is evident only in the Z series and is demonstrated by slight, yet significant, decreases in average crystal sizes (from XRD analysis), BET surface area values, pore volume (from N_2 adsorption), and micropore volume and surface area (from CO_2 adsorption). See Table I. Finally, it has been detected that these structural and textural changes are always beneficial in improving the electrocatalytic activity of ZIF-67 materials for oxygen evolution reaction (OER).

Table I. Crystallite size (XRD) and textural parameters (N_2 and CO_2 adsorption) of the pristine and modified materials.

	XRD	N_2 adsorption			CO_2 adsorption		
Sample	Crystallite size (nm) [a]	S_{BET} ($m^2\ g^{-1}$) [b]	V_{pore} ($cm^3\ g^{-1}$) [c]	Mean pore size (nm)	$V_{micropore}$ ($cm^3\ g^{-1}$) [d]	Micropore surface area ($m^2\ g^{-1}$) [d]	Mean pore size (nm)
Z	59	1820	0.91	1.30	0.33	826	0.41
Z-p30	43	1671	0.68	1.27	0.20	497	0.40
Z-p45	48	1674	0.70	1.28	0.17	429	0.40
Z-p60	45	1745	0.73	1.29	0.22	541	0.40
nZ	29	1244	0.67	1.29	0.17	417	0.40
nZ-p30	29	1310	0.65	1.34	0.17	416	0.40
nZ-p45	26	1281	0.62	1.35	0.17	431	0.40
nZ-p60	29	1302	0.63	1.35	0.16	409	0.40

[a]Average crystallite size calculated from the FWHM values of the more intense diffraction peaks in each XRD pattern by using Scherrer equation. [b]Surface area calculated from the N_2 isotherm data using the Brunauer–Emmett–Teller (BET) equation. [c]Pore volume calculated from N_2 adsorbed at $P/P_0 = 0.99$. [d]Calculated from CO_2 isotherm data using the Dubinin–Redushkevich (DR) equation.

4. Conclusions - O_2 plasmas have proven to be simple, quick, and environmentally friendly treatments for the compositional and structural modification of ZIF-67 type materials. Furthermore, the original characteristics of the starting samples are crucial in determining the extent of the various plasma-induced modifications. Lastly, regardless of the extent of these modifications, O_2 plasmas are useful tools for enhancing the electrocatalytic activity of these nanomaterials in the field of electrocatalytic oxygen production from water.

P17: Enhancing Light Olefin Recovery Using Eco-Friendly MIL 100(Fe) Adsorptive Processes

P. Carmo [1,2], A. Ribeiro [1,2], A. Rodrigues [1,2], A. Ferreira [1,2]

[1] *LSRE-LCM - Laboratory of Separation and Reaction Engineering – Laboratory of Catalysis and Materials, Faculty of Engineering, University of Porto, Rua Dr. Roberto Frias, 4200-465 Porto, Portugal.*

[2] *ALiCE - Associate Laboratory in Chemical Engineering, Faculty of Engineering, University of Porto, Rua Dr. Roberto Frias, 4200-465 Porto, Portugal.*

paulocarmo@fe.up.pt

1. Introduction – Polyethylene and polypropylene are essential materials widely utilized in packaging and various consumer goods. In 2021, their combined global production reached an estimated 180 million tons, establishing them as the most produced thermoplastics globally [1]. A major challenge in their production lies in the cost and sourcing of their chemical feedstock. To address this, it is crucial to recover monomer losses that occur during the reactor purge and resin degassing stages in the polyolefin industry, which typically range from 1% to 2% of the original feedstock [2, 3]. Traditionally, these emissions are flared to meet regulatory standards, resulting in financial losses and increased atmospheric CO_2 levels. Therefore, developing efficient monomer recovery processes is vital for reducing operational costs, enhancing industry competitiveness, and aligning with sustainability goals by reducing CO_2 emissions.
In recent decades, Metal-Organic Frameworks (MOFs) have gained significant attention due to their high porosity, large surface areas, and customizable pore structures and compositions. These properties make MOFs highly suitable for various separation processes in the chemical industry. In particular, MIL-100(Fe) has shown substantial potential due to its high capacity and tuneable selectivity for olefins, achieved through increased activation temperatures and the reduction of Fe^{3+} ions[4]. Additionally, new sustainable methods for high-capacity production have further boosted its industrial appeal, positioning MIL-100(Fe) as a key material for advancing separation technologies [5].

2. Experimental - Pure adsorption equilibrium isotherms for ethylene and propylene were measured on MIL-100(Fe) granules, using a Rubotherm magnetic suspension microbalance, for a range of 0 to 5 bar, and 303 to 373 K. Langmuir isotherm models were accurately fitted to the measured experimental results. Single, binary, and pseudo-binary breakthrough curves were performed on a bench-scale single column unit for ethylene/nitrogen and propylene/nitrogen mixtures. The dynamic behaviour of the breakthrough experiments was simulated using a 1-dimensional fixed bed mathematical model, and the pure and multicomponent extension of the Langmuir isotherm model were successfully validated using experimental data.

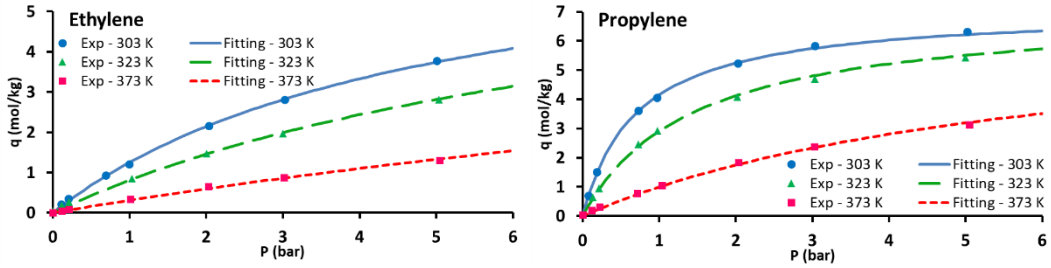

Fig.1: Adsorption Equilibrium Measurements and Model Fitting for Ethylene and Propylene on MIL-100(Fe)

3. Results and Discussion – Mathematical models are formulated to simulate the dynamic behaviour of each of the three chosen adsorption-based separation processes: Pressure-Swing Adsorption, Multitubular Temperature and Pressure Swing Adsorption, and Dual-Reflux Pressure Swing Adsorption. Furthermore, this research endeavours to design optimized adsorption-based monomer recovery units tailored to each mixture. These units are designed to yield a monomer stream suitable for direct recycling back into the polymerization unit (95 %), thus promoting process efficiency and resource conservation. Simultaneously, a pure nitrogen stream is generated, meeting emission standards for safe release into the atmosphere (20 ppm). A comparative analysis is conducted between the developed processes, evaluating their performance on an industrial scale.
For the ethylene/nitrogen Pressure-Swing Adsorption (PSA) cycle, a three-column system designed to operate between 0.3 and 9 bar produced an ethylene stream with 95.00% purity and a nitrogen stream with

ethylene contamination of 1.90 ppm, using a total adsorbent mass of 10,681 kg. This system achieved an ethylene productivity of 2.23 mol/(kg_{ads}h) and a recovery capacity of 21.03 kg_{C2H4}/(m^3_{unit}h), with a total thermal energy consumption of 10.13 MJ/kg_{C2H4}.
For the ethylene/nitrogen Multitubular Temperature and Pressure Swing Adsorption (MT-PSA) cycle, a three-multitubular adsorber system operating between 1 and 8 bar and temperatures from 303 to 393 K produced an ethylene stream with 95.15% purity and a nitrogen stream with ethylene contamination of 16.67 ppm, using a total adsorbent mass of 3,777 kg. This system achieved an ethylene productivity of 6.30 mol/(kg_{ads}h) and a recovery capacity of 24.83 kg_{C2H4}/(m^3_{unit}h), with a total thermal energy consumption of 20.81 MJ/kg_{C2H4}, including 13.02 MJ/kg_{C2H4} for heating and electrical consumption.
For the propylene/nitrogen Pressure-Swing Adsorption (PSA) cycle, a three-column system operating between 0.3 and 8 bar produced a propylene stream with 95.06% purity and a nitrogen stream with propylene contamination of 19.58 ppm, using a total adsorbent mass of 10,681 kg. This system achieved a propylene productivity of 1.48 mol/(kg_{ads}h) and a recovery capacity of 21.03 kg_{C3H6}/(m^3_{unit}h), with a total thermal energy consumption of 4.37 MJ/kg_{C3H6}.
For the propylene/nitrogen Multitubular Temperature and Pressure Swing Adsorption (MT-PSA) cycle, a three-multitubular adsorber system operating between 1 and 5 bar and temperatures from 303 to 393 K produced a propylene stream with 95.32% purity and a nitrogen stream with propylene contamination of 11.16 ppm, using a total adsorbent mass of 2,359 kg. This system achieved a propylene productivity of 6.72 mol/(kg_{ads}h) and a recovery capacity of 38.91 kg_{C3H6}/(m^3_{unit}h), with a total thermal energy consumption of 7.46 MJ/kg_{C3H6}, including 4.65 MJ/kg_{C3H6} for heating and electrical consumption.

4. Conclusions – Until the writing of this abstract, the results indicate that the proposed PSA system performs better in the separation and recovery of the ethylene/nitrogen mixture. Although the MT-TPSA cycle improves process productivity and reduces adsorbent load, its low thermal regeneration efficiency leads to significantly higher energy costs, diminishing its economic viability.
For the separation and recovery of the propylene/nitrogen mixture, both processes show potential. While the PSA system consumes less energy, it requires more than four times the adsorbent load, which may be impractical depending on material availability and space constraints.
This study supports the development of environmentally sustainable practices in the polymer industry by advancing efficient monomer recovery processes.

5. References

[1] PlasticsEurope Market Research Group and Conversio Market & Strategy GmbH, "Plastics - the Facts 2022". (Report), 2022.
[2] M. Gahleitner and C. Paulik, "Polypropylene", in Ullmann's Encyclopedia of Industrial Chemistry, 2014.
[3] D. Jeremic, "Polyethylene", in Ullmann's Encyclopedia of Industrial Chemistry, 2014.
[4] P. Carmo, A.M. Ribeiro, U-H. Lee, K.H. Cho, A.E. Rodrigues, J-S. Chang, A. Ferreira, *Micropor. Mesopor. Mat.*, **352**, (2023) p. 112510.
[5] Y.-K. Seo, J.W. Yoon, J.S. Lee, U-H. Lee, Y.K. Hwang, C.-H. Jun, P. Horcajada, C. Serre, J.-S. Chang, *Micropor. Mesopor. Mat.*, **157**, (2012) p. 137-145.

P18: Competitive adsorption of vanillin, vanillic acid, and acetovanillone onto SP700 resin

Albertina G. Rios[(1,2)], Carina A.E. Costa[(1,2)], Ana M. Ribeiro[(1,2)], Alírio E. Rodrigues[(1,2)], Alexandre F. P. Ferreira[(1,2)]

[(1)] LSRE-LCM – Laboratory of Separation and Reaction Engineering - Laboratory of Catalysis and Materials, Faculty of Engineering, University of Porto, Rua Dr. Roberto Frias, 4200-465 Porto, Portugal

[(2)] ALiCE – Associate Laboratory in Chemical Engineering, Faculty of Engineering, University of Porto, Rua Dr. Roberto Frias, 4200-465 Porto, Portugal

1. Introduction – Lignin is one of the most important components of side streams from lignocellulosic-based biorefineries and pulp and paper industries. This three-dimensional biopolymer is produced worldwide in amounts close to 70 million tonnes per year, and only 2 % is used as a precursor for chemicals and materials production [1]. Consequently, producing valuable phenolic compounds from lignin, a renewable source, emerges as a promising alternative to explore its potential. Lignin depolymerization through alkaline oxidation, at controlled conditions, is one of the possible valorisation routes, giving origin to a complex mixture of products containing lignin oligomers, dimers, low-molecular-weight phenolic monomers, and minor amounts of other secondary non-phenolic compounds [2]. Therefore, the effective and specific separation of aromatic compounds of interest is still one of the most important obstacles to their production from lignin. These compounds are usually difunctional and include aromatic aldehydes (vanillin, V), the respective aromatic acids (vanillic acid, VA), and ketones (acetovanillone, VO), whose selectivity and efficiency depend strongly on processing conditions, lignin origin, and oxidation conditions [3, 4].
This work studies the competitive adsorption behaviours of vanillin, vanillic acid, and acetovanillone on a macroporous polymeric adsorbent - resin Sepabeads SP700. Batch adsorption isotherms of vanillin, acid vanillic, and acetovanillone in single and ternary-component mixtures in aqueous solution were assessed, obtaining the respective equilibrium isotherms. Fixed bed studies were also performed to validate the mathematical model obtained, and the potential of the separation process of the phenolic monomers studied was evaluated.

2. Experimental – The adsorption equilibrium isotherms were measured by batch experiments using an orbital shaker incubator. Single and ternary-component experiments were performed using water and water/ ethanol mixtures. Then, for fixed bed experiments, a jacketed column was packed with the adsorbent material and breakthrough curves were obtained with the single and ternary mixtures of the phenolic compounds. Fixed bed experiments were performed in three steps: adsorption, elution with water, and regeneration with a solution of water/ethanol 50%/50 % (v/v).

3. Results and Discussion – Adsorption equilibrium isotherms were obtained for the three phenolic compounds and the respective multi-component mixture. The Bi-Langmuir model was used to fit the experimental data and the ethanol ratio was included in the model as a modifier of the system. These results are presented in Figure 1. V demonstrates a higher adsorption capacity, within the selected concentration range for each phenolic compound, compared to VA and VO.

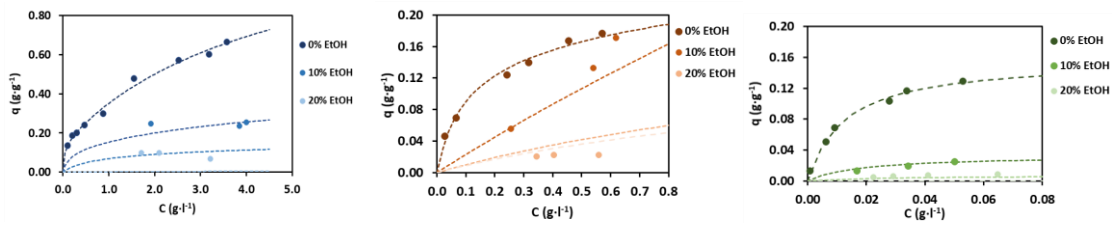

Figure 1. Adsorption equilibrium isotherms of vanillin, vanillic acid, and acetovanillone with different ethanol concentrations.

The fixed bed experiments were performed with the ternary mixture of the phenolic compounds in three steps: adsorption, elution, and regeneration. A mathematical model comprising the adsorption equilibrium isotherm and linear driving force (LDF) approximation to represent the intraparticle mass

transfer was applied to describe the dynamic adsorption behaviour and validated against the experimental results. Figure 2 presents the ternary breakthrough curve obtained, and the respective prediction by the dashed lines. As predicted by the equilibrium model, there is competition among the adsorbates, which the model well describes.

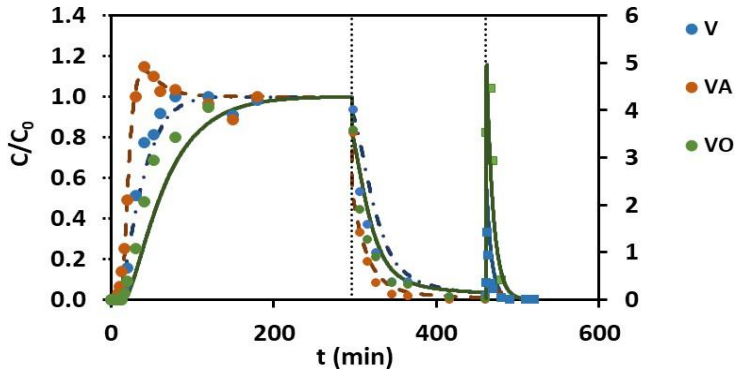

Figure 2. Fixed bed experiment for a ternary mixture with the three steps of the process: adsorption, elution, and regeneration.

4. Conclusions – Adsorption studies of vanillin, vanillic acid, and acetovanillone were performed using the macroporous adsorbent, the Sepabeads SP700 resin. Adsorption equilibrium isotherms in aqueous solutions and water/ethanol solutions were established for each phenolic compound and for the ternary mixture. Fixed bed experiments were also performed in a jacketed column. The mathematical model was validated and it represents a starting point for the possible separation of the ternary mixture by a pseudo-simulated moving bed (SMB).

Acknowledgements

This work was supported by national funds through FCT/MCTES (PIDDAC): LSRE-LCM, UIDB/50020/2020 (DOI: 10.54499/UIDB/50020/2020) and UIDP/50020/2020 (DOI: 10.54499/UIDP/50020/2020); and ALiCE, LA/P/0045/2020 (DOI: 10.54499/LA/P/0045/2020).

5. References

[1] Fernández-Rodríguez, J., X. Erdocia, C. Sánchez, M. González Alriols, and J. Labidi, *Lignin depolymerization for phenolic monomers production by sustainable processes.* Journal of Energy Chemistry, 2017. **26**(4): p. 622-631.DOI: https://doi.org/10.1016/j.jechem.2017.02.007.

[2] Costa, C.A.E., C.A. Vega-Aguilar, and A.E. Rodrigues, *Added-value chemicals from lignin oxidation.* Molecules, 2021. **26**(15): p. 4602.

[3] Costa, C.A.E., P.C.R. Pinto, and A.E. Rodrigues, *Radar tool for lignin classification on the perspective of its valorization.* Industrial & Engineering Chemistry Research, 2015. **54**(31): p. 7580-7590.DOI: 10.1021/acs.iecr.5b01859.

[4] Abdelaziz, O.Y., I. Clemmensen, S. Meier, C.A.E. Costa, A.E. Rodrigues, C.P. Hulteberg, and A. Riisager, *On the oxidative valorization of lignin to high-value chemicals: A critical review of opportunities and challenges.* ChemSusChem, 2022. **15**(20): p. e202201232.DOI: https://doi.org/10.1002/cssc.202201232.

P19: Adsorción de contaminantes orgánicos en zeolitas de tipo faujasita. Efecto de la hidrofobicidad y de la naturaleza del contaminante.

D. De Baker[(1)], J.A. González[(2)], J. Mengual[(1)*], A.E. Palomares[(1)], F. Rey[(1)]

[(1)] Instituto de Tecnología Química, Universitat Politècnica de València-Consejo Superior de Investigaciones Científicas, Avenida de los Naranjos s/n, 46022 València, Spain.
**jemencu@itq.upv.es*
[(2)] Institut Universitari d'Investigació d'Enginyeria de l'Aigua i Medi Ambient, IIAMA, Universitat Politècnica de València, Camí de Vera, s/n, 46022 València, Spain

1. Introducción – La presencia de contaminantes orgánicos en el medio natural, tales como el bisfenol A (BPA) y colorantes de tipo azoico, puede llegar a generar problemas de tipo ambiental, especialmente enel medio acuático, siendo su eliminación un desafío relevante para la adecuada gestión de los recursos hídricos. Estos compuestos, que son utilizados ampliamente en diversas industrias, presentan una alta persistencia en el medio ambiente y presentan una potencial toxicidad, afectando negativamente tanto a la salud humana como a los ecosistemas acuáticos. El BPA, empleado en la producción de plásticos, es conocido por sus propiedades como disruptor endocrino, mientras que los colorantes orgánicos azoicos, utilizados en la industria textil pueden ser tóxicos para la vida acuática [1-2], siendo ambos difíciles de degradar en las estaciones depuradoras de aguas residuales.
Se han estudiado diversas posibilidades para la eliminación de este tipo de contaminantes. Entre ellas, la adsorción es una técnica que está tomando cierta relevancia en el campo de la depuración debido a su elevada eficacia y a su coste relativamente bajo. Sin embargo, es necesario encontrar el adsorbente adecuado para las sustancias a tratar.
Las zeolitas son aluminosilicatos cristalinos con una estructura microporosa, que han mostrado ser adsorbentes altamente eficaces gracias a su gran área superficial, selectividad y a su capacidad de intercambio iónico [3]. Existen múltiples tipos de zeolitas, tanto naturales como sintéticas, que podrían ser empleadas para la adsorción de este tipo de contaminantes. Por ejemplo, la síntesis de una zeolita a partir decenizas volantes, modificada con surfactantes, ha demostrado mejorar significativamente la adsorción de BPA, debido a la interacción hidrofóbica entre el BPA y las cadenas de surfactante [4]. Asimismo, cabe resaltar que la naturaleza porosa de las zeolitas, así como su relación silicio-aluminio, que afecta directamente a su hidrofobicidad, pueden ser modificadas para adaptarse al contaminante a eliminar [5].
En base a lo anterior, en el siguiente trabajo se realiza el estudio de la adsorción de dos contaminantes orgánicos, uno de carácter más apolar (BPA) y otro de tipo iónico (naranja de metilo), sobre dos adsorbentescon una misma estructura zeolítica, pero con diferente relación silicio-aluminio, esto es, diferente hidrofobicidad.

2. Experimental – Para la realización de los diferentes ensayos se han utilizado dos zeolitas de tipo faujasitacomerciales. La zeolita pura sílice HSZ-390-HUA (zeolita Tosoh) fue suministrada por la casa comercial Tosoh Corporation, y la zeolita CBV712, de relación Si/Al = 6, fue suministrada por Zeolyst International. Las moléculas adsorbidas han sido el bisfenol A (BPA) y el naranja de metilo (NM). Los experimentos de adsorción se han llevado a cabo a temperatura ambiente por contacto de una cantidad determinada de adsorbente, ratio masa-volumen (*R*) comprendido entre 0.1 – 1.0 g L^{-1}, con una disolución de concentración comprendida entre 20 - 100 mg/L de la molécula objeto de estudio.
Una vez alcanzado el equilibrio, se ha procedido a la separación de las dos fases mediante centrifugacióny filtración para, posteriormente, caracterizar la fase líquida obtenida. La determinación de las concentraciones de ambos analitos se ha llevado a cabo mediante métodos espectrofotométricos.

3. Resultados y Discusión – Se ha estudiado la adsorción de dos compuestos orgánicos claramente diferenciados; por un lado, un colorante azoico de naturaleza iónica (NM) y por otra un compuesto más apolar (BPA). Los materiales adsorbentes utilizados fueron zeolitas con la misma estructura microporosa (estructura FAU de acuerdo con la nomenclatura de la IZA) pero de diferente relación silicio/aluminio. Se han llevado a cabo estudios cinéticos de adsorción para ambos adsorbentes y reactivos (Figura 1), así como estudios de equilibrio. Como puede apreciarse en la figura, la adsorción del BPA sobre la zeolita más hidrofóbica, zeolita Tosoh, muestra unos resultados muy prometedores, observando una eficaz eliminación del contaminante en un corto periodo de tiempo. Sin embargo, la adsorción sobre la zeolita máshidrofílica, muestra una adsorción con el tiempo prácticamente nula.

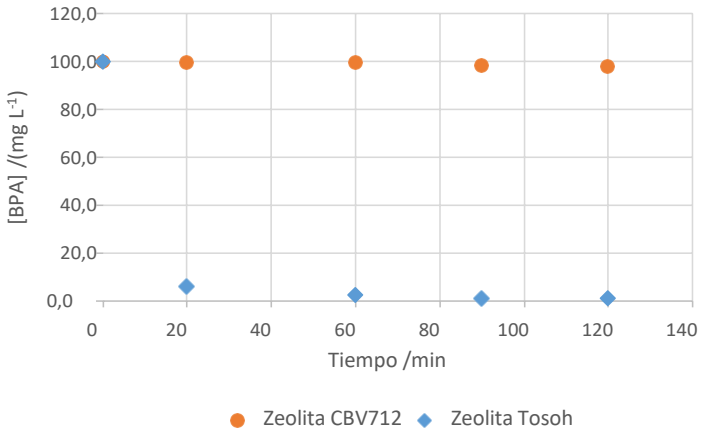

Imagen 1. Adsorción de BPA (100 mg L^{-1} inicial) sobre ambas zeolitas (R = 1 g L^{-1}).

Los estudios de equilibrio de adsorción muestran que para esta combinación de adsorbente-adsorbato se pueden obtener capacidades de adsorción del orden de 200 mg g^{-1} o incluso mayores. Sin embargo, esta elevada capacidad de adsorción disminuye cuando el adsorbente empleado es la zeolita más hidrofílica,lo que indica que existe una clara relación entre la hidrofobicidad del adsorbente y su capacidad de adsorción para moléculas tipo BPA, no siendo en este caso tan importante la estructura de la zeolita utilizada.
Este comportamiento es muy diferente del observado con el NM, compuesto orgánico iónico, el cual presenta una menor adsorción sobre la zeolita más hidrofóbica. En el caso de la adsorción del NM sobre zeolita pura sílice, zeolita Tosoh, la adsorción alcanzada es del orden de 5 mg g^{-1}, lo que pone de manifiesto la existencia de un claro efecto de la naturaleza polar del adsorbato sobre la capacidad de adsorción de la molécula seleccionada. Estos resultados permiten predecir que la zeolita FAU pura sílice permitiría la eliminación selectiva de contaminantes de baja polaridad en aguas contaminadas de forma altamente selectiva y efectiva.

4. Conclusiones – Tras la realización de este trabajo, se ha podido comprobar cómo tanto la naturaleza del adsorbente como la del propio adsorbato son clave para conseguir un proceso de eliminación eficiente. El empleo de zeolitas de naturaleza hidrofóbica de tipo faujasita presenta grandes ventajas en la eliminación de contaminantes orgánicos de naturaleza apolar, consiguiendo una elevada selectividad hacia los mismos, ya que dificulta la retención de otros tipos de especies de naturaleza más polar.

Agradecimientos
Este trabajo ha sido financiado por el Gobierno de España – MCI a través del proyecto PID2021-122755OB-I00.

5. References

[1] Chen, D. et al., Environmental Science & Technology, 50(11), (2016) p. 5438.
[2] Gupta, V. K., & Suhas, Journal of Environmental Management, 90(8), (2009) p. 2313.
[3] Dehmani, Y. et al., Arabian Journal of Chemistry, 17(1), (2019) p. 105474.
[4] Dong, Yi et al., Journal of Colloid and Interface Science, 348, (2010) p. 585.
[5] Radoor, S. et al., Colloids and Surfaces A: Physicochemical and Engineering Aspects, 611, (2021) p.125852.

P20: Graphite oxide suspension for quinoline adsorption in aqueous medium

G. F. Oliveira do Nascimento [(1)], C. M. B. Araujo [(2)], M. M. Menezes Bezerra Duarte [(1)], M. Alves da Motta Sobrinho [(1)]

[(1)] Universidade Federal de Pernambuco, Av. Prof. Moraes Rego, Recife - PE, 50670-901, Brazil
gabriel.oliveiranascimento@ufpe.br
[(2)] University of Minho, R. da Universidade, 4710-057 Braga, Portugal
mauricio.motta@ufpe.br; caroline.maria@ufpe.br

1. Introduction – Quinoline is a basic nitrogenous organic contaminant found in petroleum refineries. Commonly present in industrial effluent. It's a toxic, carcinogenic and mutagenic compound, and is difficult to degrade, therefore conventional treatment methods have difficulty removing it from the aqueous medium. Adsorption is an alternative method used to remove organic substances present in aqueous medium as it is a simple, efficient, and versatile method, which can be applicable on industrial scales [1-3]. Of many materials that can be used as adsorbents, graphite oxide (GrO) stands out due to its high surface area and negative density related to the oxygen functional groups on its surface, which makes it an attractive material for removing polar organic substances [2]. Therefore, the aim of the work is to evaluate the viability of graphite oxide in suspension as an adsorbent for removing quinoline in an aqueous medium.

2. Experimental – GrO was synthesized using the methodology inspired by the method proposed by Hummers and Offeman, (1958). Then the material was washed with a HCl solution and distilled water, the suspension was then used as an adsorbent for quinoline in an aqueous medium. A preliminary test was carried out in which 0.6 $g.L^{-1}$ of the suspension was mixed with 50 mL of a 30 $mg.L^{-1}$ quinoline solution, for 3h at 250 rpm and 298K, the supernatant was filtered and the initial and final concentration was determined using a UV-Visible spectrophotometer.
The characterization of GrO was done by X-ray diffraction (XRD), Fourier transform infrared spectroscopy (FT-IR) and Raman spectroscopy. After this, the operational conditions were then defined: m/V ratio and initial pH. The same conditions as the preliminary test were used. The m/V ratio varied from 0.4 to 1 $g.L^{-1}$ and the initial pH range studied was from 6 to 10.
The adsorption kinetics was studied. 50 mL of quinoline solution (30 $mg.L^{-1}$) remained in contact with the adsorbent for 0.5 – 60 min (250 rpm, 298 K) using the best predetermined operational conditions, being filtered and quantified right after. Then the nonlinear pseudo-first and pseudo-second order models were applied to the experimental data. After this the adsorption equilibrium experiments were carried out, the initial concentration of quinoline varied from 5 to 50 $mg.L^{-1}$. Then 50 mL of the quinoline solutions were mixed with the adsorbent for 60 min (250 rpm, 298 K) using the best operating conditions, and were subsequently filtered and quantified. The nonlinear equilibrium isotherm models of Langmuir, Freundlich and Sips were applied to the experimental data. All assays were performed in duplicate.

2. Results and Discussion – In the preliminary test, the adsorption capacity (q) of GrO was 40.02 $mg.g^{-1}$, qualifying it as a good adsorbent for quinoline. The results of the GrO characterizations are shown in Image 1. According to Image 1 (a), there is a high intensity peak at $2\theta = 10^{o}$ characteristic of graphite oxide, and a low intensity one at the point $2\theta = 26^{o}$ referring to graphite.

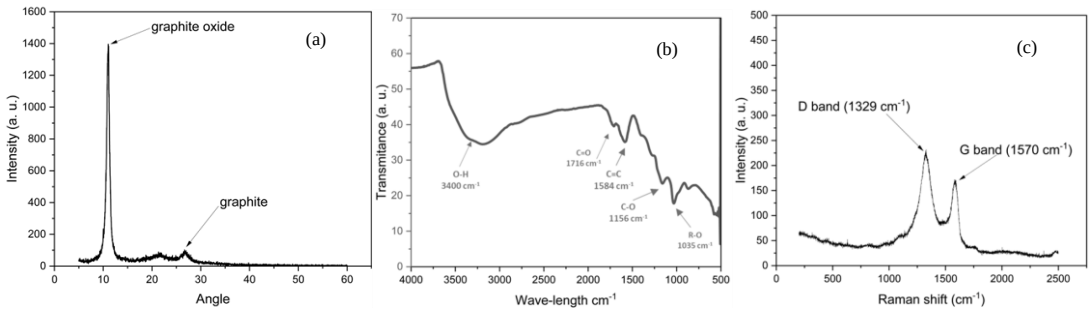

Image 1. Results of graphite oxide sample characterizations: (a) XRD; (b) FT-IR; (c) Raman spectra.

This angular shift is due to the oxygen functional groups present on the surface of the material, which increase the distance between the graphite sheets, which causes the reduction to a smaller angle. Image 1

(b) shows the presence of hydroxyl (3500 to 3000 cm^{-1}), carbonyl (1716 cm^{-1}), epoxy (1156 cm^{-1}) and alkoxy (1035 cm^{-1}) functional groups in addition to the non-oxidized graphite vibrations (C=C) at 1584 cm^{-1}. In Image 1 (c) two bands are highlighted, the D band referring to the degree of disorder of the material and the G band characteristic of crystalline graphite. The ratio between the intensities of the bands (I_D/I_G) was equal to 1.35, which indicates the disorder in the graphite sheets, caused by the insertion of oxygen functional groups on the materials surface. These characterizations confirm the success in the oxidation of graphite during the synthesis.

During the definition of the operational conditions, aiming to obtain the best correlation between the adsorptive capacity and percentage of removal, the m/V ratio selected was 0.6 $g \cdot L^{-1}$. Furthermore, it was found that for pHs below 6 there is a displacement in the quinoline peak, thus, it was decided to study the pH range from 6 to 10. The adsorptive capacity in the study did not vary significantly (2%), so it was concluded that no pH adjustments were needed.

Image 2 Shows the kinetic pseudo-first and pseudo-second order fitting the experimental data. The speed in which the adsorption occurred was quite fast, reaching equilibrium in 15 min. Both kinetic models adjusted well to the experimental data, although the pseudo-second order model had slightly better results with R^2 = 0,9997 whereas the pseudo-first order model obtained R^2 = 0,9988, also the q_{cal} (36,8 $mg.g^{-1}$) was similar to the q_{exp} (37,46 $mg.g^{-1}$). Thus, it can be inferred that the adsorption occurs through more than one mechanism.

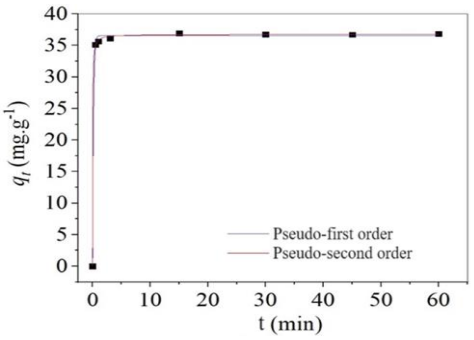

Image 2. Adsorption kinetics of GrO and quinoline.

Image 3 Shows the equilibrium isotherms of Langmuir, Freundlich and Sips fitted to the experimental data. Langmuir and Sips isotherms overlap each other, with *m* value being exactly 1 for the Sips model, which indicates the tendency to the Langmuir model which is a monolayer model. Those two were the ones who better fitted the experimental data with both having R^2 = 0,995 whereas the Freundlich model got a R^2 = 0,981, and n = 1,9 which indicates that the adsorption process is favourable. Furthermore the q_{max} value for the Langmuir model was 74,8 $mg.g^{-1}$.

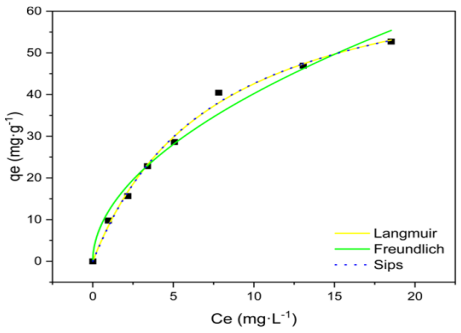

Image 3. Adsorption equilibrium isotherms of GrO and quinoline.

The adsorption capacity values of GrO shown in this work are better [1][3] or on par [2] with other materials used as adsorbent for quinoline shown in the literature, only losing to some specific composites specifically optimized for quinoline removal [2].

4. Conclusions – In this work, graphite oxide was shown to possess a good adsorption capacity compared to other materials for quinoline adsorption, except the ones produced specifically for that purpose. With a rapid kinetic and good equilibrium results, the material applied is this work might be viable as an alternative for removal of quinoline from aqueous medium through adsorption.

5. References

[1] BIAN, Y.; SUN, H.; LUO, Y.; GAO, Q.; LI, G.; WANG, Y. Effect of inorganic salt ions on the adsorption of quinoline using coal powder. **Water Science and Technology**, 78 (3) p. 496-505, 2018.

[2] SANTOS, M. B. S.; NASCIMENTO, B. F.; GHISLANDI, M. G.; ARAUJO, C. M. B.; MOTTA SOBRINHO, M. A. Production and characterization of graphene-based nanocomposites of different natures and their applications in aqueous quinoline adsorption: A comparative study. **Case Studies in Chemical and Environmental Engineering**, v. 9, p. 100605, 2024.

[3] WANG, L.; GAO, Q.; LI, Z.; & WANG, Y. Improved removal of quinoline from wastewater using coke powder with inorganic ions. **Processes**, 8(2), 2020.

P21: Gas-phase simulated moving bed for methane upgrading using pelletized maxsorb

R. O. M. Dias [1,2], M. J. Regufe [1,2], A. A. Pereira [1,2], A. F. P. Ferreira [1,2], A. E. Rodrigues [1,2], A. M. Ribeiro [1,2]

[1] *LSRE-LCM – Laboratory of Separation and Reaction Engineering – Laboratory of Catalysis and Materials, Faculty of Engineering, University of Porto, Rua Dr. Roberto Frias, 4200-465, Porto, Portugal*

[2] *ALiCE – Associate Laboratory in Chemical Engineering, Faculty of Engineering, University of Porto, Rua Dr. Roberto Frias, 4200-465, Porto, Portugal*

rmdias@fe.up.pt

mjregufe@fe.up.pt; up201806339@edu.fe.up.pt; aferreir@fe.up.pt; arodrig@fe.up.pt; apeixoto@fe.up.pt

1. Introduction

Due to the depletion of conventional natural gas wells, unconventional methane-rich sources have been increasingly explored. These sources often contain impurities, notably nitrogen, which is difficult to remove due to its similar properties to those of methane. To meet pipeline specifications, nitrogen content must be reduced to below 3% to maintain the calorific value of the stream [1]. The main technology used for this purpose is cryogenic distillation, which has very high energy costs associated and is unsuitable for medium and small-scale purification of methane streams [2]. When compared to this technology, adsorption-based processes are very appealing due to their easy scalability and lower energy requirements. However, the adsorbent performance for CH_4/N_2 separation may be an issue due to their low selectivity [3]. The use of a gas-phase simulated moving bed (SMB) process overcomes this challenge since it can separate mixtures with an adsorption selectivity close to unity by introducing a third species, the desorbent, which displaces the adsorbed phase, essentially transforming a difficult separation into two easier separations.

The design and development of a gas-SMB process for separating nitrogen-contaminated methane streams is the focus of this work, using maxsorb extruded into pellets with 10% binder, as the adsorbent material and explores argon and carbon dioxide as potential desorbent gases. The performance of the material was evaluated by measuring the adsorption equilibrium data for the four adsorbates and the dynamic behaviour of single and multicomponent adsorption through fixed-bed experiments.

2. Results and Discussion

The pure component isotherms of N_2, CH_4, Ar, and CO_2, presented in Figure 1, were measured at 303, 323, and 343 K in a pressure range of 0 - 2.5 bar using a volumetric apparatus. The data was successfully regressed with the single-site Langmuir model. The results show that CO_2 has the highest affinity to the stationary phase and Ar the lowest, over the entire range of temperature and pressure studied.

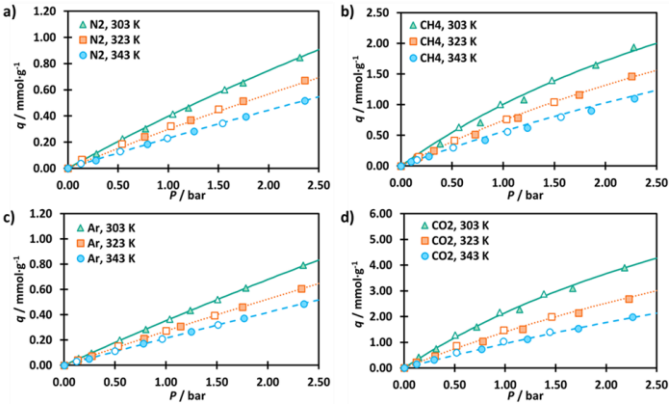

Figure 1. Amount adsorbed of a) N_2, b) CH_4, c) CO_2 and d) Ar on Maxsorb pellets at 303 (◆), 323 (■) and 343 K (●).

Single, binary, and ternary breakthrough experiments were carried out at 303 K and 1.5 bar, with a total flowrate of 0.2 SLPM. A mathematical model that encompasses mass, energy, and momentum balances was implemented in the gPROMS® software and utilized to predict the observed adsorption dynamics [4]. For example, the breakthrough experiment results with a bed initially saturated with CO_2 and a feed composition of 0.25 N_2/ 0.25 CH_4/ 0.50 CO_2 are presented in Figure 2. The experiment shows that the desorbent is easily displaced by the mixture and is equally able to displace the adsorbed phase, which is an essential step for SMB operation.

Finally, two simulated moving bed (SMB) cycles were employed to separate an equimolar CH_4/N_2 mixture using each of the desorbent gases to evaluate the impact of the desorbent strength in the process.

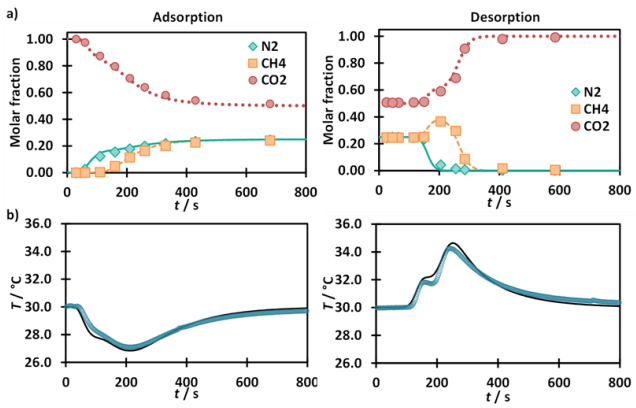

Figure 2. Breakthrough results for the ternary adsorption of a mixture of 25% methane, 25% nitrogen, and 50% carbon dioxide over the pelletized maxsorb, initially saturated with carbon dioxide: a) molar fraction of each component at the column outlet; b) temperature history in the middle of the column. Lines represent the simulation results.

while the less adsorbed species, N_2, is carried by the eluent, enriching the raffinate stream. The flow rate in section I is high enough to guarantee that the adsorbent is cleaned. In section IV, the desorbent is cleaned so it can be recycled back into section I. The desorbent-free purity for both cycles was very high (100% and 99.3% for the Argon and CO_2 experiment, respectively). A high recovery was also achieved in both cases (> 97%). When argon is used as the desorbent gas, the extract product stream is obtained with a productivity of 14.3 $kg \cdot m^{-3}_{ads} \cdot h^{-1}$.

The experiments were carried out with open loop operation, *i.e.*, with no desorbent recycle. A 2-2-2-2 four-zone system configuration was considered, with a switching time of 50 s. The SMB unit was operated at 303 K, with the backpressure, located at the end of zone IV, set at 1.5 bar. A feed composition of 50% CH_4 and 50% N_2 was used, with a feed stream of 0.130 SLPM for the argon experiment and 0.070 SLPM for the CO_2 experiment. As an example, the internal profile at 50% of the switching time for the experiment using CO_2 as the desorbent is presented in Figure 3. In zone II, the more adsorbed species, CH_4, is retained onto the material, enriching the extract stream,

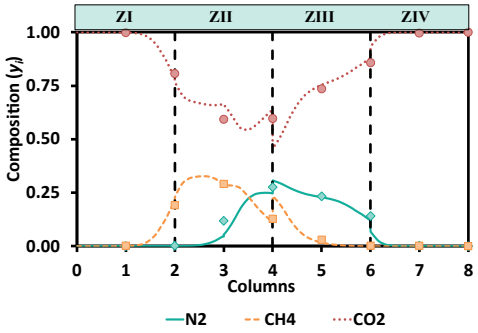

Figure 3. Internal profile at 50% of the switching time for Run 1, where carbon dioxide is used as the desorbent. Points represent experimental data and lines represent the model predictions.

3. Conclusions

Maxsorb powder was successfully extruded into pellets and its performance was evaluated for the separation of CH_4/N_2 streams. To do so, adsorption equilibrium data was measured and adsorption dynamics were assessed by breakthrough experiments. CO_2 exhibited the highest uptake among the measured adsorbates, followed by CH_4, N_2 and Ar. The breakthrough results allowed the validation of the adsorption equilibrium data measured as well as the transport parameters and model equations used in the simulations. Two SMB runs were designed for the separation of CH_4 and N_2, with both achieving high purity values (> 99%) and high recovery (> 97%) for the methane-rich stream.

4. Acknowledgements

This work was supported by national funds through FCT/MCTES (PIDDAC): LSRE-LCM, UIDB/50020/2020 (DOI: 10.54499/UIDB/50020/2020) and UIDP/50020/2020 (DOI: 10.54499/UIDP/50020/2020); and ALiCE, LA/P/0045/2020 (DOI: 10.54499/LA/P/0045/2020). Rafael Dias acknowledges his Ph.D. scholarship 2020.05095.BD, funded by FEDER funds through NORTE 2020 and by national funds through FCT/MCTES (DOI: 10.54499/2020.05095.BD).

4. References

[1] Kuo, J.C., K.H. Wang, and C. Chen, *Pros and cons of different Nitrogen Removal Unit (NRU) technology*. Journal of Natural Gas Science and Engineering, 2012. **7**: p. 52-59.
[2] Rufford, T.E., et al., *The removal of CO2 and N2 from natural gas: A review of conventional and emerging process technologies.* Journal of Petroleum Science and Engineering, 2012. 94-95: p. 123-154.
[3] Kennedy, D.A., et al., *Pure and Binary Adsorption Equilibria of Methane and Nitrogen on Activated Carbons, Desiccants, and Zeolites at Different Pressures*. Journal of Chemical & Engineering Data, 2016. 61(9): p. 3163-3176.
[4] Dias, R.O.M., et al., *Gas-Phase Simulated Moving Bed for Methane/Nitrogen Separation Using a Commercial Activated Carbon.* Industrial & Engineering Chemistry Research, 2022.

P22: Cytochrome C adsorption using graphene oxide-based composite hydrogel

C. M. B. Araujo [(1)], A. G. Rios [(2)], M. G. Ghislandi [(3)], A. F. P. Ferreira [(2)], M. A. Motta Sobrinho [(4)], A. E. Rodrigues [(2)]

[(1)]University of Minho, R. da Universidade, 4710-057 Braga, Portugal. caroline.maria@ufpe.br
[(2)]University of Porto, R. Dr. Roberto Frias, 4200-465 Porto, Portugal [(3)] UFRPE, R. Cento e Sessenta e Três, Cabo de Santo Agostinho - PE, Brazil [(4)]UFPE, Av. Prof. Moraes Rego, Recife - PE, 50670-901, Brazil
arios@fe.up.pt, marcos.ghislandi@ufrpe.br, aferreir@fe.up.pt, mauricio.motta@ufpe.br, arodrig@fe.up.pt

1. Introduction – Proteins have great importance for medicine and the pharmaceutical and food industries. However, proteins need to be purified prior to their application. Many stages are involved in separating and purifying proteins, and one of the widely used processes is adsorption. Therefore, understanding proteins adsorption mechanisms is fundamental for obtaining high capacities, selectivity, and more efficient separation processes [1]. Adsorption processes using composites based on nanomaterials, such as graphene oxide (GO), represent an alternative for efficiently isolate and purify proteins. Therefore, focusing on the comprehension of complex interactions between the biological macromolecules surfaces and nanomaterials are paramount [2].
Although applications of GO-based materials in adsorption are widely studied, the focus on semi-continuous processes remains limited. This work aimed to investigate the application of a hydrogel based on GO and agar for capturing Cytochrome C (Cyto C) heme protein by adsorption from aqueous solutions with other proteins.

2. Experimental - The synthesis of both GO and the GO-agar hydrogel were performed based on the methodology proposed by Araujo et al. [3]. Both the adsorption equilibrium and the kinetic study were performed using 25 mL of the protein solution, at pH=7. Adsorption equilibrium experiments were performed for a Cyto C initial concentration of 100 mg L^{-1}, ranging the adsorbent mass from 0.05 g to 0.80 g of the wet hydrogel. The kinetic experiments were conducted in sealed flasks for a fixed mass of adsorbent (0.20 g of wet adsorbent) and two different initial concentrations of Cyto C – 50 mg L^{-1} and 100 mg L^{-1}. The flasks were sealed and placed in the shaker at 250 rpm for 24 h and T=25°C. The supernatant was collected, and Cyto C concentration was estimated using the UV-Visible spectrophotometer at the Soret peak.
For the fixed bed tests, a stainless-steel column with 10 cm height and 2 cm internal diameter was packed with the wet composite hydrogel. The phosphate buffer (pH=7) was pumped through the column in upward flow to equilibrate the adsorbent before proceeding with the fixed bed breakthrough experiments; then the feed flow rate was switched to the protein inlet flow. The Cyto C was collected manually in the outlet stream at the top of the column, and the concentration was measured. Fixed bed experiments were performed at 25ºC, and the flow rate was periodically checked, to ensure a value close to 2 mL min^{-1}.

3. Results and Discussion - Results for the equilibrium adsorption experiment (at 25 ºC) are presented in Image 1. The maximum value of the adsorption capacity in the equilibrium obtained experimentally was 365.32 $mg.g^{-1}$ (on a dry basis). Regarding the adsorption equilibrium modelling, it is observed that all the isotherm models fitted the equilibrium data satisfactorily [4].
Results obtained during the kinetic study at two different initial concentrations are exhibited in Image 2. In this case, the pore diffusion model was used to fit the kinetic experimental data, assuming that internal diffusion is the

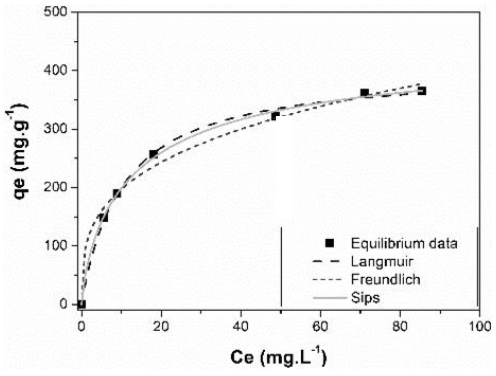

Image 1. Equilibrium adsorption isotherms (conditions: C_0 = 100 $mg.L^{-1}$, t =24 h, T =25 ºC, pH =7, V =25 mL).

slowest step, and equilibrium is reached at the liquid–solid interface [5]. Overall, all the three models showed a good fit to the kinetic data.

Regarding the adsorption mechanism of Cyto C adsorption onto the bionanocomposite, that are indications that it occurs mainly via electrostatic attraction between GO negatively charged adsorption sites in the composite and the positively charged hemeprotein Cytochrome C. Moreover, hydrogen bonds can also contribute to adsorption [3].

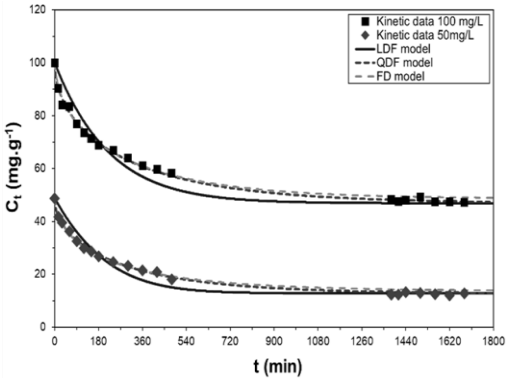

Image 2. Adsorption kinetics at different initial concentrations (conditions: C_0 = 50 and 100 mg.L^{-1}, m_{dry} = 0.004 g, T = 25 ^oC, pH = 7, V = 25 mL).

Image 3 presents experimental and simulation results of the breakthrough curve with the breakthrough time zoomed. It can be noted from the experimental points that the curve does not show a symmetrical shape. The breakthrough time is earlier (83 min) than expected when compared to the total experimental time, approximately 58 h. The average adsorption capacity calculated from fixed bed experiments was 386.64 mg g^{-1} (on a dry basis), which is slightly higher than the value calculated from batch equilibrium experiment.

The characteristic shape of the experimental breakthrough curve in proteins has also been observed by previous work. It was reported that the experimental breakthrough normally started relatively steep; then, after C_t/C_0 reached ~0.40, it bent over earlier than expected, leading to a slower approach to equilibrium. The slower equilibrium process can be attributed to the rearrangement of the adsorbed protein Cyto C within the GO layers, as the protein gradually transitions from an initially inefficient packing to its maximum packing over time [6].

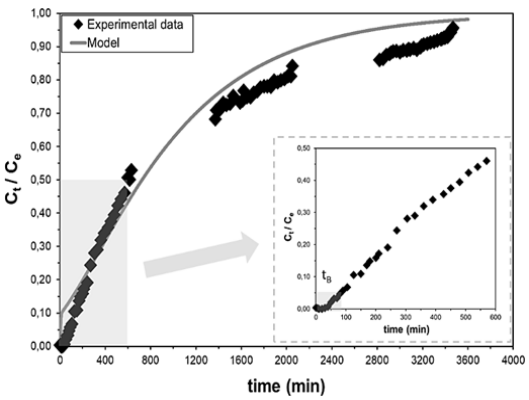

Image 3. Modelling of the breakthrough curve for Cyto C adsorption onto the GO-based composite

4. Conclusions - The application of a hydrogel produced from agar and GO was investigated as adsorbent for the adsorption of cytochrome C. All isotherm models applied for modelling the equilibrium data presented good fit to the experimental data. The maximum adsorption capacity predicted by the Langmuir isotherm model was 365.32 mg.g^{-1} (adsorbent dry). Fixed bed tests were performed and over 90% of the Cyto C adsorbed could be successfully recovered after desorption. The slower equilibrium process observed in the fixed bed breakthrough curve could be ascribed to the rearrangement of the adsorbed protein within the GO layers. Finally, the composite seems to be an effective method for Cyto C adsorption, exhibiting a notorious potential for applications in protein separation.

5. References

[1] J. C. Simoes-Cardoso, H. Kojo, N. Yoshimoto and S. Yamamoto, *Langmuir*, **36**, (2020) p.3336–3345.
[2] X. Wu, Q. Mao, Y. Hao, J. Yang, X. Zhang, Z. Chi, G. Liu, M. Wang, Q. Chen and X. Chen, *J Chromatogr A*, **1693**, (2023) p.463869.
[3] C. M. B. de Araujo, M. G. Ghislandi, A. G. Rios, G. R. B. da Costa, B. F. do Nascimento, A. F. P. Ferreira, M. A. da Motta Sobrinho and A. E. Rodrigues, *Colloids Surf., A*, **639**, (2022) p.128357.
[4] Z. Li, P. Guan, X. Hu, S. Ding, Y. Tian, Y. Xu and L. Qian, *Polymers (Basel)*, **10**, (2018) p.298.
[5] P. F. Gomes, J. M. Loureiro and A. E. Rodrigues, *Adsorption*, **23**, (2017) p.491–505.
[6] B. D. Bowes and A. M. Lenhoff, *J Chromatogr A*, **1218**, (2011) p.4698–4708.

P23: Enhanced thermal management in HKUST-1 composites through the incorporation of graphite flakes during the monolith conforming step

J. Farrando-Pérez [(1)], V. Ramírez Cerezo [(1)], J. Silvestre-Albero[(1)]

1) Department of Inorganic Chemistry/University Institute of Materials, University of Alicante, Spain. Judit.farrando@ua.es

1. Introduction- The storage of hydrogen in the cavities of nanoporous materials is emerging as a promising alternative that makes hydrogen technology more viable for large-scale applications. One of the most studied materials for this purpose is MOFs due to their high chemical flexibility and large surface area. [1] Among all existing MOFs, HKUST has proven to be one of the best for hydrogen storage due to its microporous structure. Additionally, HKUST can be compacted into monoliths using mechanical compaction techniques. This process increases the material's density, thereby improving its volumetric storage capacity without significantly reducing its surface area and porosity. [2] The compacted monoliths enhance the overall gravimetric and volumetric efficiency of hydrogen storage.

Despite all the advantages mentioned above, one of the main limitations of this material for large-scale applications is heat dissipation on the MOF surface. During hydrogen adsorption, heat is released, which can increase the temperature of the material and considerably reduce hydrogen uptake. This limitation may be overcome by mixing HKUST with a material that has good thermal conductivity, such as graphite.

Based on these premises, the aim of this study is improving the contact between the graphite and the HKUST through graphite using different conforming methods and test their heat dissipation performance during hydrogen adsorption process.

2. Experimental- Synthesis of the composites in monolithic form: Pure HKUST-1 powder was prepared using a modified hydrothermal method based on previously reported recipes. [3,4]
The monoliths were conformed into disk-shaped monoliths under a load of 0.5 Tons. In this work, two types of monoliths were prepared to evaluate their heat dissipation performance. Firstly, three mechanically mixed monoliths were prepared. For these, the corresponding amounts of graphite flakes and HKUST-1 were introduced into a vial and manually stirred until completely homogenized. The mixture was then introduced into the mold. Secondly, monoliths were prepared using a sandwich method with the same quantities as above. In this process, half of the graphite was initially added to the mold, followed by the introduction of HKUST-1, and then the final layer of graphite was added. All the material was then pressed to form the monolith. As a result, three mechanically mixed composite monoliths with 50 wt%, 33 wt%, and 25 wt% graphite were obtained, along with their corresponding sandwich monoliths. (Image. 1)

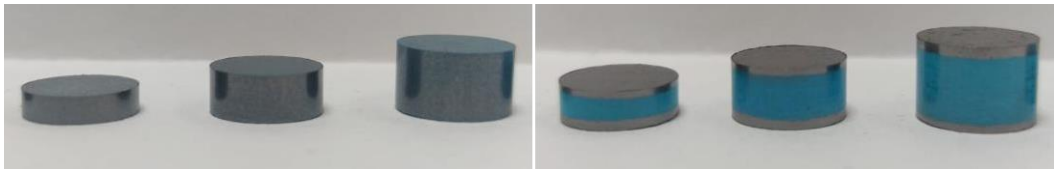

Image 1. Mechanically mixed composite monoliths with 50 wt%, 33 wt%, and 25 wt% graphite, respectively from left to right (left) and the corresponding "Sandwich" monoliths, also from left to right (right).

Thermal properties of the monoliths: The thermal heating of the samples was carried out using a LLG-uniSTIRRER 7-inch ceramic hotplate heater for sample heating and a similar ceramic plate at room temperature for the analysis of the heat dissipation of each sample. For all experiments, the temperature increase, and sample heat dissipation were monitored using a FLIR E6-XT thermographic camera and the images were treated with the FLIR Tools software and Origin 7.5. The monoliths were exposed to a thermal heating on a ceramic surface at 90 °C until reaching thermal equilibrium and the heat dissipation of the monoliths were registered from a side perspective by placing them on another ceramic surface at room temperature for 300 seconds.

3. Results and Discussion- Image 2 (left) shows the heat dissipation curves for samples HKUST-1 (**1**); HKUST-1@GO (**2**) and HKUST-1-6mm@GO (**3**). In this case, pure HKUST-1 (**1**) and sandwich HKUST- 1-6mm@GO (**3**) samples display very similar cooling profiles when the temperature is registered on the centre of the lateral side of the monoliths. In contrast, the mixed MOF-graphite oxide sample HKUST- 1@GO (**2**) displays a faster cooling rate. A more in-depth study of the thermal analysis of the thermal gradients across the lateral face of the monoliths is shown in Image 2 (right). The registered thermal images provide clear evidence that all the lateral area of the mixed MOF-graphite oxide monolith 2 dissipates heat very fast. Another interesting feature observed is that in the three samples the heat dissipation is faster on the bottom part of the monolith, which is in contact with the ceramic surface at room temperature. Indeed, after 40 and 90 seconds, the gradient distribution shows larger green and blue areas at the bottom part in agreement with a more extended temperature decrease gradient. In addition, although the heat dissipation of samples 1 and 3 is very similar in the centre of the monolith, a slightly more extended area of temperature gradient is observed at the bottom of sample 3, especially after 90 and 180 seconds. This tendency for 3 is probably due to the better thermal conductivity of the graphite oxide shell between the MOF and the ceramic surface.

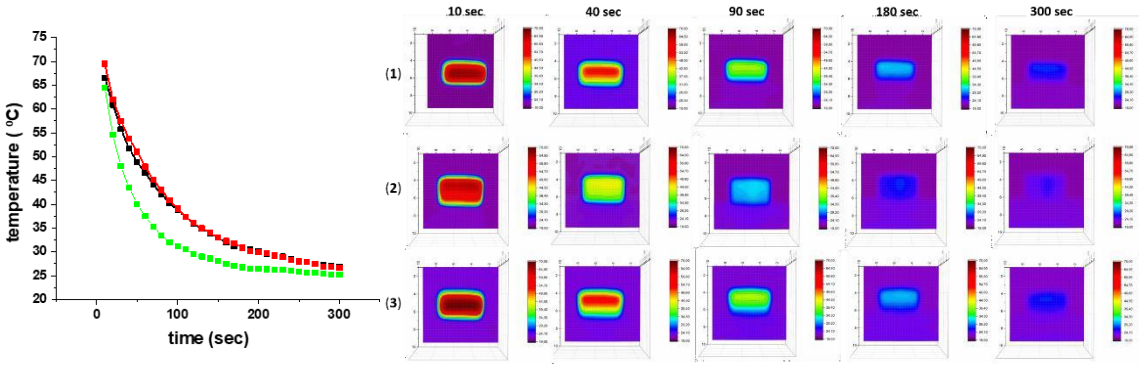

Image 2. Heat dissipation curves for pure HKUST-1 (red), HKUST-1@GO (green), and HKUST-1-6mm@GO (black). (left) and Images of heat dissipation of HKUST (1), HKUST-1@GO and HKUST-1- 6mm@GO over time. (right)

4. Conclusions This study has demonstrated how the incorporation of Graphite flakes in the HKUST-1 monolith conforming process has protected the embedded MOF crystals against amorphisation and/or plastic deformation. In addition, the presence of graphite microdomains in the formulation gives the monoliths excellent thermal properties. These properties are crucial for a fast and efficient dissipation of adsorption heat generated in high potential storage reservoirs. Finally, as for the comparison of the two types of monoliths, those prepared by mechanical mixing have shown a better heat dissipation capacity compared to the 'sandwich' type, due to a better contact between the MOF crystals and the graphite particles.

5. References

[1] M.P. Suh, H.J. Park, T.K. Prasad, D.W. Lim. Hydrogen storage in metal organic frameworks. *Chem Rev*, **112**(2), (2012), pp. 782-835.
[2] J. Farrando-Pérez, M. Rodríguez-Castillo, M. Martínez-Escandell, M. Monge, J. Silvestre-Albero. Improved thermal management in HKUST-1 composites upon graphite flakes incorporation: Hydrogen adsorption properties. *Int J Hydrogen Energy*, **48**(93) (2023), pp. 36474-36484.
[3] A. Vishnyakov, P.I. Ravikovitch, A.V. Neimark, M. Bülow, Q.M. Wang. Nanopore structure and sorption properties of Cu-BTC metal-organic framework. *Nano Lett*, **3(**6) (2003), pp. 713-718.
[4] S.S.Y. Chui, S.M.F. Lo, J.P.H. Charmant, A.G. Orpen, I.D. Williams. A chemically functionalizable nanoporous material $[Cu_3(TMA)_2\ (H_2O)_3]_n$, *Science*, **283**(5405) (1999), pp. 1148-1150.

P24: Purification of sugarcane molasses via adsorption on carbon materials and its valorization to 5-hydroxymethylfurfural

K. Morawa Eblagon*, M. V. Nunes Barros, M.F. R. Pereira, J. L. Figueiredo

LSRE-LCM - Laboratory of Separation and Reaction Engineering – Laboratory of Catalysis and Materials,
Faculty of Engineering, University of Porto, Rua Dr. Roberto Frias, 4200-465 Porto, Portugal
ALiCE - Associate Laboratory in Chemical Engineering, Faculty of Engineering, University of Porto, Rua Dr. Roberto Frias, 4200-465 Porto, Portugal
Corresponding author's e-mail: keblagon@fe.up.pt

1. Introduction – The industrial transition from a linear fossil-fuels-based economy to a more sustainable circular economy requires utilizing easily available and renewable raw materials that do not compete with the food supply [1]. In this sense, sugarcane molasses (SCM), a low-value by-product of the sugar industry, can be applied as a feedstock for producing important platform chemicals, such as 5-hydroxymethylfurfural (HMF). SCM is a viscous dark brown syrup containing a high concentration of sugars, mainly sucrose (up to 50 %), glucose, and fructose, apart from impurities such as organic acids, metal salts, and colorants (i.e., caramels, polyphenols, and melanoidins) [2].

HMF is a versatile molecule that can be transformed into biofuels and/or fuel additives, solvents, polymers, resins, and pharmaceuticals to substitute conventional petroleum-derived products. HMF can be produced from SCM via a cascade reaction catalyzed by acids, which involves the following steps: i) the hydrolysis of sucrose into glucose and fructose, ii) the isomerization of glucose into fructose, and iii) fructose dehydration to HMF. During the conversion of SCM to HMF, the impurities above can significantly affect the catalyst's performance by adsorbing on its surface and blocking the active sites. Alternatively, they can homogenously catalyze side reactions such as HMF degradation to humin [3]. Thus, in the present work, the purification of SCM was studied via adsorption on commercial activated carbon (AC) and carbon xerogel (CX). The efficiency of these processes was assessed by measuring the total amount of organic carbon, sugars, and metals in the SCM solution before and after the adsorption pre-treatments. Subsequently, the purified SCM was used as feedstock for HMF production using a microwave reactor, and the obtained catalytic results were compared with those achieved using untreated SCM.

2. Experimental –

2.1. Preparation and characterization of the adsorbents.

Carbon xerogel (CX) was obtained via polycondensation of resorcinol (R) and formaldehyde (F) in DI water, as described in our previous work [4]. The precursor's pH was adjusted to 5.7 using 0.1 M NaOH. After preparing the dry organic gel, the material was crushed into small pieces and carbonized in a vertical furnace under N_2 flow (100 mL/min) at 800 °C for 2h. The activated carbon Epibon Y, abbreviated AC, was obtained from Chimiefree Portugal. The materials were crushed and sieved through 100 µm mesh and dried overnight at 100 °C in the laboratory oven before the adsorption tests. The carbon materials were characterized using N_2 Adsorption/Desorption at −196 °C, Elemental and Thermogravimetric analyses.

2.2. Purification of SCM via adsorption

The substrate was obtained by dissolving 100 g of industrial-grade SCM (supplied by sugar refinery RAR, Portugal) in 1L of ultrapure water, using an ultrasonic bath for 20 min. Subsequently, the solution was centrifuged applying VWR MEGA STAR 1.6 centrifuge set at 4500 rpm for 20 min. The solid residue was removed by decantation, resulting in the substrate abbreviated SCM-simple. The SCM-simple was stored in a fridge at 4 °C. In the typical pre-treatment of SCM-simple, 2.1 g of the carbon adsorbent (AC or CX) was dispersed in 40 mL of the SCM-simple using a 50 mL beaker. The batch adsorption experiments were carried out for 1h at 25 °C under magnetic stirring set at 650 rpm. When the time was finished, the adsorbent was separated from the liquid via filtration. The SCM treated via adsorption on AC was abbreviated SCM-AC, and that treated with CX was labelled SCM-CX._

2.3 Characterisation of the substrates

SCM-simple, SCM-AC, and SCM-CX were characterized using Total Organic Carbon (TOC) measurements, and the color removal was obtained from UV-absorption at λ =280 or 400 nm measured using UV-1800 Shimadzu ultraviolet spectrophotometer. The concentration of sugars in SCM was obtained from High-Performance Liquid Chromatography (HPLC). The ash content of the substrates was accessed by weight difference before and after the combustion of the material at 700 °C. The amounts of metals were measured by Inductively Coupled Plasma (ICP).

2.4. Catalytic testing

The conversion of SCM-simple, SCM-AC, and SCM-CX feedstocks was carried out in a microwave reactor (Anton Paar Monowave 200) using carbon catalyst containing -SO_3H as Brønsted acid sites. The catalyst

was prepared using hydrothermal carbonization in the presence of diluted H_2SO_4, as described in [3]. In a typical catalytic experiment, 0.07 g of catalyst was placed inside a 30 mL glass vial, followed by 10 mL of the 10 % SCM feedstock (i.e., SCM-simple, SCM-AC, or SCM-CX) and a magnetic stirrer. The catalytic testing was conducted at 180 °C for 20 min, with a magnetic stirring set at 600 rpm. At the end of the tests, the stirring was stopped, and the microwave was allowed to cool to 55 °C (t < 2 min) by blowing cold air. The reaction mixtures were analyzed using HPLC equipped with C18 and UV detector or Altech OA-1000 organic acid column coupled with RI detector. The details of the analysis can be found in our previous work [3].

3. Results and Discussion -

The N_2 adsorption/desorption isotherms at −196 °C revealed that AC was a micro-mesoporous material with a BET surface area (S_{BET}) of 1408 m^2 g^{-1}. In addition to a large volume of micropores ($V_{micro,}$=0.95 m^3/g, it also presented an extended mesoporosity with a surface area higher than that of CX (1242 vs 219 m^2 g^{-1}). On the other hand, CX showed S_{BET}=620 m^2/g and V_{micro}=0.2 m^3/g. The elemental analysis results demonstrated that CX contained 5.3 wt% of oxygen compared to 7.3 wt% found in AC. The analysis of the SCM feedstocks before and after the purifications showed that SCM-simple had 13.3 % ashes, which decreased to 12.7% in the case of SCM-AC and 9.8% for SCM-CX. The ICP analysis of the ashes in the SCM-simple identified the presence of large amounts of Ca (27%). After the pre-treatments, SCM-AC contained only 8% of Ca, lower than the 14% present in SCM-CX. AC was generally found to be more efficient than CX in removing metal ions from SCM. AC was also more effective in the adsorption of colorants. UV-VIS results demonstrated 93% removal of color in SCM-AC compared to only 85% observed in SCM-CX. However, the treatment of SCM-simple via adsorption on AC resulted in the significant retention of sucrose, which is undesirable from the view of the application of SCM as feedstock for HMF. The catalytic results demonstrated that pre-treatment with AC showed the highest selectivity to HMF of 23%, whereas only 15% was obtained from SCM-CX and 14% was measured from SCM-simple. Interestingly, the feedstock conversion showed reverse order, with 62%, 55%, and 46% for SCM-simple, SCM-CX, and SCM-AC, which evidenced that the impurities in SCM can catalyze undesired side reactions of sugars.

4. Conclusions—Purification of industrial-grade SCM via adsorption was found to be an important step for its application as feedstock in future biorefineries. The adsorption of impurities such as ashes and colorants was more effective using AC, which resulted in much higher selectivity to HMF obtained in the subsequent catalytic process. The demonstrated pre-treatment process requires further development and optimization to minimize the sucrose losses and decrease the substrate/adsorbent ratio to become competitive and commercially viable approach.

5. Acknowledgments

This work was supported by national funds through FCT/MCTES (PIDDAC): LSRE-LCM, UIDB/50020/2020 (DOI: 10.54499/UIDB/50020/2020) and UIDP/50020/2020 (DOI: 10.54499/UIDP/50020/2020); and ALiCE, LA/P/0045/2020 (DOI: 10.54499/LA/P/0045/2020). KE is grateful to FCT for her Junior Researcher grant (# 2021.00535.CEECIND)

5. References

[1] N.C. Joshi, S. Sinha, P. Bhatnagar, Y. Nath, B. Negi, V. Kumar, P. Gururani, *Microbiol. Curr. Res.* 6, (2024) p.100237.

[2] M. Sjölin, J. Thuvander, O. Wallberg, F. Lipnizki, *Membranes*, 10, (2020) p. 5.

[3] K. Morawa Eblagon, J.L.Figueiredo, M.F. R. Pereira, *Catalysis Today*, (2024) under review.

[4] K. Morawa Eblagon, N. Rey-Raap, J.L. Figueiredo, M.F. R. Pereira, *Appl. Surf. Sci*., 548 (2021) p.149242.

RIA 43
XLIII Reunião Ibérica de Adsorção
Porto, Portugal
1-4 September 2024

P25: Xylene Adsorption on Barium-Potassium Exchanged Faujasite Zeolite

B. Castro [1,2], A. Ferreira [1,2]

[1] 1 LSRE-LCM – Laboratory of Separation and Reaction Engineering - Laboratory of Catalysis and Materials, Faculty of Engineering, University of Porto, Rua Dr. Roberto Frias, 4200-465 Porto, Portugal
[2] ALiCE – Associate Laboratory in Chemical Engineering, Faculty of Engineering, University of Porto, Rua Dr. Roberto Frias, 4200-465 Porto, Portugal.
up201505452@up.pt
aferreir@up.pt

1. Introduction – Xylenes are a group of aromatic compounds widely used in the chemical industry, as its isomers, ortho (*o*), meta (*m*), and para (*p*), are used as intermediates of various compounds. *p*-Xylene is the most used isomer as it can be oxidized to form terephthalic acid, which is of great relevance since it is used in the synthesis of polymers, such as polyethylene terephthalate (PET) and polybutylene terephthalate (PBT) [1-3].
The separation of xylene isomers is considered one of the seven world-changing separations and the complexity of this separation is related to their similar physicochemical properties, which prevents their separation by conventional methods, such as distillation [2, 4].
Normally, for the separation of *p*-xylene from the other C_8 aromatics, the solid phase of the SMB unit is a faujasite-type zeolite, X or Y, exchanged with alkali and/or alkaline earth metal ions, being preferable to use barium, potassium, or a combination of both [5-7]. The nature of the counter ion also plays an important role in the choice of the desorbent. For example, if toluene is the desorbent, it is preferable to use zeolite Y, exchanged with both barium and potassium. On the other hand, if the desorbent is *p*-diethylbenzene, the preferred adsorbent is zeolite X, almost completely exchanged with barium [8].

2. Experimental - The adsorbent (zeolite Y - SiO_2/Al_2O_3 = 5.1) was first subjected to an ion exchange step to replace the sodium (Na^+) cations, initially present in the zeolite, with potassium (K^+) and barium (Ba^{2+}) cations through contact with a solution containing 1.0 M of barium chloride and 0.3 M of potassium chloride. The zeolite was treated 8 times for 20 min each and then washed intensively with deionized water to remove any traces of chloride anions. This treatment took place at around 353 K, under reflux, with magnetic stirring at a speed high enough to maintain a homogenous mixture, 500 rpm in this case. The temperature was controlled by the condenser using water from the thermostatic bath.
Afterwards, the zeolite was dried overnight at 353 K. Then the adsorbent was shaped into pellets through an extrusion-spheronization process using Caleva Multi Lab-CML (Caleva, UK). The zeolite was mixed with kaolin, which acts as a binder (40 wt%). The mixing process was conducted at 80 rpm for 30 min while adding 0.42 mL of ultrapure water per gram of solid. The extrusion and spheronization processes were carried out at 60 and 650 rpm, respectively. Finally, the pellets were calcined at 823 K for 5 h.
The pellets were packed into a fixed bed column and left to dry overnight under a constant flow rate of nitrogen at 473 K. To obtain the breakthrough curves, the column was heated up to the desired operating temperature (453 to 513 K) while feeding a continuous stream of *i*-octane. When the defined temperature was reached, the feed was changed from *i*-octane to a mixture of *i*-octane and xylenes (1-15 wt%) or *i*-octane and toluene (1-15 wt%). The results of these breakthrough curves were used to determine the respective isotherms.

3. Results and Discussion - The adsorption equilibrium data for *m*-xylene, *p*-xylene and toluene, obtained from the breakthrough curves, were adjusted to fit the dual-site Langmuir model. These results are represented in Image 1. As an example, for the experiments with 1 wt% in *i*-octane at 453 K, the adsorption amounts of *m*-xylene, *p*-xylene, and toluene were 0.17, 0.23, and 0.14 $mol \cdot kg^{-1}$ respectively.

According to these results, it is possible to conclude that *p*-xylene has greater affinity towards the adsorbent than the other two components, which means that it can be more easily separated from a mixture of xylene isomers and toluene. As all of these components are present during the isomerition of xylenes, given that toluene is a secundary product, it could be advantageous to combine these two reactons into one single process, namely in a Simulated Moving Bed Reactor (SMBR), because by removing *p*-xylene from the reaction medium, the conversion of the other isomers can surpass the limit imposed by the thermodynamic equilibrium.

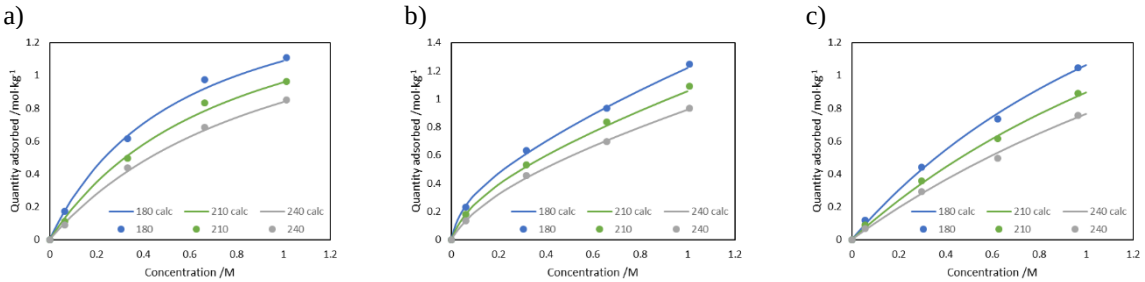

Image 1. Adsorption equilibrium curves for a) *m*-xylene, b) *p*-xylene, and c) toluene.

Additionally, several breakthrough experiments with a binary mixture of *m*-xylene and *p*-xylene (1-15 wt%) in *i*-octane were performed. Here, as an example, is represented the results of the experiment with 5wt% of xylenes (equimolar) in *i*-octane at 453 K (**Image 2**). These results indicate the *m*-xylene is the first component to saturate and therefore leave the column. When the front of *p*-xylene reaches the adsorption sites filled with *m*-xylene, it can displace the *m*-xylene, as seen by the roll-up in **Image 2**. This once again confirms the higher affinity of *p*-xylene displays towards the solid phase.

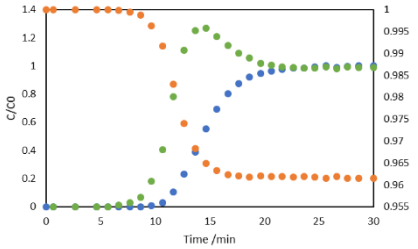

Image 2. Breakthrough curve for a binary mixture of *m*-xylene (●) and *p*-xylene (●) in *i*-octane (●).

4. Conclusions – The faujasite zeolite exchanged with barium and potassium shows greater affinity for *p*-xylene than toluene and *m*-xylene, which demonstrates it is a suitable absorbent for this separation. These are encouraging results that indicate that these reaction could occur simultaneously with isomerization (such as in a SMBR) as all of these components are present.

5. Future Perspectives – The main objective of this work is to develop a Simulated Moving Bed Reactor (SMBR) process for the production of *p*-xylene, employing a hybrid particle composed of both the adsorbent and the catalyst that will be used in a sorption-enhanced reactive process to maximize the isomers conversion and the selectivity towards *p*-xylene. The revolutionary aspect of this approach is the proximity between the adsorbent and the catalyst, which creates a lower resistance to mass transfer. Besides, as the separation of *p*-xylene by adsorption makes its concentration in the liquid medium decrease, isomerization of *o*- and *m*-xylenes can go beyond the thermodynamic equilibrium, further increasing the production of this isomer.

6. References

[1] C. Perego, P. Pollesel, Advances in Aromatics Processing Using Zeolite Catalysts, in: S. Ernst (Ed.) Advances in Nanoporous Materials, Elsevier2010, pp. 97-149.
[2] Y. Yang, P. Bai, X. Guo, Separation of Xylene Isomers: A Review of Recent Advances in Materials, Industrial & Engineering Chemistry Research, 56 (2017) 14725-14753.
[3] Y. Ma, N.C. Bruno, F. Zhang, M. Finn, R.P.J.P.o.t.N.A.o.S. Lively, Zeolite-like performance for xylene isomer purification using polymer-derived carbon membranes, Proceedings of the National Academy of Sciences of the United States of America, 118 (2021).
[4] D.S. Sholl, R.P. Lively, Seven chemical separations to change the world, Nature, 532 (2016) 435-437.
[5] H. Jobic, A. Méthivier, T. Seydel, On the adsorption and diffusion of water in BaX zeolite, Comptes Rendus Chimie, 8 (2005) 411-417.
[6] J.-P. Bellat, J.C. Moise, V. Cottier, C. Paulin, A. Methivier, Effect of Water Content on the Selective Coadsorption of Gaseous p-Xylene and m-Xylene on the BaY Zeolite, Separation Science and Technology, 33 (1998) 2335-2348.
[7] G.C. Anderson. 1992. Process for separating para-xylene from a C_8 and C_9 aromatic mixture. US 5,171,922 A: UOP.
[8] G. Hotier, C.R. Guerraz, T.N. Thanh. 1999. Process for the separation of *p*-xylene in C_8 aromatic hydrocarbons with a simulated moving bed adsorption and a crystallization. US 5,922,924 A: IFP Energies Nouvelles IFPEN.

P26: Synthesis and Functionalization of Monolithic Adsorbents: Impregnation and Grafting for Optimal CO_2 Capture

A. Kasiri, E.S. Sanz-Pérez A. Arencibia

Departamento de Tecnología Química, Energética y Mecánica, ESCET, Universidad Rey Juan Carlos, C/Tulipán s/n, 28933 Móstoles, Madrid, Spain.
amaya.arencibia@urjc.es

Introduction

The increasing concentration of atmospheric CO_2 is a critical driver of climate change, inducing the rapid development of effective carbon capture technologies to mitigate its environmental impact. Among various adsorbent materials, mesostructured materials functionalized with amino groups have proven especially effective for CO_2 capture due to their large surface areas and tailored pore structures that facilitate chemisorption of CO_2 [1]. Since more than 15 years ago, huge efforts have been done to probe these materials under a great vary of conditions. However, they are pulverulent materials, with very small particle sizes that often face high pressure drops and handling challenges in industrial settings [2], thus leading to important disadvantages for practical applications.

In contrast, monolithic adsorbents are engineered to overcome these limitations, thereby providing enhanced manageability and operational efficiency. Their robust structure not only mitigates pressure drop and facilitates easier handling but also reduces material loss and operational hazards associated with dust. This design allows to prepare adsorbents more suitable for sustainable and safe industrial applications.

This research focuses on the synthesis and comprehensive evaluation of three distinct types of monolithic adsorbents, trying to obtain functionalized mesostructured silica materials with a monolithic external morphology. With this aim, two types of procedures have been explored to develop monoliths for CO_2 capture: i) direct synthesis of the monolithic silica using structure directing agents able to produce the mesoporous framework and ii) preparation of the monolithic with a pre-synthesized mesostructured silica material.

2. Experimental

Three monolithic silica structures were synthesized using tailoring methods and further modified through two impregnation and grafting to optimize each adsorbent properties. SBA-15 monoliths were prepared through a gel-casting approach, starting with a precursor aqueous solution containing acrylamide and N′-methylenebisacrylamide, and ammonium persulfate. Pre-synthesized SBA-15 powder was added to the previous solution and was vigorously stirred. The mixture was then molded and went through a gelation process, followed by systematic drying and calcination to ensure structural integrity and optimal porosity. Similarly, silica monoliths prepared by direct synthesis were obtained by a sol-gel process using two structure directing agents (Pluronic P-123 and Pluronic F-127), typical for mesostructured silica development. This procedure involved the combination of a pre-hydrolyzed silica precursor with the respective surfactant, allowing the mixture to undergo controlled evaporation to form a gel. The gel was then aged and calcined to remove organic components and stabilize the pore structure [3, 4].

To enhance their CO_2 adsorption capabilities, each monolith was functionalized with amino groups. Tetraethylenepentamine (TEPA) and Polyethylenimine (PEI) were used to impregnate the monoliths and to optimize surface chemistry for better CO_2 interaction. Conversely, the grafting method employed aminosilanes to chemically bind functional groups directly onto the monolithic structural framework, aiming to create a durable modification that enhances stability and adsorption capacity under a great variety of experimental conditions. The so-prepared functionalized monoliths were thoroughly characterized to determine their structural, textural and chemical properties as well as their CO_2 adsorption behavior. These evaluations provided a comprehensive overview of the adsorbents' performance, allowing further optimizations and adjustments in the synthesis and functionalization processes.

3. Results and Discussion

A preliminary study of the silica monoliths obtained from the different procedures was carried out. All the three samples (Mon-SBA-15, Mon-P123 and Mon-F127) could be prepared as monolithic morphology (Figure 1). According to the XRD and N_2 adsorption-desorption isotherms, they exhibit mesostructured internal porosity with small differences in their textural properties.

Figure 1 Monolith P-123 and Mon P-123/ TEPA (70%)

The comparative analysis of CO_2 adsorption of functionalized monolithic materials revealed that the use of different precursors as structure directing agent significantly affect to the final properties. As an example, monoliths obtained using Pluronic P-123 and functionalized by the impregnation method with TEPA (70%) exhibited high CO_2 uptake (190 mg/g), due to a very high nitrogen content (29.7 wt.%). These monoliths outperformed those made with Pluronic F-127, due to the surfactant effect on the polymer framework and functional group distribution (Table I). Regarding the comparison with TEPA impregnated monolithic materials that were prepared using SBA-15, it was found also an important uptake (177 mg/g) and better structural properties (surface area of 25 m^2/g).

Table I. Physico-chemical properties, nitrogen content and pure CO_2 adsorption properties (45 ºC, 1 bar) of amino-functionalized Monoliths

Sample	mg CO_2/g sample	SBET (m^2/g)	Vp (cm^3/g)	N content (wt.%)	mol CO_2/ mol N
Mon-P-123/ TEPA (70%)	190	12	0.03	29.7	0.20
Mon-SBA-15/ TEPA (70%)	177	25	0.05	20.1	0.28
Mon-F-127/ TEPA (70%)	169	45	0.10	19.1	0.28

On the other hand, monoliths grafted with amino-propyl and diethylenetriamine yielded very different results in CO_2 capture compared to the impregnated monoliths. As can be seen in the Table I, samples contained smaller amount of nitrogen (6.6-13.4 wt.%), with higher efficiency of amino groups, as expected for this type of amino-functionalized adsorbents although the adsorption capacity is smaller. In this case, the use of a previously SBA-15 silica to prepare monoliths (SBA-15/2DT) seems to be more stable, since maintained higher textural properties (surface area of 65 m^2/g and pore volume of 0.11 cm^3/g) although having lower adsorption capacities (94 mg/g).

4. Conclusions

This study demonstrated that monolithic silica materials that maintained their mesoporous internal structure can be obtained and used for CO_2 capture after functionalization. The effect of using different organic functionalizing agents, amount, and methods for organic incorporation on the final CO_2 adsorption performance was found to be similar while it is possible to achieve higher adsorption uptakes.

Acknowledgments
The authors acknowledge the financial support to the Agencia Estatal de Investigación (Ministerio de Ciencia e Innovación, Spain) through the Project TED2021-131144B-I0.

5. References

[1] C. H. Yu, C. H. Huang, and C. S. Tan, *Aerosol Air Qual. Res.*, 12 (5), (2012) pp. 745.
[2] W. Gao *et al.*, *Chem. Soc. Rev.*, 49, 23, (2020) pp. 8584.
[3] C. Zhou *et al.*, *Chem. Eng. J.*, 413, (2020) pp. 2021
[4] G. L. Drisko *et al.*, *Microporous Mesoporous Mater.*, 148 (1), (2012) pp. 137.

P27: Production of Activated Carbons from Technical Lignin for Arsenic and Cadmium simultaneous adsorption

B. F. M. L. Gomes [(1)], S. Vaz Júnior [(2)], L. V. A. Gurgel [(3)]

[(1)] Graduate Program in Environmental Engineering, School of Mines, Federal University of Ouro Preto, Campus Universitário Morro do Cruzeiro, Rua Nove, s/n, Bauxita, 35402-163 Ouro Preto, Minas Gerais, Brazil brener.gomes@aluno.ufop.edu.br

(2) Brazilian Agricultural Research Corporation (Embrapa), Parque Estação Biológica, s/n, Av. W3 Norte, Asa Norte, 70770-901 Brasília, Distrito Federal, Brazil silvio.vaz@embrapa.br

(3) Physical Organic Chemistry Group, Department of Chemistry, Institute of Exact and Biological Sciences, Federal University of Ouro Preto, Campus Universitário Morro do Cruzeiro, Rua Quatro, 786,Bauxita, 35402-136 Ouro Preto, Minas Gerais, Brazil legurgel@ufop.edu.br

1. Introduction – The Brazilian state of Minas Gerais is one of the territories most affected by water contamination with toxic species such as arsenic (As), cadmium (Cd), and lead (Pb), with high concentrations of arsenic already identified in open-pit mine waste [1], as well as in soils, waters, and in tissues of plants and fish [2-4]. The presence of these toxic substances in water at significant concentrationsis undesirable, requiring the use of appropriate treatment technologies for their removal from industrial effluents. Adsorption has been the most widely studied methodology for the removal of toxic pollutants due to its simplicity, low operating cost, and high efficiency compared to other existing methods.Furthermore, the efficiency of the adsorption process can be enhanced by choosing an adsorbent with suitable properties, i.e., an adsorbent that exhibits greater affinity for the species of interest in the water treatment. In this work, activated carbons (ACs) were synthesized under different conditions to assess theirpotential and versatility in the simultaneous adsorption of As(V) and Cd(II) in aqueous solutions.

2. Experimental

2.1. Synthesis of ACs – Technical lignin (TL) from a Brazilian second-generation ethanol plant was used asthe raw material. All reagents used (CSN_2H_4, $FeCl_3$, and KOH) showed analytical purity. For the synthesis of ACs, six different experimental conditions were established. In condition 1, TL was impregnated with athiourea solution (0.8 mol L^{-1}) for 3 hours, followed by pyrolysis at 800 ºC with a heating rate of 10 ºC min^{-1}under a flow of 150 mL min^{-1}, activation of the obtained carbon with KOH in a 1:1 ratio, and final impregnation with $FeCl_3$ solution (0.8 mol L^{-1}). In condition 2, after the initial impregnation with thiourea,the material was impregnated with $FeCl_3$ for 3 hours before pyrolysis and activation with KOH. Condition 3 involved impregnation with thiourea, pyrolysis, and subsequent impregnation with $FeCl_3$. In condition 4,TL underwent pyrolysis with KOH, followed by sequential impregnations with thiourea and $FeCl_3$. In condition 5, pyrolysis with KOH preceded impregnation with $FeCl_3$. Finally, in condition 6, TL was impregnated with thiourea and $FeCl_3$, followed by pyrolysis under the same mentioned conditions, except for the KOH activation. Each condition was carefully controlled to investigate synthesis variables and theirinfluence on the properties of activated carbons.

2.2. Adsorption experiments - In different flasks containing a bicomponent aqueous solution of As(V) andCd(II) at a concentration of 24 mg L^{-1}, 20 mg of the ACs obtained in the previous section were added and stirred for 24 hours. At the end of this time, the samples were properly filtered, and the final concentrationof the supernatant solution was analyzed using an ICP-OES.

3. Results and Discussion - In Table I, the adsorption capacity values for As(V) and Cd(II) of each obtained AC are shown. Based on the results (Table I), it was possible to observe that condition 2 exhibited the highest adsorption capacity for both species (As(V) and Cd(II)) simultaneously, indicating the bi-functionality of the material. The experimental arrangement of condition 2 appears to have favoured the incorporation of the N, S, and Fe elements, derived from the CH_4N_2S and $FeCl_3$ activation agents, into theinternal structure of the carbon when compared to the other conditions. These elements seem to have beenwell fixed to the surface and internal structure of the carbonaceous material, providing electrostatic affinity adsorption sites for As(V) and Cd(II), especially after KOH activation. The activation agent (KOH) seemsto play a fundamental role because, when comparing the results between conditions 2 and 6, which differedonly in the final activation step, absent in the latter condition. It is possible to note that the activation of thecarbon increased the adsorption capacity for As(V) and Cd(II) by approximately 385% and 3440%, respectively. The increase in adsorption performance by the material obtained in condition 2 suggests thatactivation promotes access to adsorption sites inside the carbon through micropores.

Table I. Adsorption capacity of ACs for As(V) e Cd(II).

Condition	*q* As(V) (mg g^{-1})	*q* Cd(II) (mg g^{-1})
1	10.79 ± 1.38	4.07 ± 0.58
2	95.88 ± 2.57	89.09 ± 2.89
3	3.22 ± 0.98	25.07 ± 0.75
4	28.77 ± 3.11	0.00 ± 0.00
5	9.99 ± 0.40	1.91 ± 0.33
6	24.91 ± 1.49	2.59 ± 0.93

Similar behavior was observed by Han et al. [5] when activating carbons with steam subsequent to lignin impregnation by $FeSO_4$. The authors observed that 78% of the iron is carbonized within the carbon structure and 22% on its surface. Thus, upon carbon activation, there was an increase in the Fe content available foradsorption because the Fe atoms previously inaccessible in the internal structure of the carbon became accessible through the porous structure of the activated carbon.

In addition to iron, N and S are also elements of affinity for toxic species, especially when available on thesurface of adsorbent materials in the form of $-NH_2$ and -SH functional groups [6]. The importance of the co-activation agent (CH_4N_2S) for the adsorption of As(V) and Cd(II) can be observed from the results obtained in conditions 4 and 5. In condition 4, N and S doping occurred after the thermal pyrolysis process, and possibly, such particles filled the pores of the carbon. In the subsequent impregnation step with iron, the Fe particles possibly adhered to the surface of the carbon, representing an obstacle to the nitrogenous and sulfonated groups. Thus, although As(V) and Cd(II) did not compete for the same active sites, the presence of As(V) likely promoted the inhibition of Cd(II) adsorption in this case. While in all other synthesis conditions the ACs obtained showed superior adsorption capacity for either As(V) or Cd(II), in the absence of CH_4N_2S as a co-activation agent (condition 5), AC exhibited low adsorption capacity for both species, suggesting that the presence of N and S on the AC surface is beneficial for the adsorption of As(V) and Cd(II) [6-8].

4. Conclusions - From the obtained results, it was possible to notice the relevance of the co-activation agents (CSN_2H_4 and $FeCl_3$) and activation (KOH) for increasing the adsorption capacity for As(V) and Cd(II) of the obtained carbons. Condition 2 proved to be the ideal experimental design for the synthesis of an AC with higher adsorption capacity for both species simultaneously. Furthermore, this AC demonstrates potential as an adsorbent material for arsenic and cadmium removal from water and industrial effluents throughout treatment systems. Also, the production of AC from TL with higher performance for toxic species removal may represent an excellent opportunity to promote the economic viability of biorefineries.

5. References

[1] H. F. D. Neto *et al.*, Environmental and human health risks of arsenic in gold mining areas in the eastern Amazon,, *Environmental Pollution*, vol. 265, p. 13, Oct 2020, Art no. 114969, doi: 10.1016/j.envpol.2020.114969.

[2] P. G. Costa *et al.*, Temporal and spatial variations in metals and arsenic contamination in water, sediment and biota of freshwater, marine and coastal environments after the Fundao dam failure, *Science of the Total Environment*, vol. 806, p. 23, Feb 2022, Art no. 151340, doi: 10.1016/j.scitotenv.2021.151340.

[3] C. E. T. Parente *et al.*, First year after the Brumadinho tailings' dam collapse: Spatial and seasonal variation of trace elements in sediments, fishes and macrophytes from the Paraopeba River, Brazil, *Environmental Research*, vol. 193, p. 10, Feb 2021, Art no. 110526, doi: 10.1016/j.envres.2020.110526.

[4] M. C. Teixeira, A. C. Santos, C. S. Fernandes, and J. C. Ng, Arsenic contamination assessment in Brazil - Past, present and future concerns: A historical and critical review, *Science of the Total Environment*, Review vol. 730, p. 21, Aug 2020, Art no. 138217, doi: 10.1016/j.scitotenv.2020.138217.

[5] T. Han, X. C. Lu, Y. J. Sun, J. C. Jiang, W. H. Yang, and P. G. Jönsson, Magnetic bio-activated carbon production from lignin via a streamlined process and its use in phosphate removal from aqueous solutions, *Science of the Total Environment*, vol. 708, p. 10, Mar 2020, Art no. 135069, doi: 10.1016/j.scitotenv.2019.135069.

[6] J. X. Liu, Z. L. Xu, and W. J. Zhang, Unraveling the role of Fe in As(III & V) removal by biochar via machine learning exploration, *Separation and Purification Technology*, vol. 311, p. 11, Apr 2023, Art no. 123245, doi: 10.1016/j.seppur.2023.123245.

[7] C. Saka, I. Tegin, K. Kahvecioglu, and O. Yavuz, Nitrogen- and oxygen-doped carbon particles produced from almond shells by hydrothermal method for efficient Pb(II) and Cd(II) adsorption, *Biomass Conversion and Biorefinery*, ; Early Access p. 14, 2023 Feb 2023, doi: 10.1007/s13399-023-03920-8.

[8] C. Saka, I. Tegin, and K. Kahvecioglu, Sulphur-doped carbon particles from almond shells as cheap adsorbent for efficient Cd(II) adsorption, *Diamond and Related Materials*, vol. 131, p. 10, Jan 2023, Art no. 109542, doi: 10.1016/j.diamond.2022.109542

P28: Adsorção contínua de losartana em leito poroso utilizando nanotubos de carbono funcionalizados por rota verde

H. P. de S. Costa [(1)], M. G. C. da Silva [(1)], M. G. A. Vieira [(1)]

[(1)] *Universidade Estadual de Campinas, Faculdade de Engenharia Química, Departamento de Desenvolvimento de Processos e Produtos*
helocst@gmail.com

1. Introdução - A contaminação de águas por compostos farmacêuticos é um problema crescente visto que os sistemas tradicionais de tratamento de água e efluentes não conseguem removê-los eficientemente. Esses compostos são amplamente utilizados e, consequentemente, liberados no meio ambiente e podem causar diversos efeitos nocivos devido à sua persistência e tendência à bioacumulação em organismos vivos [1]. Técnicas avançadas, como a adsorção com nanomateriais, mostram-se promissoras para a remoção desses poluentes. Nanotubos de carbono (NTCs), especialmente quando funcionalizados com nanopartículas metálicas, têm grande potencial como adsorventes eficazes [2]. Este estudo investiga a adsorção de Losartana, um dos anti-hipertensivos mais utilizados mundialmente, utilizando NTCs funcionalizados com nanopartículas de ferro por rota verde, empregando resíduos de casca de café como agente redutor. Para otimizar e compreender o processo visando possível aplicação industrial, o sistema contínuo em coluna porosa foi investigado via aplicação de modelos matemáticos e fenomenológicos.

2. Experimental - A solução sintética de losartana foi preparada utilizando o composto ativo do fármaco (>100%, Geolab, Brasil) e água ultrapura. Foram utilizados nanotubos de carbono de paredes múltiplas pré- funcionalizados com grupos OH e COOH (grau de funcionalização = ± 9%). A funcionalização com nanopartículas de Fe seguiu a metodologia de rota verde adaptada pelo grupo de pesquisa [3],[4]. O adsorvente foi previamente caracterizado por análises de MEV/EDS, FTIR, TGA e BET. Para os experimentos em leito-fixo os nanotubos funcionalizados foram suportados em areia inerte (Altura = 10 cm) e os experimentos foram realizados utilizando soluções com concentração inicial de 0,2 mmol/L e vazão de 0,2 mL/min foram bombeadas com auxílio de uma bomba peristáltica. A coleta dos pontos na saída do sistema foi realizada utilizando um coletor de frações automático, coletando alíquotas em intervalos regulares de tempo. As Equações de 1 a 5 foram utilizadas para calcular os parâmetros de eficiência do sistema, sendo eles: capacidade adsortiva até a ruptura (q_r), capacidade de adsorção na exaustão (q_e), comprimento da zona de transferência de massa (ZTM) e percentuais de remoção na ruptura ($\%R_r$) e na exaustão ($\%R_e$). Aos dados obtidos foram aplicados os modelos propostos por Yan et al. [5] e Dual Site Diffusion [6].

$$q_r = \frac{C_0 Q}{w}\int_0^{t_r}\left(1-\frac{C}{C_0}\right)dt \quad (1)$$

$$q_e = \frac{C_0 Q}{w}\int_0^{t_s}\left(1-\frac{C}{C_0}\right)dt \quad (2)$$

$$ZMT = \left(1-\frac{q_u}{q_s}\right)\cdot H_t \quad (3)$$

$$\%R_r = \frac{q_r m}{C_0 Q t_r} \quad (4)$$

$$\%R_e = \frac{q_e m}{C_0 Q t_e} \quad (5)$$

3. Resultados e Discussão - As caracterizações do material funcionalizado foram apresentadas em artigos publicados anteriormente [8],[9] pelo grupo de pesquisa. Os resultados de MEV indicaram que após a funcionalização com as nanopartículas metálicas, o NTC interagiu com os compostos polifenólicos das cascas de café, formando um material mais agregado. Através da análise EDS foi observada a presença de elementos Fe no material, comprovando a eficácia do processo de funcionalização. O FTIR apresentou bandas relacionadas à presença de anéis benzênicos (C=C) do NTC, além de ligações O-H e C-O, relacionadas aos grupos funcionais COOH e OH já existentes no material. Além disso, foram detectadas bandas relacionadas às ligações CH, formadas entre os nanotubos e as nanopartículas de ferro, comportamento esperado na metodologia da rota verde. A análise termogravimétrica demonstrou melhoria na estabilidade térmica do material após a funcionalização, o que deve ser diretamente associado à presença das nanopartículas metálicas em sua superfície. Os resultados de BET mostraram características mesoporosas dos NTCs, com aumento da área superficial e volume de poros após a funcionalização. A Figura 1 apresenta a curva de ruptura obtida para o processo de remoção de losartana em sistema de adsorção dinâmica. Enquanto a Tabela 1 apresenta os parâmetros de eficiência e de transferência de massa calculados.

Figura 1. Curva de ruptura obtida para a adsorção de losartana em sistema dinâmico de leito poroso.

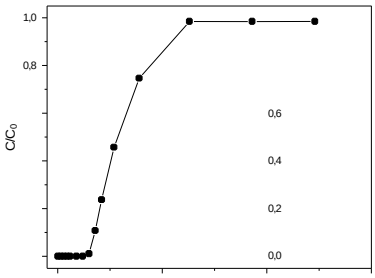

Tabela 1. Parâmetros de eficiência e de transferência de massa para a adsorção de losartana em NTC verde.

t_r (min)	t_e (min)	q_r (mmol.g^{-1})	q_e (mmol.g^{-1})	ZTM (cm)	%R_r	%R_e
161,99	630	0,065	0,131	5,00	99,05	50,94

Analisando os valores obtidos para tempo de ruptura (tr), momento até no qual a remoção do composto é superior a 95%, e tempo de exaustão (te), etapa de decaimento do desempenho da coluna (C/C0 = 1), nota-se que o sistema foi eficiente para a remoção de losartana. Além disso, a curva obtida se assemelha ao formato de uma função degrau, indicando que há menor resistência à transferência de massa. O valor de ZTM obtido condiz com o observado na literatura para sistemas dinâmicos de remoção de losartana. Entretanto a capacidade adsortiva no ponto de ruptura e de saturação obtidas no presente trabalho se mostram superiores ao reportado na literatura [5]. A Tabela 2 apresenta os resultados obtidos pelo ajuste dos modelos de Yan et al. (2001) e Dual SD (2020) aos dados da curva de ruptura.

Tabela 3. Parâmetros obtidos a partir do ajuste de modelos dinâmicos à curva de ruptura obtida.

Modelos	Parâmetros	LOS
Experimental	**q_e (mmol/g)**	**0,131**
Yan *et al.*	a_Y	4,197
	q_Y (mmol/g)	0,115
	R^2	0,996
	AICc	-150,24
DualSD	D_a	0,000986
	α	0,278
	$K_{S,1}$	0,000903
	$K_{S,2}$	1,48E-04
	$q_{e,pred}$ (mmol/g)	0,142
	R^2	0,999
	AICc	-165,83

Os modelos matemáticos apresentaram a tendência de subestimar os valores da capacidade adsortiva do sistema na etapa de exaustão. Essa tendência pode ser observada pelo ajusto do modelo de Yan e colaboradores. Apesar de ser menos representativo na etapa de saturação, devido ao longo tempo do processo (1230 min), esse modelo descreve bem os pontos iniciais da curva de ruptura. O modelo DualSD, por outro lado, apresentou um excelente ajuste aos dados experimentais. O melhor ajuste deste modelo indica que duas taxas de difusão influenciam as curvas de ruptura em momentos diferentes do processo de adsorção. Além disso, esse modelo também foi capaz de prever valores de capacidade adsortiva mais próximos ao obtido experimentalmente, sendo mais adequado para descrever o comportamento da remoção de losartana em sistema adsortivo dinâmico.

4. Conclusão – Os resultados obtidos mostram a remoção satisfatória de losartana em sistema contínuo utilizando leito-fixo de nanotubos de carbono funcionalizados com Fe por rota verde. Espera-se que tal resultado contribua para possíveis aplicações desse sistema em escala industrial, uma vez que estudos visando à remoção desse composto farmacêutico, especialmente em sistemas dinâmicos, ainda são escassos apesar do risco ambiental que apresentam. Além disso, o desenvolvimento de um material adsorvente utilizando uma metodologia alternativa e ambientalmente amigável também pode ser destacado.

5. Referências

[1] T. Rasheed et al., *Environ. Res.*,**184**, (2020) p. 109436.
[2] C. Jung et al., *J. Ind. Eng. Chem*., **27**, (2015) p. 1-11.
[3] J. Diel et al., *Chemosphere*, **283**, (2021) p. 131193.
[4] M. Spaolonzi et al., *J. Clean. Prod.*, **373**, (2022) p. 133961.
[5] G. Yan et al., *Bioresour. Technol.*, **78**(3), (2001) p. 243–249.
[6] J. de Andrade et al., *J. Mol. Liq.*, **58**, (2020) p. 113427.
[7] H. Costa et al., *J. Clean. Prod.*, **251**, (2024) p. 118733.
[8] H. Costa et al., *J. Water Process Eng.*, **58**, (2024) p. 104923

P29: Propane and Propylene separation with carbon dioxide at mild temperatures by gas-phase SMB in binderfree zeolite 13X

Rute Seabra [1,2], Rafael Dias [1,2], Maria J. Regufe [1,2], Ana M. Ribeiro [1,2], Alírio E.Rodrigues [1,2], Alexandre P. Ferreira [1,2]

[1] *LSRE-LCM - Laboratory of Separation and Reaction Engineering – Laboratory of Catalysis and Materials, Faculty of Engineering, University of Porto, Rua Dr. Roberto Frias, 4200-465 Porto, Portugal*
[2] *ALiCE - Associate Laboratory in Chemical Engineering, Faculty of Engineering, University of Porto, Rua Dr. Roberto Frias, 4200-465 Porto, Portugal*
ruteseabra@fe.up.pt

1. Introduction – Propylene is a versatile building block to manufacture commodities used in several industries worldwide, from pharmaceuticals and cosmetics to all kinds of plastics and textiles [1]. The annual propylene production was approximately 100 million tons worldwide in 2016 and has an expected growth rate of 3.6% by 2025 [2]. This light olefin is usually obtained by the steam cracking of naphtha, or alternatively, as a by-product of fluid catalytic cracking of gas oils in refineries. Different propane/propylene mixtures are obtained by the two processes, and to get the polymer-grade olefin (99.5–99.8%), a separation ought to be made [1].

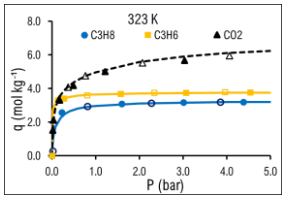

Figure 1. Adsorption equilibrium isotherms at 323 K.

The state-of-the-art process to obtain high-purity propylene is the cryogenic distillation process [3]. Due to the similar properties of propane and propylene, this separation is energy-intensive, estimated to equal the annual energy expenditure of Singapore [4]. Being a very cost-intensive route, alternative processes have been studied in the last decades, as the gas-phase simulated moving bed (Gas-SMB).

In this work, the adsorbent/desorbent pair binderfree zeolite 13X/carbon dioxide was tested in the propane/propylene separation, by the SMB technology, at mild temperatures, at 323 K, i.e. 100 K below the previous work. As far as the authors know, this is the first study with the application of binderfree zeolite 13X/carbon dioxide at such low temperatures in gas-phase SMB

Regarding the process simulation, the multicomponent adsorption equilibrium is usually predicted based on pure component measurements. Although this approach allows good results for ideal interactions between adsorbate-adsorbent, it fails when predicting non-ideal behaviors. In 1994, Huang *et. al.* experimentally determined the binary adsorption equilibrium of propane-propylene on 13X molecular sieves at 398, 323, and 343 K. The authors compared the experimental values with IAST. They concluded that at 398 K the prediction is accurate, but at 323 and 343 K, the relative differences increase significantly, exhibiting nonideal adsorption behavior that is not appropriately described with IAST [5]. In 2001, Siperstein and Myers, measured the adsorption equilibrium isotherms of the binary mixture carbon dioxide – propane at 295 K on zeolite 13X, having reported the highly nonideal behavior and existence of an azeotrope [6]. The present work also found non-ideal behavior in the system C_3H_8 – C_3H_6– CO_2 – 13X, and to predict multicomponent adsorption equilibrium RAST-aNRTL was used.

2. Experimental - The propane, propylene and carbon dioxide adsorption equilibrium isotherms were measured by a gravimetric method using a magnetic suspension microbalance (IsoSORP Rubotherm, Germany). Pure C_3H_8, C_3H_6, and CO_2 adsorption equilibrium measurements were performed at 323, 373, and 423 K for the hydrocarbons and 303, 323 and 423 K for CO_2. For the dynamic studies in the binderfree zeolite 13X granules, breakthrough experiments were performed in the lab-scale unit. The simulated moving bed cycles were carried out on the gas-phase SMB unit described in detail in a previous work of our group [1].

3. Results and Discussion - To apply RAST-NRTL, binary interaction parameters must be obtained from binary adsorption equilibria. The common method to obtain that multicomponent adsorption equilibrium data is simple breakthrough experiments [38]. The adsorbed phase molar fraction as a

function of the gas phase molar fraction predicted by the RAST-aNRTL model and the experimental points, are presented in **Figure 2**.

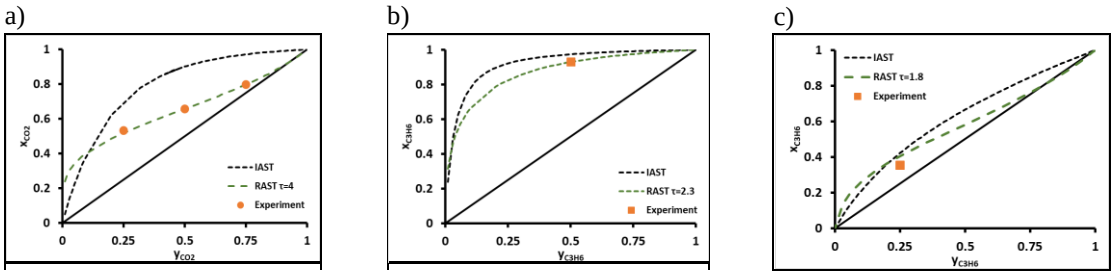

Figure 2 – Adsorbed phase molar fraction as a function of the gas phase molar fraction: Lines – Predictedby the RAST-aNRTL and IAST; Square – experimental point. a) CO_2 -1 C_3H_8 – 2; b) C_3H_6 – 1 C_3H_8 – 2;c) C_3H_6 – 1 CO_2 – 2

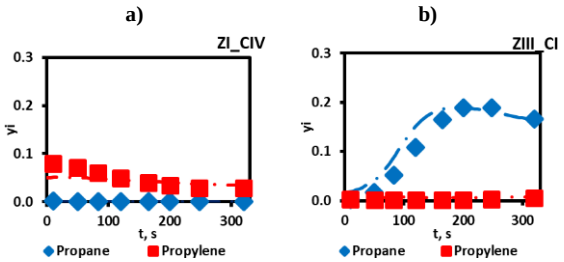

Figure 3- Experimental and simulated molar fractions profiles obtained at cyclic steady-state: a)composition of the Extract b) composition of the raffinate, as a function of step time.

A simulated moving bed experiment was performed, at 323 K and 3 bar, in the gas-SMB unit. For the feed of 0.5/0.5 propane/propylene (molar based) feed composition, a propylene purity of 98.8% was obtained, with a recovery above 98% and productivity of 39.3 kg $_{C3H6}$ h^{-1} m^{-3}. **Figure 3** presents the experimental molar fractions profiles obtained at cyclic steady-state for the extract and raffinate streams.

4. Conclusions - Adsorption equilibrium isotherms of propylene, propane, and carbon dioxide were measured gravimetrically in a temperature range from 323 K to 423 K, and pressure up to 5 bar. Breakthrough experiments were performed at 323 K and 3 bar. Binary adsorption equilibrium data was obtained from the dynamic experiments. Non-ideal adsorption behavior was observed for the adsorbate-adsorbent pairs, therefore the multicomponent adsorption equilibrium was predicted with the RAST – aNRTL model. A simulated moving bed experiment was performed in the gas-SMB unit. For the 0.5/0.5 propane/propylene (molar based) feed composition, a propylene purity of 98.8% was obtained, with a recovery above 98% and a productivity of 39.3 kg_{C3H6} h^{-1} m_{bed}^{-3}. This work experimentally demonstrated it is possible to produce high-purity propylene with a high recovery using binderfree zeolite 13X as adsorbent and carbon dioxide as desorbent, at mild temperature (323 K).

5. References

1. Martins, V.F.D., et al., *Gas-phase simulated moving bed: Propane/propylene separation on 13Xzeolite.* Journal of Chromatography A, 2015. **1423**: p. 136-148.
2. Nakayama, N. *Global Supply and Demand of Petrochemical Products Relied on LPG as Feedstock*. in *International LP Gas Seminar: Tokyo, Japan*. 2017.
3. Saha, D., et al., *Elucidating the mechanisms of Paraffin-Olefin separations using nanoporous adsorbents: An overview.* iScience, 2021. **24**(9): p. 103042.
4. Sholl, D.S. and R.P. Lively, *Seven chemical separations to change the world.* Nature, 2016. **532**(7600): p. 435-437.
5. Huang, Y.-H., et al., *Experimental determination of the binary equilibrium adsorption and desorption of propane-propylene mixtures on 13X molecular sieves by a differential sorption bedsystem and investigation of their equilibrium expressions.* Separations Technology, 1994. **4**(3): p. 156-166.
6. Siperstein, F.R. and A.L. Myers, *Mixed-gas adsorption.* AIChE journal, 2001. **47**(5): p. 1141-1159.

P30: Contributions of the caustic material to enhance the reactive adsorption ability for H2S removal at ambient conditions

M. Abid [(1)], J. Silvestre. Albero [(1)]

[(1)] *1Advanced Materials Lab, Inorganic Chemistry Department, University of Alicante, Spain*
Abidmeriem095@gmail.com
joaquin.silvestre@ua.es

1. Introduction

Problems associated with odor removal from the air have become controversial issues, given that H_2S detrimentally affects various aspects of human life including the environment, health, industrial infrastructure, and catalytic processes, its removal from various gas streams is of paramount importance. As the most promising alternative, room-temperature H_2S adsorption /catalytic oxidation on carbon-based materials attracted extensive attention owing to its low costs, high efficiency, and the possibility of sulfur recovery. activated carbon is one of the most suitable candidates, especially working at low temperatures. This is the result of its unique properties such as large surface area, and high pore volume as well as its rich surface chemistry [1]. this study focuses on ambient H_2S removal using a commercial activated carbon RGC-30 which was impregnated with caustic materials such as sodium hydroxide, it also highlights the importance of various factors governing and influencing the performance (e.g. relative humidity) of the mentioned purpose. The introduction of NaOH not only promoted the dissociation of H_2S but also enhanced the desulfurization process. This study presents the effective application of RGC-30 as a support for NaOH for fine desulfurization at room temperature which resulted in an excellent hydrogen sulfide removal performance of 797 mg/g.

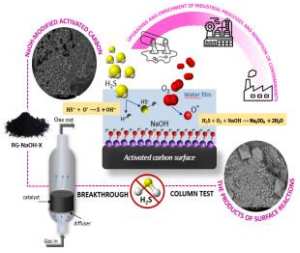

Image 1. schematic illustration of the H_2S oxidation process over RG-NaOH-X.

2. Experimental

The adsorbents were prepared by wetness impregnation method as describe in the **Image 2**.
The synthesized samples have been characterized by different techniques, such as N_2 adsorption measurements at -196 ºC, FE-SEM, TG, and XRD.

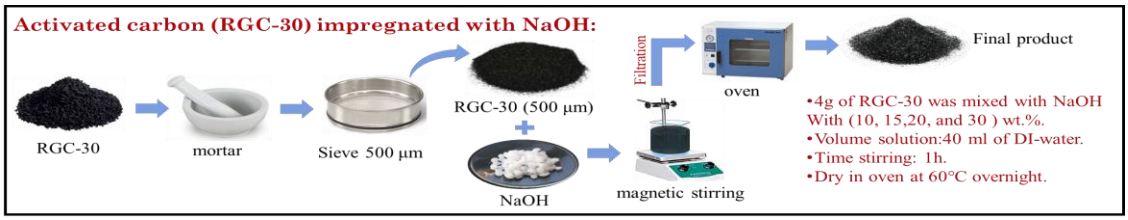

Image 2. Schematic illustartion of the preparation method of the RG-NaOH-X adsorbents.

3. Results and Discussion -

The performance data and the adsorption activity of virgin and modified carbons are presented concerning the times at which emissions of hydrogen sulfide were detected in the column outlet and the H_2S breakthrough capacity. **Image 3**. shows the breakthrough curves of impregnated carbon materials. Both H_2S removal capacity and the time breakthrough remarkably increased with the increase of NaOH loading on the surface of carbon support and all the adsorbents were able to adsorb hydrogen sulfide and exhibit good activity even at ambient conditions.

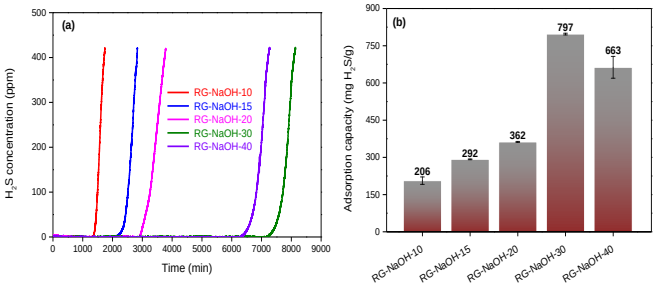

Image 3: The breakthrough curves (a) and H_2S removal capacity (b) of the prepared adsorbents.

It was noted that the sample with 30wt.% NaOH content has the highest hydrogen sulfide removal capacity of 797 mg/g, where the reduced H2S uptake ability of RG-NaOH-40 is caused by introducing a high

concentration of NaOH that significantly decreases the surface area and pore volume of the support, which leads to reduces in H2S performance. An excess of the caustic material likely results in pore blocking. This clearly demonstrates that there is a threshold in the amount of NaOH introduced to the surface of the carbon matrix.

Relative humidity (RH) is one of the key factors leading to enhanced H_2S removal under ambient temperature. In fact, to assess the effect of moisture content on H_2S capture, four breakthrough experiments were performed for the sample impregnated with 30% NaOH content at different relative humidity values of 40%, 50%, 60%, and 70%. **Image 4.** shows the H_2S breakthrough curves and the adsorption capacities of RG-NaOH-30 adsorbent under different RH. As expected, it was found that the presence of moisture in the gas stream significantly affected the H_2S adsorption capability of our adsorbent. As indicated elsewhere, water is a very important factor in the discontinuous desulfurization process [2]. By increasing the relative humidity from 40 % to 60 %, the breakthrough time, and hydrogen sulfide capacity dramatically increased. in contrast, catalytic performance decreases rapidly at RH values of 70%. suggesting that high moisture can lead to a decrease in H_2S removal capacity since the thick water film deposited on the surface of the solid may block the pores, preventing H_2S to diffuse through the sorbent and access the active site.

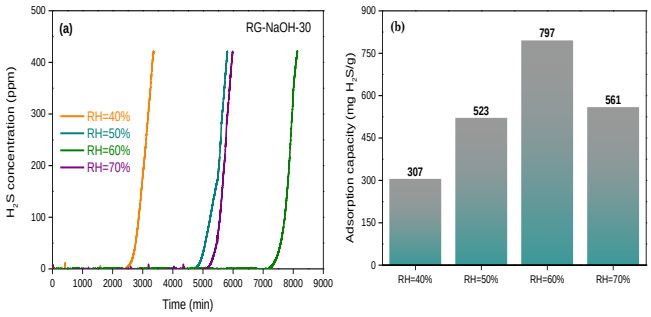

Image 4. The breakthrough curves (a) and H_2S removal capacity (b) of the prepared adsorbents under various relative humidity (RH %).

4. Conclusions

- The results presented in this paper show the importance of catalytic centers on the surface of adsorbents in the process of H_2S removal from the gas stream in the presence of moisture.
- Carbonaceous adsorbents can act as efficient media for air desulfurization provided that sufficient conditions for hydrogen sulfide oxidation exist. These conditions include a basic local pH, well-dispersed active sites able to enhance H_2S oxidation, and pore space where oxidation products can be stored.
- Impregnation with NaOH as the main agent makes the AC become an efficient adsorbent for H_2S adsorption. where the adsorbent with 30%wt. has the highest H_2S adsorption capacity of 797 mg/g.
- The impregnation with NaOH results in a high concentration of hydrosulfide ion (HS^-) and enhances the oxidation of H_2S. the reduced hydrogen sulfide uptake can be a result of the formation of sulfuric acid, where, the sulfuric acid suppresses H_2S dissociation and leads to the rapid deactivation of the AC.
- In the case of our adsorbents, the impregnated NaOH provides a basic environment and avoids its deactivation until the pores are almost completely saturated.
- The challenge is finding an optimum combination of the crucial surface features leading to efficient, cost-effective air desulfurization Further, improvement in using the different types of AC as a support could be made in order to examine the versatility of this strategy.

5. References

[1] T. J. Bandosz, Journal of Colloid and Interface Science **246**, (2002) p. 1–20.
[2] R. Sitthikhankaew et al, Fuel Processing Technology **124** (2014) p 249–257.

P31: Synthesis and evaluation of laccase-modified biochar for the removal of anti-inflammatory drug diclofenac from aqueous systems

H. F. Rocha[(1)], A. Almeida[(1)], M. Pereira[(2)], A. Peleja[(1)], G. Pereira[(1)], D.L.D. Lima [(3)], V. Calisto[(1)]

[(1)] Department of Chemistry and CESAM, University of Aveiro, 3810-193, Aveiro, Portugal
hugofmr@ua.pt
[(2)] Department of Chemistry, University of Aveiro, 3810-193, Aveiro, Portugal
[(3)] H&TRC – Health & Technology Research Center, Coimbra Health School, Polytechnic University of Coimbra, Rua 5 de Outubro, S. Martinho do Bispo, 3054-854 Coimbra, Portugal
aaalmeida@ua.pt; marta.pereira01@ua.pt; catarina.malpique@ua.pt; goreti.pereira@ua.pt; diana.lima@estesc.ipc.pt; vania.calisto@ua.pt

1. Introduction – Conventional wastewater treatment plants are not effective in removing pharmaceutical compounds, leading to their accumulation in the aquatic environment. Consequently, enhancing wastewater treatment processes is crucial to mitigate the introduction of these contaminants into the environment. Numerous advanced wastewater treatment methods have been evaluated for this purpose, including adsorption and enzymatic degradation. Although adsorption using carbon materials is quite effective, the challenges associated with regeneration and reutilization cycles remain a significant drawback. In this context, functionalizing the adsorbent surface with enzymes presents a promising strategy to extend the lifetime of these materials. Hence, this study aims to investigate the combination of adsorption and enzyme- mediated degradation of pharmaceuticals, specifically focusing on the immobilization of biocatalysts in biochar, as a viable advanced treatment for the removal of microcontaminants from water.

2. Experimental – A waste-based biochar was produced from spent-brewery grains (SBG) through microwave pyrolysis at 800 ºC for 20 min. The resulting biochar was subsequently functionalized with commercial laccase, an oxidoreductase enzyme, via physical immobilization. The composites produced were assessed for immobilization efficiency, enzyme activity and enzymatic stability with temperature andstorage time.

The adsorption and degradation performance of the composite was tested for the removal of the anti-inflammatory pharmaceutical diclofenac (DCF) from aqueous solutions with a concentration of 5 mg/L, atcontrolled pH levels of 5 and 7, and a temperature of 40 ºC, under batch conditions with stirring at 350 rpmfor 24 h. In the described adsorption-degradation experiments, the remaining concentration of DCF in the aqueous phase was quantified by capillary electrophoresis with UV detection, allowing to determine the removal percentage of DCF for each evaluated condition. The results obtained were compared with the removal efficiency of non-functionalized biochar and biochar functionalized with inactive enzyme, to delineate the contributions to the overall DCF removal efficiency.

3. Results and Discussion – The quantification of the enzyme in the leachate of the immobilization solution revealed that immobilization was achieved and was stable, as consecutive washings of the composite did not result in the release of the enzyme to the washing solution. Also, immobilized laccase maintained enzymatic activity after the immobilization; yet, the enzymatic activity decreased over the weeks that followed the production of the material.

Batch removal tests were performed using 500 mg/L of composite material (synthesised using a suspensionof biochar in a solution with 5 mg/mL of laccase) with a DCF solution of 5 mg/L in acetate buffer, at pH 5and pH 7. Despite the optimal working pH of laccase being slightly acidic (pH 5) it was also possible to achieve some degree of enzymatic degradation at higher pH (pH 7) indicating that this enzyme has potentialto be applied in pH conditions relevant for urban wastewater. The comparison of the performance of the enzyme-modified biochar with the non-functionalized biochar reveals that adsorption is still the predominant removal mechanism at the tested timescale.

4. Conclusions – Physical immobilization of laccase onto the surface of a waste-based biochar was successfully achieved with a simple procedure and with the enzyme maintaining enzymatic activity in the composite material. Adsorption is the dominant process in the overall removal of DCF with the produced composite. Yet, to establish more solid conclusions, reutilization cycles need to be assessed to understand if the enzyme maintains its activity after the saturation of the material´s adsorption sites.

Acknowledgments
This work was developed within the project SYNERGY (2022.02028.PTDC), supported by national funds (OE), through FCT/MCTES. The authors also acknowledge financial support to CESAM by FCT/MCTES(UIDP/50017/2020+UIDB/50017/2020+ LA/P/0094/2020), through national funds. Diana Lima also acknowledges financial support to H&TRC by FCT/MCTES (UIDP/05608/2020 (https://doi.org/10.54499/UIDP/05608/2020) and UIDB/05608/2020 (https://doi.org/10.54499/UIDB/05608/2020)).

P32: Aging of chabazite on natural gas dehydration by TSA

P. A. S. Moura [(1)], E. Vilarrasa-García [(1)], M. Bastos-Neto [(1)], E. Rodríguez-Castellón [(2)], D. C. S. Azevedo [(1)]

[(1)] Grupo de Pesquisa em Separações por Adsorção, Federal University of Ceara – 60440-900, Brazil
[(2)] Departamento de Química Inorgánica, Facultad de Ciencias, University of Malaga – 29071, Spain
mbn@ufc.br

1. Introduction – The aging of molecular sieves is a critical issue in the dehydration of natural gas (NG) [1]. Chabazite (CHA), a zeolite with high water adsorption capacity, is commonly used in this process. However, its long-term performance in pre-salt NG processing significantly deteriorates due to aging effects. To better understand the aging phenomenon and the associated loss of adsorption capacity, a chabazite sample with a Si/Al ratio of approximately 2 in its sodium form was subjected to conditions analogous to those in the pre-salt NG dehydration process.

2. Experimental – To simulate the conditions of a real TSA process for NG dehydration and assess the impacts on material aging, various factors were investigated, including exposure to heavier hydrocarbons (n-heptane), concentrations of CO_2 and CH_4, and high temperatures throughout the procedure. The procedure is described in the literature [2]. The adsorption capacities of N_2, CO_2 and H_2O were measured at various intervals throughout the simulated aging cycles to evaluate the modifications experienced by the pristine CHA sample. N_2 and CO_2 isotherms were measured with the aid of an Autosorb iQ3 (Quantachrome) and H_2O isotherms were measured in a IGA-002 (Hiden Isochema).

3. Results and Discussion – Although the aging of chabazite resulted in similar XRD patterns, the reflection peaks showed varying magnitudes, decreasing over the aging period, which in turn affected the material's crystallinity (Figure 1). The main reflection peaks are located in the 2θ range from 20° to 32° (20.4, 22.9, 24.7, 25.8 and 30.4°) [3]. The crystallinity of the aged material decreased by approximately 67%, showing a continued decline with longer aging periods. However, the degradation levels off after 45 days of the aging procedure, with the most pronounced deterioration occurring within the first 30 days.

The N_2 isotherms at 77 K for the pristine CHA sample (Figure 2) presented a type I behavior according to the IUPAC classification [4], which is typical for microporous solids. The measured adsorbed amounts agree well with literature data for CHA zeolite [5]. The N_2 adsorption isotherms for all aged samples, regardless of the aging duration, show a considerable decrease in uptake compared to the pristine sample.

Carbon dioxide was also used to evaluate the adsorption properties throughout the aging process, because CO_2 can diffuse more easily in small micropores at 273 K compared to N_2 at 77 K. Figure 3 shows the CO_2 isotherms at 273 K for the analyzed samples, indicating a progressive decrease in uptake, which suggests that aging leads to pore obstruction. The pristine sample has a maximum adsorption capacity of 110.7 $cm^3\ g^{-1}$, while the most severely aged sample retains less than 30% of this capacity. The micropore volumes of the samples, as estimated by the DR method [6], corroborate with this observation.

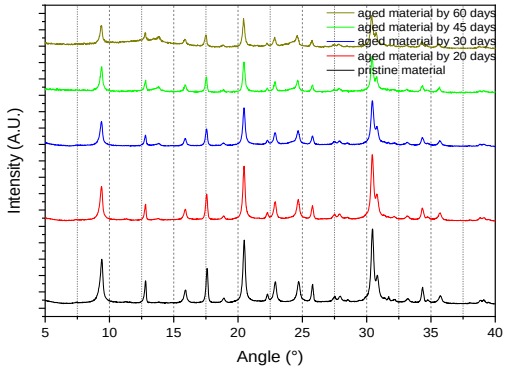

Figure 1. XRD patterns.

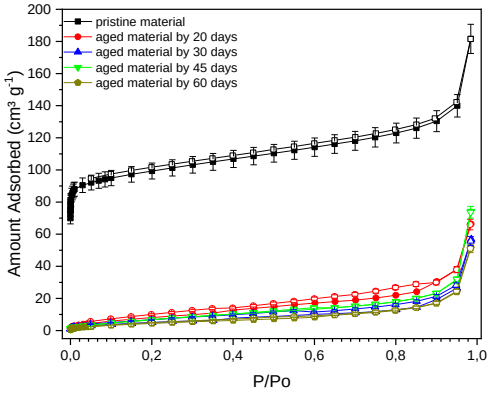

Figure 2. N_2 isotherms at 77 K.

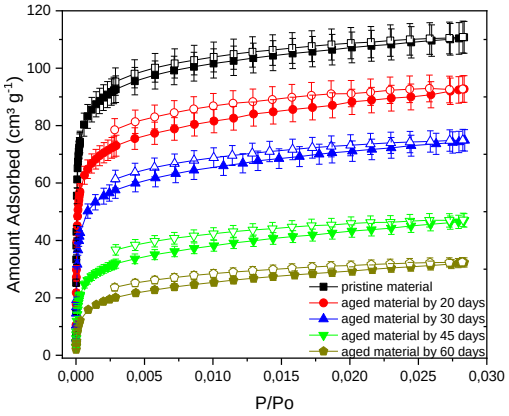

Figure 3. CO_2 isotherms at 273 K.

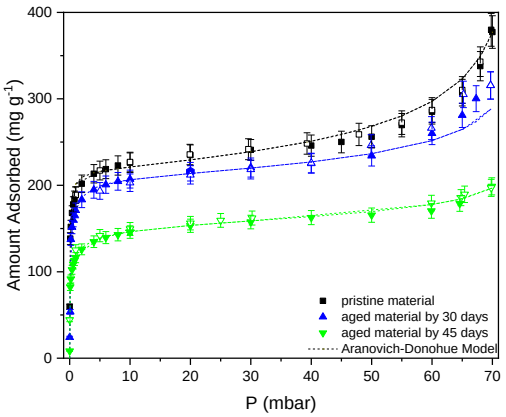

Figure 4. $H_2O_{(v)}$ isotherms at 313 K.

The water vapor isotherms at 313 K (Figure 4) also show that the adsorption capacities of the aged zeolites are lower than that of the pristine sample. However, the difference in uptake is significantly more modest compared to the CO_2 adsorption data. All isotherms have a steep rise in the low-pressure range (up to 5 mbar), indicating the existence of strong adsorbate-adsorbent interactions, which are retained throughout the aging process. In the pressure range of 5 to 40 mbar, all isotherms reach a plateau and the aging process results in a water adsorption capacity loss of about 35%. Some strong adsorption sites appear to be preserved despite the aging, as evidenced by the CO_2 isotherms and further confirmed by the water isotherms in the low-pressure range, although the overall capacity decreases. The analysis of the textural properties and CHN data (Table I) corroborate the presented findings, indicating that carbon deposition in aged samples is proportional to the aging time and reduces the capacity of the molecular sieve.

Table 1. Effects of the aging on textural properties and carbon content of chabazite samples

sample	S_{BET} ($m^2\ g^{-1}$)	V_{mic} ($cm^3\ g^{-1}$)	%C
pristine CHA	308.0	110.7	< 0.3
aged CHA (60 days)	19.0	32.3	3.1

4. Conclusions - The longer the aging time is, the greater the observed degradation degree in the studied properties of chabazite. The applied aging methodology effectively demonstrated the impact of heavy hydrocarbons at high temperatures on chabazite and its water adsorption properties. The aging process deteriorated the textural characteristics, which appeared to be directly correlated with carbon deposition in the pores.

5. References

[1] B. O. Nascimento *et al.*, "Water adsorption in fresh and thermally aged zeolites: equilibrium and kinetics," *Adsorption*, Aug. 2021, doi: 10.1007/s10450-021-00331-x.

[2] P. A. S. Moura *et al.*, "Water adsorption and hydrothermal stability of CHA zeolites with different Si/Al ratios and compensating cations," *Catal Today*, 2021, doi: 10.1016/j.cattod.2021.11.042.

[3] J. Cejka *et al.*, "IZA - Chabazite Synthesis," 1985.

[4] M. Thommes *et al.*, "Physisorption of gases, with special reference to the evaluation of surface area and pore size distribution (IUPAC Technical Report)," *Pure and Applied Chemistry*, vol. 87, no. 9–10, pp. 1051–1069, Jan. 2015, doi: 10.1515/pac-2014-1117.

[5] F. N. Ridha, Y. Yang, and P. A. Webley, "Adsorption characteristics of a fully exchanged potassium chabazite zeolite prepared from decomposition of zeolite Y," *Microporous and Mesoporous Materials*, vol. 117, no. 1–2, pp. 497–507, 2009, doi: 10.1016/j.micromeso.2008.07.034.

[6] G. Rouquerol, F., Rouquerol, J., Sing, K., Llewellyn, P., Maurin, *Adsorption by powders and porous solids.*, Academic P., vol. 11, no. 3. San Diego, 2014. doi: 10.1002/vipr.19990110317.

P33: Simulated Moving Bed Cascade for the Separation of Dihydroxyacetone from Glycerol Catalytic Oxidation Products

Pedro M. Walgode [(1)], Rui P. V. Faria [(2)], Alírio E. Rodrigues [(3)]

[(1) (2)(3)]*LSRE-LCM - ALiCE, Faculdade de Engenharia, Universidade do Porto, Rua Dr. Roberto Frias, 4200-465 Porto, Portugal*
[(1)]*up201200744@edu.fe.up.pt*
[(2)]*ruifaria@fe.up.pt* [(3)]*arodrig@fe.up.pt*

1. Introduction

Glycerol (GLY), the main reaction by-product of the biodiesel industry, can be valorized through various established pathways such as catalytic oxidation, yielding high-added-value products, including dihydroxyacetone (DHA), which has major applications in the cosmetics industry. While numerous studies have explored DHA production by GLY catalytic oxidation in the liquid phase [1], there exists a gap in the literature concerning DHA purification.

The cosmetics industry demands DHA of at least 97% purity; therefore, it must be separated from unreacted GLY and reaction by-products: oxalic acid (OXA), tartronic acid (TTA), glyceric acid (GCA), and glycolic acid (GCO). For that, a separation process by adsorption was developed. Adsorption isotherms of GLY and its oxidation products were determined at 293 K using a commercial polystyrene-divinylbenzene ion-exchange resin functionalized with sulfonic groups, the Dowex® 50WX-2 resin in H^+ form and a 5mM H_2SO_4 aqueous solution as eluent. All species showed a linear adsorption isotherm, with DHA and GLY being the most retained species, except OXA, the least retained compound, whose adsorption data was better described by a Freundlich isotherm. Adsorption data of GLY and DHA at 293 K using the Dowex® 50WX-2 resin in Ca^{2+} form and water as eluent, and the data was well described by a linear adsorption isotherm, with DHA being again the most retained compound [2].

Due to the low separation selectivity of DHA from GLY in the resin in H^+ form, (α = 1.04), compared with the Ca^{2+} form (α = 1.28), a DHA purification process on a cascade of two Simulated Moving Bed (SMB) units is herein proposed. Initially, DHA will be separated from the organic acids on an SMB packed with the resin in H^+ form (SMB-H^+), being collected in the extract stream together with a fraction of the GLY. This stream will be fed to a second SMB packed with the resin in Ca^{2+} form (SMB-Ca^{2+}) to separate DHA from GLY. This process was implemented on the gPROMS model builder V7.0.7 (PSE, UK) and validated experimentally on the lab-scale FlexSMB-LSRE® SMB unit with six fixed-bed columns (10x2 cm, 1-2-2-1 configuration), considering the solution from the aerobic oxidation of a 1 M GLY aqueous solution with a commercial catalyst, Bi-doped Pt nanoparticles supported in activated carbon, in a semi-batch reactor [2].

2. Experimental

The columns were packed with resin and characterized via pulse injections of a tracer into the columns pre-equilibrated in the eluent. A fixed-bed column model assuming an axially dispersed plug flow model to describe the fluid flow and linear driving force for the mass transfer between the liquid and the solid, isothermal operation, homogeneous spherical particles with uniform size, constant fluid velocity, bed porosity, and bed length, and no bed radial gradients was implemented in gPROMS model builder software. The model was validated using data from single and multi-component breakthrough experiments [2]. This model was extended to the SMB process, accounting for the FlexSMB-LSRE® unit specifics such as tubes, dead volumes, column filters, manifolds, and time switch delays, described elsewhere [3].

For each SMB, the regeneration region $\gamma_I^*, \gamma_{IV}^*$ was obtained by applying a safety factor of 15% to the γ_j^* (liquid and solid flow rate ratio in each SMB section) given by the equilibrium theory. The separation region was delineated by running the FlexSMB-LSRE® model for different $\gamma_{II}^*, \gamma_{III}^*$ values, considering a minimum extract purity and DHA recovery in the extract stream.

The solution with the composition: 1.2 g_{OXA} L^{-1}, 12.9 g_{TTA} L^{-1}, 8.2 g_{GCA} L^{-1}, 6.9 g_{GCO} L^{-1}, 22.0 g_{GLY} L^{-1}, and 29.8 g_{DHA} L^{-1} was fed to the SMB-H^+ and 5mM H_2SO_4 aqueous solution as used as eluent. The flow rate of the inlet and outlet streams was monitored at every SMB cycle. The composition of the raffinate and extract streams was quantified by HPLC, and upon stabilization of the species' average concentration (<5% variation during five successive cycles), cyclic steady state (CSS) conditions were reached. At this point, samples were collected at 25%, 50%, and 75% of the t^* to obtain internal concentration profiles. The extract stream of the SMB-H^+ was fed to the SMB-Ca^{2+} to separate DHA from GLY, using water as the eluent.

3. Results and Discussion

The columns showed an average porosity of 0.37 and an average Peclet number of 600. To design the separation in the SMB-H^+, a minimum DHA recovery in the extract of 85% and an extract purity on a GLY-

free basis of 97% were defined. The operation point γ_I^* = 2.88, γ_{II}^* = 2.44, γ_{III}^* = 2.47, γ_{IV}^* = 1.41 and a t^* of 1.5 min were defined. The unit reached CSS conditions after 30 cycles (**Figure 3** right). The internal concentration profiles at CSS were represented in **Figure 3** left).

DHA recovery in the extract stream was 87.0% and the extract purity on GLY free basis was 96.8. The species' average concentration in the extract stream was 1.82 g L^{-1} of DHA and 0.58 g L^{-1} of GLY, and the main contaminant was GCO (0.06 g L^{-1}, 2.3%), see **Figure 3** right.

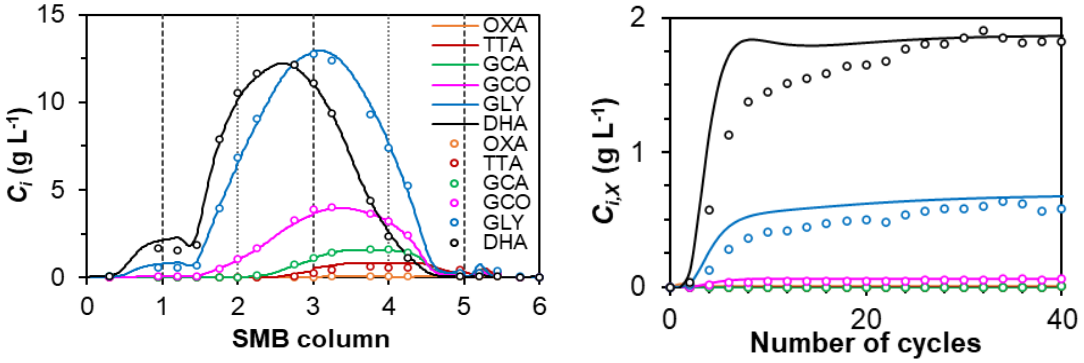

Figure 3. SMB-H^+ internal concentration profiles at CSS conditions (**Left)** and species' average concentration in the extract stream **(Right)**

The extract stream obtained from the SMB-H^+ was fed to the SMB-Ca^{2+}. A minimum DHA recovery in the extract stream of 90% and an extract purity of 97% were considered for the separation region. The operation point γ_I^* = 3.31, γ_{II}^* = 2.59, γ_{III}^* = 2.81, γ_{IV}^* = 2.07 and a t^* of 2 min were defined. CSS conditions were achieved after 30 cycles (see **Figure 4** right) and the internal concentration profiles at CSS were represented in **Figure 4** left. with a DHA recovery in the extract stream of 89.0% and an extract purity of 98.6% and the species average concentration in the extract stream was 0.50 g L^{-1} of DHA and 0.01 g L^{-1} of GLY.

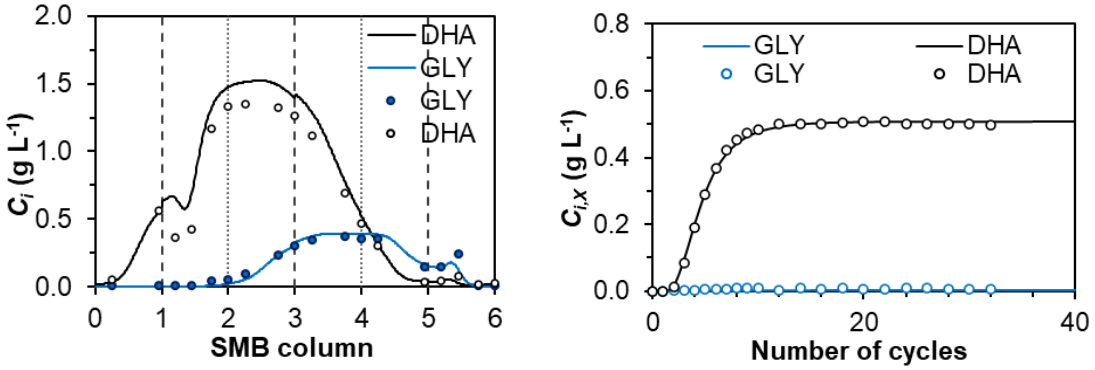

Figure 4. SMB-Ca^{2+} internal concentration profiles at CSS conditions (**Left)** and species' average concentration in the extract stream **(Right)**

The model fitted well both the internal concentration profiles and the species' concentration in the outlet streams of both SMB experiments. The two-SMB cascade produced DHA with 98.6% of purity, and the cascade showed a global productivity of 21.7 kg_{DHA} (m^3_{ads} day)$^{-1}$ and an eluent consumption of 5.7 m^3_{ads} kg_{DHA}^{-1}.

4. Conclusions

The purification of DHA from GLY oxidation products was successfully achieved on the lab-scale FlexSMB-LSRE® SMB unit, highlighting the potential of SMB technology for future industrial applications. A detailed SMB model was validated using fixed-bed column and SMB experimental data.

5. References

[1] B. Katryniok *et al.*, *Green Chem.*, vol. 13, no. 8, pp. 1960-1979, 2011.
[2] P. M. Walgode *et al.*, *Industrial & Engineering Chemistry Research*, 2021.
[3] A. Rodrigues, Elsevier, Ed. 1st Edition ed. Amsterdam: Butterworth-Heinemann, 2015, p. 304.

RIA 43
XLIII Reunião Ibérica de Adsorção
Porto, Portugal
1-4 September 2024

P34: Impact of moisture on CO_2 adsorption equilibrium on zeolite 13X

R. G. Santiago [(1)], E. Vilarrasa-García [(1)], A. E. B. Torres [(1)], D. C. S. de Azevedo [(1)], C.L. Cavalcante Jr [(1)], M. Bastos-Neto [(1)]

[(1)] *Grupo de Pesquisa em Separações por Adsorção, Federal University of Ceara – 60440-900, Brazil.*
mbn@ufc.br

1. Introduction – CO_2 capture from the flue gas of power plants is extensively studied as a means to mitigate atmospheric CO_2 emissions [1]. Adsorption on porous solids using cyclic operation of multiple beds is an attractive technology for this purpose. Hence, the choice of material is a key factor in the process performance [2].
Mathematical models of column dynamics for adsorption-based CO_2 capture are useful for determining performance parameters and optimizing process conditions. Developing these models and efficiently operating the process requires an understanding of the adsorption equilibrium between the gas components and the adsorbent material. Given the presence of moisture in flue gases, it is crucial to understand how water interferes with the equilibrium and competes for adsorption sites of the adsorbent material.
The main objective of this work is to investigate the effects of water vapor on the adsorption of CO_2 on zeolite 13 X considering a post-combustion scenario for different moisture concentrations.

2. Experimental - The studied adsorbent material was a commercial zeolite 13X in pellet form (~2 mm), acquired from Shanghai Hengye Chemical Industry Co. (Shanghai, China). CO_2 adsorption isotherms were measured using a magnetic suspension balance from Rubotherm (Bochum, Germany) and water vapor adsorption isotherms were evaluated using an IGA-002 (Hiden Isochema Ltd., United Kingdom).
The isotherms were obtained at different temperatures (50, 70 and 90 °C) for water vapor and for CO_2 with different amounts of water previously loaded on the adsorbent sample. The Sips equation [3] was modified to fit the CO_2 adsorption equilibrium data after preloading a certain amount of water on the adsorbents to predict the impact of moisture on CO_2 uptake by the zeolite. The modification involves correlating the constant *K*, which is related to the adsorbent-adsorbate affinity for the CO_2 isotherm under dry conditions, with the *K* values for CO_2 isotherms at various water loadings, according to the following equations.

$$q_i = \frac{q_m (K_i P_i)^t}{[1+(K_i P_i)^t]} \quad (1)$$

$$K_i = K_{dry}(1-f)^{a_i} \quad (2)$$

$$a_i = a_0 - a_1 f \quad (3)$$

where f is a parameter defined as the ratio of the initial water loading to the water concentration at the saturation point of the material; a_o and a_1 are fitting parameters with no physical meaning; and q_{mi} and t are the limiting adsorbed concentration, and the heterogeneity factor, respectively.

3. Results and Discussion – To evaluate the influence of the presence of water on the CO_2 adsorption capacity of the zeolite 13X, the material was initially loaded with a water concentration lower than its saturation point, allowing the adsorbent to subsequently adsorb CO_2. The CO_2 adsorption isotherm was measured and compared to the pure CO_2 isotherm (Figure 1). The experiments were conducted at 50, 70 and 90 °C in view of the post combustion scenario. The pure water vapor adsorption isotherms for 13X zeolite are plotted in Figure 2. The shape of the isotherms may be considered as Type I of the IUPAC classification, which is typical for microporous adsorbents [4].
The decrease in CO_2 uptake observed in Figure 1, when compared to the pure-component adsorption isotherm at 50 °C, indicates that H_2O preferentially occupies the adsorption sites, reducing the availability of those sites for CO_2 adsorption as water loading increases. The deterioration in CO_2 adsorption performance is observed at all temperatures in the presence of moisture (not shown).

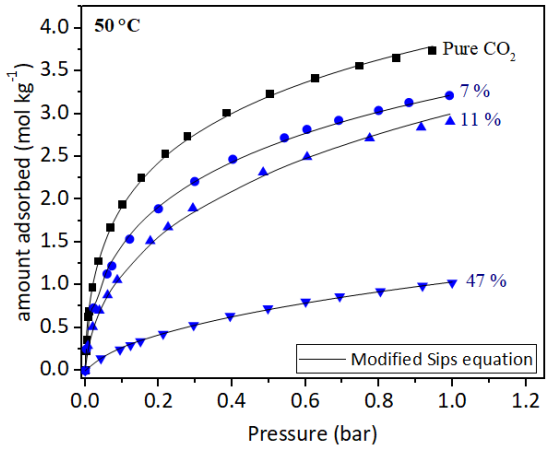

Figure 1. CO_2 adsorption isotherms at 50 °C for 13X with different preloaded water vapor concentrations. The percentages (%) represent the *f* factor, *i.e.*, the ratio of the initial water loading to the water concentration at the saturation point of the material (n_s), Continuous line for Sips modified equation.

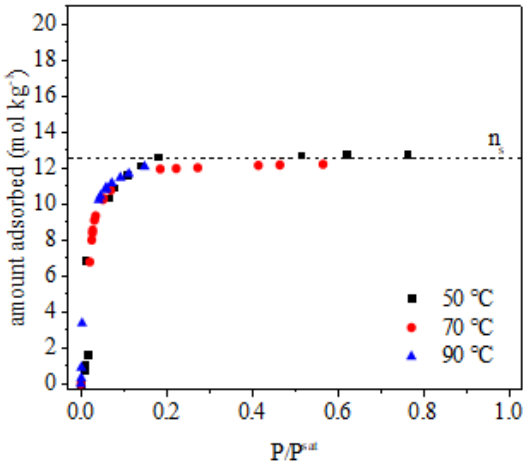

Figure 2. H_2O adsorption isotherms at 50, 70 and 90 °C for 13X zeolite.

4. Conclusions – The presence of moisture in flue gas can severely impact CO_2 adsorption and should not be disregarded when analyzing equilibrium. Water can strongly adsorb on zeolite sites, preventing CO_2 from adsorbing and thus decreasing the material's capacity. This effect can be further intensified in long-term cyclic processes, as water tends to accumulate on the surface, necessitating careful and costly regeneration. The proposed modification of the Sips equation showed good agreement with experimental data and might be an interesting tool to predict the CO_2 uptake at any load of preadsorbed water.

5. References

[1] Wang X and Song C, Carbon Capture From Flue Gas and the Atmosphere: A Perspective. *Frontiers in Energy Research.*, **8**, 2020. doi: 10.3389/fenrg.2020.560849

[2] Morales-Ospino et al. Assessment of CO2 desorption from 13X zeolite for a prospective TSA process. Adsorption, **26**, 2020. doi:10.1007/s10450-019-00192-5

[3] Sips, Robert. On the structure of a catalyst surface. II. The Journal of Chemical Physics, [*s. l.*], 1024–1026, **8(8)**, 1950. doi: 10.1063/1.1747848

[4] Thommes, M., Kaneko, K., Neimark, A.V., Olivier, J.P., Rodriguez-Reinoso, F., Rouquerol, J., Sing, K.S.W.: Physisorption of gases, with special reference to the evaluation of surface area and pore size distribution (IUPAC Technical Report). Pure and Applied Chemistry **87(9-10)**, 2015. doi:10.1515/pac-2014-1117

RIA43
XLIII Reunião Ibérica de Adsorção
Porto, Portugal
1-4 September 2024

P35: Engineering Carbon Nanotubes for Water Remediation

C. Abreu-Jaureguí [(1)], A. Sepúlveda-Escribano [(1)], J. Silvestre-Albero[(1)]

[(1)] *Laboratorio de Materiales Avanzados, Departamento de Química Inorgánica, Instituto Universitario de Materiales, Universidad de Alicante, Spain*
coset.abreu@ua.es

1. Introduction

Advanced oxidation processes driven by natural sunlight are the key to the next generation of water treatment technologies. Photocatalysis using semiconductor materials constitutes a promising approach to degrade organic contaminants in wastewater with minimal generation of secondary pollutants. In this scenario, carbon-based nanomaterials have emerged as promising modifying co-catalysts. The incorporation of the carbon structure manages to enhance the photocatalytic activity under visible light and the overall yield of the reaction. More specifically, single-walled carbon nanotubes (SWCNTs) have been anticipated as superior modifiers that can enhance the photocatalytic performance of flagship catalysts like TiO_2 for practical applications. The improved performance is attributed to the textural features associated with this type of nanostructure and the newly developed heterojunction. More specifically, the resulting high-surface composite is rather interesting for surface chemistry modulation. Heteroatom doping is an effective and more environmentally sustainable approach to modulate the presence of specific superficial groups. Various nonmetals, such as sulphur (S), fluorine (F), boron (B), nitrogen (N), phosphorus (P), and oxygen (O), can potentiate either the reduction or the oxidation of the pollutant. In particular, nitrogen, phosphorous, and oxygen have shown great capability to serve as mediators and enhance the electronic properties of the composite, facilitating the creation of active sites within the catalyst's surface. In this context, our investigation focused on modulating carbon nanotubes with oxygen, nitrogen, or phosphorous functional groups, enriching TiO_2 (P25) through meticulously tailored chemical pathways.

2. Experimental.

This investigation is centred on evaluating the effect of the SWCNT's superficial chemistry modification with oxygen, nitrogen, or phosphorous to use as modifying agents of commercial titanium dioxide and further testing in Rhodamine B photodegradation. The heteroatom doping went through different chemical paths adapted to each element. Oxygen functionalization involved overnight drying of the SWCNT, oxidizing it with a 12 N H_2O_2 solution (precursor) for 48 hours, followed by filtering, washing until it no longer presents oxidizing characteristics, drying, and finally grinding the oxidized SWCNT. Nitrogen doping consisted of 3 main steps: physical mixture with Melamine (precursor), thermal treatment under N_2 flow, and ultimately, grinding the NSWCNT. Regarding the phosphorous introduction, the procedure included a physical mixture of Phytic Acid (precursor) and SWCNT followed by a pre-polymerization step and a thermal treatment under N_2 flow with the eventual grinding of the obtained PSWCNT. Once the SWCNTs were functionalized, a wet impregnation approach with methanol and 90% commercial TiO_2 (P25) secured the composite formation.

A wide variety of techniques were applied to get insights into the textural and chemical properties of the synthesized photocatalysts, i.e. N_2 adsorption, TEM, TGA/MS, XPS, XRD, RAMAN, UPS, and DR. The degradation of RhB was evaluated in a home-built photoreactor equipped with 24 lamps (18 W/lamp) and five integrated stirring positions. Four different irradiation environments were considered for this study: (i) visible light, (ii) ultraviolet light, (iii) simulated solar irradiation (4% UV), and (iv) dark conditions (as a reference). Regarding reaction specifications, 25 mg of the photocatalyst was dispersed in 50 mL of the corresponding RhB solution (40 ppm unless otherwise stated). Additionally, a cycling experiment was designed to evaluate the durability of the most promising catalysts (TiO_2/OSWCNT; TiO_2/PSWCNT) against the reference material TiO_2 (P25). Finally, a desorption experiment was conducted on the recovered catalyst using a Methanol:Water solution, followed by an N_2 adsorption experiment to restore the textural properties. In all cases, the amount of RhB in solution was analysed using an HPLC equipment Shimadzu SCL-40 Nexera Series coupled to an Inductively Coupled Plasma Mass Spectrometer from Agilent. The m/z signals detected helped to identify the reaction photodegradation mechanism.

3. Results and Discussion

Upon wet impregnation of the carbon nanostructures, an improved adsorption performance was observed compared to pristine TiO_2 (90 wt.%), reaching up to 120 m^2/g of specific surface area (BET). The composites exhibited a similar crystallographic structure, independently of the functionalization incorporated, in accordance with the characteristic crystallographic pattern of commercial TiO_2. TEM microscopy confirmed the successful dispersion of TiO_2 nanocrystals in the SWCNT support, anticipating the success in the development of proper oxide-carbon heterojunctions at the interface. XPS and Raman

suggested significant interface phenomena, especially in the TiO_2/OSWCNT and TiO_2/PSWCNT samples. These observations might confirm the presence of strong oxide-carbon interactions at the formed heterojunction, which are associated with significant changes in the electronic density. Additionally, TGA-MS (under N_2 atmosphere) helped to elucidate the catalyst composition in terms of surface groups by evaluating its thermal decomposition.

In photocatalytic terms, the most promising photocatalysts for Rhodamine B (RhB) photodegradation were TiO_2/OSWCNT and TiO_2/PSWCNT, with nearly 100% conversion in less than 2 h under simulated solar irradiation and at 40 ppm. These outstanding findings are likely linked to the fundamental physicochemical adjustments at the newly formed heterojunction structure, along with the composite materials' dual capability to simultaneously adsorb and degrade RhB. Cyclability tests confirm the long-term (5 cycles) enhanced performance of the composites (i.e., TiO_2/OSWCNT; TiO_2/PSWCNT) due to the combined adsorption/degradation ability. Additionally, the regeneration of the SWCNT textural properties was achieved almost immediately by subjecting the recovered catalysts to a final desorption step. Overall, this research provides a thorough comparison of the most used heteroatoms for photocatalytic doping. Simultaneously, it highlights the importance of understanding the complex nature of carbon materials in photocatalytic applications and presents an efficient mechanism for restoring the original textural characteristics of the catalysts.

Figure 1. Highlights of the catalyst's physicochemical characterization and photocatalytic performance: a) TEM microscopy images of SWCNT and b) TiO_2/OSWCNT; c) XPS spectra of composites and pristine TiO_2 at Ti2p core level; d) CO evolution in TGA-MS profiles of the composites under N_2 atmosphere; e) Photocatalytic performance of all tested catalysts with no irradiation/simulated solar irradiation; f) Desorption experiment on recovered TiO_2/OSWCNT catalyst.

4. Conclusions

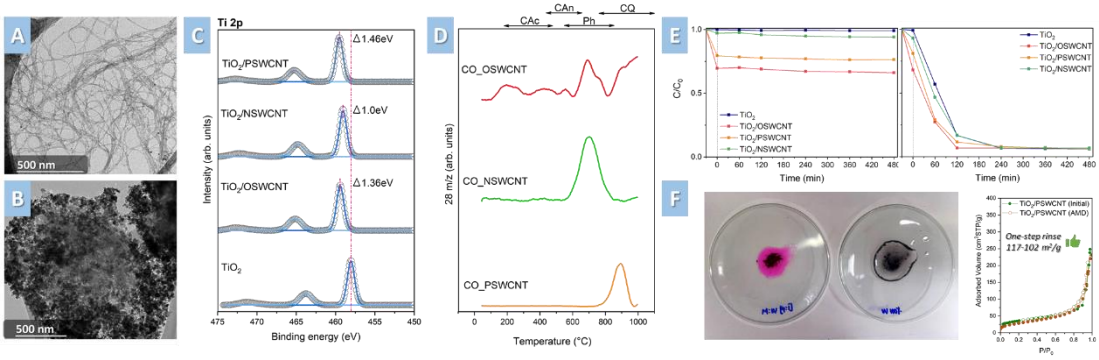

Figure 1. Highlights of the catalyst's physicochemical characterization and photocatalytic performance: a) TEM microscopy images of SWCNT and b) TiO_2/OSWCNT; c) XPS spectra of composites and pristine TiO_2 at Ti2p core level; d) CO evolution in TGA-MS profiles of the composites under N_2 atmosphere; e) Photocatalytic performance of all tested catalysts with no irradiation/simulated solar irradiation; f) Desorption experiment on recovered TiO_2/OSWCNT catalyst.

This study demonstrates that tailoring the electronic structure of carbon nanotubes significantly enhances their photocatalytic activity for pollutant degradation. The engineered nanotubes exhibit a dual capability, effectively adsorbing and breaking down pollutants like Rhodamine B under simulated sunlight. Moreover, these nanotubes can be efficiently regenerated for multiple cycles using a simple methanol-water solution, highlighting the sustainability of this approach.

Acknowledgements: The authors acknowledge financial support from MCIN (PID2019-108453GB-C21), MCIN/AEI/10.13039/501100011033, and EU "Next Generation/PRTR" (PCI2020-111968/ERANET-M/3D-Photocat).

5. References

[1] P. Ayala, R. Arenal, M. Rümmeli, A. Rubio, T. Pichler, Carbon. 2010, 48, 575–586.
[2] T. J. Bandosz, in Carbon Materials for Catalysis, John Wiley & Sons, Ltd. 2008, pp. 45–92.
[3] J. L. Faria, W. Wang, in Carbon Materials for Catalysis, John Wiley & Sons, Ltd. 2008, pp. 481–506.

P36: Separation of Branched Alkanes Feeds by a Synergistic Action of Zeolite 5A and Metal-Organic Framework MIL-160(Al)

A. Henrique [1,2], P. F. Brântuas [1,2], L. F. A. S. Zafanelli [1,2,3,4], E. Aly [1,2,5], A. E. Rodrigues [3,4], G. Maurin [6], C. Serre [7], J. A. C. Silva [1,2]

[1] *Centro de Investigação de Montanha (CIMO), Instituto Politécnico de Bragança, 5300-253 Bragança, Portugal.*

[2] *Laboratório Associado para a Sustentabilidade e Tecnologia em Regiões de Montanha (SUSTEC), Instituto Politécnico de Bragança, 5300-253 Bragança, Portugal.*

adriano_henrique@ipb.pt

[3] *LSRE-LCM – Laboratory of Separation and Reaction Engineering – Laboratory of Catalysis and Materials, Faculty of Engineering, University of Porto, 4200-465 Porto, Portugal*

[4] *Alice – Associate Laboratory in Chemical Engineering, Faculty of Engineering, University of Porto, 4200-465 Porto, Portugal*

[5] *Aveiro Institute of Materials, CICECO, Department of Chemical Engineering, University of Aveiro, Campus Universitario de Santiago, 3810-193 Aveiro, Portugal*

[6] *ICGM – Univ. Montpellier, CNRS, ENSCM 34293 Montpellier, France*

[7] *Institut des Matériaux Poreux de Paris, ESPCI Paris, Ecole Normale Supérieure, CNRS, PSL University, 75000, Paris, France*

pedro.brantuas@umontpellier.fr; zafanelli@ipb.pt; ezzeldin@ipb.pt; arodrig@fe.up.pt; guilaume.maurin1@umontpellier.fr; christian.serre@espci.psl.eu; jsilva@ipb.pt

1. Introduction – The total isomerisation process (TIP) developed by the universal oil products (UOP) for upgrading the octane rating of light hydrocarbon fractions, especially mixed feedstocks containing pentane (C5) and hexane (C6) isomers, is among the first and most successful adsorption processes applied in the industry [1]. Typically, the light naphtha, characterised by a low research octane number (RON, ≈70), undergoes an incomplete catalytic isomerisation that generates an effluent containing unconverted linear paraffins, mostly n-pentane (nC5; RON 61.7) and n-hexane (nC6; RON 30), mixed with their respective branched isomers, i.e., isopentane (iC5; RON 93.5), 2-methylpentane (2MP; RON 74.5), 3-methylpentane (3MP; RON 75.5), 2,2-dimethylbutane (22DMB; RON 94), and 2,3-dimethylbutane (23DMB; RON 105). After that, the output of the isomerisation reactor is fed into an adsorber packed with zeolite (LTA type) that behaves as a molecular sieve, adsorbing only the linear paraffins (which are then recycled to the catalytic reactor for further processing). This results in a final branched isomerate product with an average RON ≈87–90. However, with the actual TIP process, the monobranched hexanes 2MP and 3MP represent up to 30% of the final product composition, which is detrimental to the octane improvement of gasoline for RON values higher than 90 [1]. Accordingly, this work shows a novel adsorptive separation process, based on the synergistic action of the zeolite 5A and the MIL-160(Al) metal-organic framework (MOF), to efficiently fractionate C5/C6 alkane isomers according to classes of high RON (HRON – 22DMB, 23DMB, and iC5) and low RON (LRON – nC5, nC6, 2MP, and 3MP) compounds.

2. Experimental - The robust, easily scalable with a predicted low-cost industrial production, and bio-derived Al-dicarboxylate MIL-160(Al) MOF is in the shaped form of beads (inorganic binder (silica sol solution 10 wt.%)) with a diameter ranging from 2.0 to 3.35 mm [2]. The zeolite 5A, with the commercial name *KÖSTROLITH® 5A BFK*, is in the shape of binder-free beads with a 1.2 to 2.0 mm diameter.

3. Results and Discussion - The core of the proposed technology is based on the outstanding property of MIL-160(Al) to separate C6 mixtures according to the degree of branching [3]. Image 1a shows the breakthrough curves measured on a fixed bed of MIL-160(Al) at 423 K and a total alkane pressure of 50.0 kPa. The HRON di-branched 22DMB and 23DMB elute first, and they are completely separated from the LRON mono-branched 3MP and 2MP, while the LRON linear nC6 elutes much later. The shape of the breakthrough curves for each isomer indicates that this excellent mixture segregation in MIL-160(Al) is primarily based on thermodynamically equilibrium competition due to their steepness and overshoot phenomenon. Moreover, the calculated ideal productivity for an accumulated RON of 92 is 1.02 $mol.dm^{-3}$, which outperforms all current adsorbent materials.

As a next step, MIL-160(Al) was associated with the commercially available zeolite 5A to design a single adsorption bed to feed all the C5/C6 alkane isomers. The corresponding experimental breakthrough data collected for the mixed bed of 70 wt% MIL-160(Al) and 30 wt% zeolite 5A demonstrated the desired discrimination between fractions of HRON (22DMB, 23DMB, and iC5) and LRON (nC6, nC5, 2MP, and 3MP) compounds (Image 1b). An ideal sorption hierarchy: nC6 ≫ nC5 ≫ 2MP ≈ 3MP ⋙ 23DMB > iC5 ≈ 22DMB is associated with an excellent productivity of 1.14 $mol.dm^{-3}$ for an accumulated RON of 92.

Further, a preliminary cyclic experiment was conducted to see how these results could be relevant to industrial applications. Image 1c displays the cyclic steady state (CSS) of a simplified 2-step PSA experiment, i.e., (i) pressurisation and adsorption with feed and (ii) vacuum countercurrent depressurisation with inert (helium) purge (desorption). At step I (adsorption), the mass front of the HRON 22DMB and iC5 has completely left the column, while the mass transfer front of 23DMB is concentrated at the edge of the column. The other LRON molecules mostly remain inside the bed, with only a small concentration leaving the column at the end of the adsorption step I. Also, the real-time RON history shows that the product mixture has an average RON higher than 92.

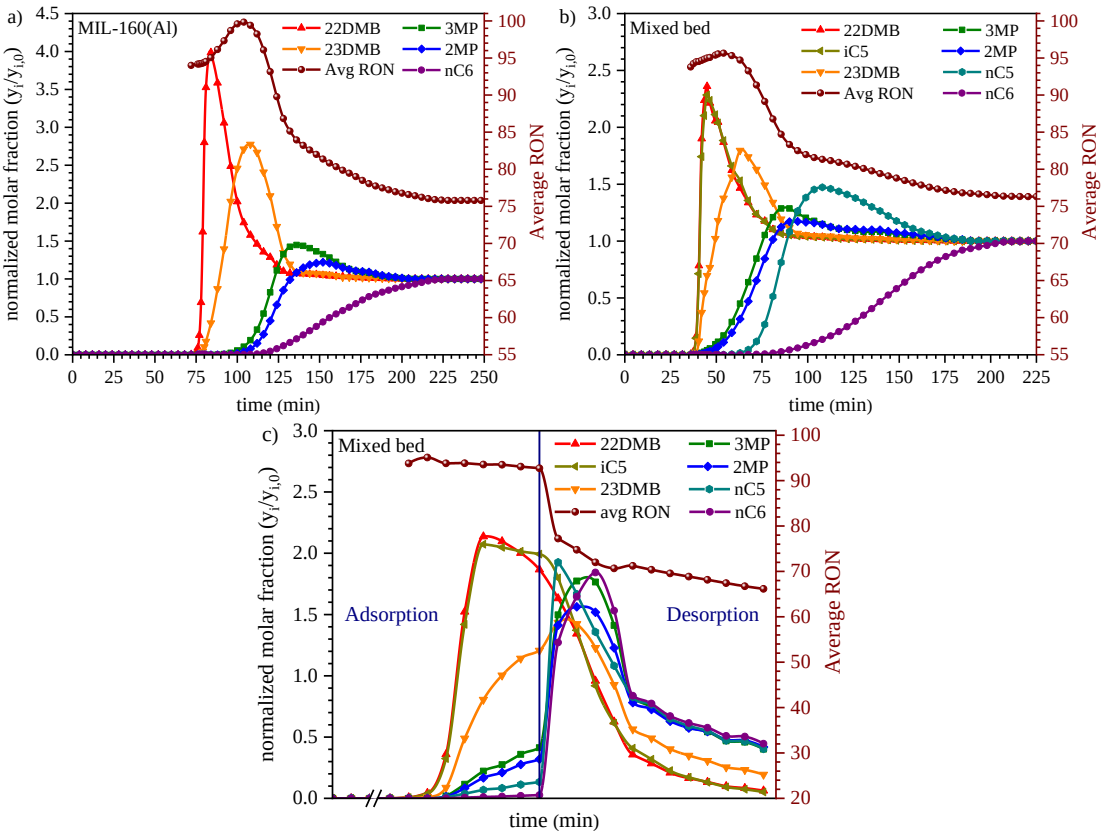

Image I. **a)** Breakthrough data for an equimolar C6 mixture fed in MIL-160(Al). **b)** Breakthrough data for an equimolar C5/C6 mixture fed in the mixed-bed adsorber of 70 wt% MIL-160(Al) and 30 wt% zeolite 5A. **c)** Cyclic steady-state data of a PSA experiment with an equimolar C5/C6 mixture fed in the mixed-bed adsorber of 70 wt% MIL-160(Al) and 30 wt% zeolite 5A.

4. Conclusions - This work reveals that the synergistic action of a mixed bed made by the MOF MIL-160(Al) together with the commercially available zeolite 5A led to the complete fractionation of light naphtha (RON < 70) into an HRON hydrocarbon final product (RON > 92) under relevant industrial operating conditions. As MIL- 160(Al) can be produced at a multi-kilogram scale, while zeolite 5A is already commercially available, this gives the building block for further pilot-scale testing before envisaging industrial commercialisation.

5. References

[1] R. A. Meyers, "Handbook of petroleum refining processes"; McGraw-Hill Education, New York, 2004.
[2] M. I. Severino, E. Gkaniatsou, F. Nouar, M. L. Pinto, C. Serre, *Faraday Discuss.*, **231**, 2021,231, p. 326-341.
[3] P. F. Brantuas, A. Henrique, M. Wahiduzzaman, A. Von Wedelstedt, T. Maity, A. Rodrigues, F. Nouar, U.-H. Lee, K. H. Cho, G. Maurin, J. A. C. Silva, C. Serre, *Adv. Sci.*, **9**(22), 2022, 2201494.

P37: Fluoroquinolone antibiotic-ciprofloxacin- removal by adsorption on a lab-synthesized carbon xerogel from several environmentally relevant wastewater matrices

A.B. Hernández-Abreu, S. Álvarez-Torrellas*, V.I. Águeda, J.A. Delgado, J. Garcia

Catalysis and Separation Processes Group (CyPS), Chemical Engineering and Materials Department, Faculty of Chemistry, Complutense University, Avda. Complutense s/n, 28040 Madrid, Spain.
satorrellas@ucm.es

1. Introduction – Antibiotics are one of the most widely used types of drugs today, instrumental in combating many infectious diseases in humans and animals. As a consequence of an incomplete metabolization and direct elimination of unused antibiotic residues, these compounds have been frequently detected in the aquatic environment [1]. The aim of this work is to evaluate the removal of the antibiotic ciprofloxacin (CPX) onto a synthesized carbon xerogel (RFX) from wastewater in a stirred tank.

2. Experimental - The xerogel (RFX) was synthesized following the procedure described by Job et al [2]. The polycondensation reaction of resorcinol (R) and formaldehyde (F) was carried out in aqueous medium under the following conditions: molar ratio R: F=0.5; pH=5.8 (adjusted with NaOH solutions). The dried solid was pyrolyzed under inert atmosphere (N_2 = 100 cm^3-min^{-1}) according to the following heating schedule: (1) 2°C-min^{-1} to 150°C and an isothermal stage of 15 min; (2) 5°C-min^{-1} to 400°C, for 60 min; (3) 5°C-min^{-1} to 800°C for 120 min; (4) slow cooling to room temperature. Finally, the material was ground and sieved between 250-500 μm.

3. Results and Discussion - The N_2 adsorption-desorption isotherm of RFX corresponds to I-IV Type, suggesting that the material has a high degree of microporosity with a large contribution of macroporosity on its porous structure. As can be seen in Figure 1a, regarding to the influence of pH on CPX adsorption, the adsorption capacity shows a high decreasing at pH = 10. This can be explained by the occurrence of repulsive electrostatic forces between the negatively charged surface of the adsorbent and the adsorbate, which is in its anionic form. On the other hand, in the studies using different aqueous matrices (Figure 1b), a slight decrease in the adsorption capacity of CPX was observed in the experiments with river water and WWTP effluent, while in the adsorption experiments using hospital effluent the decrease was much more drastic (23%).

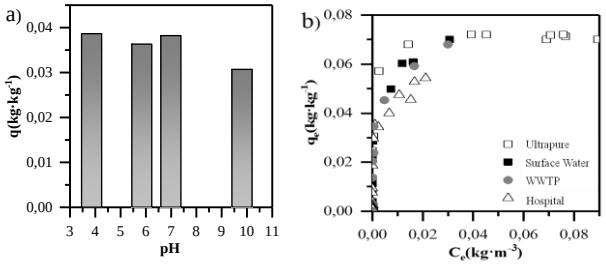

Figure 1. CPX batch adsorption experiments: **(a)** influence of the pH solution, and **(b)** influence of the aqueous matrix on CPX adsorption capacity.

4. Conclusions - In this work, the removal of CPX by adsorption onto a carbon xerogel (RFX) from wastewater has been studied. The batch adsorption experiments revealed that pH and organic matter content of the effluent are factors that significantly affect the removal of CPX and can lead to a decrease in the adsorption capacity.

Acknowledgments. This work has been supported by the MICINN PID2020-116478RB-I00 project.

5. References

[1] D.H. He, J. Li, W.H. Yu, et al., *Sci. Total Environ.* ***926*** (2024) 171806.
[2] N. Job, R. Pirard, J. Marien, J.P. Pirard, *Carbon*, ***42*** (2004) p. 619.

P38: Magnesium-modified cork biochars for the removal of phosphate from water

Ariana M.A. Pintor[1,2], Nuno F. R. Sousa[1,2], O. Salomé G.P. Soares[1,2], M. Fernando R. Pereira[1,2] and Cidália M.S. Botelho[1,2]

[1] LSRE-LCM - Laboratory of Separation and Reaction Engineering – Laboratory of Catalysis and Materials, Faculty of Engineering, University of Porto,Rua Dr. Roberto Frias, 4200-465 Porto, Portugal
[2] ALiCE - Associate Laboratory in Chemical Engineering, Faculty of Engineering, University of Porto, Rua Dr. Roberto Frias, 4200-465 Porto, Portugal
fpereira@fe.up.pt
ampintor@fe.up.pt
up201504455@edu.fe.up.pt
salome.soares@fe.up.pt
cbotelho@fe.up.pt

1. Introduction

Phosphorus is an essential nutrient for life, namely the growth of plants, and is, therefore, widely used in the fertilisation of crops. Conventional fertilisers are usually extracted from phosphate rock, a finite, non-renewable resource predicted to be exhausted in the next 50 to 100 years [1]. For this reason, better phosphorus management, given a circular economy, is being sought. At the same time, phosphorus leaching into water bodies through wastewater disposal or agricultural runoff causes eutrophication, a grave environmental problem that endangers the health of aquatic life [2]. Therefore, the sequestration of excess phosphorus from water and wastewater is increasingly regarded as an alternative path for recycling this nutrient. Adsorption is an easy-to-operate methodology that is adequate for treating low phosphate concentrations. It also concentrates phosphorus on a solid surface, from where it can be recovered.

Biochar is a black carbon material produced by pyrolysis of lignocellulosic biomass in the absence of oxygen. It presents numerous advantages as a soil amendment, leading to the sequestration of carbon, which contributes to climate change mitigation [3]. Cork, the bark of Quercus suber L., is a good candidate for biochar production, given its unique cellular structure and chemical composition [4]. Biochar can be engineered to improve its contents in specific components and enhance its adsorption capacity, promoted by the larger surface area than its precursors [5]. When modified with calcium or magnesium, they have shown high capacities for phosphate adsorption [4].

In this study, magnesium-modified biochars using cork were produced to uptake phosphorus from water.

Image 1. A black carbon material produced through the pyrolysis of cork

2. Experimental

Cork granulates were transformed into magnesium-modified biochars by chemical modification and thermal treatment. A design of experiments was used to study several production factors, such as impregnation time, pyrolysis temperature, heating ramp, duration, and gas (N_2 or CO_2), to optimise biochar production for maximum phosphate uptake from water. Phosphorus (P) adsorption tests were carried out in a solution using Na_2HPO_4. After the contact time, the solution was filtered for subsequent phosphorus (P) and magnesium (Mg) analysis.

3. Results and Discussion

The materials were found to have an excellent uptake capacity for phosphorus compared to similar biochars previously reported. A best-performing biochar was selected, also considering the environmental aspects of production, such as energy expenditure and pyrolysis yield. Figure 1 shows the isotherm profile of the best-performing material. The P adsorption is favoured at lower pH.

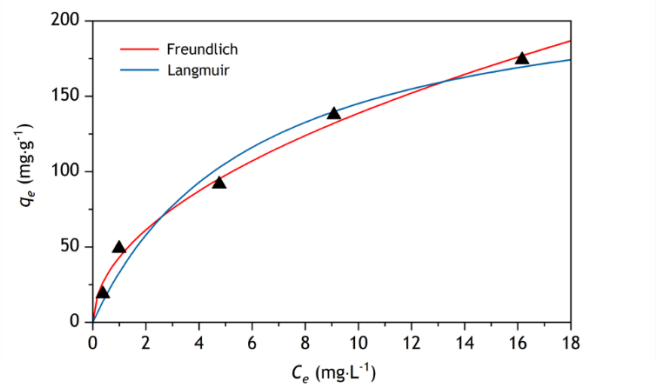

Figure 1. Isotherm of adsorption of P over the optimized biochar.

The carbon materials enriched with magnesium and phosphorus can further be applied as fertilisers in the soil since both magnesium and phosphorus are essential to plants' growth [6]. Through this process, the recycling of phosphorus from water and wastewater flows is achieved while at the same time providing added value to a byproduct of the cork industry.

4. Conclusions

Magnesium-modified biochars produced from the pyrolysis of cork granulate are effective at adsorbing phosphate from water, with performance optimization achievable through adjusting pyrolysis temperature and gas to ensure high magnesium content in micro and nano surface structures; phosphate uptake is enhanced at lower pH levels.

5. Acknowledgements

This work was financially supported by LSRE-LCM - UIDB/50020/2020 (DOI: 10.54499/UIDB/50020/2020) and UIDP/50020/2020 (DOI: 10.54499/UIDP/50020/2020); and ALiCE - LA/P/0045/2020 (DOI: 10.54499/LA/P/0045/2020).

6. References

[1] D.P. Van Vuuren, A.F. Bouwman, and A.H.W. Beusen, *Global Environ. Change*, **20** (3), (2010) p. 428-439.
[2] C.P. Mainstone, and W. Parr, *Sci. Tot. Environ*., **282-283**, (2002) p. 25.
[3] D. Mohan, A. Sarswat, Y.S. Ok, and C.U. Pittman Jr., *Biores. Technol*., **160**, (2014) p. 191.
[4] Q. Wang, Z. Lai, J. Mu, D. Chu, and X. Zang, *Waste Manag*., **105**, (2020) p. 102.
[5] Pintor, A.M.A.; Ferreira, C.I.A.; Pereira, J.C.; Correia, P.; Silva, S.P.; Vilar, V.J.P.; Botelho, C.M.S.; Boaventura, R.A.R., *Water Research*, **46**(10), (2012) p. 3152.
[6] H. Bacelo, A.M.A. Pintor, S.C.R. Santos, R.A.R. Boaventura, C.M.S. Botelho, *Chem. Eng. J*., **381**, (2020) p. 122566.

P39: Adaptive Digital Twin for Pressure Swing Adsorption Systems: Integrating a Novel Feedback Tracking System, Online Learning and Uncertainty Assessment for Enhanced Performance

Erbet Almeida Costa [(1)], Carine de Menezes Rebello [(1)], Leizer Schinitman[(2)], José Miguel Loreiro[(3)] [(4)], Ana Mafalda Ribeiro[(3)] [(4)] and Idelfonso B. R. Nogueira[(1)]

[(1)] Chemical Engineering Department of the Norwegian University of Science and Technology, Gløshaugen, Trondheim, 7034, Norway.
erbet.a.costa@ntnu.no
[(2)] Programa de pós-graduação em Mecatrônica, Universidade Federal da Bahia, Rua Prof. Aristides Novis, n 2., Salvador, 40210-630, Brasil
[(3)]LSRE-LCM - Laboratory of Separation and Reaction Engineering – Laboratory of Catalysis and Materials, Faculty of Engineering, University of
Porto, Rua Dr. Roberto Frias, Porto, 4200-465, Portugal
[(3]ALiCE - Associate Laboratory in Chemical Engineering, Faculty of Engineering, University of Porto, Rua Dr. Roberto
Frias,, Porto, 4200-465, Portugal

Abstract – This paper presents a novel approach to digitizing and modeling pressure swing adsorption (PSA) processes using an uncertainty-aware digital twin. PSA modeling presents unique challenges due to its complex and cyclic behavior, which lacks a steady state. By contributing to the literature on periodic systems, we provide valuable insights into the potential applications of artificial intelligence and digital twins beyond the field of cyclic processes. Our proposed methodology can enhance the understanding and optimization of complex systems across various industries and applications. The proposed digital twin is uncertainty-aware and reliable, continuously updating itself through online learning and utilizing a novel feedback tracker to accurately represent the PSA system. This robust and adaptable methodology supports optimal PSA system operation and facilitates informed decision-making for enhanced process operation. The results demonstrate that the proposed approach yields a reliable digital twin for the PSA unit, capable of tracking the process's complex dynamics and adapting to changes, including adsorbent degradation, which is a significant challenge in PSA operations. Overall, this work highlights the potential of advanced technologies, such as digital twins and artificial intelligence, to improve performance and efficiency in the field of process engineering. This work contributes to the ongoing efforts to optimize industrial processes and support sustainable development by providing a reliable and adaptable methodology for digitizing PSA processes.

P40: Hierarchical Y and MCM-22 zeolites prepared through surfactant mediated technology

A.P. Carvalho [1,2], B. Matos [1,2], M. Matos [2,3] N. Nunes [2,3], M. S. Santos [1,2], J. Coelho [3,4], A. Martins [2,3]

[1] *Centro de Química Estrutural – Institute of Molecular Sciences, Universidade de Lisboa, Portugal*
[2] *Departamento de Química e Bioquímica, Faculdade de Ciências da Universidade de Lisboa, Portugal*
apcarvalho@ciencias.ulisboa.pt
[3] *DEQ, Instituto Superior de Engenharia de Lisboa, Instituto Politécnico de Lisboa, Portugal*
[4] *Centro de Química Estrutural - Institute of Molecular Sciences, Universidade de Lisboa, Portugal*
fc54692@alunos.ciencias.ulisboa.pt; mariana.matos@isel.pt; nelson.nunes@isel.pt; mssantos@ciencias.ulisboa; jose.coelho@isel.pt; amartins@deq.isel.ipl.pt

1. Introduction – In the past few decades, hierarchical zeolites have emerged has an alternative to the purely microporous ones. Among the several available strategies, the alkaline treatment in the presence of surfactants comprises the combination of a basic agent, such as NaOH, with a surfactant molecule, like CTAB, followed by a thermal treatment under autogenous pressure [1]. This method allows to produce hierarchical materials with regular size and shape of mesopores, in contrast with solely alkaline treatment that leads to a random distribution of mesopores (Figure 1). The modification of HY zeolite through surfactant assisted treatment has been deeply investigated [1-3] whereas for HMCM-22 there are no reported studies. In this work, HMCM-22 and HY zeolites were modified through NaOH + CTAB methodology, using previously optimized protocols [1-3] but slightly modified, according to each zeolite structure. The structural and textural properties of parent and modified materials were studied, foreseeing further applications as catalysts or catalyst supports.

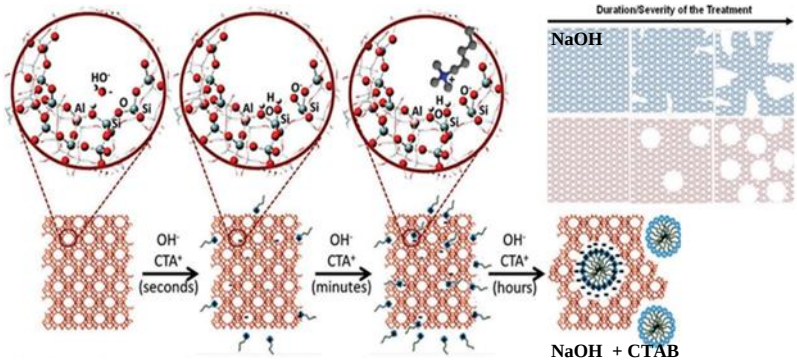

Figure 1. Production of hierarchical zeolites using NaOH + CTAB surfactant under autogenous pressure. Adapted from [1].

2. Experimental – HMCM-22, synthesized according to Güray et al. [4] and commercial HY zeolite (Zeolyst Si/Al=5.4) were use as parent materials. Both zeolites were modified through alkaline treatment assisted by CTAB surfactant under autogenous pressure at 150 ºC. For HY zeolite samples the amounts of NaOH and CTAB were fixed (0.7 g CTAB /1 g zeolite, and [NaOH] = 0.37 M) and the duration of the treatment changed from 6 to 24 h. For HMCM-22 samples the duration of the treatment was 6 h and [NaOH] = 0.05, 0.1 or 0.2 M, keeping the amount of CTAB the same as used for HY. After quenching the autoclaves the powders were recovered, dried, and calcined at 550 ºC for 4 h. The samples were labeled Z_[NaOH]_Ct, where Z is the zeolite designation, followed by the NaOH concentration, C means the surfactant CTAB, followed by the duration of the treatment (h). The samples were characterized by powder X-ray diffraction in a Pan' Analytical PW3050/60X'Pert PRO diffractometer and N_2 adsorption isotherms at -196 ºC obtained in an automatic apparatus ASAP2010 from Micromeritics. Prior to the adsorption measurements about 50 mg of zeolite samples were outgassed at 300 ºC for 2 h under vacuum greater than 10^{-2} Pa.

3. Results and Discussion - The diffractograms of HMCM-22 and HY modified samples (data not shown) reveal that the samples keep the long-range crystal ordering, meaning that the crystal structure was kept despite of the treatments. The N_2 adsorption isotherms and pore size distribution for parent and modified HMCM-22 and HY samples are displayed in Figure 2.

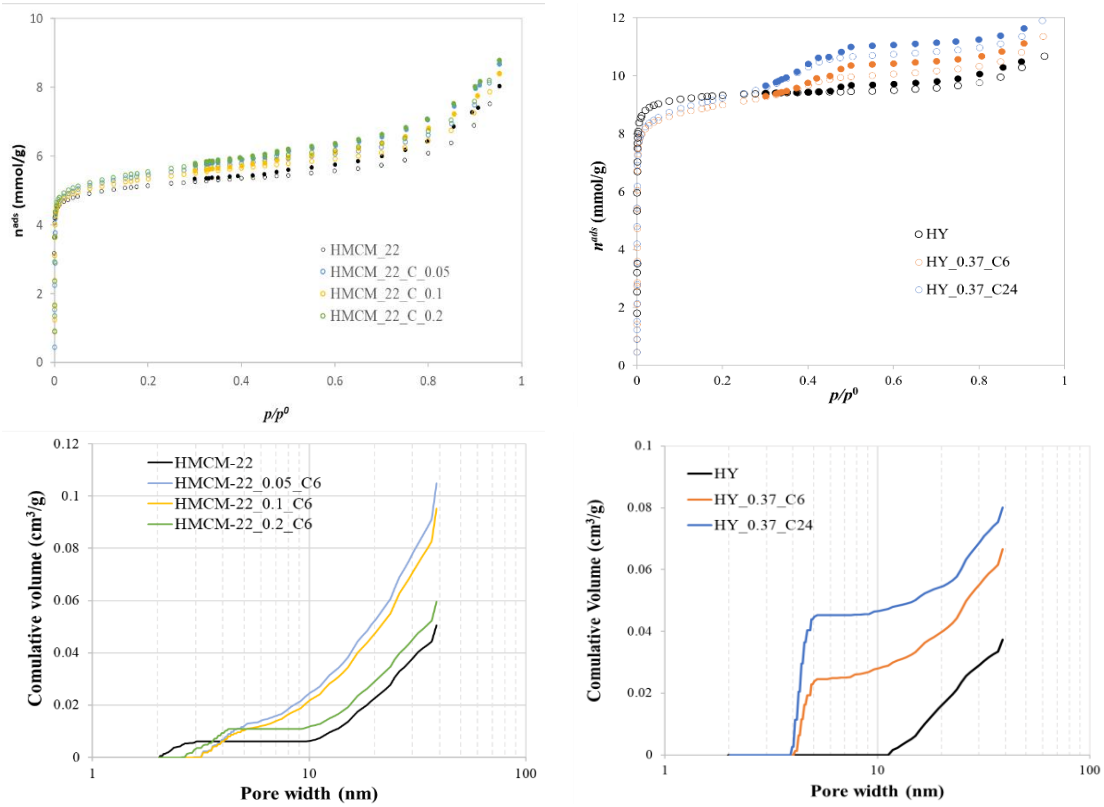

Figure 2. N_2 adsorption isotherms at -196 ºC (top) and mesopore size distribution (bottom) for parent and treated samples with NaOH + CTAB.

The NaOH + CTAB treatment has distinct effect on the textural properties of the two zeolite structures. In the case of parent HMCM-22 there is a continuous mesopore distribution starting from 2 nm pores while in the modified samples there are a larger volume of mesopores starting only around 3 nm, most probably resulting on the enlargement of the inner supercages characteristic of this zeolite structure (MWW). On the other hand, for HY materials a preferential formation of narrow mesopores (4-5 nm) is observed.

4. Conclusions – Hierarchical materials based on HMCM-22 and HY through NaOH treatments assisted by CTAB surfactant were obtained pointing out the influence of the structure for the textural characteristics of the modified samples. The potentialities of these materials will be explored as bifunctional catalysts, upon metal loading, in hydrodeoxygenation (HDO) reaction aiming to transform biomass into biofuels.

Acknowledgements
This research was funded by Fundação para a Ciência e Tecnologia (FCT) through UIDB/00100/2020, https://doi.org/10.54499/UIDB/00100/2020 UIDP/00100/2020 https://doi.org/10.54499/UIDP/00100/202 and LA/P/0056/2020 https://doi.org/10.54499/LA/P/0056/2020 and IPL through Project IPL/2023/Zeo@BioRef ISEL

5. References
[1] M. J. Mendoza-Castro, E. Serrano, N. Linares, J. Garcia-Martinez, *Adv. Mater. Interfaces* (2020) 202001388.
[2] A. Martins, V. Neves, J. Moutinho, N. Nunes, A.P. Carvalho, *Microporous Mesoporous Mater.* **323** (2021) 111167.
[3] A. Martins, B. Amaro M. Soledade C.S. Santos, N. Nunes, R. Elvas-Leitão, A. P. Carvalho, *Molecules*, **29** (2024) 517.
[4] I. Güray, J. Warzywoda, N. Baç, A. Sacco Jr, *Microporous Mesoporous Mater*. **31** (1999) 241.

RIA 43
XLIII Reunião Ibérica de Adsorção
Porto, Portugal
1-4 September 2024

P41: Modified ZSM-5 and BEA through chemical and mecanochemical methods for Fenton reactions

A. P. Carvalho [1,2], J. Costa [3], A. Martins [2,3], N. Nunes [2,3]

[1] Departamento de Química e Bioquímica, Faculdade de Ciências Universidade de Lisboa, Ed.C8, Campo Grande, Lisboa, Portugal.
apcarvalho@ciencias.ulisboa.pt
[2] Centro de Química Estrutural, Faculdade de Ciências, Institute of Molecular Sciences, Universidade de Lisboa, Campo Grande, Lisboa, Portugal
[3] Departamento de Engenharia Química, Instituto Superior de Engenharia de Lisboa, Instituto Politécnico de Lisboa, R. Conselheiro Emídio Navarro, 1, Lisboa, Portugal
a46246@alunos.isel.pt; angela.nunes@isel.pt; nelson.nunes@isel.pt

1. Introduction – Fenton reactions are a type of oxidation reaction that involves the use of hydrogen peroxide (H_2O_2) as oxidizing agent in the presence of a transition metal, typically iron (II). The reaction can be used to decompose organic pollutants and contaminants found in wastewater. More recent approaches include the incorporation of transition metals into zeolites to enhance the decomposition rate and the process efficiency [1].
Zeolites are crystalline microporous materials with a unique combination of properties such as high surface area and well-defined microporosity, and high thermal and mechanical stability. These features make them suitable for many applications in separation processes and catalysis. Yet, their use in liquid-phase processes has some restrictions since molecules cannot easily diffuse to the active sites located inside the micropores. To overcome this limitation, several types of modifications have been proposed [2]. For instance, desilication is a chemical treatment that aims to selectively remove Si from the zeolite framework originating hierarchical materials with inner micro+mesopores. Alternatively, mechanochemical procedures have the purpose of reducing the particle size and, thus, generate additional intercrystalline porosity. In this wok ZSM-5 and BEA zeolites are modified through chemical alkaline + acid leaching and mechanochemistry. The behaviour of zeolites loaded with iron (Fe) will be examined as catalysts for degrading methylene blue dye in Fenton reactions.

2. Experimental – Commercial powder zeolites from Zeolysts International, ZSM-5 (Si/Al=15) and BEA (Si/Al=12.5) were used to (a) chemical desilication and (b) mechanochemical modifications. Chemical: alkaline treatment with NaOH (0.8 or 0.1 M for ZSM-5 and BEA, respectively), at 65 ºC and 30 min, followed by an acid leaching with HCl (0.1 M) at 70 ºC for 3 h to remove extra-framework debris located at the pore mouths. The solids were recovered by centrifugation, dried, and calcined in a muffle at 550 ºC for 4 h. The samples were labelled as ZEO_D_AT, where D means desilication and AD indicates the acid treatment. Mechanochemical: both zeolites were modified in a shaker mill (VWR Star-Beater) with a stainless-steel jar with 5 spheres of 3 mm diameter. The samples were milled for 10 min with 10 Hz frequency, giving ZEO_ M samples. The impact of the treatments was assessed through powder X-ray diffraction (Pan'Analytical PW3050/60X'Pert PRO), textural analysis was achieved through low temperature N_2 adsorption isotherms (Micromeritics ASAP 2010) obtained after a previous treatment at 300 ºC for 3 h under vacuum greater than 10^{-2} Pa. Particle size distribution was evaluated by light scattering experiments (Malvern, Master 3000) and TEM microscopy (JEOL JEM-2100-HT). The metal ion Fe^{2+} was introduced by ion exchange or through mechanochemistry using the condition previously described. In all cases the targeted metal loading was (0.7 wt.%). In the Fenton reaction, 10 mg of the samples were accurately weighted and placed into stoppered flasks along with 40 mL of dye solutions. The flasks were then immersed in a thermostatically controlled bath at 40 °C (Julabo MP), which was positioned over a multiposition magnetic stirrer (Selecta Multimatic 9-S). The adsorption process was allowed to reach equilibrium after a period of one hour. Prior to initiating the reaction, the solution pH was adjusted to 5 using NaOH. The reaction commenced by adding 0.5 mL of a 0.07 M hydrogen peroxide (H_2O_2) solution. To halt the reaction, when necessary, sodium thiosulfate was added, and the catalyst was removed via centrifugation at 6,000 rpm for 10 minutes using a Hermle Z300 centrifuge. Aliquots of the supernatant solution were subsequently taken and their absorbances measured in a double-beam spectrophotometer (Jasco V530) to quantify the remaining methylene blue in solution.

3. Results and Discussion – ZSM-5 and BEA commercial zeolites display different morphologies and particle sizes (Figure 1), being clear the presence of crystal agglomerates, especially in the case of BEA zeolite.

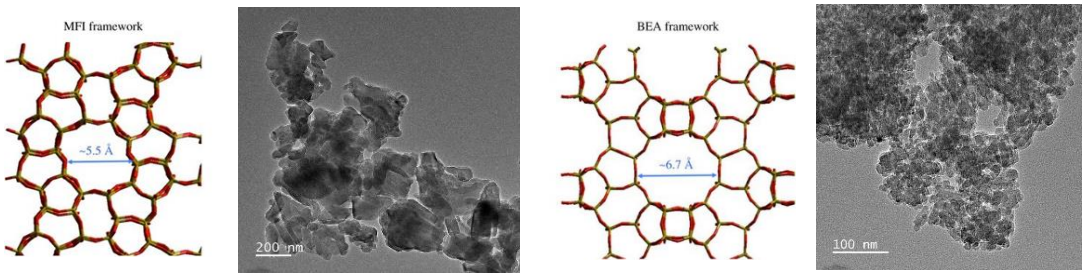

Figure 1. TEM images of ZSM-5- MFI structure- (left), and BEA (right).

The crystallinity and textural parameters of parent and modified materials are present on Table 1 revealing that the crystal arrangements of the zeolites were kept although some loss of crystallinity occurs especially in the case of BEA based materials. Concerning the textural parameters, microporous volume (V_{micro}) was quantified through the application of αs method and V_{meso} was calculated by the difference between the total volume (V_{total}), corresponding to the amount of N_2 adsorbed at $p/p^0 \approx 0.95$, and V_{micro}.

Table1. Crystallinity and textural parameters of parent and modified samples.

Sample	C_{XRD} **(%)**	V_{micro} **(cm^3 g^{-1})**	V_{meso} **(cm^3 g^{-1})**
ZSM-5	100	0.15	0.07
ZSM-5D_AT	100	0.15	0.13
ZSM5_M	95	0.14	0.07
BEA	100	1.17	0.40
BEA_D_AT	71	0.15	0.44
BEA_M	87	0.15	0.41

As can be observed, the chemical treatment (desilication + acid leaching) allowed to keep V_{micro} and promoted a substantial increase of V_{meso} in the case of ZSM-5_D_AT, whereas in the case of BEA_D_AT a slight decrease in V_{micro} and a small increase of V_{meso} was noted. For the mechanochemical treatment the textural parameters were kept for both milled samples, for the applied experimental conditions.

4. Conclusions – Preliminary results regarding the modification of ZSM-5 and BEA zeolites through chemical and mechanochemical treatments are presented. BEA zeolite proved to be a more sensitive structure, leading to a more substantial loss of crystallinity. Further studies will proceed with characterization of the Fe^{2+} loaded samples through classic ion exchange and mechanochemistry, thus allowing a deeper insight of the catalytic performance in Fenton reactions.

Acknowledgements
This research was funded by Fundação para a Ciência e Tecnologia (FCT) through UIDB/00100/2020, https://doi.org/10.54499/UIDB/00100/2020 UIDP/00100/2020 https://doi.org/10.54499/UIDP/00100/202 and LA/P/0056/2020 https://doi.org/10.54499/LA/P/0056/2020.

5. References

[1] S. Navalon, M. Alvaro, H. Garcia, *Appl. Catal., B*, **99**(1-2), (2010) p. 1.
[2] A. Carvalho, N. Nunes, A. Martins, "Hierarchical Zeolites: Preparation, Properties and Catalytic Applications", Nova Science Publishers, New York, 2015.

P42: Techno-economic analysis of the industrial production of MIL 120(Al)

M. Bordonhos, [1][2] A. Al Mohtar, [1] B. Chen, [3] R. V. Pinto, [3][4] M. L. Pinto, [1]

F. Nouar, [3] G. Mouchaham, [3] Christian Serre [3]

[1] *CERENA, Departamento de Engenharia Química, Instituto Superior Técnico, Universidade de Lisboa, Lisboa, 1049-001 Portugal*

[2] *CICECO – Aveiro Institute of Materials, Department of Chemistry, University of Aveiro, Campus Universitário de Santiago, Aveiro, 3810-193 Portugal*

[3] *Institut des Matériaux Poreux de Paris, Ecole Normale Supérieure, ESPCI Paris, CNRS, PSL University, 75005 Paris, France*

[4] *Service de Thermodynamique et de Physique Mathématique, Faculté Polytechnique, Université de Mons, 7000 Mons, Belgium.*

marta.bordonhos@tecnico.ulisboa.pt

1. Introduction – MIL-120(Al) [1] is a robust and cost-effective aluminium-based metal-organic framework (MOF) that has been recently studied as a candidate for the post-combustion capture of CO_2 from flue gases by adsorption-based processes [2]. In this work, the synthesis of MIL-120(Al) by an eco-friendly procedure using inexpensive raw materials has been scaled-up to the kilogram scale, a thorough multidisciplinary experimental and computational study of the material has been conducted, and a techno-economic analysis of its industrial production has been performed.[2] Herein, we present our contribution to this work, the techno-economic evaluation of the industrial-scale batch production process of 1 kton/year of MIL-120(Al). Based on our economic model, we have estimated a production cost of *ca*. 13 $/kg for MIL-120(Al). A sensitivity analysis has also been performed based on the organic ligand and energy prices, as well as the base equipment cost. This analysis has revealed the production cost to be more sensitive to the ligand price.

2. Economic Model – The industrial-scale batch production process, represented in Image 1, has been designed based on the water-based and ambient-pressure pilot-scale (1 kg) synthesis reported, that uses 1,2,4,5-benzenetetracarboxylic acid (H_4BTeC) as the organic ligand, sodium aluminate ($NaAlO_2$) as the metal source and acetic acid (CH_3COOH) as a pH modulator, and has a space-time yield (STY) of *ca*. 100 $kg \cdot m^{-3} \cdot day^{-1}$.[2] The industrial process starts with the raw materials, kept in a storage tank (CH_3COOH) and silos (H_4BTeC and $NaAlO_2$), being fed into a batch-stirred reactor with a propeller agitator. Next, the solid produced in the reactor is washed and filtrated in a plate-and-frame filter, followed by drying in a rotary dryer. The dry MIL-120(Al) is then transported in a conveyor belt to a final storage silo. The process equipment was designed for a yearly production of 1 kton/year (*ca*. 5% of the total yearly requirements for adsorbents for CO_2 capture from cement plants), considering a reaction yield of 76% and 260 full days of work per year, and was based on typical chemical engineering heuristics, the properties of the materials and process conditions.

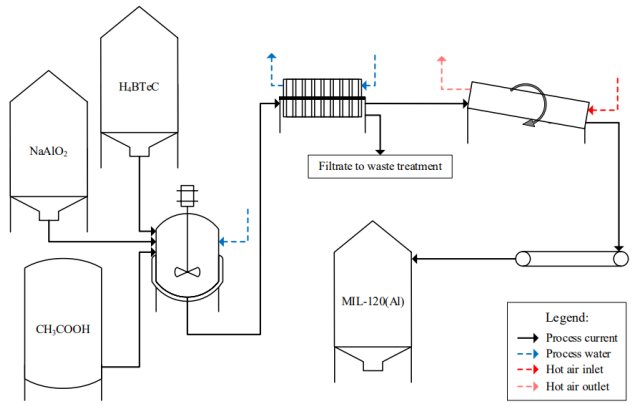

Image 1. Simplified process block diagram of the industrial production of MIL-120(Al).

The economic model considers the total investment and production costs. The total investment is the sum of the fixed investment, working capital and interim interests paid over the bank loan. The fixed investment has been calculated based on the base equipment cost and common cost factor heuristics [2,3], the working capital has been calculated based on the fixed investment, and the interim interests considered a borrowed capital from the bank of 60% of the total investment cost, with a 5% interest rate and 24 months of interim interest payment (corresponding to the duration of the plant construction). The production costs consider the manufacturing costs (comprised of direct, indirect and fixed costs) and general expenses. The direct manufacturing costs consider different segments, namely total raw

materials, utilities (only the electricity was considered), and labour (25 plant operators and 5 shifts were considered). Other segments of the direct manufacturing costs, the indirect and fixed manufacturing costs, as well as the general expenses have been calculated based on cost factors and other parcels.[2,3] All currency values were converted to USD ($) and all prices were updated based on the Chemical Engineering Plant Cost Index (CEPCI), for the years 2019 and 2022.

3. Results and Discussion – Considering the economic model described above and the techno-economic analysis performed for 2022, the total base equipment cost has been estimated to be *ca*. 2.5 M$, with a total investment of *ca*. 14.5 M$. The final estimated production cost has been *ca*. 13 $/kg, lower than that reported for other MOFs [4,5]. When scaled to 2019 prices, the production cost for MIL-120(Al), *ca*. 10 $/kg, is almost a third of the cost reported by some of us for another aluminium-based MOF, MIL-160(Al), 29.5 $/kg [4]. This can be explained by two cumulative factors that favour the production costs of MIL-120(Al) over MIL-160(Al): the more affordable organic ligand used in the synthesis (H_4BTeC) and the lower ligand-to-aluminium mass ratio of MIL-120(Al).

To have a better understanding of how the production cost could be influenced by variations in cost segments more significant to its estimation and more prone to price fluctuations, we have performed a sensitivity analysis. For this, on a first approach we have selected the organic ligand and energy prices. The organic ligand is the raw material more prone to price fluctuations, as the aluminium source ($NaAlO_2$) and acetic acid (CH_3COOH) are raw materials commonly used in the industry. The results of this sensitivity analysis are illustrated in Image 2A, and from this analysis, the ligand price can be seen to have a higher influence on the production cost. We have then analysed the effect of varying the cost of the base equipment, as depicted in Image 2B, and it can be seen that a variation of ± 20% would result in a fluctuation in the production cost of ± 1.1 $/kg.

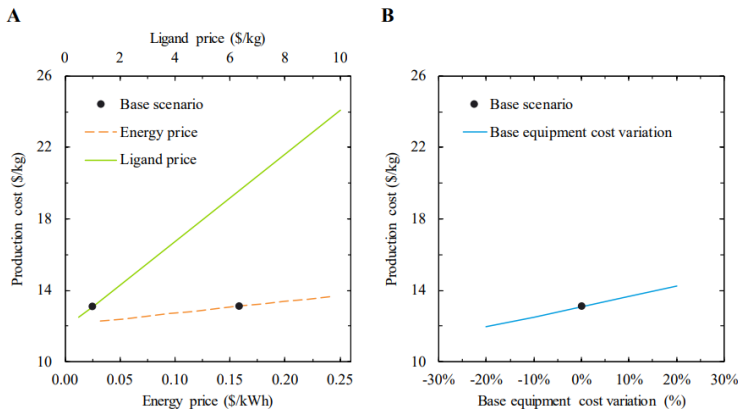

Image 2. Sensitivity analysis of the ligand and energy prices (A) and base equipment cost variation (B) on the production cost of MIL-120(Al).

3. Conclusions – A techno-economic analysis of a proposed industrial-scale production process for the MIL-120(Al) MOF has been developed. The resulting estimated production cost, *ca*. 13 $/kg (for a production of 1 kton/year), is lower than the production costs estimated for other MOFs. Considering the principle of the economy of scale, this production cost could even be expected to decrease for larger production scales. Furthermore, additional optimisations of the material's synthesis could lead to higher yields, further decreasing the overall costs. As such, not only due to its favourable production process conditions and costs, but also to its intrinsic characteristics and adsorption performance, MIL-120(Al) can be seen as a viable candidate for application in CO_2 capture.

4. References

[1] C. Volkringer, T. Loiseau, M. Haouas, F. Taulelle, D. Popov, M. Burghammer, C. Riekel, C. Zlotea, F. Cuevas, M. Latroche, D. Phanon, C. Knöfelv, P. L. Llewellyn, G. Férey, *Chem. Mater*. **2009**, *21*, 5783.

[2] B. Chen, D. Fan, R. V. Pinto, I. Dovgaliuk, S. Nandi, D. Chakraborty, N. García-Moncada, A. Vimont, C. J. McMonagle, M. Bordonhos, A. Al Mohtar, I. Cornu, P. Florian, N. Heymans, M. Daturi, G. De Weireld, M. Pinto,
F. Nouar, G. Maurin, G. Mouchaham, C. Serre, *Adv. Sci.* **2024**, *2401070*, DOI 10.1002/advs.202401070.

[3] M. S. Peters, K. D. Timmerhaus, R. E. West, *Plant Design and Economics for Chemical Engineers*, McGraw-Hill Higher Education, **2003**.

[4] M. I. Severino, E. Gkaniatsou, F. Nouar, M. L. Pinto, C. Serre, *Faraday Discuss.* **2021**, *231*, 326.

[5] F. Nouar, C. Serre, M. L. Pinto, M. I. Severino, V. Pimenta, C. Freitas, *Cost Estimation of the Sustainable Production of MIL-100(Fe) at Industrial Scale from Two Upscaled Synthesis Routes*, Cambridge, **2023**

P43: Effect of water loading on the stability of pristine and defected UiO-66. A simulation study

E. Acuna-Yeomans [(1,2)], P. J. Goosen [(1)], J. J. Gutierrez-Sevillano[(3)], D. Dubbeldam[(4)], S. Calero[(1,2)]

[(1)]Materials Simulation and Modelling, Department of Applied Physics, Eindhoven University of Technology, 5600MB Eindhoven, The Netherlands.
[(2)]Eindhoven Institute for Renewable Energy Systems, Eindhoven University of Technology, PO Box 513, Eindhoven 5600 MB, The Netherlands.
[(3)]Department of Physical, Chemical and Natural Systems, Pablo de Olavide University, Ctra. Utrera Km. 1, 41013 Seville, Spain.
[(4)]Van't Hoff Institute for Molecular Sciences, University of Amsterdam, 1098XH Amsterdam, The Netherlands.

Principal Author's e-mail: e.acuna.yeomans@tue.nl

1. Introduction – For industrial applications, materials used in water treatment must be stable in moist conditions for easy handling and cost-effectiveness. Despite many Metal-organic frameworks (MOFs) developed, few are stable enough for water treatment, including the prototypical MOF UiO-66. Over the past decade, UiO-66 has garnered attention for its high hydrothermal and mechanical stability, due to its high zirconium cluster coordination, and tunability through defect control. Recently, computational simulations using rigid force fields have studied the adsorption properties of pristine and defected UiO-66, focusing on water and CO2 adsorption. Likewise, flexible models have been used in the past to study the structural and mechanical properties of the pristine and defected framework when it is not loaded with adsorbates. The main goal of this work is to study how water affects the structural and mechanical properties of both pristine and defected UiO-66 using classical molecular simulations. Correctly modeling the interactions between the framework and water molecules is crucial for this analysis. We implement and compare two methodologies for treating Lennard-Jones parameter mixing between the framework atoms and water molecules. Our study examines the spatial arrangement of water molecules within the framework, the affinity for interaction sites, the pore filling process, and their impact on the framework's structural parameters under atmospheric conditions, high hydrostatic pressures, and increased water loading. Additionally, we explore how the inclusion of linker vacancies, which creates open metal sites, affects these properties.

2. Experimental – This work was developed purely in-silico, via classical molecular simulations. The interactions between framework atoms were modelled using the force fields proposed by Rogge et al.[1] for the UiO family of materials, which have proven to provide an accurate prediction of the structural properties of the unloaded crystal relative to often used ad-hoc modifications of generic force fields. Water was modelled using SPC/E. Two methods were implemented to model water-framework interactions with Lennard-Jones potentials. The first method applied Lorentz-Berthelot (L-B) mixing rules, combining the SPC/E water model and MM3 parameters for the framework. The second method used Universal force field [2] parameters for the framework atoms while retaining MM3 parameters for intra-framework interactions, creating a hybrid of the two. Along with the pristine structure, 8 defected structures were considered: one of them corresponds to a system with one linker vacancy per unit cell and the rest to structures in which a different additional linker defect is introduced to the former. These structures were loaded with different amounts of water molecules, from 10 molecules per unit cell of the framework to 120 molecules per unit cell, near the water saturation point at room temperature. Molecular dynamics simulations were run in order to: obtain radial distribution functions of water with respect to potential principal interaction sites in the inorganic cluster, monitor the change in framework structural parameters upon loading and determine the loss-of-crystallinity pressure upon water loading of the pristine and defected structures at high pressures.

3. Results and Discussion - Our findings reveal that in the complex system of UiO-66 and water, the choice of guest-host interaction parameters greatly affects water distribution within the pore volume. Hybrid mixing methods align better with previous studies on water diffusion and pore-filling in UiO-66 and similar

structures. In contrast, direct Lorentz-Berthelot (L-B) mixing rules predict unusually strong coordination between water molecules and linker oxygen atoms, restricting water movement and preventing cluster formation at moderate loadings. Both methods show that water molecule spatial arrangement at various loadings impact the structural parameters of the framework, with L-B mixing predicting significant loading-induced expansion and hybrid mixing predicting slight system contraction. Looped NPT simulations reveal that the pressures at which the structure collapses (amorphization) decreases with increased water loading (Image 1). Both models predict similar amorphization pressure values at low water loading and start to differ at moderate water loading, with hybrid mixing predicting higher values. The results obtained for the structures containing 1 linker vacancy per unit cell reveals a similar comparative behavior to the pristine structures. Interestingly, a different trend is observed for structures containing 2 linker vacancies per unit cell, where hybrid mixing results in a sharper decrease in amorphization pressure values at low loadings and unlike with the less defected structures, both models predict comparable values at high loadings. Simulations with the defected structures at atmospheric conditions using hybrid mixing indicate that due to interactions with open metal sites at low loadings the systems expand, and once those sites are occupied the decreasing volume trend for increased water loading is recovered (Image 2).

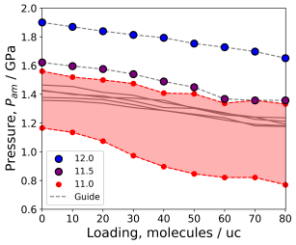

Image 1. Amorphization pressure with respect to water loading for pristine and defected UiO-66 using L-B mixing.

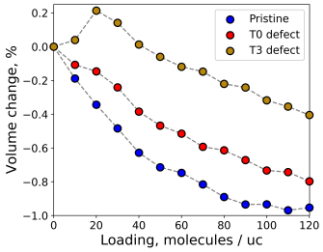

Image 2. Framework volume change upon water loading (hybrid mixing) for the pristine, 11.5-coordinated and 11.0 coordinated structures.

4. Conclusions – Our findings indicate that the selection of guest-host interaction parameters significantly impacts the distribution of water within UiO-66 and therefore the impact it has on the framework structural parameters. Hybrid mixing provides a more realistic representation of the water-framework system when compared to direct L-B mixing. Our simulations indicate that water weakens the bonds between the zirconium clusters and organic linkers, which leads to framework loss of crystallinity at lower hydrostatic pressures. The availability of open metal sites for the water molecules to directly interact with, in structures containing defects, modify the way in which the crystal responds to external pressure.

5. References

[1] Rogge, S. M. J. et al. Chemistry of Materials, 28, 5721-5732, 2016.
[2] Rappe, A. K. et al. Journal of the American Chemical Society, 114, 10024-10035, 1992.

P44: Innovative adsorbent of TiO_2/SiO_2 monolithic aerogels with cellulose fiber reinforcement

H. M. Sales[1,2,3], C. M. R. Almeida[1], L. Durães[1], J. F. De Conto[2,3], S. M. Egues[2,3]

[1] University of Coimbra, CERES, Department of Chemical Engineering, Rua Sílvio Lima, 3030-790, Coimbra, Portugal. E-mail: havila.maria@souunit.com.br
[2] Tiradentes University (UNIT), Aracaju – SE, Brazil.
[3] Laboratory of Materials Synthesis and Chromatography (LSINCROM), Institute of Technology and Research (ITP), Aracaju - SE, Brazil.
E-mail: claudio@eq.uc.pt; luisa@eq.uc.pt; jfconto@gmail.com; smsegues@gmail.com

1. Introduction – Environmental contamination by organic pollutants demands innovative, effective and sustainable solutions [1]. In this context, the present work proposes the development of a TiO_2/SiO_2 aerogel composite reinforced with cellulose fibers from *Luffa Cylindrica* to remediate water bodies polluted by contaminants, minimizing risks to human health and the environment. This material aims to combine the beneficial properties of silica aerogels, such as high surface area, high porosity, and low density, with the mechanical strength provided by cellulose fibers and the photocatalytic activity of TiO_2 [2, 3]. TiO_2 is a well-known photocatalyst with high efficiency in degrading organic pollutants under UV light due to its ability to generate reactive oxygen species. However, TiO_2 nanoparticles often suffer from limitations such as low adsorption capacity, electron-hole pairs recombination, and the difficulty of recycling in powder form. By incorporating TiO_2 onto SiO_2 aerogel matrices, the photocatalytic efficiency can be improved by reduced electron-hole recombination rates and increased surface area for adsorption of pollutants near TiO_2 active sites [4]. The monolithic form of this composite material also facilitates easy recovered and reused, making it a promising solution for environmental applications. Moreover, the addition of cellulose fibers to the aerogel composite not only contribute to the mechanical reinforcement of the aerogel structure, improving its stability and handling, but also offer additional surface area for adsorption of organic pollutants, making it a multifunctional material with improved adsorption and photocatalytic properties [2, 5]. This aerogel aims to effectively adsorb atrazine in water, representing a contribution to environmental decontamination, in the face of the challenges associated with pesticide contamination.

2. Experimental - The aerogel synthesis used tetraethoxysilane, vinyltrimethoxysilane and titanium isopropoxide as precursors, and environmentally friendly solvents and *Luffa cylindrica* fibers (Image 1). The composite underwent hydrolysis, condensation of the sol particles, aging, and supercritical drying with ethanol at high temperature, resulting in the TiO_2/SiO_2 aerogel monolith reinforced with *Luffa cylindrica* fibers, identified as AeroTi-Luf. For comparison, an aerogel without titania particles was produced, resulting in the sample identified as Aero-Luf (SiO_2 aerogel monolith and *Luffa cylindrica* fibers). Subsequently, the produced samples were characterized using different physicochemical, thermomechanical, and microstructural analysis techniques, such as apparent density measurement, nitrogen adsorption, scanning electron microscopy, X-ray diffraction, thermal analysis, mechanical compression tests, Fourier transform infrared spectroscopy, among others. The adsorption tests will be carried out using an atrazine solution (1 to 5 mg/L) in a batch reactor for 2 hours. All experiments will be carried out in duplicate under the same experimental conditions at room temperature (25 ºC). Sampling will be done at different time intervals. Preliminary tests of atrazine adsorption were conducted at room temperature, initial concentration of 5 mg/L, 0.02 g of the adsorbent dosage over 24 hours.

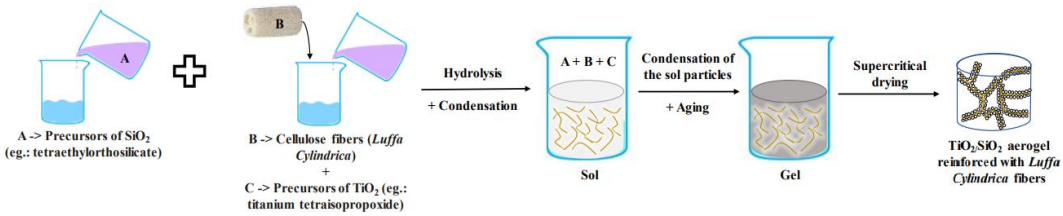

Image 1. Representation of the synthesis process for the TiO_2/SiO_2 aerogel monolith reinforced with *Luffa cylindrica* fibers.

3. Results and Discussion - The initial characterization results indicated a good dispersion of TiO_2 and fibers in the silica matrix, resulting in a yellowish and rougher appearance of the aerogels (Image 2). The volumetric shrinkage after supercritical drying was approximately 21.57% for Aero-Luf and 27% for AeroTi-Luf. Although the AeroTi-Luf monolith did not show significant shrinkage, some cracks were observed in its structure, in contrast to Aero-Luf monolith. This can be attributed to differences in shrinkage during the drying process between the two systems, as well as variances in the interaction between the oxides and cellulose. Further studies with different TiO_2 content in the aerogel must be done to reduce the cracks. Both aerogels exhibited a free-standing structure, suggesting that the presence of fibers did not compromise the structural integrity [6].

The apparent densities were low, being 0.19 g/cm³ for Aero-Luf and 0.28 g/cm³ for AeroTi-Luf, typical of highly porous materials. The addition of TiO_2 to the SiO_2/*Luffa* aerogel monolith increased its density, consistent with the incorporation of another oxide into the system, given that TiO_2 has a higher density than silica. The final density of the aerogel depends on the composition and relative amount of each oxidepresent.

Preliminary efficiency tests of atrazine adsorption over AeroTi-Luf monolith, resulted in 44,25% removal. The hydrophilic nature of the composite aerogel, due to the hydroxyl groups of the silica and titania, and the polar groups of the cellulose fibers, increases affinity with atrazine in an aqueous medium,contributing to its adsorption capacity.

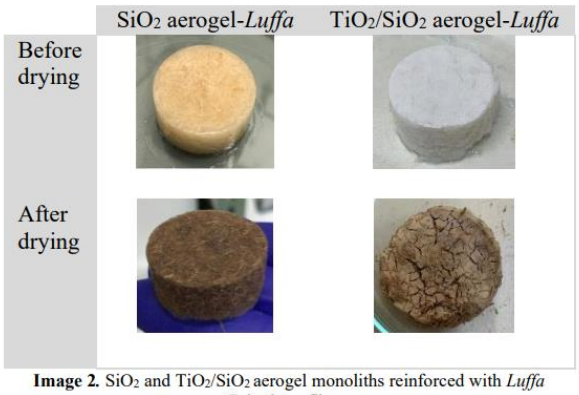

Image 2. SiO_2 and TiO_2/SiO_2 aerogel monoliths reinforced with *Luffa Cylindrica* fibers.

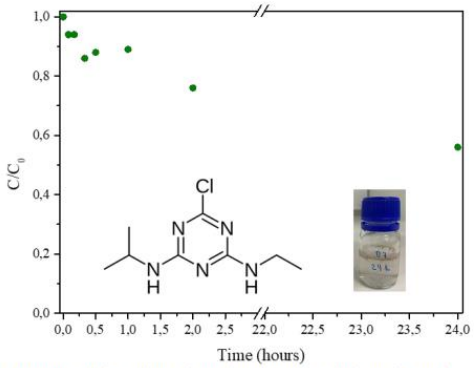

Image 3. Adsorption of atrazine aqueous solution of 5 mg/L.

4. Conclusions – The synthesis of the TiO_2/SiO_2 composite reinforced with *Luffa Cylindrica* fibers was successful. The high-temperature ethanol supercritical drying allowed obtaining intact monoliths, with moderate shrinkages. The fibers were incorporated without compromising the monolithic structure. The aerogels exhibited low apparent densities, indicating high porosity. The addition of TiO_2 resulted in a yellowish and rough appearance, without excessive shrinkage. The initial results are promising for these new cellulose fiber-reinforced materials. The combination of the inorganic matrix and the organic reinforcement results in an effective and environmentally friendly adsorbent for the removal of atrazine from aqueous solutions.

5. References

[1] L. Posthuma, M.C. Zijp, D. De Zwart et al., *Scientific reports*, **10**(1), (2020) p. 14825.
[2] T. Linhares, M. T. P. Amorim, L. Durães, *J. Materials Chemistry A*, **7**(40), (2019) p. 22768-22802.
[3] M.A. Santos, T.S.L. Da Silva, I.F.S. Oliveira et al., *J Mater Sci: Mater Electron*, **34**, (2023) p. 2225.
[4] V. G. Parale, T. Kim, K-Y. Lee et al., *Ceramics International*, **46**(4), (2020) p. 4939-4946.
[5] C. Ruan, Y. Ma, G. Shi et al., *Applied Surface Science*, **592**, (2022) p. 153280.
[6] H. Dai, Z. Jun, Y. Yin et al., *IOP Conf. Ser.: Mater. Sci. Eng.*, **587**, (2019) p. 012016.

P45: High-pressure CO_2 capture using Monolithic Silica Aerogels

T.L. Silva [(1)], M.R. Oliveira [(2)], T.R. Menezes [(1)], K.C. Santos [(1)], K.S. Santos [(2)], G.R. Borges [(1,2)], C. Dariva [(1,2)], J.F. De Conto [(1,2)], S.M. Egues*[(1,2)]

[(1)] *Postgraduate Program in Process Engineering (PEP)/ Tiradentes University (UNIT), Aracaju, SE Brazil. e-mail: smsegues@gmail.com*

[(2)] *Laboratory of Materials Synthesis and Chromatography (LSINCROM), Center for Studies in Colloidal Systems (NUESC)/Institute of Technology and Research (ITP), Aracaju, SE, Brazil. E-mail: claudio.dariva@gmail.com; jfconto@gmail.com*

1. Introduction – The Brazilian Pre-Salt fields hold significant reserves of natural gas (NG), characterizedby high levels of carbon dioxide (CO_2), ranging from 30 to 90% in raw NG. Consequently, substantial efforts have been dedicated to finding more efficient adsorbents for gas separation, particularly CO_2/CH_4 [1]. Among these, monolithic silica aerogel stands out for its exceptional properties: low density, high porosity, low thermal conductivity, and selectivity. Furthermore, its synthesis offers flexibility for modification with amine groups. Generally, the syntheses of these structures are produced in the form of fine powders and therefore are not suitable for direct use in high-scale adsorption processes. To address this issue, an alternative approach is to synthesize the adsorbent in monolith form. Monolith adsorbents offer several advantages over compacted bed adsorbents, such as: reduced pressure drop, leading to more efficient adsorption processes and reduced energy consumption; enhanced mass transfer kinetics, allowing for more rapid adsorption and desorption processes; manufacturing efficiency, as they can be used immediately after drying, without the need for additional compaction steps [2]. Thus, this study aimed to synthesize monolithic silica aerogel via supercritical drying, characterize its physical and chemical properties, and evaluate its efficacy in CO_2 adsorption under pressurized conditions up to 50 bar, with the goal of developing an advanced adsorbent material for high-pressure CO_2 capture and storage applications.

2. Experimental - The silica aerogel monolith (Si-Aeg) was synthesized following the methodology outlined by De Conto [3], undergoing supercritical CO_2 drying at 40 °C and 90 bar pressure for 3 hours, while the Pebax-modified aerogel monolith (Si-Peb) underwent a similar process with the addition of a Pebax solution. Physicochemical properties were assessed through FTIR, CHN, and N_2 Adsorption/Desorption analyses, with CO_2 adsorption isotherms conducted at temperatures of 45, 55, and 65 °C up to 50 bar to comprehensively evaluate the materials' performance and characteristics.

3. Results and Discussion - The development of a new Pebax-modified silica aerogel monolith has proven effective, showing a reduction in synthesis time through the sol-gel route combined with supercritical drying. It was observed that the Si-Aeg had a translucent appearance and a fragile structure due to numerous fissures throughout the material (Figure 1a, upper). On the other hand, it was noted that the Si-Peb monolith has a more regular formation, greater robustness in monolith shape, and minimized internal cracks (Figure 1a, lower). Through N_2 adsorption/ desorption analysis, it was found that Si-Peb has a lower surface area and pore volume compared to Si-Aeg, due to polymer occupying the pores. As expected, CHN analysis showed a higher amount of carbon, hydrogen, and nitrogen for Si-Peb monolith (Table 1). The FTIR spectra shown in Figure 1b present the main chemical groups present in the Si-Aeg and Si-Peb monoliths. The spectrum of pure Pebax was addedto observe the contributions of the polymer to the Si-Peb monolith. The functionalization of silica with Pebax silica caused some changes in the position and intensity of the characteristic peaks of Pebax, due tosilica-polymer interactions. The peak at 1636 cm^{-1} is due to stretching frequency of H-N-C=O group of Pebax, which showed a decline in intensity and a shift to 1641 cm^{-1} in the Si-Peb monolith [4]. Pebax peakaround 2890 cm^{-1}, due to aliphatic –C–H stretching, also reduced its intensity after functionalization of silica aerogel. The broad band at around 3300 cm^{-1} on the surface of Si-Peb, is more related to –N–H stretching vibrations of Pebax chain than characteristic of Si-OH groups [4]. The most intense band at 1054cm^{-1} present in Si-Aeg and Si-Peb corresponds to the asymmetric stretching of Si-O-Si bonds, which has a typical asymmetric shape attributed to the presence of siloxane groups in the samples [3, 5]. Aerogels samples presented characteristic peaks of silica. The peak at 945 cm^{-1} corresponds to the asymmetric stretching of Si-OH

Table I. BET specific surface area (SBET) and elemental compositions obtained from CHN analyses.

Sample	S_{BET} ($m^2\ g^{-1}$)	V_p ($cm^3\ g^{-1}$)	C (%)	H (%)	N (%)
Si-Aeg	511	1.28	2.37	0.59	0.07
Si-Peb	277	0.58	4.02	8.55	2.14

groups, while the symmetric stretching of Si-O-Si chains appears at 780 cm^{-1} [3, 5].

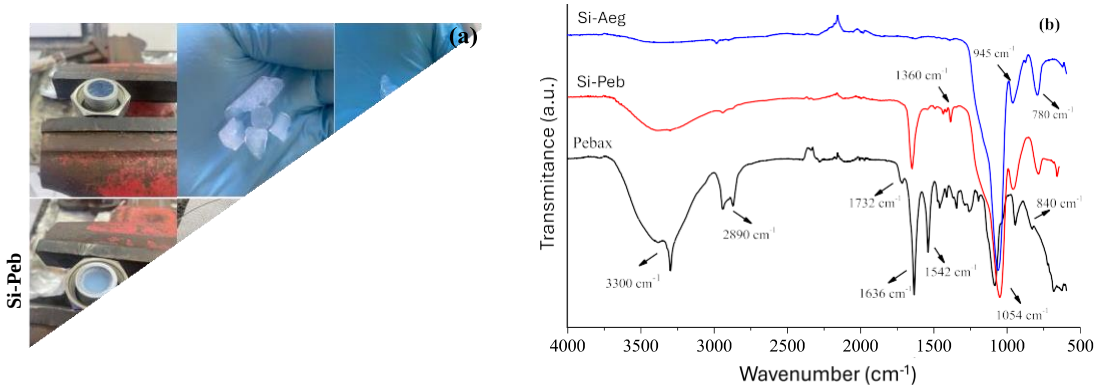

Image 1. (a) Images of Si-Aer and Si-Peb and (b) FTIR spectra of monoliths and Pebax.

Adsorption isotherms showed that the CO_2 adsorption capacity of Si-Peb monoliths decreased with increasing temperature from 45 °C to 65 °C. The amount of CO_2 adsorption was 11,98 mmol g^{-1} at 50 bar and 45 °C (Figure 2b). The gas adsorption capacity of nanoparticles is greatly affected by gas temperature and pressure, decreasing significantly with increasing temperature [6]. The results also revealed that functionalization with Pebax effectively increased the CO_2 adsorption capacity, as Si-Aeg at the same conditions reached 7.34 mmol g^{-1}. The Dual-Site Langmuir model showed good agreement with the experimental data at 55 °C and 65 °C and accurately predicted CO_2 adsorption sites. However, at 45°C, the model did not fit well. Nevertheless, the sum of errors between the experimental adsorbed amount and the model-predicted one was 5%, indicating an acceptable value.

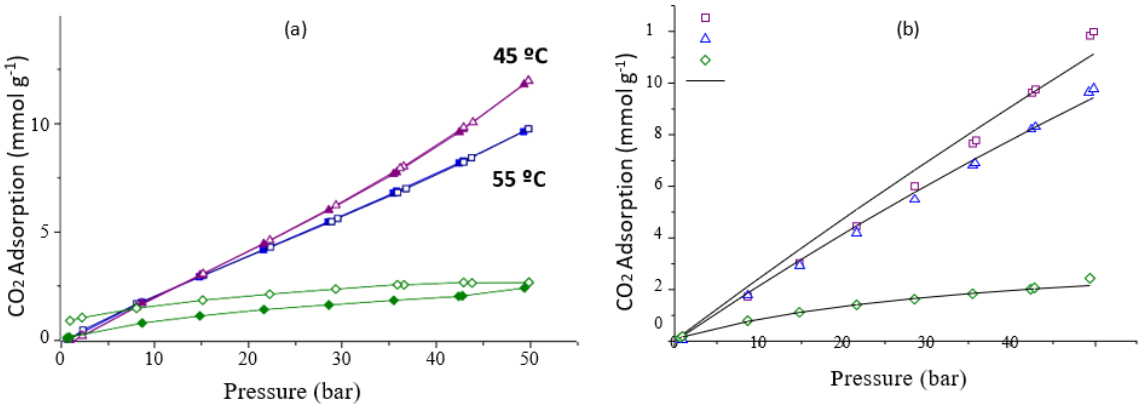

Image 2. CO_2 adsorption equilibrium isotherms for Si-Peb at 50 bar (a) and Langmuir isotherm fitting (b).

Conclusions - The development of a new monolithic material using Pebax in the silica structure has proven effective. It was possible to achieve silica monoliths with a significant reduction in synthesis time through the sol-gel synthesis route combined with supercritical drying. Monolithic silica showed promising results for CO_2 capture processes with a great adjustment to the Langmuir model. It is noteworthy that this study is new about existing materials, where it is observed that the silica monolith has good CO_2 adsorption capacity when compared to the literature.

4. References

[1] K. Santos et al., *Separation and Purification Technology*, **271**, (2021) p. 119409.
[2] N. Politakos et al., *Industrial & Engineering Chemistry Research*, **59**, (2020) p. 8612–8621.
[3] J.F. De Conto et al., *Journal Non-Crystalline Solids*, **471**, (2017) p. 209−214.
[4] M. Isanejad et al., *Journal applied polymer science*, **134**, (2016) p. 44531.
[5] M.R. Oliveira et al., *Journal of Sol-Gel Science and Technology*, **105**, (2023) p. 370–387.
[6] Z. Aghaei et al., *Separation and Purification Technology*, **199**, (2018) p. 47–56.

P46: Fixed bed adsorption column studies for the removal of antibiotics from water using biochar prepared from brewery residues

É.M.L. Sousa [(1)], M. Otero [(2)], M.V. Gil [(3)], V.I. Esteves [(1)], V. Calisto [(1)]

[(1)] Department of Chemistry and CESAM, University of Aveiro, 3810-193 Aveiro, Portugal.
erikamousa@ua.pt
[(2)] Departamento de Química y Física Aplicadas, Universidad de León, Spain.
[(3)] Instituto de Ciencia y Tecnología del Carbono, INCAR (CSIC), Francisco Pintado Fe 26, 33012 Oviedo, Spain.
marta.otero@unileon.es; victoria.gil@incar.csic.es; valdemar@ua.pt; vania.calisto@ua.pt

1. Introduction – Residual biomass from the brewery industry, specifically spent brewery grains (SBG), is produced in large amounts and is a valid option to be used as a precursor of carbon adsorbents for further application in water treatment systems [1,2]. In fact, the use of agro-industrial wastes as precursors of adsorbent materials contributes to the environmental sustainability of this process, avoiding the use of non-renewable raw materials. Sustainable wastewater treatment with advanced processes is crucial to meet environmental standards and safeguard water systems from harmful pollutants. In this regard, this work aims to assess the fixed-bed adsorption performance of biochar produced from SBG for the removal of three antibiotics, namely sulfamethoxazole (SMX), trimethoprim (TMP) and ciprofloxacin (CIP), from water. For this purpose, the impact of flow rate and single/multi-component adsorption on the breakthrough adsorption curves was determined. Thermal regeneration of the exhausted material was also considered to evaluate its possible reutilization.

2. Experimental – Biochar (BC) from SBG was produced by microwave-assisted pyrolysis at 800 °C and a residence time of 20 min followed by acid washing with HCl and final washing with water until a neutral pH was reached in the leachate. BC was characterized by the point of zero charge (PZC), N_2 adsorption isotherms for specific surface area (S_{BET}) and microporosity determination, and mercury intrusion experiments to determine the apparent density. The fixed-bed performance of BC in the removal of antibiotics under continuous operation mode was evaluated using column reactors. All fixed-bed experiments were performed in a CHROMAFLEX® glass column (13 cm total height, 1 cm internal diameter), with an acrylic jacket at a constant temperature of 25 ± 1 °C, using a thermostatic recirculating bath (HAAKE A10, Thermo Scientific). The column was packed with BC with a constant bed depth (Z) of 4.4 cm, corresponding to ~2 g of BC, using a flow adapter of 20 µm porosity HDPE bed support.
Fixed-bed studies on the adsorptive removal of pharmaceuticals by BC in continuous operation mode were carried out in three subsequent stages: *i)* Study of the effect of flow rate on the adsorption of SMX, TMP, and CIP, using buffered distilled water (pH 8.0) as a matrix; for this purpose, the fixed-bed column was fed with single solutions of SMX, TMP, and CIP (influent concentration of 20 µmol L^{-1}) at flow rates of 1, 2, and 4 L d^{-1}. *ii)* Study of the adsorption of SMX, TMP, and CIP from single (20 µmol L^{-1}) or ternary (20 µmol L^{-1} of each pharmaceutical) solutions in buffered distilled water fed at the previously optimized flow rate (2 L d^{-1}). *iii)* Thermal regeneration of exhausted BC was performed by microwave pyrolysis (600 °C under N_2 atmosphere for 20 min). The regenerated BC was packed into the column for a second adsorption cycle using TMP as the case study, under a flow rate of 2 L d^{-1}. Subsequently, the regenerated and exhausted BC was subjected to a second thermal regeneration and fixed-bed adsorption was repeated under the same conditions.
Experimental data from the breakthrough curves were modeled using Thomas, Yan, Yoon–Nelson, and Clark models.

3. Results and Discussion – The material obtained had an SBET value of 280 m2 g-1 and an apparent density of 0.905 g cm-3. BC showed a PCZ of 5, indicating a slightly acidic surface.
Based on the breakthrough curves, the optimal flow rate was determined to be 2 L d-1 (as shown in Figure 1). The highest bed adsorption capacity, either from a single or ternary solution, was observed for TMP, followed by CIP and then SMX, which may be related to non-favorable electrostatic interactions between SMX and BC at the working pH (pH 8).
For all three antibiotics, the bed adsorption capacity from the ternary solution was notoriously lower than that of their respective single solutions, decreasing in the order SMX>CIP>TMP. Regeneration studies showed that the BC adsorption capacity decreased after the first and second stages of thermal regeneration.
The fits of the experimental breakthrough curves to the Thomas, Yoon-Nelson and Yan models showed high R^2 values (≥0.995).

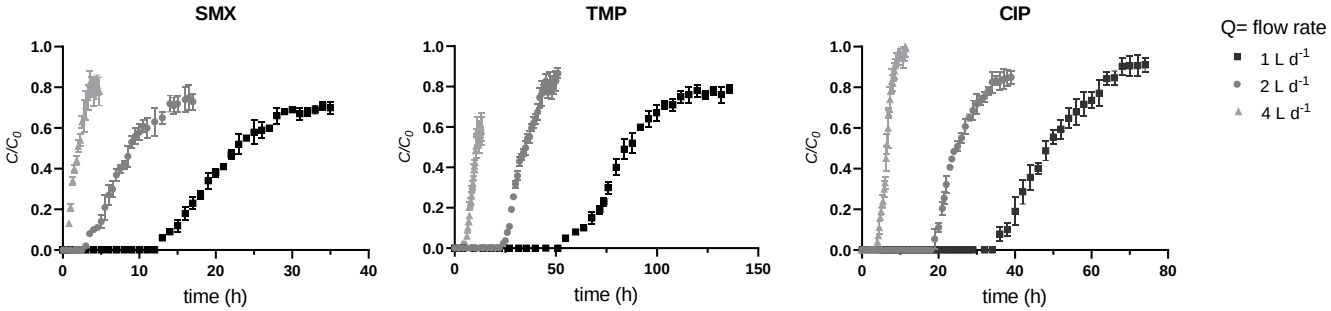

Figure 1. Breakthrough curves for the adsorption of SMX, TMP and CIP onto BC at flow rates of 1 L d^{-1}, 2 L d^{-1}, and 4 L d^{-1}.

4. Conclusions – Fixed-bed adsorption of SMX, TMP, and CIP was successfully performed using BC from SBG as adsorbent. The adsorption of these antibiotics from their single solution in distilled water showed that the bed capacity decreased in the order TMP>CIP>SMX. Due to competitive effects, the bed capacity was lower for the ternary solution of these antibiotics than for their single solution, decreasing in the order SMX>CIP>TMP. The thermal regeneration process carried out with the exhausted BC provided good results in terms of reusability, but only for one cycle. It must be highlighted that few studies have explored the application of BC derived from industrial residues for the removal of pharmaceuticals from water in fixed-bed systems. Therefore, our research fills this critical gap and provides a novel approach to wastewater treatment.

Acknowledgements: This work was developed within the project SYNERGY (2022.02028.PTDC), supported by national funds (OE), through FCT/MCTES. The authors acknowledge financial support to CESAM by FCT/MCTES (UIDP/50017/2020+UIDB/50017/2020+LA/P/0094/2020) supported by national funds. Érika M.L. Sousa thanks her PhD grant (2020.05390.BD), supported by FCT.

5. References

[1] É.M.L. Sousa, M. Otero, M. V Gil, P. Ferreira. *Environ. Technol. Innov.* **30** (2023) 103074.
[2] É.M.L. Sousa, M. Otero, L.S. Rocha, M. V. Gil, P. Ferreira, V.I. Esteves, V. Calisto,. *J. Hazard. Mater*. **431** (2022) 128556.

P47: Selective recovery of platinum group metals from HCl-based leachates using bio-based materials

A. Nobahar [(1)], F. H. B. Sosa[(1)], H. Passos[(2)(3)], J.A.P. Coutinho[(1)]

[(1)]CICECO - Aveiro Institute of Materials, Department of Chemistry, University of Aveiro, 3810-193 Aveiro, Portugal
anobahar@ua.pt
[(2)]LSRE-LCM – Laboratory of Separation and Reaction Engineering – Laboratory of Catalysis and Materials, Faculty of Engineering, University of Porto, Porto, Portugal
[(3)]ALiCE – Associate Laboratory in Chemical Engineering, Faculty of Engineering, University of Porto, Porto, Portugal.
filipesosa@ua.pt; hpassos@fe.up.pt; jcoutinho@ua.pt

1. Introduction

The recovery of Platinum Group Metals (PGMs) such as platinum, palladium, and rhodium is of significant interest due to their high economic value and essential role in various industrial applications. Traditional recovery methods often involve complex and expensive processes with various environmental impacts. Previous studies have highlighted the potential of biological materials in metal recovery due to their specificity and eco-friendliness [1-3]. Bio-based materials are known to adsorb metals through different mechanisms including ion exchange, complex formation, electrostatic interaction, chelation, redox mechanisms, and precipitation [4]. In this study, we investigated the selective interaction of lyophilized egg white with PGMs from a model multimetallic solution and an HCl-based leaching solution derived from spent catalytic converters. For comparison, we tested the PGM adsorption efficiency of pure egg albumin. Finally, we explored the mechanisms involved in the separation of PGMs by the tested bio-based materials from multimetallic solutions.

2. Results and Discussion

Results of this study showed a high adsorption tendency of tested material toward PGMs. Lyophilized egg white as raw material demonstrated superior performance in selective separation and recovery of PGMs, with minor co-adsorption of other metals. Pure albumin revealed similar PGMs adsorption rates with lyophilized egg white, indicating the significant role of this protein in adsorption behaviour of the lyophilized egg white.
Various factors including adsorption isotherms and kinetics, adsorption capacity, effect of pH, temperature and contact time were studied.

3. Conclusions

This study demonstrates that lyophilized egg white is effective, sustainable material for the selective recovery of PGMs from HCl-based solutions. These findings offer a promising alternative to conventional methods, potentially leading to more cost-effective and environmentally friendly recovery processes.

This work was supported by national funds through FCT/MCTES (PIDDAC): LSRE-LCM, UIDB/50020/2020 (DOI: 10.54499/UIDB/50020/2020) and UIDP/50020/2020 (DOI: 10.54499/UIDP/50020/2020); ALiCE, LA/P/0045/2020 (DOI: 10.54499/LA/P/0045/2020); CICECO, UIDB/50011/2020, UIDP/50011/2020 & LA/P/0006/2020. This work was also financially supported by national funds through FCT – Fundação para a Ciência e a Tecnologia, I.P., within the scope of the project PlatILPlus (2022.04478.PTDC, DOI: 10.54499/2022.04478.PTDC). F.H.B. Sosa acknowledge FCT for the researcher contract CEECIND/07209/2022 (DOI 10.54499/2022.07209.CEECIND/CP1720/CT0019).

5. References

[1] Grilli, M.L., Slobozeanu, A.E., Larosa, C. et al. *Crystals*, 13(4), (2023), p. 550 .
[2] MacDonald, L., Zhang, D. and Karamalidis, A. *RCR Advances*, 205, (2024), p. 107590.
[3] Kinas, S., Jermakowicz-Bartkowiak, D. Pohl, P. et al. *Hydrometallurgy* 223, (2024), p. 106222.
[4] Bilal, M., Ihsanullah, I. and Younas, M. et al. *Sep. Purif. Technol.* 278, (2021), p. 119510.

P48: Enhancement of gas transport properties of polyurethane-based membranes for blood oxygenation

Tiago Ferreira[(1)*], Rita F. Pires[(1)], Inês Coelho[(1)], Sérgio B. Gonçalves[(2)], Vasco D.B. Bonifácio[(3)], Moisés L. Pinto[(4)], Mónica Faria[(1)]

[(1)] Center of Physics and Engineering of Advanced Materials (CeFEMA), Laboratory for Physics of Materials and Emerging Technologies (LaPMET), Chemical Engineering Department, Instituto Superior Técnico, Universidade de Lisboa, Lisbon, Portugal
tiago.j.ferreira@tecnico.ulisboa.pt
[(2)] IDMEC, Instituto Superior Técnico, Universidade de Lisboa, Av. Rovisco Pais, 1049-001 Lisbon, Portugal
[(3)] iBB-Institute for Bioengineering and Biosciences and i4HB-Institute for Health and Bioeconomy, Bioengineering Department, Instituto Superior Técnico, Universidade de Lisboa, Lisbon, Portugal
[(4)] Centro de Recursos Naturais e Ambiente (CERENA), Chemical Engineering Department, Instituto Superior Técnico, Universidade de Lisboa, Lisbon, Portugal

1. Introduction – Extracorporeal Membrane Oxygenation (ECMO) is essential for severe respiratory and cardiac failures. Its core component is a membrane blood oxygenator (BO). The current BOs, even though they have large membrane surface areas, exhibit poor hemocompatibility, which triggers coagulation. Despite technological advances, there is no BO currently available that efficiently supports prolonged ECMO. Our research team has previously reported on the production of membranes using polyurethane (PUR) and polycaprolactone (PCL) [1], which exhibited good hemocompatibility and high permeability to carbon dioxide (CO_2). However, permeability to oxygen (O_2) fell below the requirements for efficient blood oxygenation. Therefore, our research has focused on the development of new PUR-based blend membranes that can offer improved O_2 permeability, hemocompatibility, and durability, in association with a good flex-life and mechanical strength [2,3].

2. Results and Discussion - In this work, two groups of nonporous symmetric membranes were prepared by the solvent evaporation technique: pure polyurethane (PU) membranes, and polyurethane blend membranes prepared with different total polymer/solvent and polyurethane/second reagent weight ratios. All the membranes were fully characterized, and their mechanical properties were evaluated. Single gas O_2 and CO_2 permeation studies were conducted using the constant volume method at 37°C in an in-house built gas permeation set-up. The permeability coefficients ranged from 239 to 347 Barrer for CO_2 and 26 to 30 Barrer for O_2. The ranges obtained for the diffusion coefficients by the time-lag method were $1.4x10^{-6}$-$3.0x10^{-6}$ cm^2/s for CO_2 and $2\ x10^{-6}$-$2.5x10^{-6}$ cm^2/s for O_2, and the ranges obtained for the solubility coefficients were $116x10^{-4}$-$186x10^{-4}$ $cm^3/cm^3.cmHg$ for CO_2, and $11x10^{-4}$-$13x10^{-4}$ $cm^3/cm^3.cmHg$ for O_2. Gas adsorption measurements are also performed using an experimental setup based on the barometric method [2] to independently measure the solubility coefficients of the studied gases in a test membrane. This is done to further validate the estimates of the solubility (and hence also diffusion) coefficients obtained by the application of the time-lag method to the pressure vs. time results obtained with the built gas permeation setup. The solubilities obtained by the barometric method coincide, within the experimental uncertainty, with the results obtained from the time-lag method for the studied gases, fully validating the application of this method to the pressure vs. time data, and the solubility and diffusion coefficients obtained therefrom.

3. Conclusions – PU-based membranes can afford high permeability to CO_2, but the permeability values of O_2 still fall below the requirements for efficient blood oxygenation. Future work includes exploring the preparation of PU-based mixed matrix membranes incorporating metal-organic frameworks (MOFs) to improve the O_2 permeability while maintaining high CO_2 permeability.

Acknowledgments: This work was supported by Fundação para a Ciência e a Tecnologia (FCT, Portugal) through project PTDC/MEC-ONC/29327/2017 and CeFEMA programmatic funding UIDB/04540/2020 and UIDP/04540/2020 and through IDMEC, under LAETA, project UIDB/50022/2020. The preparation of PU-based mixed matrix membranes incorporating metal-organic frameworks (MOFs) is included in a project that has received funding from the European Union's Horizon Europe research and innovation programme under grant agreement Nº 101130006. Views and opinions expressed are however those of the author(s) only and do not necessarily reflect those of the European Union or European Innovation Council. Neither the European Union nor the granting authority can be held responsible for them.

5. References

[1] M. C. Besteiro, A. J. Guiomar, C. A. Gonçalves, V. A. Bairos, M. N. de Pinho, M. H. Gil, J. Biomed. Mater. Res. Part A, 93A(3), (2010) pp. 954-964.
[2] T. M. Eusébio, A. R. Martins, G. Pon, M. Faria, P. Morgado, M. L. Pinto, E. J. M. Filipe, M. N. de Pinho, Membranes, 10(1), (2020) 8.
[3] I. Coelho, R. F. Pires, S. B. Gonçalves, V. D. B. Bonifácio, M. Faria, Membranes, 12(9), (2022) 826.

P49: Porous Ti-MOF for Dual Release of NO/H2S for Therapeutic Applications

M. Batista [(1)] , S. Wang [(2)], C. Serre[(2)], M.L. Pinto [(3)], J. Pires[(1,*)]

[(1)] *CQE, Centro de Química Estrutural, Institute of Molecular Sciences, Departamento de Química e Bioquímica, Universidade de Lisboa, Campo Grande, 1749-016, Lisboa, Portugal.*
**jpsilva@ciencias.ulisboa.pt*
mkbatista@ciencias.ulisboa.pt
[(2)] *Institut des Matériaux Poreux de Paris, Ecole Normale Supérieure, ESPCI Paris, CNRS, PSL University, 75005 Paris, France*
[(3)] *CERENA, Departamento de Engenharia Química, Instituto Superior Técnico, Universidade de Lisboa, Campus Alameda, 1049-001, Lisboa, Portugal.*
moises.pinto@tecnico.ulisboa.pt

1. Introduction – Gasotransmitters such as nitric oxide (NO) and hydrogen sulfide (H_2S) play crucial roles in several physiological processes, including vasodilation, angiogenesis, immune and inflammatory responses, neurotransmission, apoptosis, and regulation of gene transcription [1]. This broad spectrum of functions prompted the intense research for vehicles to target deliver these gases at controlled rates, and for predetermined durations, as a potential treatment for medical conditions where exogenous delivery therapy may be beneficial to supplement or regulate local NO and H_2S levels. Although current knowledge indicates that cooperation between NO and H_2S signalling pathways is essential for many of their shared physiological roles, the development of porous materials for the simultaneous release of these gasotransmitters is still in a primordial stage of study, since most research efforts focus on singular gas delivery. In this context, we propose a titanium-based metal-organic framework (MOF), named MIP-177, as a potential dual carrier for NO/H_2S. The characterization of the sample MIP-177 and NO adsorption/release capacity for therapeutic applications has already been studied [2]. The current research on this material has assessed its adsorption capacity for H_2S using a volumetric method and examined the H_2S-release under physiological conditions (Fig. 1).

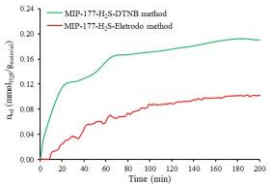

Fig. 1. H_2S release in liquid phase obtained from the two methodologies at room temperature.

2. Experimental - The experimental determination of the H_2S amounts released from the porous materials in the liquid phase was time-consuming and challenging. For this, two methodologies were used, the detection through the DTNB reaction and an H_2S-electrode. To evaluate the influence of NO on the H_2S release kinetics in the MIP-177 system loaded simultaneously with NO/H_2S, two systems were studied. For this, the composite pellets were loaded with H_2S and NO/H_2S, respectively. Then the H_2S release in both system loads was obtained by the DTNB and H_2S-electrode methods.

3. Results and Discussion - Currently, studies are underway to evaluate the additional effects of H_2S on the overall gas (NO and H_2S) delivery potential, as well as its impact on physiological phenomena such as wound healing.

4. Conclusions – The MIP-177, a titanium-based metal-organic framework-MOF, is a most promising material for therapeutic applications, showing a good balance between H_2S/NO adsorption and release.

Acknowledgments:
This research was financed by Fundação para a Ciência e a Tecnologia (FCT) in the scope of the projects UIDB/00100/2020 (CQE), UIDB/04028/2020 (CQE), UIDB/04028/2020, and UIDP/04028/2020 (CERENA), and the Institute of Molecular Sciences (IMS) Associate Laboratory funded by FCT through project LA/P/0056/2020 and the project 2022.05605.PTDC (DOI 10.54499/2022.05605.PTDC)

5. References

[1] J. Fu, Y. Mao, J. Han, P. Zhang, Y. Tan, J. Hu, P. H. Seeberger and J. Yin, Biomat. Adv., 144 (2024) p. 213309.
[2] R. V. Pinto, S. Wang, S. R. Tavares, J. Pires, F. Antunes, A. Vimont, G. Clet, M. Daturi, G. Maurin, C. Serre and M. L. Pinto, Angew. Chem. Int. Ed., 59, (2020) p. 5143.

P50: Adsorption desalination using LTA type zeolites: A molecular simulation approach

A. Smetsers [(1)], S. Calero [(1)], A. Martin-Calvo [(2)]

[(1)] *Department of Applied Physics, Eindhoven University of Technology, Eindhoven, The Netherlands*
a.a.smetsers@student.tue.nl
Eindhoven University of Technology, 5600MB Eindhoven, The Netherlands
[(2)] *Center for Nanoscience and Sustainable Technologies (CNATS), Universidad Pablo de Olavide, Seville, Spain.*
s.calero@tue.nl, amarcal@upo.es

1. Introduction – Drinking water is an essential good for life, but its supply is not infinite. The increasing lack of rain, the exponential population growth and water consumption make the water scarcity a global problem. Increasing the production of water from unconventional water sources, such as seawater or wastewater, is an increasingly widely supported solution to meet the demand for freshwater consumption and irrigation [1]. However, converting saline water into freshwater remains a major challenge on the production process [2]. Commonly, distillation and reverse osmosis are used as desalination processes, as these are the most developed techniques, but the cost-effective provision of freshwater using these techniques is not straight forward due to their high energy demand [3]. It is found that adsorption desalination is a promising method for desalinating seawater due to its low running costs, low environmental impact through its use of waste energy resources, and high salt removal efficiency [4]. For adsorption desalination, zeolites are one of the most suitable and accessible adsorbents for desalinating water through water adsorption and cationic exchange [5]. Besides their functional benefits, zeolites are also a more environmental-friendly alternative due to their non-toxicity and safe operation.

2. Methods and Materials - This work has performed GCMC simulations using the RAPSA software [6] to investigate the effects of various NaCl and $CaCl_2$ solutions and cation compositions on the water adsorption and cation exchange in the commercially available LTA zeolite with different cation compositions: LTA_SI, NaLTA, CaLTA, and NaCaLTA. The systems are analysed through water adsorption isotherms, Average Density Profiles, and Radial Distribution Functions at a water saturation pressure of 10 kPa.

3. Results and Discussion - Water adsorption isotherms for the salt concentrations per LTA structure show that high amount of $CaCl_2$ yields to the greatest adsorption in all structures. Comparing the isotherms per structure among each other reveals that CaLTA produces the highest water adsorption across all salt concentrations. These findings support the notion that Ca^{2+} cations benefit the adsorption of water in the structure. Average Density Profiles show a significant influence of salt type and concentration in the pure silica LTA (Figure 1), and a perceived influence of the type of extra-framework cations in systems without salt. Furthermore, it is found that water molecules cluster together in the structures, presumably around the present cations. Higher salt concentrations and Ca^{2+} cations have the largest effect on the nucleation of water molecules. Radial Distribution Functions for the distance between the Oa atoms in the structure and the cations in the water saturated system configuration reveal that NaLTA and NaCaLTA have interesting properties for cation exchange for the higher concentrations of $CaCl_2$. A slight shift in position of the extra-framework cations is observed as a consequence of adding salt in the system. For which, independent of the type of salt added, the Na^+ framework cations move closer to the structure in NaLTA, and the Ca^{2+} framework cations move further away from the structure in CaLTA, in the presence of higher salt concentrations. This effect can be attributed to the hydration of the cations due addition of salt.

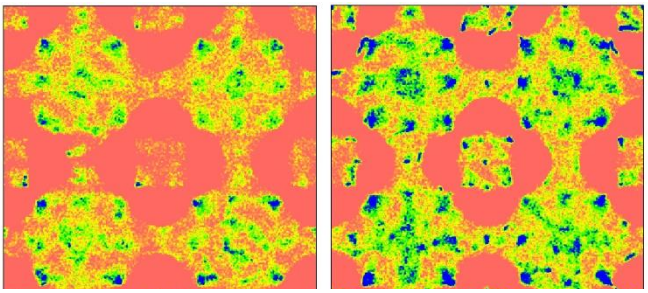

Figure 1: Average density profile of water in LTA-SI with low (left) and high (right) amount of NaCl. Color gradation goes from orange to blue from the less to the most populated parts of the structure

4. Conclusions - In this study, the LTA structures, especially when containing $Ca^{2+,}$ show increased hydrophilicity and water nucleation, revealing potential to be used in desalination through water adsorption. NaLTA and NaCaLTA show possibility for selective desalination of Ca^{2+} salt cations through cation exchange and their suitability could be compared with other porous structures by measuring their Cation Exchange Capacity or salt removal percentages.

5. References

[1] Y. Ibrahim, et al. Desalination, 498, 114798 (2021)
[2] M. Elimelech and W. A. Phillip. Science, 333(6043), p712–717 (2011)
[3] H. Manchanda and M. Kumar. Environmental Progress & Sustainable Energy, 37(1), p444–464 (2018)
[4] P. G. Youssef, et al. Energy Procedia, 61, p2604–2607 (2014)
[5] B. Qiu, et al. Chinese Journal of Chemical Engineering, 42, p151–169, (2022)
[6] D. Dubbeldam, et al. Molecular Simulation, 42(2), p81–101, (2016)

P51: Unveiling acid sites of Nb2O5 for microalga Chlorella sp. valorisation by ssNMR

M. Ilkaeva [1], S. Lima [2], E. García-López [2], I. Krivtsov [1], C. Bornes [3], L. Mafra [3], F. Scargiali [2], G. Marcì [2]

[1] *Department of Chemical and Environmental Engineering, University of Oviedo, Av. Julián Clavería 8, 33006 Oviedo, Spain*
ilkaevamarina@uniovi.es
[2] *University of Palermo, Department of Engineering, Viale delle Scienze Ed. 6, 90128 Palermo, Italy*
giuseppe.marci@unipa.it
[3] *CICECO - Aveiro Institute of Materials, Department of Chemistry, University of Aveiro, Campus Universitário de Santiago, 3810-193 Aveiro, Portugal*

1. Introduction – Exploration of the alternative and sustainable feedstocks has recently attracted substantial attention because of the shortage, high cost and environmental impact of fossil resources. Biomass, which is available in large amounts is an important part of renewable energy. In particular, microalgae are quite attractive as a renewable biomass with a wide range of applications. 5-hydroxymethylfurfural (5-HMF) is one of the top value-added bio-based platform chemicals produced from lignocellulosic biomass or biomass-derived hexose sugars by an acid-catalysed dehydration reaction. Among heterogeneous solid acid catalysts Nb_2O_5 stands out as abundant and cheap material with water-tolerant and tunable acid-base properties showing promising performance in sugar conversion reactions. In this work a systematic study of the structure-activity relationships of niobium oxide calysts applied for aqueous phase dehydration of algal biomass substrates to obtain furanic derivatives has been conducted [1].

2. Experimental - A set of niobia catalysts has been prepared and thoroughly characterized. The acidity of the materials was evaluated using temperature-programmed NH_3 desorption (NH_3-TPD) approach, but also applying P-bearing probe molecule-assisted solid-state nuclear magnetic resonance (NMR) technique enabling acidity assessment of non-thermally treated catalysts allowing for the distinction between Lewis and Brønsted acid sites. The glucose dehydration has been used as a model reaction to study its catalytic isomerisation to fructose occurring on Lewis acid sites and the successive fructose dehydration to 5-HMF over Brønsted acid sites. Eventually, the microalgae *Clorella sp.* biomass was used as real substrate to obtain 5-HMF and furfural products.

3. Results and Discussion – The best Nb_2O_5 catalysts for valorizing *Chlorella sp*. into furans exhibited a larger number of Brønsted acid sites. Employing these catalysts, we achieved yields of 5-HMF and furfural of ca. 20-22 % with respect to the extracted sugars from algae. The results showed a discernible dependence of the yields to 5-HMF and furfural on catalyst overall acidity, specific surface area, and the presence of the Brønsted acid sites. The acid properties studied by ssNMR indicates that the Nb_2O_5 prepared by an hydrothermal method in the presence of H_2O_2 and calcined at 300°C is the sample with the greatest amount of Lewis sites, therefore, justifying the higher yield of 5-HMF starting from a glucose solution [1]. Instead, when *Chlorella sp.* aqueous suspension was the starting material after the a preliminar stage dedicated to the release of carbohydrates present in the algae cells and the hydrolysis of the long chains of polymeric sugars, part of them remained in the form of polysaccharides whose hydrolysis to hexoses and pentoses is favored by the presence of Brønsted acids.

4. Conclusions –The feasibility of the valorisation process of *Chlorella sp.* as substrate in the presence of Nb_2O_5 using an eco-friendly catalytic approach was demonstrated. It was found that the most acidic catalysts (having more Lewis and Brønsted acid sites) are those capable of better hydrolysing residual polysaccharides into monosaccharides that can be transformed to 5-HMF with the highest yields.

5. References

[1] S. Lima et al., J. Catal., 434, (2024) p. 115457.

P52: Separation of volatile fatty acids with adsorption-based methods

C. Gomes [(1),(2)], A. M. Ribeiro [(1),(2)], A. Rodrigues[(1),(2)], A. Ferreira[(1),(2)]

[(1)] LSRE-LCM – Laboratory of Separation and Reaction Engineering - Laboratory of Catalysis and Materials, Faculty of Engineering, University of Porto, Rua Dr. Roberto Frias, 4200-465 Porto, Portugal
[(2)] ALiCE – Associate Laboratory in Chemical Engineering, Faculty of Engineering, University of Porto, Rua Dr. Roberto Frias, 4200-465 Porto, Portugal.
up201403931@edu.fe.up.pt
apeixoto@fe.up.pt, arodrig@fe.up.pt, aferreir@fe.up.pt

1. Introduction – Volatile Fatty Acids (VFA) are usually used as precursors in the food, pharmaceuticals, chemicals, cosmetics, bioenergy industries, making them attractive and valuable compounds in the market. Typically, VFA are produced via petrochemical routes. However, due to the negative health and environmental effects, the interest in developing sustainable processes for volatile fatty acids production has increased. An alternative and more sustainable VFAs production method is via biological means, like acidogenic fermentation of wastewater [1]. However, not processed, and mixed VFAs are less valuable than the refined acids or even pure. Therefore, separating the acids into a more worthy form is needed to be used for their intended purpose. Several methods have already been researched for this end, such as precipitation, distillation, electrocoagulation, pervaporation, adsorption, nanofiltration, reverse osmosis. Adsorption is a highly studied method for VFAs separation, since it is relatively easy to operate, has high selectivity, and has a variety of materials [2]. Different adsorbents have been tested to recover volatile fatty acids. Adsorbents with polystyrene-divinylbenzene or acrylic matrixes are most widely used for this end, especially those containing functional groups, such as primary, secondary, tertiary amines and quaternary ammonium. The tertiary amino resins have the strongest interactions with VFAs at optimal pH 2.5-4.5, and non-functionalized ones present different affinities to each acid [3-6].
This work intends to report a complete analysis of adsorption/desorption of volatile fatty acids. Therefore, batch experiments were carried out in different adsorbents to assess the adsorption equilibrium data and to select the resin more suitable for acids separation. VFA adsorption and desorption was also analysed in a dynamic system through fixed-bed experiments. All experiments were coupled with mathematical modelling. Furthermore, a SMB unit was modelled to assess the VFA separation.

2. Experimental - Different resins (one non-functionalized – Amberlite XAD-4, two functionalized with tertiary amines – Amberlite IRA-67 and Amberlyst A21, and one with quaternary ammonium – Dowex Marathon MSA) were evaluated in terms of adsorption equilibrium, in batch mode, with single-component aqueous solutions of the following VFA: acetic, propanoic, butyric, isobutyric, valeric, isovaleric and hexanoic acids. Single-site Langmuir model was adjusted to the equilibrium experimental results. Single and multicomponent breakthrough experiments were also performed using a lab-scale fixed-bed set-up, packed with the adsorbent that achieved the best performance in the batch experiments, i.e., that showed different affinities to each volatile fatty acid. Single and multicomponent breakthrough curves were used to validate the fixed-bed mathematical model. To evaluate the VFA separation with a Simulated Moving Bed (SMB) unit, the separation region was computed.

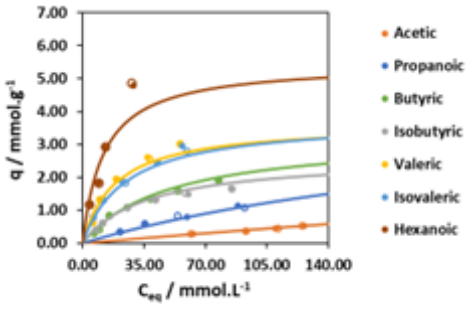

Image 1. Adsorption equilibrium isotherms.

3. Results and Discussion – Adsorption equilibrium isotherms were obtained for each individual acid at pH 3 and 25 °C, in the four adsorbents: Amberlyst A21, Amberlite IRA-67, Amberlite XAD-4 and Dowex Marathon MSA. From the equilibrium results obtained, it was concluded that the non-functionalized resin (Amberlite XAD-4) would be the most suitable adsorbent to separate/fractionate the volatile fatty acids since it displays different selectivity to each acid, allowing a higher potential for the VFAs fractioning. Image 1 shows the adsorption equilibrium data for the Amberlite XAD-4 adsorbent, as well as the isotherm model fitting.

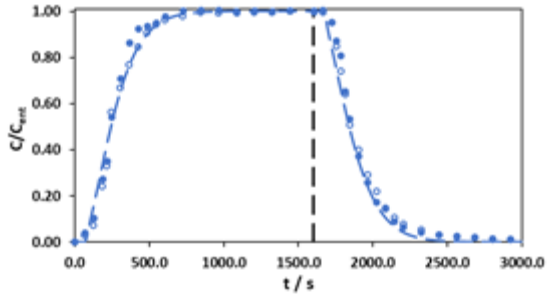

Image 2. Single-site breakthrough curve of acetic acid

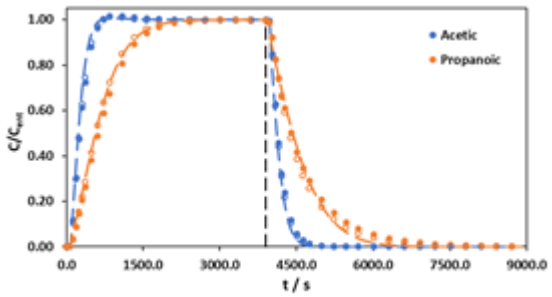

Image 3. Binary breakthrough curve of acetic and propanoic acids

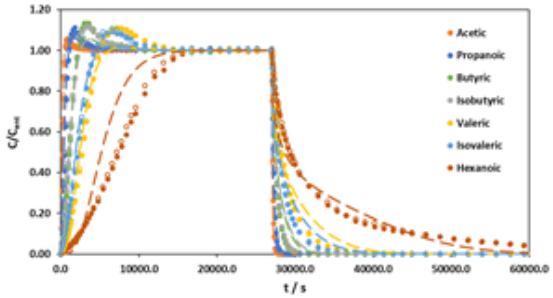

Image 4. Multicomponent breakthrough curve

Breakthrough curves were acquired for single-component solutions of every acid in study, for binary solutions of acetic acid with every other acid, propanoic acid with every other acid and for a multicomponent solution with all VFA, at pH 3 and room temperature (22-25 °C). In the desorption step, water was used as desorbent, that way the adsorption equilibrium isotherms could be used in the mathematical model simulations for both breakthrough steps. Single-component breakthrough curve of acetic acid, binary breakthrough curve of acetic and propanoic acids and breakthrough curve with all the acids are shown in Images 2, 3 and 4, respectively, as well as the mathematical model simulations (in dashed lines). The mathematical model applied was able to give a good prediction of the experimental results, which means that the equilibrium and kinetics parameters determined are accurate enough to estimate the behaviour of VFA adsorption. Bearing in mind all the results performed of single and multicomponent breakthrough curves, it is important to highlight that when the adsorbent is regenerated and reused, the breakthrough curves obtained, under the same conditions, did not show significant differences, confirming the efficiency of water as desorbent and the complete reversibility of the adsorption phenomenon in the Amberlite XAD-4 adsorbent.

The separation of volatile fatty acids was then assessed in a SMB unit, firstly by drawing the separation region for a solution with acetic and propanoic acids and simulating an operating point inside that region.

4. Conclusions - This study explored the adsorption equilibrium of acetic, propanoic, butyric, isobutyric, valeric, isovaleric and hexanoic acids, in four different adsorbents. From the four adsorbents studied, the non-functionalized resin (Amberlite XAD-4) was selected, due to the different adsorption capacity achieved for each acid and higher potential to separate the volatile fatty acids. In the fixed-bed experiments, the adsorption equilibrium was proved to be the same in batch and dynamic modes and the mathematical model applied was capable of predicting the experimental data for the single and multicomponent breakthrough curves.

Acknowledgement

This work was supported by national funds through FCT/MCTES (PIDDAC): LSRE-LCM, UIDB/50020/2020 (DOI: 10.54499/UIDB/50020/2020) and UIDP/50020/2020 (DOI: 10.54499/UIDP/50020/2020); and ALiCE, LA/P/0045/2020 (DOI: 10.54499/LA/P/0045/2020). This work was also financially supported by CONSERVAL Project, 0679_CONSERVAL_1_E, co-financed by the European Regional Development Fund (ERDF) through the Interreg V-A Spain-Portugal Program (POCTEP). Cristiana Gomes acknowledges her PhD scholarship 2021.05666.BD funded by FEDER funds through NORTE 2020 and by national funds through FCT/MCTES.

5. References

[1] Aghapour Aktij, S., et al., Journal of Industrial and Engineering Chemistry, 81, (2020) p. 24-40.
[2] Yesil, H., et al., Water Science & Technology, 69, (2014) p. 2132.
[3] Reyhanitash, E., et al., ACS Sustainable Chemistry & Engineering, 5, (2017) p. 9176-9184.
[4] Rebecchi, S., et al., Chemical Engineering Journal, 306, (2016) p. 629-639.
[5] Fargues, C., et al., Industrial & Engineering Chemistry Research, 49, (2010) p. 9248-9257.
[6] Eregowda, T., et al., Separation Science and Technology, (2019) p. 1-13.

P53: Fast method for the evaluation of CO2 adsorption capacity of materials

V. Silva [(1)], B. Abreu [(2)], L. Gando-Ferreira [(3)]

[(1)] University of Coimbra, CIEPQPF, Department of Chemical Engineering, Faculty of Sciences and Technology, Polo II, Rua Sílvio Lima, 3030-790 Coimbra, Portugal;
CeNTI – Centre for Nanotechnology and Advanced Materials;
vsilva@centi.pt
[(2)] CeNTI – Centre for Nanotechnology and Advanced Materials;
babreu@centi.pt
[(3)] University of Coimbra, CIEPQPF, Department of Chemical Engineering, Faculty of Sciences and Technology, Polo II, Rua Sílvio Lima, 3030-790 Coimbra, Portugal;
lferreira@eq.uc.pt

1. Introduction – Over the past few years, climate change on our planet has become a major concern. The Earth's average global temperature has increased by about 1 degree Celsius since the pre-industrial period. This increase is driven by the burning of fossil fuels, leading to higher levels of greenhouse gases, with carbon dioxide being the most harmful. To combat climate change and achieve decarbonization, the evaluation and implementation of CO_2 capture technologies are necessary. This capture can be classified as pre-combustion, oxy-combustion, or post-combustion, with the latter being the focus of this work. Post-combustion CO_2 capture involves separating and storing carbon dioxide from combustion gases after combustion. This technology can be carried out by several techniques, with adsorption being one of the most promising [1]. Adsorption can be either chemical (covalent bonds) or physical (van der Waals molecular interactions) in nature, with adsorbents similarly classified as chemical or physical. Compared to chemical adsorbents, physical adsorbents offer benefits in terms of energy efficiency, selectivity, adsorption capacity and regeneration. The most promising physical adsorbents for use in post-combustion technologies are zeolites, carbon-based materials, silica-based materials, and metal-organic frameworks (MOFs) [2][3]. To evaluate the adsorption capacity of each adsorbent, it is first necessary to perform adsorption isotherms and later fixed-bed adsorption tests. However, these methods are commonly expensive, difficult to access, and do not provide real-time results, presenting a limitation when investigating new materials for CO_2 adsorption that require progressive optimization, involving the analysis of a large number of samples [4]. Thus, the need arose to develop a low-cost real-time characterization method that would allow for this optimization in a short period. In this work, a method was developed that uses a thermogravimetric balance and a gas injection reactor under controlled pressure allowing us to compare and select the most efficient materials in real time, in an iterative approach.

2. Experimental - Different groups of materials were prepared, to compare their CO_2 adsorption capacity: 1) non-covalent hybrid materials combining silica or zeolites with graphene (*via* electrostatic attractions in aqueous medium); 2) dry hydrogels (prepared through freeze drying). Hydrogels were prepared with polyethyleneimine, hydroxypropyl cellulose, and carboxymethyl cellulose [5]. Further, the impact of the addition of carbon nanotubes was evaluated. To evaluate the CO_2 adsorption capacity, the material is placed in the thermogravimetric balance, where it undergoes drying at 120 °C to remove moisture and impurities. It is then exposed to air for 15 minutes and dried again in the balance at 120°C. Next, it goes to the reactor, where it is in contact with pure carbon dioxide at 1 bar for 15 minutes, and finally, it is dried again in the balance at 120 °C. The mass of adsorbed CO_2 is thus calculated by the difference in mass lost with and without CO_2 injection.

3. Results and Discussion – In this work, several materials were prepared and tested for their CO_2 adsorption capacity at atmospheric conditions using a developed methodology. For each material, a control test was conducted for air exposure, for proper comparison with pure carbon dioxide exposure. It was found that the combination of materials through electrostatic attractions has a negative impact on CO_2 adsorption, with zeolites showing better performance without modifications. For hydrogels, the efficiency was clearly improved, which can be attributed to the morphology of these materials, reaching a CO_2 adsorption capacity of 113 mg/g. To enhance the mechanical and thermal properties of these materials, carbon nanotubes were added. However, it was found that carbon nanotubes impaired the adsorption capacity of the hydrogels, as corroborated by TGA analysis and adsorption isotherms.

4. Conclusions – The methodology developed in this work allowed for a fast evaluation of the CO_2 adsorption capacity of materials, permitting a progressive optimization of the preparation method and composition of materials, in an iterative approach. This work paves the way for further material optimization, using a cost-effective and fast methodology to evaluate CO_2 adsorption.

5. References

[1] M. A. Scibioh and B. Viswanathan, "CO2 - Capture and Storage," in Carbon Dioxide to Chemicals and Fuels, Elsevier, 2018, pp. 61–130. doi: 10.1016/b978-0-444-63996-7.00003-1.
[2] R. Ben-Mansour et al., "Carbon capture by physical adsorption: Materials, experimental investigations and numerical modeling and simulations - A review," Applied Energy, vol. 161. Elsevier Ltd, pp. 225–255, Jan. 01, 2016. doi: 10.1016/j.apenergy.2015.10.011.
[3] B. Dziejarski, J. Serafin, K. Andersson, and R. Krzyżyńska, "CO2 capture materials: a review of current trends and future challenges," Materials Today Sustainability, vol. 24. Elsevier Ltd, Dec. 01, 2023. doi: 10.1016/j.mtsust.2023.100483.
[4] M. Thommes et al., "Physisorption of gases, with special reference to the evaluation of surface area and pore size distribution (IUPAC Technical Report)," Pure and Applied Chemistry, vol. 87, no. 9–10, pp. 1051–1069, Oct. 2015, doi: 10.1515/pac-2014-1117.
[5] Y. Guo, V. Bolongaro, and T. A. Hatton, "Scalable Biomass-Derived Hydrogels for Sustainable Carbon Dioxide Capture," Nano Lett, vol. 23, no. 21, pp. 9697–9703, Nov. 2023, doi: 10.1021/acs.nanolett.3c02157.

P54: Adsorption of n-hexane isomers in montmorillonite and laponite zeolite L pellets

Daniel Pereira [(1)], João Pires [(1,*)]

[(1)] *CQE, Centro de Química Estrutural, Institute of Molecular Sciences, Departamento de Química e Bioquímica, Faculdade de Ciências, Universidade de Lisboa, Campo Grande, 1749-016 Lisboa, Portugal.*

** jpsilva@ciencias.ulisboa.pt*

fc56619@alunos.ciencias.ulisboa.pt

1. Introduction – A strategy to improve the research octane number is to promote branched isomers over their linear counterparts, as is the case of hexane isomers. The hexane isomers have similar properties (i.e. boiling points), which makes it difficult to separate them by distillation and, additionally, distillation is a large energy consuming process. Is this way, selective separation by adsorption using porous materials as adsorbents has emerged as a promising alternative approach in the separation industry.
In the present work we used two smectite clays, a natural (Montmorillonite) and a synthetic (Laponite) to obtain pellets in combination with in the case the zeolite L. The plastic properties of clays (Cáceres et al., 2021) makes them particularly suitable to produce shaped pellets by affordable and environmentally friendly methodologies, namely by just adding water. The clays were chosen due not only to their different origin, natural and synthetic, but also due to the marked difference in the clay particle sizes: in the micrometer and nanometer scale for Montmorillonite and for Laponite, respectively.

2. Experimental – Pellets with the proportions (in weight) clay/zeolite of 0.25, 0.5 and 1 were prepared. Characterization was made by N_2 adsorption at 77 K and Nano-Computed Tomography. Adsorption isotherms of hexane isomers were determined by the gravimetric method at 298K.

3. Results and Discussion – One example of the obtained adsorption isotherms is given in Fig. 1, that shows that the curves are differentiated amongst themselves, which is a first indication for a possible application in the separation of the isomers. Selectivity values were estimated by the IAST theory [1,2].

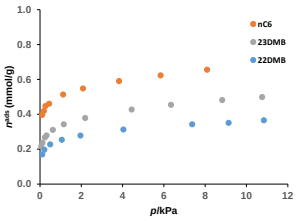

Fig 1. Adsorption isotherms of hexane isomers at 298 K in pellets of Laponite/zeolite L (clay/zeolite = 0.5)

4. Conclusions – High selectivity values (as high as 30) were found for some systems. Highest amounts of clay, particularly Laponite, are more beneficial for the separation that involve the linear n-hexane molecule.

Acknowledgments:
This research was financed by Fundação para a Ciência e a Tecnologia (FCT) in the scope of the projects UIDB/00100/2020 (CQE), UIDB/04028/2020 (CQE), UIDB/04028/2020, and the Institute of Molecular Sciences (IMS) Associate Laboratory funded by FCT through project LA/P/0056/2020

5. References

[1] J. Pires, S. Carvalho, J. Environ. Chem. Eng., 10, (2022) p. 107689.
[2] C.M. Simon, B. Smit, M. Haranczyk, Comput. Phys. Commun. 200 (2016) p. 364.

P55: Ionic carbon nitrides for photocatalytic hydrogen peroxide production in biphasic systems

I. Krivtsov[(1)], D. Mitoraj [(2)], R. Beranek [(2)]

[(1)] *Department of Chemical and Environmental Engineering, University of Oviedo, 33006 Oviedo, Spain*
krivtsovigor@uniovi.es
[(2)] *Institute of Electrochemistry, Ulm University, 89081 Ulm, Germany*

1. Introduction – The heptazine-based polymeric carbon nitrides are well established as promising photocatalysts for light-driven selective redox transformations. One of the most promising photocatalytic application of this family of materials is the light-driven O_2 reduction enabling formation of H_2O_2, a valuable chemical whose use extends from disinfection and pollutants degradation to energy storage systems. Alkaline metal poly(heptazine imides) (PHI), the ionic representatives of the broad family of polymeric carbon nitrides, are known to possess higher activity in photocatalytic hydrogen peroxide production than their covalent counterparts. However, the inability of this class of materials to oxidise water requires that an electron and the proton donor must be used, in order to achieve the two-electron dioxygen reduction. The choice of electron donor is far from being a trivial task and extreme care must be taken to avoid possible pitfalls related to autocatalytic behavior of the sacrificial chemical compound [1]. Moreover, hydrogen peroxide is a notoriously unstable chemical that can be easily reduced or oxidized, therefore ensuring the stability of this product in irradiated systems is challenging and requires modification of conventionally implemented suspension-based systems for its photocatalytic generation.

2. Results and Conclusions – One of the key figures of merit of photocatalytic H_2O_2 production is its concentration that can be achieved in the reaction medium. This, however, is conditioned by the decomposition rate of the photoproduced H_2O_2 on the surface of the irradiated photocatalyst. We approached the solution of this problem by devising a hydrophobic poly(heptazine imide) photocatalyst able to operate in biphasic conditions by oxidizing a lipophilic organic substrate in the organic layer, while the reduction product, H_2O_2, is immediately extracted into the aqueous phase. This method enables obtaining a ready to be used 0.12 mol/L solution of H_2O_2 already separated from the photocatalyst's particles and the electron donor [2]. We expect that the set of synthetic and post-synthetic procedures developed in this work will contribute to the devising of practical photoredox processes for synthesis of valuable chemicals.

3. References

[1] I. Krivtsov, A. Vazirani, D. Mitoraj, R. Beranek, ChemCatChem. 15, (2023) p. e202201215.
[2] I. Krivtsov, A. Vazirani, D. Mitoraj, R. Beranek, et al. J. Mater. Chem. A 11, (2023) p. 2314.

P56: CH4/CO2 separation by Pressure Swing Adsorption process using shaped MOF MIL-160(Al): Experimental and Simulation assessment

M. Karimi [(1)], R. M. Siqueira [(1)], A. E. Rodrigues [(1)], F. Nouar [(2)], J. A. C. Silva [(3)], C. Serre [(2)], A. F. P. Ferreira [(1)]

[(1)] *Laboratory of Separation and Reaction Engineering (LSRE), Associate Laboratory LSRE/LCM, Faculty of Engineering, University of Porto, Rua Dr. Roberto Frias, 4200-465 Porto, Portugal.*
mohsen.karimi@fe.up.pt, rafaelsqra@gmail.com, arodrig@fe.up.pt, aferreir@fe.up.pt
[(2)] *Institut des Matériaux Poreux de Paris, ESPCI Paris, Ecole Normale Supérieure, CNRS, PSL University, Paris, France*
farid.nouar@espci.fr, cristian.serre@ens.fr
[(3)] *Centro de Investigação de Montanha (CIMO), Instituto Politécnico de Bragança, Campus de Santa Apolónia, 5300-253 Bragança, Portugal*
jacsilvaipb@gmail.com

1. Introduction – In order to reduce the greenhouse gas emissions, policies of sustainable development have been established many legislative measures to increase the use of renewable energy source or alternative fuels and decrease carbon dioxide (CO_2) emission from exhaust gas. Carbon Capture and Storage (CCS) technology is one of the most prominent solutions for capture and storage CO_2 from natural gas purification or biogas upgrading [1]. Biogas is derived from the anaerobic digestion (AD) of organic matter, in digesters or landfills, which based on the origin of the organic samples, it is mainly composed of CH_4 (35–70%) and CO_2 (15–50%), also minor quantities of H_2S, H_2O, NH_3, N_2, O_2, and CO, as well as volatile organic compounds can be traced in the biogas [2]. Various technologies have been developed for biogas upgrading including. Accordingly, the highest specific energy consumption and specific production cost can be attributed to the cryogenic technology. Currently, most of the installed biogas upgrading plants ascribe to the water scrubbing and membrane technology due to the lowest energy consumption. However concerning the cost, energy consumption, efficiency and environmentally friendly, pressure swing adsorption is among the most favorable ones [3]. Designing a highly efficient PSA unit require a full set of engineering details and material characters. In this way, several operating factors including times and schedule of the various steps, flow rates, and pressure levels must be considered and optimized to develop an effective process. On the other hand, the type of adsorbent is also one of the key elements in the adsorption process. Metal-Organic Frameworks (MOFs) as a novel class of crystalline porous materials received a significant interest for gas adsorption processes [4]. The potential of MIL-160(Al) sample for separation of CO_2/CH_4 concerning the biogas application has been investigated using the PSA process for the first time. To this end, firstly, the dynamic of fixed-bed adsorption of carbon dioxide and methane is accomplished, experimentally, and validated numerically. Afterwards, a 5-step PSA process is simulated and experimentally validated for biogas upgrading in a lab-scale set-up. Finally, a PSA process has been designed to evaluate the capacity of shaped MIL-160(Al) for biogas upgrading in the industrial scale.

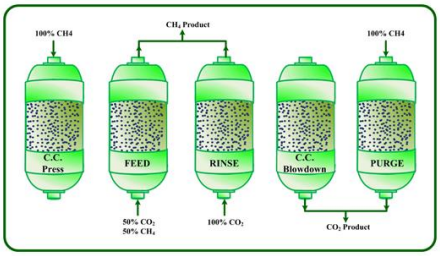

Image 1. Employed cycle sequences in the developed PSA experiments.

2. Experimental - The dynamic breakthrough experiments and cyclic process were performed using a fixed-bed dynamic system. The gases flow rates were measured by mass flow controllers, while a mass flow meter was employed to monitor the flow rate at the outlet stream. In addition, the compositions of outlet gases from the adsorption column were continuously recorded using an infrared gas analyzer. A thermocouple was improvised at the middle of the column to record the temperature history during the adsorption process. Furthermore, a backpressure regulator was provided by Bronkhorst to control the pressure of the system. To perform the single component breakthrough test, the column was firstly saturated with methane, afterwards, the feed (pure carbon dioxide) was infused to the system, which after getting the equilibrium conditions in the composition, pressure and temperature, the desorption process was performed by shifting the inlet stream to the CH_4. However, to accomplish the pseudo binary experiment, the column was firstly saturated with

CH_4, then, a feed containing CO_2(50%)/CH_4(50%) was fed to the adsorption column. In the next phase, the PSA cycles containing five steps were designed and developed at 318 K and 4.6 bar (Image 1). To this end, the first cycle of PSA process initiated with a counter-current pressurization step with pure methane, then the feed step was accomplished, afterwards, the rinse step performed using pure carbon dioxide, followed by blowdown and purge steps. The simulation of PSA process was performed by employing proper boundary conditions, coupled with developed dynamic fixed-bed adsorption model. Additionally, the performance of the PSA process can be assessed by product purity, recovery, and productivity factors.

3. Results and Discussion – The results of breakthrough experiments present molar fraction, flowrate and temperature history of CH_4-CO_2 onto shaped MOF MIL-160(Al) accompanied with prediction/simulation during both the adsorption−desorption steps. During the adsorption-desorption processes, in the second step, CO_2 is adsorbed as long as CH_4 is desorbed. Regarding the temperature history (Figure 4c), there is a temperature increment related to the adsorption of carbon dioxide (around 20 K) due to the adsorption heat of CO_2 is higher than adsorption heat of CH_4. Thus, the temperature history of all process is influenced mainly by CO_2 adsorption-desorption process. Therefore, during the CO_2 desorption step the temperature decreases, even occurring the CH_4 adsorption. Relying on the dynamic fixed-bed adsorption outcomes, a cyclic adsorption PSA process containing five main steps was designed and experimental validated for biogas upgrading. The experimental outcomes are properly described with the designed simulation. To evaluate the potential of shaped MOF MIL-160(Al) for large scale applications, in the next attempt, an industrial scale PSA was designed concerning biogas upgrading. The performances of the developed process were calculated according to equations and the CH_4 is produced by the purity of 99.5%, while the purity of CO_2 reached 77%. Further, as the recovery of CH_4 and CO_2 are around 98.7% and 65.6%, respectively. It is worth mentioning that Cyclic Steady State of the PSA designed process was achieved around the 7^{th} cycle.

4. Conclusions - The shaped MOF MIL-160(Al) was successfully investigated for separation of carbon dioxide and methane concerning the biogas upgrading application using a pressure swing adsorption (PSA) process. he breakthrough results proved the potential of considered model for predicting and developing the PSA process. Accordingly, a lab-scale PSA process with 5-steps demonstrated the well potential of MIL-160(Al) MOF for biogas upgrading. Afterwards, an industrial-scale PSA process was designed considering a mixture of 50%-50% CO_2:CH_4 at 318 K and 4 bar. The designed PSA illustrated the purity and recovery of methane around by 99% and 66%, also in the case of carbon dioxide around 76% and 97%, respectively. The obtained results in this work indicated the superb potential of MOF MIL-160(Al) for biogas upgrading concerning its unparalleled specifications such as adsorption performance, synthesized cost, easy shaping, and stability comparing with other sorbents.

5. References

[1] B. Yuan, X. Wu, Y. Chen, J. Huang, H. Luo, S. Deng, Environ. Sci. Technol., 47 (2013) 5474–5480.
[2] D. Papurello, S. Silvestri, A. Lanzini, Sep. Purif., Technol. 210 (2019) 80–92.
[3] A. Naquash, M.A. Qyyum, J. Haider, A. Bokhari, H. Lim, M. Lee, Renew. Sustain. Energy Rev., 154 (2022) 111826.
[4] A.F.P. Ferreira, A.M. Ribeiro, S. Kulaç, A.E. Rodrigues, Chem. Eng. Sci., 124 (2015) 79–95.

P57: Microwave-Assisted Synthesis of Zeolites from clays for CO2 Adsorption

M.R. Oliveira[(1)] , J.A. Cecilia[(2)], D. Ballesteros-Plata[(2)] , I. Barroso-Martín[(2)] , P. Núñez[(3)], A. Infantes-Molina[(2)] and E. Rodríguez-Castellón[(2)]

[(2)] Departamento de Química Inorgánica, Facultad de Ciencias, Universidad de Málaga, 29071 Málaga, Spain
castellon@uma.es
[(1)(3)] Center for Studies in Colloidal Systems (NUESC), Laboratory of Materials Synthesis and Chromatography, Institute of Technology and Research (ITP), Tiradentes University (UNIT), Aracaju 49032-490, SE, Brazil; Department of Chemistry, Institute of Materials and Nanotechnology, University of La Laguna, 38200 Tenerife, Spain;
pnunez@ull.es
jacecilia@uma.es, daniel.ballesteros@uma.es, Isabel.barroso@uma.es, ainfantes@uma.es

1. Introduction – The global demand for energy and industrial growth has generated an exponential use of fossil fuels in recent years. It is well known that carbon dioxide (CO_2) is mainly produced, but not only from fuels, which has a negative impact on the environment, such as the increasing emission of greenhouse gases. Thus, thinking about reducing this problem, this study analyzes microwave irradiation as an alternative to conventional heating to optimize zeolite A synthesis conditions for CO_2 capture. Synthesis reaction parameters such as different temperatures (60–150 ◦C) and different time durations (1–6 h) were evaluated. The CO_2 adsorption capacity was evaluated by CO2 adsorption–desorption isotherms at 25 ◦C and atmospheric pressure. The results showed that the synthesis of zeolite A by microwave irradiation was successfully obtained from natural kaolinite (via metakaolinization), reducing both temperature and time. Adsorption isotherms show that the most promising adsorbent for CO_2 capture is a zeolite synthesized at 100 ◦C for 4 h, which reached an adsorption capacity of 2.2 mmol/g.

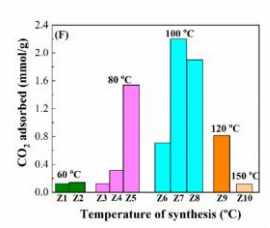

Figure 1. Comparison of CO_2 uptake for all prepared zeolites

2. Experimental - Kaolinite (a silicon- and aluminum-rich clay mineral) was obtained from Vimianzo deposits (Galicia, Spain). Synthesis of Zeolites*:* The kaolinite was previously calcined at 600 °C for 4 h in a furnace to convert it into metakaolinite. Then, the metakaolinite was added to a 3.0 M NaOH aqueous solution and stirred for 15 min at room temperature for homogenization. The solid–liquid ratio used in this process was 2 g of metakaolinite per 50 mL of alkaline solution. The stirred mixture was placed in a Teflon container and inserted into the microwave reactor (ETHOS, Milestone, Denmark), varying the temperatures (60 °C to 150 °C) and times (0.5 to 6 h) of synthesis. After microwave-assisted treatment, the samples were subjected to centrifugation at 1500 rpm for 25 min. Subsequently, the solids were carefully washed several times with deionized water (approximately 300 mL) to remove any remaining moisture and alkaline residue. Finally, the samples were dried in an oven overnight at 60 °C.

3. Main results and conclusions - The use of microwave irradiation in the synthesis of zeolites from metakaolinite has shown its potential to achieve faster and more cost-effective methods. The results of this study demonstrate the advantages of microwave-assisted synthesis, not only in expediting the preparation of zeolites but also in enhancing their adsorption capabilities for CO_2. This approach yielded zeolites of high crystallinity and purity and revealed a significant correlation between synthesis time and temperature within the microwave reactor.
Through the CO_2 adsorption isotherms, it was possible to analyse that the adsorption capacity of zeolites increases with increasing temperature, except for temperatures higher than 120 °C due to the formation of mixtures of phases whose pore diameter is larger. The zeolite A synthesized under microwave irradiation at 100 °C for 4 h exhibited the highest CO_2 adsorption capacity (q_{ads} = 2.18 mmol/g at 25 °C and 1 bar pressure). This result is particularly noteworthy as it substantially outperforms the results achieved in many prior studies that demanded significantly longer synthesis times, ranging from 24 to 96 h.
Thus, it was seen that microwave irradiation not only accelerates the synthesis of zeolites but also obtains adsorbents with a greater number of active sites available for CO_2 adsorption and, consequently, a greater adsorption capacity than zeolites synthesized by the conventional method.

Acknowledgements – M.R. Oliveira thanks to Conselho Nacional de Desenvolvimento Científico e Tecnológico (CNPq, National Council for Scientific and Technological Development, Brazil) for financial support. J.A. Cecilia, D. Ballesteros-Plata, I. Barroso-Martín, A. Infantes and E. Rodríguez - Castellón thank to the Spanish Ministry of Science and Innovation, project PID2021-126235OB-C32, funded by MCIN/AEI/10.13039/501100011033/ and FEDER funds. Moreover, P.Núñez. thanks Cajacanarias under grant 2021-ECO-05.

4. References

[1] M.R. Oliveira, J.A. Cecilia, D. Ballesteros, I. Barroso-Martín, P. Núñez, A. Infantes-Molina, E. Rodríguez -Castellón. International Jornal of Molecular Science 24 (2023) 14040.
[2] M.R. Oliveira1, J.A. Cecilia, J.F. De Conto, S.M. Egues, Enrique Rodríguez-Castellón. Journal Sol Gel Technology 105 (2023) 370-387.
[3] J.A. Cecilia, E. Vilarrasa-García, R. Morales-Ospino, E. Finocchio, G. Busca, K. Sapag, J. Villarroel-Rocha, M. Bastos-Neto, D.C.S. Azevedo, E. Rodríguez-Castellón. Fuel 320 (2022) 123953.

P58: Polyxometalates supported on silicon xerogels. New materials for catalysis and sensorics

B. Rosales-Reina[(1)], G. Cruz-Quesada[(1)], S. Reinoso[(1)], C. Elosúa[(2)], M.V. López-Ramón[(3)], J.J. Garrido [(1)(4)]

[(1)] *Institute for Advanced Materials and Mathematics (INAMAT2), Departamento de Ciencias, Universidad Pública de Navarra (UPNA), Campus de Arrosadia, 31006 Pamplona, Spain*
[(2)] *Institute of Smart Cities (ISC), Departamento de Ingeniería Eléctrica, Electrónica y de Comunicación, Universidad Pública de Navarra (UPNA), Campus de Arrosadia, 31006 Pamplona, Spain*
[(3)] *Departamento de Química Inorgánica y Orgánica; Facultad de Ciencias Experimentales, Universidad de Jaén, 23071, Spain*
[(4)] *j.garrido@unavarra.es*

1. Introduction – Xerogels (XG) are materials known for their one-pot sol-gel synthesis and their wide variety of chemical and textural properties. In fact, during the synthesis, the use of silicon molecular precursors containing organic groups has been proven effective to customize the textural properties of hybrid xerogels [1]. Furthermore, functional substances can be embedded within the porous network of these materials endowing those new properties. For instance, silica xerogel films containing luminescent probes have been tested as coatings for optical fibre humidity sensors [2]. Polyoxometalates are substances that exhibit interesting properties such as photoactivity and luminescence. The aim of this work was to synthesize new xerogels containing polyoxometalates, where the xerogel matrix acts as a support that allows the application of these materials in catalysis and sensorics.

2. Experimental – The synthesis of XG has been carried out following the sol-gel method as indicated in a previous work [1], although slight modifications have been made to achieve the inclusion of polyoxometalates. To accomplish this, 1.5 mL of polyanion solution (([Ti2(HGeMo7O28)2]10– or H5[PV2Mo10O40]) is mixed with 2.6 mL of ethanol under stirring, followed by the dropwise addition of

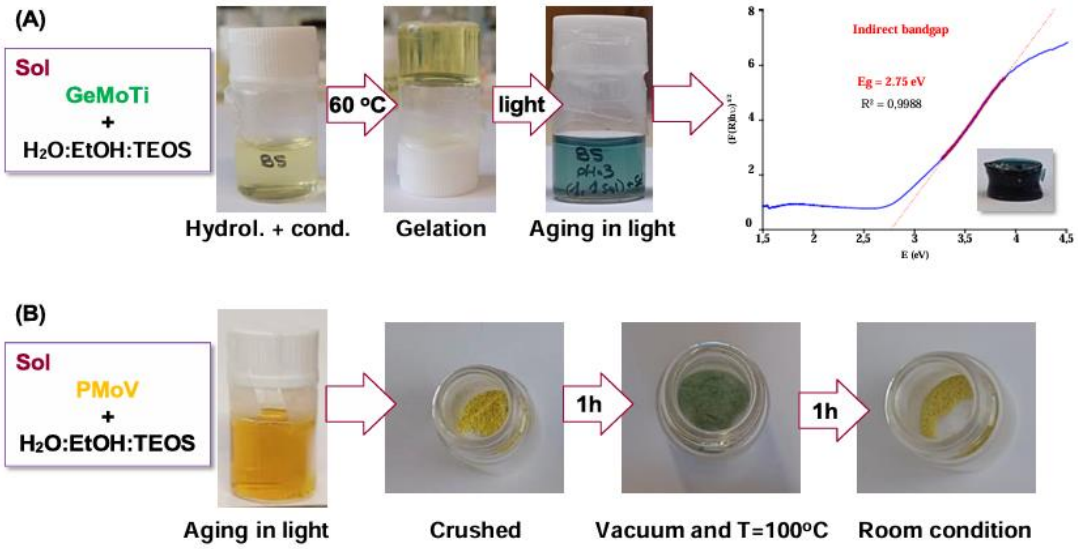

Figure 1. (A) GeMoTi XG colour change with the aging and the indirect bandgap obtained, (B) PMoVO XG color change under specific conditions.

triethoxysilane (TEOS). Subsequently, the pH is adjusted to a value of 3.5 with 0.1 M hydrochloric acid solution. The mixture is then deposited in an oven where it is maintained until it reaches its gel point, and finally allowed to dry at room temperature.

3. Results and Discussion – Figure 1 shows the two TEOS+polyoxometalates synthesized (GeMoTi ([Ti2(HGeMo7O28)2]10–)+TEOS (A), and PMoV (H5[PV2Mo10O40]+TEOS) (B)) with different visual studies. For GeMoTi, color [U1] degradation with solar light has been observed passing from a pale-yellow color to a dark green color, proving the reduction of the polyoxometalates. The bang-gap for GeMoTi was

measured, a value of 2.75 eV, being acceptable to be used as a photocatalyst. And for the reduction of the PMoV is necessary to apply specific conditions (0.1 atm and 100°C) and the XG color changing from a bright yellow to a greenish-blue, being this is a reversible process. Figure 2 shows the N2 adsorption

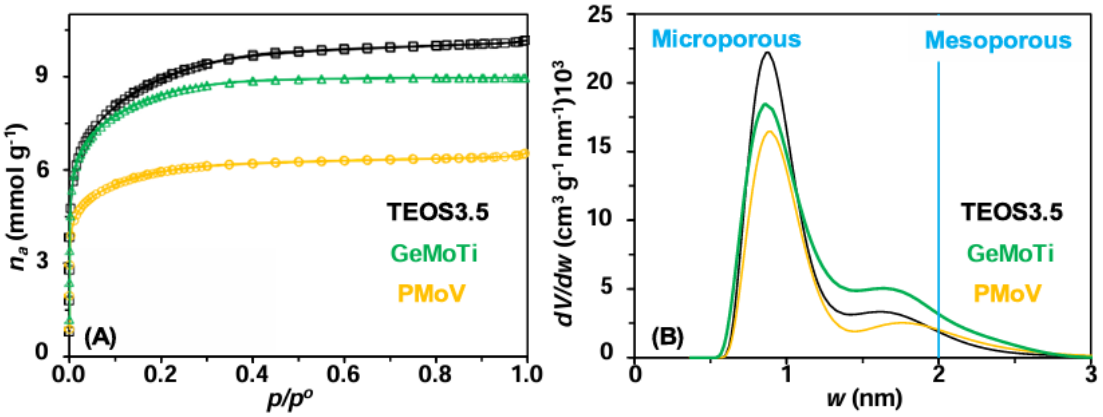

Figure 2. N_2 (77 K) adsorption isotherms of 3 studied XG (A) and pore size distribution (B).

Table 1. Textural parameters of xerogels.

XG	a_{BET} (m^2g^{-1})	V_{micro} (cm^3g^{-1})	V_{meso} (cm^3g^{-1})	V_{total} (cm^3g^{-1})	BJH^{AP5} (nm)
TEOS3.5	605	0.25	0.02	0.28	2.45
GeMoTi	590	0.30	0.01	0.31	2.70
PMoVO	498	0.19	0.02	0.22	2.47

isotherm (77 K) and the pore size distribution (PSD) for the XG reference (TEOS) and two TEOS+polyoxometalates. The isotherms of the studied XG show a type I(b) isotherm, which indicates that these materials are mainly microporous with a narrow distribution of micropore sizes. The textural parameters obtained from the isotherms and gathered in [br3], indicate that GeMoTi and the reference have similar texture with the difference that GeMoTi have a bigger volume of microporous (Vmicro). On the other hand, PMoV has a significant lower specific surface area (aBET) to that of the reference and lower volume of pores (Vtotal). [U4]

4. Conclusions – The inclusion of a polyoxometalate in the matrix of an XG has been achieved without adversely affecting the textural properties of the xerogel. The resulting XG shows photosensitive properties similar to those of its starting salts. Therefore, it is a promising candidate to be used as a material for future applications as a photosensitive material.

5. References

[1] G. Cruz-Quesada, M. Espinal-Viguri, M.V. López-Ramón, J.J. Garrido. Polymers, 13(9), (2021) p. 1415.

[2] G. Cruz-Quesada, B. Rosales-Reina, D. López-Torres, S. Reinoso, M.V. López-Ramón, G. Arzamendi, C. Elosúa, M. Espinal-Viguri, J.J. Garrido. Sens. Actuators, B C 406, (2024) p. 135369.

P59: Improved adsorption system for hydrogen drying

T. Santos [1, 2, 3], R. Moreira[1, 2], F. Relvas[3], P. Ribeirinha[3], A. Mendes[1, 2]

[1] *LEPABE - Laboratory for Process Engineering, Environment, Biotechnology and Energy, Faculty of Engineering, University of Porto, Rua Dr. Roberto Frias, 4200-465 Porto, Portugal.*
[2] *ALiCE – Associate Laboratory in Chemical Engineering, Faculty of Engineering, University of Porto, Rua Dr. Roberto Frias, 4200-465 Porto, Portugal*
up201306235@up.pt
[3] *Amnis Pura, Parque Empresarial Laborim, 100 Armazém C3, 4430-246 Vila Nova de Gaia, Portugal*
armoreira@fe.up.pt
fredericorelvas@amnispura.pt; pauloribeirinha@amnispura.pt; mendes@fe.up.pt

1. Introduction – In the last century and since the Industrial Revolution, the energy stored in fossil fuels has been a key driver in the technological advancement of society. The heavy reliance on these carbon-based fuels created an environmental stress that threatens the environment. The energetic shift towards the use of renewable energy sources and conversion to storable chemicals becomes imperatively urgent. Hydrogen gas has a highly gravimetric energy density (120 MJ/kg), is the most abundant element in the universe, and water is produced when oxidized to release its energy. It can also be converted to chemicals with a greater volumetric energy density, such as methanol and other synthetic fuels. Currently, most of the produced hydrogen feedstock is fossil fuels, but hydrogen production from the electrochemical splitting of water molecules has been increasing. The safe compression of hydrogen for storing and transport to pressures of 350 bar and 700 bar requires that the contaminants be reduced to standard levels as specified in ISO 14687-2 standard [1]. The theoretical contaminants of hydrogen produced through water splitting are oxygen and water. For the particular case of water, the maximum contamination concentration is 5 $\mu mol \cdot mol^{-1}$, equivalent to a temperature dew point (Tdp) of -65.5 °C to prevent condensation inside high-pressure vessels and thus corrosion of sensitive parts compromising its safety [1]. Gas drying is a common issue easily solved with adsorption technologies. In particular, air drying is usually done with adsorption with high-purity grades [2]. Hydrogen purification for gasification of biomass or coal is also well established [3]. Due to low interactions between hydrogen and most commercial adsorbents [4], it becomes straightforward to design a unit cantered on water adsorption using an activated alumina or zeolite molecular sieve [5]. The challenge becomes optimizing the unit to recover as much hydrogen as possible, producing a pure stream with an average water concentration lower than the standard limit. To do so, the regeneration of the packed bed should be improved within the limits of the adsorption cycle. In this work, a Pressure Swing Adsorption (PSA) laboratory prototype was modified to take a vacuum pump and study different regeneration methods.

2. Experimental - A lab-scale PSA prototype fed with a humidified hydrogen stream with 50 % relative humidity was designed and built. The unit consists of three columns loaded with activated alumina beads (0.5 – 1.0 mm diameter). The columns are made of stainless steel with a length of 100 mm and inner and outer diameters of 10 mm and 11.5 mm, respectively. The hydrogen feed stream – flow rate of 1.5 $LN \cdot min^{-1}$ (Bronkhorst El-FlowF-201CV, 0−10 $LN \cdot min^{-1}$), was humidified in a water column to 50 % relative humidity. The humidity of the product stream was recorded using a CS-Instruments FA500. A vacuum pump (Vacuubrand RZ 2.5) was employed for purging the adsorbent columns. Tables I, II, and III depict the experimental PSA adsorption cycles; Table I shows a regular PSA cycle using 1 % of its purified feed or purge-to-fee ratio (*P/F*) to regenerate the saturated column; Table II shows a cycle using only reduced pressure to promote desorption and no purge gas and; Table III shows a cycle using both purge (1 % *P/F*) and reduced pressure for regeneration. The adsorption time for all three cycles is 7.5 h.

Table I: Adsorption cycle when the regeneration is performed under atmospheric pressure using 1 % of purified feed – named Purge cycle.

Time / s	1	1	8998	1	1	8998	1	1	8998
Column 1	AD			DPE	BD	PG	PPE	BF	

Column 2	PPE	BF		AD		DPE	BD	PG
Column 3	DPE	BD	PG	PPE	BF	AD		

Table II: Adsorption cycle when the regeneration is performed under a reduced pressure atmosphere without and purging gas – named Vacuum cycle.

Time / s	**1**	**1**	**8998**	**1**	**1**	**8998**	**1**	**1**	**8998**
Column 1	AD			DPE	BD	EV	PPE	BF	
Column 2	PPE	BF		AD			DPE	BD	EV
Column 3	DPE	BD	EV	PPE	BF		AD		

Table III: Adsorption cycle when the regeneration is performed under a reduced pressure atmosphere with 1 % purging gas – named Purging under vacuum cycle.

Time / s	**1**	**1**	**2**	**8996**	**1**	**1**	**2**	**8996**	**1**	**1**	**2**	**8996**
Column 1	AD				DPE	BD	EV	PGV	PPE	BF		
Column 2	PPE	BF			AD				DPE	BD	EV	PGV
Column 3	DPE	BD	EV	PGV	PPE	BF			AD			

Concerning the Purge cycle, Table I, the adsorption (AD) stage comprehends three steps. After the saturation of the column, the depressurization pressure equalization (DPE) stage occurs when column 1 equalizes its pressure with recently regenerated column 3. This follows the blowdown (BD) stage and purging (PG) stage when purified gas from column 2 is fed to column 1. The newly regenerated column 1 equalizes with saturated column 2 during the pressurization pressure equalization (PPE) stage and, repressurizes to the adsorption pressure using purified gas from column 3 – the backfill (BF) stage. In the vacuum-only cycle, the PG stage is replaced by an evacuation (EV) stage, and in the purge and vacuum stages, an additional stage of evacuation is added to reduce pressure below atmospheric pressure, followed by a purge under vacuum (PGV) stage.

3. Results and Discussion - The three cycles were run until a fully developed cyclic steady state was reached, after which the results were collected and analyzed. Table VI displays the results of the three cycles.

Table IV: Operating conditions and results for each cycle.

Cycle	t_{AD} / h	F_{dry} / LN·min-1	*P/F*	P_{AD} / MPa	P_{regen} / bar	R_{rec} (%)	T_{dp} / °C
1	2.5	1.5	1%	0.8	1	98.61%	-9.62
2	2.5	1.5	0%	0.8	0.04	99.37%	-49.01
3	2.5	1.5	1%	0.8	0.04	98.34%	-70.05

Only purging under vacuum cycle to reach the -65.5 °C dewpoint milestone; when purging gas improved the vacuum regeneration even further.

4. Conclusions – Three different cycles were tested using a PSA unit loaded with activated alumina. Only Purging under vacuum cycle, when the purging stage is performed under vacuum, allowed to reach and overcome the demanding milestone of -65.5 °C of dew point, required by ISO 14687-2 standard.

5. References

[1] T. Bacquart et al., "Probability of occurrence of ISO 14687-2 contaminants in hydrogen: Principles and examples from steam methane reforming and electrolysis (water and chlor-alkali) production processes model", International Journal of Hydrogen Energy, 43, (2018) pp. 11872-11883.
[2] V. Sureshkannan, S. Vijiayan and V. R. Lenin, "Design and performance analysis of compressed air adsorption dryer with heatless regeneration mode", Heat and Mass Transfer, 58, (2022) pp. 631-641.
[3] P. Häussinger, R. Lohmüller and A. M. Watson, "Hydrogen, 3. Purification", Ullmann's Encyclopedia of Industrial Chemistry, (2012) pp. 309-333.
[4] K. M. Thomas, "Hydrogen adsorption and storage on porous materials", Catalysis Today, 120, (2007) pp. 389-398.
[5] D. M. Ruthven, S. Farooq and K. S. Knaebel, "Pressure Swing Adsorption", (1994), pp. 389-398.

P60: Waste-Based Magnetic Activated Carbon and its Microwave-Assisted Regeneration for the Removal of Low Concentrations of Sulfamethoxazole from Water

D. Pereira [(1)], M. V. Gil [(2)], N. J. O. Silva [(3)], V. Calisto [(1)], M. Otero [(4)]

[(1)] *Department of Chemistry & CESAM, University of Aveiro, Campus de Santiago, Aveiro, Portugal*
[(2)] *Instituto de Ciencia y Tecnología del Carbono (INCAR), CSIC, Francisco Pintado Fe, Oviedo, Spain*
[(3)] *Department of Physics & CICECO, University of Aveiro, Campus de Santiago, Aveiro, Portugal*
[(4)] *Departamento de Química y Física Aplicadas, Universidad de León, Campus de Vegazana, León, Spain*

marta.otero@unileon.es
diogoepereira@ua.pt; victoria.gil@incar.csic.es; nunojoao@ua.pt; vania.calisto@ua.pt

1. Introduction

Pharmaceuticals are recurrently found at relative low concentrations in the aquatic environment across the globe. Still, their nefarious impact on aquatic ecosystems and human health is undeniable and poses significant hazards due to their recalcitrant nature. Among pharmaceuticals, antibiotics ubiquity in natural waters is particularly alarming due to the development of antimicrobial resistance. The last update of the watch-list of substances for monitoring in the European Union waters included several pharmaceuticals, such as the antibiotic sulfamethoxazole (SMX), which is regarded as a top candidate for risk management and remediation efforts [1]. Moreover, pharmaceuticals are considered the main sources of micropollutants in urban wastewater by the forthcoming Urban Wastewater Treatment Directive [2] that is expected to come into force at the end of this year. Hence, developing sustainable solutions for the removal of pharmaceuticals from wastewater is of utmost importance for the protection of aquatic resources. Powdered activated carbon (PAC) has proven to be highly efficient in the removal of several persistent contaminants, namely pharmaceuticals, from water. A generalized incorporation of PAC treatments in wastewater treatment plants (WWTP) for the removal of pharmaceuticals is still limited due to its small particle size, which hampers its after-use recuperation. As a potential alternative, coating PAC with iron oxides nanoparticles to produce magnetic activated carbon (MAC), enables a quick and effective separation of the material after saturation, which allows for its regeneration and reutilization.
This work has two main objectives. First, evaluate the adsorption performance of an ex-situ MAC in removing trace concentrations of SMX from WWTP effluents. Most of published results on adsorption of pharmaceuticals from water use unrealistic initial concentrations that can be several orders of magnitude higher than those found in effluents. Second, study the regeneration by microwave radiation to thermally decompose adsorbed SMX so to reuse MAC.

2. Experimental

An ex-situ MAC was produced by combining paper mill sludge-based PAC with magnetic iron oxides in a water suspension with controlled pH in between the point of zero charge of both particles.
Batch adsorption studies were performed in ultrapure water and final effluent from a municipal WWTP by contacting SMX solutions and MAC under shaking. Initial concentration of SMX was 50 µg L^{-1} (0.20 µmol L^{-1}) and MAC dosage was 1 mg L^{-1} in ultrapure water and 65 mg L^{-1} in effluent. Adsorption kinetics (5-360 min) and equilibrium studies were carried out in both matrices. After saturation, MAC was recuperated and thermally regenerated at 700 ºC (SMX decomposition) for 20 min, under N_2 stream using a microwave furnace. Adsorption tests were performed after each regeneration cycle.

3. Results and Discussion

Kinetic results on the adsorption of SMX onto MAC (Figure 1 – left) indicate that equilibrium was reached within 3 hours of adsorption in either ultrapure water or effluent.
In a previous study [3] with the ex-situ MAC but at an initial concentration of SMX around 10 times higher (20 µmol L^{-1}), adsorption equilibrium was reached within 30 min, which shows that adsorption velocity is strongly reduced at near trace level concentrations.

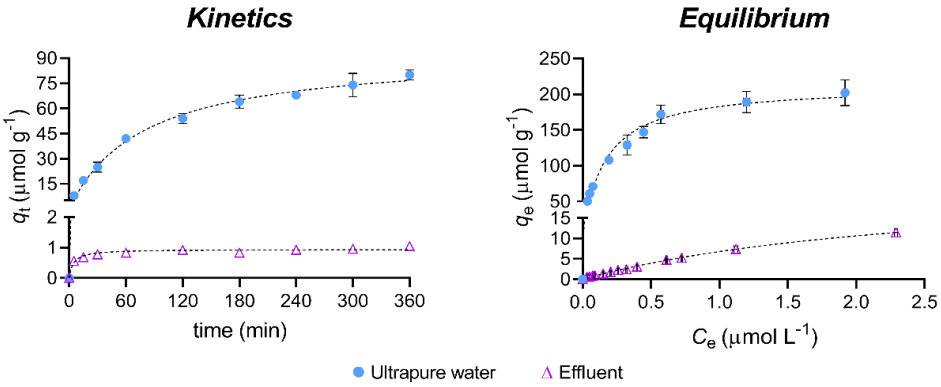

Figure 1. Kinetic and equilibrium results on the adsorption of SMX from ultrapure water and WWTP effluent together with fittings (dotted lines) to pseudo-second order kinetic model and Langmuir equilibrium model.

The equilibrium data (Figure 1 – right) adequately fit the Langmuir adsorption model in ultrapure water and also in effluent. The reduction of SMX adsorption from the effluent may be related to its complex composition and pH. Natural organic matter competes for active sites on the surface of MAC and the pH affects the speciation of SMX, which is mostly negatively charged as is the surface of MAC at effluent pH. Thus, the combination of these effects explains the plummeting of the Langmuir maximum adsorption capacities (q_m) which were 213 ± 8 and 25 ± 1 µmol g^{-1} in ultrapure water and effluent, respectively.

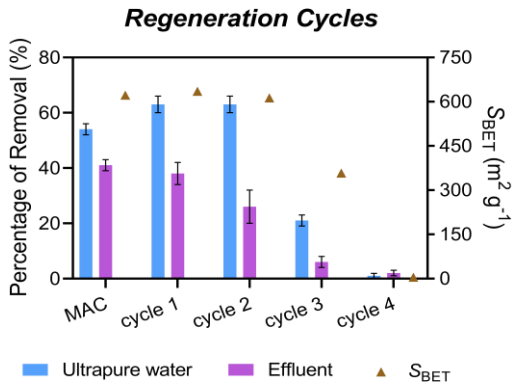

Figure 2. SMX removal percentages in ultrapure water and. Materials' specific surface area (S_{BET}) is also represented.

Figure 2 represents the SMX percentage of removal by the original MAC and after successive regeneration cycles (principal axis) and its surface area (S_{BET}, secondary axis). Adsorption performance in both ultrapure water and effluent, as well as S_{BET}, remained mostly similar after two cycles of regeneration. However, after the third cycle, SMX adsorption, S_{BET} and micropore volume (not shown) decreased around 41 % and were close to null after the fourth regeneration cycle. What this suggests is that, at the temperature required to decompose SMX (700 ºC), MAC porous structure deteriorates abruptly after the third cycle as result of pore collapse and pore blocking from charred residue.

4. Conclusions

This study realistically demonstrates that a waste-based MAC is effective in the removal of a recalcitrant antibiotic at near trace level concentration from WWTP effluents. It also proves that thermal regeneration of the exhausted MAC can be achieved through microwave radiation up to two cycles without significantly affecting its structure integrity. This are relevant findings when considering large scale implementation.

Acknowledgements

The authors acknowledge financial support to CESAM by FCT/MCTES (UIDP/50017/2020+UIDB/50017/2020+ LA/P/0094/2020), through national funds. Diogo Pereira thanks FCT for PhD grant (2020.05389.BD).

5. References

[1] Yang, Y. et al. Which Micropollutants in Water Environments Deserve More Attention Globally? Environ Sci Technol 56, 13–29 (2022).
[2] European Parliament Legislative Resolution of 10 April 2024 (P9_TA(2024)0222).
[3] Pereira, D. et al. Ex-situ magnetic activated carbon for the adsorption of three pharmaceuticals with distinct physicochemical properties from real wastewater. J Hazard Mater 443, 130258 (2023).

P61: 3D Activated Carbon Structures for Carbon Dioxide Capture

Henrry Ortega[1], I. Fonseca[1], J.P.B. Mota[1], I. Matos[1], R.P.P.L. Ribeiro[1,2]

(1) *LAQV-REQUIMTE, NOVA School of Science and Technology, NOVA University of Lisbon, Caparica, Portugal*
(2) *HyLab – Green Hydrogen Collaborative Laboratory, Estrada Nacional 120-1, Central Termoeléctrica, Sines, Portugal*
rpp.ribeiro@fct.unl.pt; rui.ribeiro@hylab.pt

1. Introduction – 3D printing has recently become a widely available tool that enables anyone to create objects from scratch. This disruptive approach has potential to influence procedures in virtually every field of work. 3D printing is used in the automotive, space, footwear, clothing, and jewellery industries.
The introduction of 3D printing in the chemical engineering field is also occurring at a fast pace. Novel reactors, mixers, structured catalysts and adsorbents have been 3D printed. [1]
The printing of adsorbent structures can have a huge impact on adsorption processes. Many adsorbents are synthesized as powders that are unfeasible for utilization in separation processes, due to the huge pressure drop generated, and must be shaped into bigger particles. Traditionally, pellets or beads are used although the use of structured adsorbents such as honeycomb monoliths presents several advantages [2]. These monoliths are typically obtained by extrusion which limits the obtainable structures to monoliths with parallel (non-interconnected) channels. On the other hand, with 3D printing novel and more complex shapes can be obtained, adding more degrees of freedom to the design of structured adsorbents. Furthermore, the use of computer aided design tools allows changing the structures with ease, permitting the rapid prototyping of different shapes.
Among the several 3D printing techniques available, until now most of the adsorbent structures printed were based on the direct ink writing (DIW) technique. [3, 4] Some studies have also focused on the development of novel formulations for use in stereolithography 3D printers [5].
In this work, we have developed a straightforward templating methodology for the preparation of carbon-based adsorbent structures for carbon dioxide (CO_2) capture.

2. Results and Discussion – The 3D structures are designed in BlenderTM software, generating STL files that can be 3D-printed. The structures are printed in an CreatBot F160 printer using a commercial polyvinyl alcohol (PVA) filament. Subsequently, the three-dimensional piece is filled with a previously prepared phenol-formaldehyde resole resin and left curing at 353 K for approximately one week. Then, the template is removed in water and the self-sustained resole structure is pyrolyzed. Various activation conditions with CO_2 were tested to evaluate its influence in the porosity of the obtained activated carbons. Figure 1 shows the obtained structures, which were thoroughly characterized through nitrogen (N_2) adsorption at 77 K, SEM, and Hg porosimetry. The CO_2 and N_2 adsorption equilibrium are also determined to evaluate the potential of the materials for CO_2 capture.

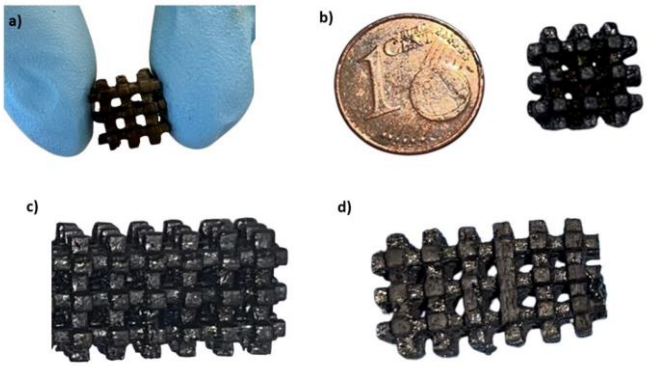

Figure 1. Examples of the 3D Activated Carbon structures obtained

The structured activated carbons present microporosity suitable for gas adsorption. The adsorption equilibrium isotherms of CO_2 and N_2 at 303 K on three activated carbon samples, prepared at different activation conditions are shown in Figure 2. The data obtained demonstrates that the adsorption capacity increases with the CO_2 activation time employed.

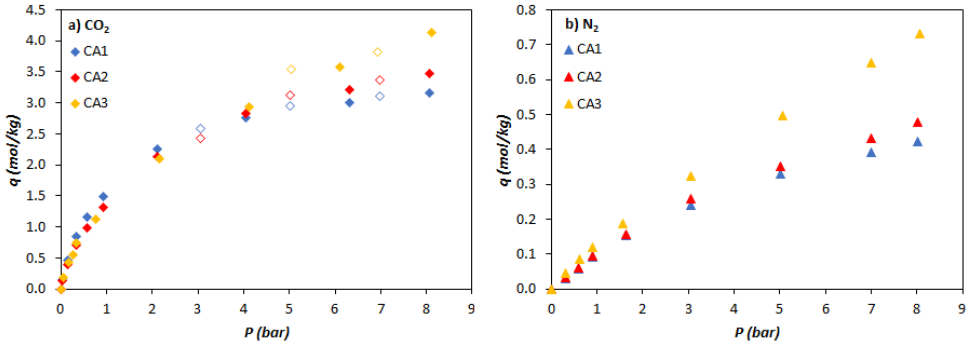

Figure 2. CO_2 and N_2 adsorption equilibrium isotherms at 303 K on the 3D Activated Carbon structures

3. Conclusions – The results obtained show that the approach proposed presents a straightforward and efficient option for the preparation of 3D adsorbent structures with good potential for CO_2 capture. It is once more showed that 3D printing will surely be an important tool in the chemical engineering sector in the near future.

Acknowledgements
This work was financed by through project Print3d4Capture (2022.15637.UTA) from the UT Austin-Portugal Program. It was also partially supported by FCT/MCTES through the Associate Laboratory for Green Chemistry–LAQV [LA/P/0008/2020, UIDP/50006/2020, UIDB/50006/2020)]. Inês Matos also acknowledges the Individual Call to Scientific Employment Stimulus contract CEECIND 004431/2022.

4. References
[1] C. Parra-Cabrera, C. Achille, S. Kuhn, R. Ameloot, Chem. Soc. Rev., 47 (2018) p. 209.
[2] Y.Y. Li, S. P. Perera, B.D. Crittenden, Chem. Eng. Res. Des., 76 (1998) p. 931.
[3] S. Couck, J. Lefever, S. Mullens, L. Protasova, V. Meynen, G. Desmet, G. Baron, J. Denayer, Chem. Eng. J., 308 (2017) p. 719.
[4] H. Thakkar, S. Eastman, A. Hajari, A. Rownaghi, J. C. Knox, F. Rezaei, ACS Appl. Mater. Interfaces, 8 (2016) p. 27753.
[5] L.F.A.S. Zafanelli, A. Henrique, H. Steldinger, J.L. Diaz de Tuesta, J. Gläsel, A.E. Rodrigues, H.T. Gomes, B.J.M. Etzold, J.A.C. Silva, Micropor. Mesoporous Mat., 335 (2022) p. 111818.

RIA43

XLIII Reunião Ibérica de Adsorção

Porto, Portugal

1-4 September 2024